81
13

DR 2010

MASTER

ORNL-4751
UC-70 – Waste Disposal and Processing

RADIOACTIVE WASTE REPOSITORY PROJECT: TECHNICAL STATUS REPORT FOR PERIOD ENDING SEPTEMBER 30, 1971

OAK RIDGE NATIONAL LABORATORY
operated by
UNION CARBIDE CORPORATION
for the
U.S. ATOMIC ENERGY COMMISSION

BLANK PAGE

Printed in the United States of America. Available from
National Technical Information Service
U.S. Department of Commerce
5285 Port Royal Road, Springfield, Virginia 22151
Price: Printed Copy $6.00; Microfiche $0.95

BLANK PAGE

ORNL-4751

Contract No. W-7405-eng-26

RADIOACTIVE WASTE REPOSITORY PROJECT:
TECHNICAL STATUS REPORT FOR PERIOD ENDING SEPTEMBER 30, 1971

A. L. Boch, Project Director
J. O. Blomeke, Assistant Director
W. C. McClain, Assistant Director
B. F. Bottenfield, Project Engineer

DECEMBER 1971

OAK RIDGE NATIONAL LABORATORY
Oak Ridge, Tennessee 37830
operated by
UNION CARBIDE CORPORATION
for the
U.S. ATOMIC ENERGY COMMISSION

CONTENTS

CONTENTS (Continued)

CONTENTS (Continued)

CONTENTS (Continued)

RADIOACTIVE WASTE REPOSITORY PROJECT: TECHNICAL STATUS REPORT FOR PERIOD ENDING SEPTEMBER 30, 1971

SUMMARY

Background

To ensure the successful application of nuclear power for mankind's benefit, a satisfactory means must be found for the disposal of the long-lived, toxic radionuclides that will accrue as waste materials. Most of the isotopes of concern appear in the high-level liquid wastes generated by the reprocessing of spent fuels and in solid refuse from AEC and industrial manufacturing operations. For the past 15 years the AEC has promoted the development of processes for converting the liquid wastes to stable, solid forms and, in consultation with the National Academy of Sciences and members of the geologic community, has sponsored work at ORNL to examine the suitability of bedded salt formations as a final Repository for these materials.

Salt deposits are considered to be most attractive for this purpose because of their wide distribution and great abundance; they are easily mined, have good thermal properties, and are free of circulating groundwater. Other possibilities that have been studied or seriously considered either require excessive surveillance, are more costly, or are more limited in their applicability.

The selection of the Lyons site was based primarily on a consideration of the favorable depth, thickness, and extent of the salt there; the amount of information available concerning key aspects of the site; the availability of the existing mine; and the generally favorable reception expected from the local inhabitants. Since the announcement of this site's tentative selection, we have completed a conceptual design of the Repository and initiated an investigative program designed to provide positive assurance of the Repository's safety and feasibility.

Geohydrological Characteristics of the Proposed Site and Considerations of Natural Containment of the Wastes

To determine and define the geological, as well as the hydrological, conditions at the Repository site and its immediate surroundings, an investigative program has been initiated that includes such things as surface mapping, core drilling, auger and rotary drilling, geophysical well logging, hydrologic testing, and measurements of the physical, chemical, and thermal properties of the rocks. To date, two core holes about 1300 ft deep have been completed at the northeast and southeast corners of the site. In addition, four 300-ft hydrologic test holes have been drilled at the approximate corners of the 1-square-mile site. Also, a series of some 45 auger borings have been made within a 9-square-mile area centered on

the Repository site to aid in delineating the unconsolidated surface sediments and in appraising the shallow groundwater aquifers. Data from this test program have revealed that the rocks in this region are all of sedimentary origin and flat-lying for the most part. A thin blanket of unconsolidated sands, silts, and gravels of Pleistocene age covers the land surface. This is underlain by Cretaceous age sandstones, while Permian rocks are found beneath the Cretaceous deposits. The salt member lies within the Permian rocks and is about 300 ft in thickness, lying from about 800 to 1100 ft below the land surface. Pennsylvanian and Cambro-Ordovician sediments comprise most of the rock section below the salt, with the Precambrian basement lying at a depth of about 4000 ft. Beginning some several hundred feet to a thousand feet below the salt bed, the rocks contain numerous permeable and porous beds that contain salt water and, locally, gas and oil. In general, the only important supplies of freshwater are found in the thick accumulations of sand and gravel in stream valleys. Some water may also be obtained from Cretaceous and Permian beds that outcrop at the surface, but the quality of the water is generally poor and the quantities small. Thus, the salt beds are separated from freshwater aquifers above, as well as oil and gas reservoirs below, by several hundred to a thousand feet or more of impermeable shales and other sedimentary rocks.

Thermal Analysis

Tentative criteria for limiting temperatures in and near the Repository are: temperature of the high-level waste, ≤1100-2000°F (depending on the type of waste); nominal maximum temperature of the alpha waste, ≤350°F; temperature of the salt approximately 8 in. from the surface of the waste container and approximately midway between the waste packages, ≤482 and ≤392°F, respectively; earth's surface temperature rise, ≤1°F; temperature rise in the geologic formation at the edge of the Repository buffer zone, ≤1°F; stagnant aquifer temperature rise at a depth of 300 ft below the earth's surface, ≤50°F.

Heat transfer from the waste packages and throughout the surrounding geologic formation is primarily by conduction. Finite difference techniques are used to solve the differential heat conduction equation. Three-dimensional analysis is required for calculating temperatures within several feet of the heat source, while two-dimensional models are used for determinations in the outlying region.

The permissible high-level mine loading in terms of initial power per unit gross surface area of the Repository is nearly independent of the power per package and of room size, but is dependent upon the age of the waste at the time of burial. For a 10-year-old waste (the oldest permitted to be stored at a reprocessing plant site), a loading of about 150 kW/acre is consistent with the limiting criteria. The shorter effective thermal-power half-life of a 1-year-old waste allows a loading of about 350 kW/acre, but the amount of waste required to produce this higher power level is only one-third that of 10-year-old waste. Therefore, it appears more economical to postpone burial to the 10-year limit. If all waste is 10 years old at

burial, the proposed 1000-acre site will accommodate the amount accumulated through the year 2000.

Temperatures close to the source reach a maximum in 1 to 25 years; the greater the mine space per package, the shorter the time. Peak times are: 40 years midway between the packages, 50 years in the pillar, 500 years near the earth's surface, and 2000 years at the edge of the Repository. Extensive sensitivity studies indicate that the existing uncertainties in thermal properties and stratigraphic detail do not affect the results substantially.

Temperatures calculated for the proposed alpha mine loading are well below permissible values, indicating that higher compaction factors than presently proposed would be acceptable.

Rock Mechanics Analysis

The objective of the rock mechanics analysis is to evaluate the mechanical effects which the operation of the Repository has on the surrounding rock strata and their potential for leading to conditions whereby the geologic containment of the wastes could be breached. These mechanical effects are the transient and permanent displacements and strains caused by the combined influences of the designed closure of the mine openings and thermal expansion of the entire rock column resulting from the transient elevation in temperature.

Preliminary estimates of these effects indicate that a total vertical subsidence of about 4 ft will be reached, with over 95% of it occurring in the first 100 years. On the other hand, the thermal expansion will produce an uplift of the ground surface amounting to a maximum of about 5 ft approximately 200 years after the operation of the facility, which thereafter is very slowly recovered as the thermal anomaly is dissipated. The sum of these two effects produces a ground deformation, which causes the surface over the Repository to rise slowly about 1 ft during the first 200 years and then subside very slowly, reaching a net depression of about 4 ft but only after several thousands of years.

The most serious potential consequence of these deformations is the development of a throughgoing fracture in the shales overlying the salt, which would render the salt subject to leaching by percolating groundwater. Such fracturing is directly related to the amount of strain absorbed by the shale. These strains will be calculated for the current mining design and also for other usable mine excavation patterns over the entire Repository area, using a deformation model calibrated by comparison with the deformations that took place throughout the experimental area of Project Salt Vault. More detailed finite-element calculations will also be performed for the regions experiencing the maximum strains and strain rates. These calculated strains and strain rates will then be compared with a failure criterion for the shales, based upon both laboratory experiments (including the possible thermal alteration of the physical properties of the materials) and selected field examples where similar rocks have experienced similar deformations.

Rock Property Testing

Analyses of the Repository behavior require knowledge of the physical and mechanical properties of the involved geological formations. Experimental measurements that have been made, or are planned, on cores from test holes 1, 2, and 3 are discussed. Physical properties of interest include thermal conductivity, specific heat capacity, and coefficient of thermal expansion within the range 0 to 200°C. Mechanical properties include stress-strain characteristics, creep behavior, and elastic and plastic moduli in the same temperature range. Standard analyses and potential mineralogical changes will be used to interpret and guide these measurement programs to establish needed property profiles.

Facility Description

A conceptual design study of the physical facilities of the Repository was completed in April 1971 by Kaiser Engineers under contract with the Atomic Energy Commission and under the technical guidance of the Oak Ridge National Laboratory project staff. The Lyons, Kansas, site is served by two railroads and a federal highway, which connect with the site directly. In addition, a third railroad and a state highway serve the Lyons community. The Repository includes both surface and mine-level facilities for the receipt, handling, and burial of both alpha-contaminated and high-level wastes. The facilities in which all waste handling operations are performed will be designed for tornado and earthquake resistance, and all such facilities will have controlled ventilation and confinement systems to protect against routine or inadvertent release of radioactive particulates. In-mine studies will be performed to confirm both the calculated effects of heat and radiation on the salt rocks and the capability to bury and retrieve wastes. Assuming Congressional authority is forthcoming, Title I engineering of the Repository facilities and leasing of the site and a surrounding buffer zone will begin late in CY-1971.

Characteristics of Wastes

Solid wastes containing plutonium and other transuranium elements, frequently referred to as alpha wastes, are routinely produced during operation of nuclear production and spent fuel reprocessing plants as well as operation of AEC laboratories and production facilities. The transuranium content of the wastes ranges from trace amounts to several grams per cubic foot. A series of heating tests was carried out to study the oxidation and pyrolysis of typical combustible solid wastes in wooden crates and steel drums at temperatures up to 215°C for extended periods of time. The wastes were packed into the containers to give a density of about 5 lb/ft^3 – a value that corresponds closely to the average density achieved in actual practice. The pressure buildup and weight losses on heating were recorded. Among the general conclusions drawn from these tests are that (1) combustible wastes in combustible containers should not be accepted at the Repository, and (2) combustible wastes in noncombustible containers, such as DOT 17C and 17H specification metal drums or equivalents, should be acceptable at the Repository.

Solutions containing fission products and small quantities of uranium, plutonium, and other heavy elements are generated during the processing of spent reactor fuels. These are generally referred to as high-level wastes because of their very intense, penetrating radiation and high heat-generation rates. Four processes have been developed for converting these liquid wastes to solid forms with a high degree of chemical, thermal, and radiolytic stability.

The products from the processes can be described as calcine cake for the pot calcination process, microcrystalline or rock-like solids for the spray solidification process, phosphate glass for the phosphate glass process, and a powder for the fluidized-bed calcination process. The pot and fluidized-bed products have lower thermal conductivities and higher leach rates than do the spray solidifier and phosphate glass products. However, the pot calcine material is more stable at elevated temperatures. The spray, phosphate glass, and the fluidized-bed products can be packaged in mild-steel containers, while stainless-steel containers must be used in the pot calcination process.

Isotope Transport

Three general modes of transport can be identified as potential mechanisms for the dispersal of radioactivity within the salt formation, once the metal waste container has been breached. These are gas-phase (and aerosol) transport, migration along free surfaces, and solid-state bulk and grain-boundary diffusion. Each of these phenomena has received varying degrees of attention during the past year.

The most obvious result of a breach in the radioactive waste container is a change in the chemical environment of the exposed waste species, and thus the possibility of gas-phase transport as a result of the formation of volatile fission product forms. Therefore, studies were initiated on two fronts. On one, the degree to which a crushed salt bed would retard gas transport was of primary interest, whereas the other was concerned with the possible formation of volatile species as a result of interactions between the waste and the salt environs. Although the gas permeability and diffusion investigations on crushed salt beds which were performed under this task indicated insignificant holdup relative to free-space transport prior to reconsolidation of the salt, the parallel studies that were conducted regarding volatility enhancement, and initially limited to interactions between water vapor and fission product oxides, suggested negligible transport by this mechanism owing to the anticipated temperatures involved.

A survey of the literature relative to solid-state bulk diffusion in salts indicates completely negligible transport by this mechanism as well, except for cases where the formation of space charges within the salt is a possibility. A similar study was also made of surface diffusion. This investigation revealed inconsistencies in the available experimental data; and, for this reason, plus a belief that transport along free surfaces ought to be more rapid than solid-state diffusion, an experimental program

of investigation was developed. The results of a rather crude, preliminary experiment with La_2O_3 tend to indicate that transport via a surface diffusion mechanism is acceptably slow, although an anomaly, as yet unresolved, has been observed (which may be an artifact of the experimental procedure).

Experiments have also been designed to verify the final results which the studies of the individual transport mechanisms are anticipated to yield. These "integrated" experiments involve investigations of the migration of simulated waste material through crushed salt beds under various conditions.

Energy Storage

Radiation produces defects in solid materials. This lattice disorder usually causes the crystal to be in a higher energy state, so that, upon thermal annealing, energy can be released. If the amount of stored energy that is released is greater than the heat capacity of the material, runaway heating can take place. For the case of the Repository, energy can be stored in the waste oxides due to heavy particle self-irradiation, and energy can be stored in the salt due to the more penetrating gamma rays emitted by the wastes. A survey of results in the literature, together with some extrapolations, lets us estimate that on the order of 50 cal/g can be stored in many oxides and between 1 and 20 cal/g can be stored in the salt, the amount depending very sensitively on impurity content and temperature of irradiation. Analyses based on upper-limit values of stored energy show that its release under the most pessimistic conditions could have no serious consequences. Additional work is required, however, to establish actual values for energy storage in the salt and solidified wastes under the transient thermal and radiation conditions that will prevail in the Repository.

Radiolysis and Hydrolysis in Salt-Mine Brines

Salt deposits of the type to be used for radioactive waste disposal contain a small volume-fraction of brine inclusions (~0.5%). Some brine from these inclusions will enter the open and unconfined spaces around a waste can as a result of the migration of the inclusions, which takes place in the presence of thermal gradients in the salt, and as a result of salt-fracture, which takes place at high temperatures (starting at about 250°C). The brine, vapors, and salts around a can will be exposed to high gamma-ray intensities and doses and to high temperatures. Accordingly, they will be subject to radiolysis and to other changes in composition brought about by thermally induced reactions.

We made a detailed review and analyses of literature information relative to the rates of inflow of brine and to the radiation and thermal chemistries of the salt and brines within the vicinity of a buried waste can. Our objective was to provide information on the identities of the final radiolysis- and thermal-reaction products and on the amounts formed

and released into the spaces around a can. Radiolysis products that were identified included, importantly, H_2, O_2, and possibly ClO_3^- and BrO_3^-. Most of the ClO_3^- and BrO_3^- will decompose to halides and O_2 at the high temperatures around a can; $Mg(BrO_3)_2$, if present, may give rise to some Br_2. Nearly all of this H_2, and the accompanying oxidized species, are formed within the migrating brine inclusions by the radiations absorbed within the brine and by dissolution of the trapped electrons and holes from the irradiated solid salt. The brine is rich in $MgCl_2$ (2.3 to 3 M), and hydrolysis of the $MgCl_2$ around a can will give rise to HCl. Corrosion reactions between the metal waste can and water vapor are possibly large sources of H_2. Experimental work and additional literature-type work are planned to establish more firmly the identities and amounts of radiolytic and thermal reaction products around a waste can.

Ecological Assessments

The objective of ecological investigations of the Repository project is to establish base lines that can be used for evaluating normal ecological changes, and, by comparison, determine impacts on the environment from Repository operations. Methodologies are being developed which will be used to evaluate possible impacts from radioactivity and thermal effects on plants, animals, and people living in the surface environment. Results from ecological studies will provide a framework for assessing alleged or real impacts such as effects resulting from either chronic or accidental releases of radioactivity, particularly ^{90}Sr, ^{137}Cs, and plutonium. Pathways of radioactivity movement, reconcentration in food chains, and possible hazards to man will be examined for different sources of release and modes of exposure. Another potential impact on the environment may involve thermal effects on surface biota manifested by heat dissipation from high-level waste deposits in the salt formation. On-site energy and water balance evaluations will be performed to verify preliminary conclusions of a negligible effect on surface biota. The initial phase of the ecological assessment has focused on: (1) ecological surveys by consultants from Kansas State University on plants, animals, and local environmental factors; (2) identification of the most probable pathways of radionuclide movement to man by using the results of these surveys and existing information on radioactivity flow in ecosystems; (3) formulation of predictive models for estimating radioactivity concentrations in ecosystem components by coupling pathway data with concepts of radioactivity behavior in the environment; and (4) summarization of meteorological conditions for the central Kansas region in order to identify the normal as well as extreme climatic conditions that could influence the design and operation of a Repository facility. Background information gathered from initial-phase assessment has been used to identify the principal environmental systems in the vicinity of the proposed Repository. These are Cow Creek, a stream with a variable flow rate; a grassland pasture, the projected plant community for the Repository site; and a wheat agroecosystem, the predominant crop of the area.

Safety Analysis

The only significant source of off-site exposure to radioactive or other materials originating from the Repository will be from very small quantities of airborne radioactive materials that escape through high-efficiency particulate air (HEPA) filters. It is planned that there will be no discharge of liquid waste from the Repository. Solid wastes generated at the Repository will be packaged and buried in the mine. Aqueous wastes will be recycled, with any excess water being evaporated to the atmosphere.

The maximum off-site concentrations that will result from the release of radioactive materials from the Repository to the atmosphere are estimated to be less than 0.1% of the applicable standards for exposure of the public and, in general, well below the concentrations of the same materials that exist at present due to natural and man-made sources. It is estimated that the buildup of off-site surface contamination of various species over the life of the Repository will ultimately result in a level that is less than 1% of the level that presently exists for the same species (including such radioisotopes as ^{90}Sr, ^{137}Cs, and ^{239}Pu, which have been deposited by fallout).

1. BACKGROUND

J. O. Blomeke

If nuclear fission is to be tapped as a major source of energy for our nation's growing needs, reliable methods must be developed to protect the environment from the ever-increasing inventories of radioactive wastes that will be generated in the course of producing nuclear power. Some of the radioisotopes present in these wastes are so long-lived that they must be contained outside the environment for hundreds of thousands of years. They appear principally in the high-level liquid wastes from reprocessing spent fuels and in a wide assortment of solid refuse, contaminated with transuranium elements, that is generated in various Atomic Energy Commission (AEC) and industrial manufacturing operations. The AEC first became concerned about the problem of ultimate disposal of these wastes more than 15 years ago, when it initiated the development of processes for converting the high-level liquid wastes to stable, solid forms, and when, in consultation with the National Academy of Science and others, it inaugurated investigations here at Oak Ridge National Laboratory into the suitability of natural salt formations as a final repository for these materials.

The progress of both the waste solidification and the salt investigations over the intervening years was such that the AEC felt justified recently in establishing the requirement that industries solidify their high-level liquid wastes for eventual shipment to a federal repository.[1] Furthermore, to prevent the accumulation of large quantities of plutonium in conventional burial grounds, the AEC has established a policy within its own complex which requires that wastes containing known or detectable amounts of transuranium nuclides be kept segregated, packaged, and stored in a readily retrievable manner for eventual shipment to a repository. A little over a year ago, the AEC announced the "tentative selection" of a site near Lyons, Kansas, for a demonstrational salt-mine repository for these two types of solid radioactive wastes.[2]

In this section, some of the work and considerations that led to the selection of the Carey mine at Lyons as the site for this first waste repository is reviewed. Subsequent sections, for the most part, will deal with many of the newer aspects that have received attention during the past 12 to 18 months.

1.1 Magnitude of the Problem

Projections to the year 2000 of the two types of wastes for which this first repository is being established give an idea of the magnitude of the problem that is facing us. Table 1.1 presents our estimates of the volumes of high-level wastes that will be generated by fuel reprocessing. These estimates are based on a nuclear power economy that is expected to expand from an installed capacity of about 6000 MW in 1970 to 940,000 MW in the year 2000. In this instance, we have assumed that the nuclear economy is based on power generation by LWRs using both ^{235}U and recycled plutonium fuels. LMFBRs are expected to come on-stream in the mid-1980s and assume an increasingly important role in the economy thereafter. At the end of the century, we anticipate that there will be only eight or ten reprocessing plants handling the fuel from the thousand or more reactors that will be producing electricity. The annual rate of waste generation in the form of concentrated liquids will approach 6 million gallons by 2000. The 77 million gallons predicted to be accumulated by the year 2000 (assuming that the wastes would all be accumulated as liquids) compares with greater than 80 million gallons of waste currently in storage at AEC production sites, but the total activity and the quantities of significant long-lived nuclides predicted for 2000 exceeds present AEC inventories by many orders of magnitude. Solidification reduces volumes by more than a factor of 10 and facilitates transport and retention of the wastes outside the environment. The total heat generation rates, beta activities, and individual isotopes that are shown in Table 1.1 include the ^{85}Kr and tritium which are currently released from reprocessing plants. They will probably eventually be separated from effluent streams and methods will be devised for their immobilization and long-term storage, although present plans do not provide for their storage at this first repository. A small percentage of the ^{239}Pu, which is present in the spent fuels, appears in the wastes as a processing loss, and it is representative of a number of long-lived alpha-emitting isotopes of the heavy elements which are also present in the high-level wastes.

Table 1.2 presents the estimated volumes of so-called "alpha" wastes which, because of their plutonium content, will probably be shipped to

Table 1.1. High-Level Wastes from Predicted Nuclear Power Economy

	Calendar Year			
	1970	1980	1990	2000
Installed Nuclear Capacity, 10^3 MW(e)	6	150	450	940
Liquid: Annual generation, 10^6 gal	0.017	1.0	3.3	5.8
Accumulated, 10^6 gal	0.4	4.4	29	77
Solidified: Annual generation, 10^3 ft^3	0.17	9.7	33	58
Accumulated, 10^3 ft^3	0.17	44	290	770
Total heat generation rate, MW	0.9	80	410	1,040
Isotopes accumulated, MCi				
Total beta activity	200	19,000	100,000	270,000
28.9-y ^{90}Sr	4	960	5,700	12,000
30-y ^{137}Cs	5	1,300	8,000	20,000
10.8-y ^{85}Kr	0.6	120	690	1,500
12.3-y ^{3}H	0.03	7.3	44	110
24,400-y ^{239}Pu ($\approx$0.5% processing loss)	0.0001	0.02	0.3	1.7

Table 1.2. Projections of Compacted Alpha Wastes

	Calendar Year		
	1980	1990	2000
Volume generated, 10^3 ft^3			
Annually	350	1,000	2,500
Accumulated	2,100	10,300	25,000
Isotopes accumulated			
Mass of actinides, metric tons	1.4	16	53
87.4-y ^{238}Pu, MCi	0.23	2.6	8.3
24,400-y ^{239}Pu, MCi	0.05	0.6	1.9
6600-y ^{240}Pu, MCi	0.07	0.8	2.8
433-y ^{241}Am, MCi	0.06	1.0	6.5
Shipments[a]			
Number per year	350	1,000	2,500
Volume per shipment, ft^3	1,000	1,000	1,000
Plutonium per shipment, kg	0.8	2.5	2.5
Vehicles in transit	8	23	58

[a]In ATMX-600 railcars.

repositories. These estimates pertain to solid, low-radiation-level wastes that contain greater than 10 μCi of long-lived alpha activity per kilogram and are to be generated by both AEC and industry. Thus far, the AEC has stated that only alpha wastes of AEC origin will be sent to the repository; however, since the volume of alpha wastes from industrial sources will probably exceed the volume generated at AEC sites even before 1980, we assume that their storage in repositories will likewise soon be required. By 2000 we will be generating 2.5 million ft^3 annually of these wastes, which will be compacted or otherwise reduced in volume by a factor of 10.[3] Twenty-five million cubic feet containing more than 50 tons of actinide elements will have been accumulated by 2000, and 2500 railcar shipments per year will be required for transport to repositories. We estimate that from 80 to 90% of these wastes will be generated at reactor fuel fabrication and preparation plants, with the remainder being generated at reprocessing plants.

1.2 Management of High-Level Wastes

In the mid-1950s, soon after work began on methods for solidifying high-level wastes and on the investigation of salt formations, we decided to make an evaluation of the technical and economic feasibility of the overall approach that was being pursued. This evaluation effort, which is still under way, initially consisted of a series of studies, on paper, of the various operational steps that constituted high-level waste management. These studies served as a very useful tool both in justifying and in directing much of the experimental work.

Management of high-level liquid wastes is viewed as consisting of a series of operational steps carried out over a period of years or decades following fuel reprocessing (Fig. 1.1). (The ORNL numbers shown in this figure refer to published reports.) Following their generation in a fuel reprocessing plant, the wastes could be subjected to such preliminary operations as partial removal of fission products, interim storage as liquids in tanks, conversion to solids by a process such as pot calcination, interim storage of the solids, and, finally, shipment of the solids to a repository. Although burial in salt was our preferred method of

ORNL-LR-DWG 72614 R6

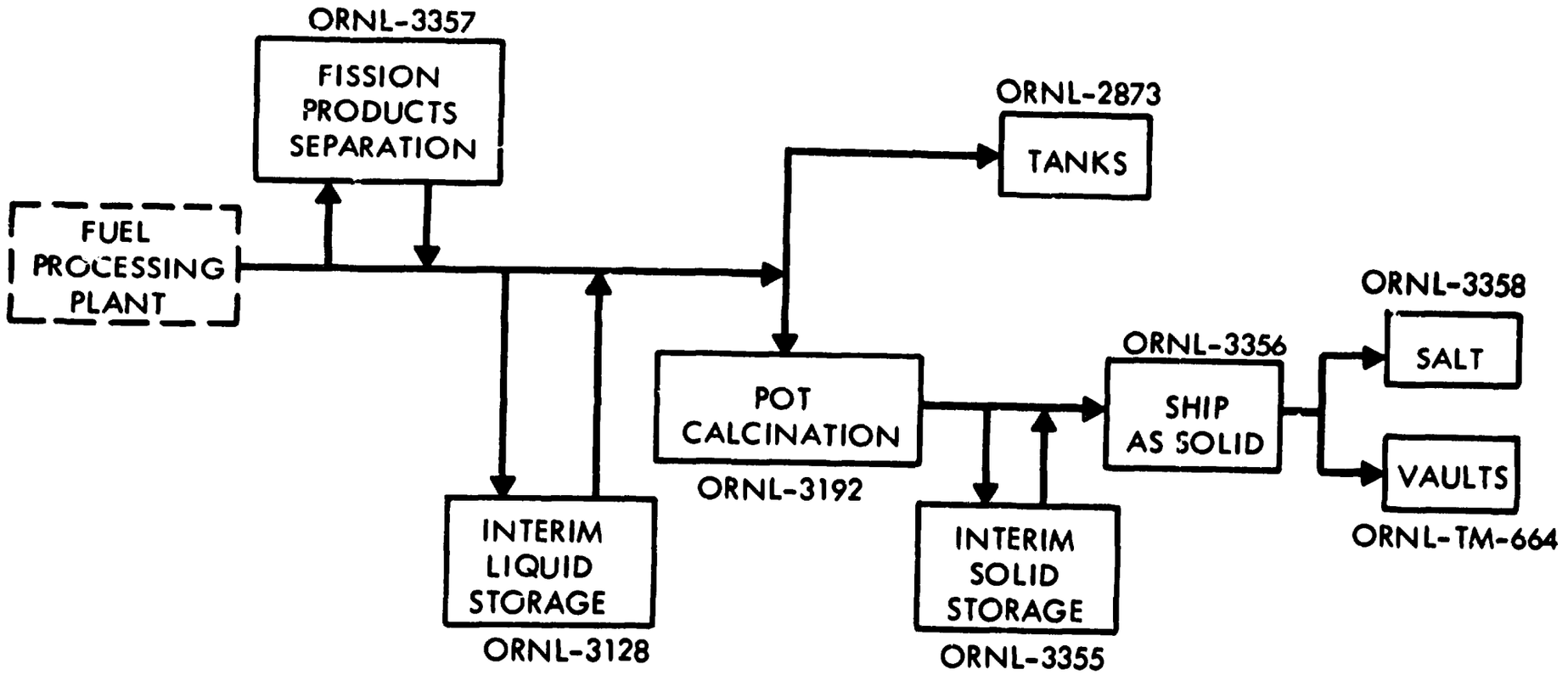

Fig. 1.1. Management of High-Activity Wastes.

ultimate disposal, it was (and still is) conceivable that vaults or other specially constructed monolithic structures at the surface might be constructed to serve for very long-term storage. Although "perpetual" storage in tanks was not considered acceptable, we carried out an economic analysis of this method to serve as a basis for comparison with the preferred approach.

With regard to fission-product removal, it should be pointed out that, according to current federal regulations, any inert material which is removed from a typical high-level waste for release to an uncontrolled area must be decontaminated, by factors ranging from 10^{11} to 10^{15}, from a dozen or more of the most hazardous elements that are present. Such high degrees of separation would be prohibitively expensive, if not technically impossible to achieve, in the case of some of the substances that are present in these wastes. On the other hand, we found that the cost of managing wastes which are 90 to 99% depleted in fission products (a degree of separation currently attainable) is still about 70% as much as the cost of management with no fission products removed. The difference, about $2000 to $3000 per ton of fuel processed, is not adequate to pay for the separation, encapsulation, and eventual disposal of the separated fission-product concentrates. We concluded, therefore, that the removal of radioisotopes must be justified and paid for by the market for these materials as radiation or heat sources, with only a marginal credit from reduced costs of waste management. This clearly does not offer a very promising approach, much less a permanent solution, to the waste management problem.

Our estimates of the costs of waste management, if carried out over a period extending up to 10 years after fuel reprocessing, are summarized in Table 1.3. These costs were computed for a fixed-size economy and are based on an economic model representative of corporate financing.[4] The important parameter considered here is time, or the point in time at which the various operations are carried out, and costs are given in units of thousandths of a mill per kilowatt-hour of electricity produced. Basically, what they show is that high-level waste management by the route of solidification, shipment, and storage in a salt-mine repository should be less than 0.05 mill/kWhr, or about 1% of the cost of electricity and perhaps

Table 1.3. Range of Management Costs for LWR Fuel Reprocessing Wastes (20,000 MW(e) economy[a])

Operation	Cost Range (10^{-3} mills/kWhr)
Interim liquid storage from 1 to 10 years	14 to 26
Solidification in 6- to 12-in.-diam pots[b]	4 to 17
Interim solids storage from 1 to 10 years	1 to 10
Shipment (2000-mile round trip)	1 to 3
Burial in salt after aging 1 to 10 years	3 to 11
Total costs	37 to 45

[a]688 tons of fuel per year exposed to 33,000 MWd/ton at 30 MW/ton.
[b]1 cubic foot of solids produced per 10,000 MWd (thermal).

25% of the current cost of fuel reprocessing. Although this is 10 to 20% greater than the cost we estimated for perpetual storage in tanks, it was (and still is) considered by most of us to be an acceptable price to pay. Also, it provided reassurance that we were not developing an approach that was likely to be economically self-defeating.

1.3 Advantages of Salt Formations

Salt formations were first recommended for use in the disposal of radioactive wastes by the National Academy of Sciences-National Research Council (NAS-NRC).[5] This recommendation was based on a number of characteristics which make it particularly attractive for this purpose. It is widespread and abundant, underlying about 500,000 square miles in portions of 24 states; it has good structural properties, with a compressive strength and radiation-shielding characteristics similar to concrete; it is relatively inexpensive to mine; its thermal properties are better than those of most other rock types; and it occurs generally in areas of low seismicity. Most

importantly, bedded salt deposits are completely free of circulating groundwaters and are isolated from underground aquifers by essentially impermeable shale. This situation tends to be preserved because any fractures that might develop may be healed by plastic deformation and recrystallization of the salt.

1.4 Principal Alternatives to Salt

Several other possibilities have been studied or seriously considered, either at ORNL or elsewhere. In general, these alternatives require excessive surveillance, are more costly, or are more limited in their applicability. "Perpetual" storage as liquids in tanks requires continuing surveillance, mechanical means for removal of decay heat for several centuries, and periodic replacement of the tanks. Disposal as liquids in bedrock caverns, as has been suggested for use at the Savannah River Plant, would be restricted only to those sites with the proven geological characteristics necessary to ensure long-term confinement; and the relative scarcity of potential sites and the extensive explorations required to verify their suitability would place a serious limitation on the siting of reprocessing plants. We were able to show, in the course of the economic evaluations discussed above, that disposal as solids in surface vaults and granite caverns would cost several times more than would the use of salt formations. Furthermore, a salt repository would almost certainly be safer than concrete vaults; and, as a general rule, salt has more desirable natural attributes for our purposes than do granite and other available geologic structures. Finally, the practical application of such advanced techniques as transmutation or disposal into space is not in the realm of present, or probably even near-future, technology. Both methods would require extremely complicated separations and packaging techniques and the development of sophisticated hardware. Even then, it is questionable whether transmutation of all the isotopes of concern would be possible. Disposal into space may someday become feasible if reliability and cost factors can be overcome.

1.5 Historical Development

The history of the salt-mine repository dates back to September 1955, when a committee of geologists and geophysicists was established by the NAS-NRC to consider the possibilities for disposal of high-level wastes in geologic structures within the United States (Table 1.4). This committee proposed storage in natural salt formations as the most promising method for the near future. Early investigations in the laboratory and in the field were aimed at the disposal of liquid wastes. These investigations were prompted by the fact that, while processes for converting liquid wastes to solids had been proposed, they were then in only a very early stage of development.

Table 1.4. Historical Development of Salt-Mine Repository

Event	Date
Consideration and recommendation by NAS-NRC	1955-1957
Laboratory and field studies with liquid wastes	1957-1961
Review and confirmation by NAS-NRC	1961
Feasibility studies of radioactive demonstration	1962
Project Salt Vault	1963-1967
Review and endorsement by NAS-NRC	1966
Feasibility study of high-level waste repository	1968-1969
Conceptual design of high-level waste repository	1969-1970
Conceptual design of dual facility	1970-1971
Review and endorsement by NAS-NRC	1970

In December 1961, the NAS-NRC committee reviewed developments that had taken place since the 1955 meeting and concluded that the experimental and other investigative work which had been in progress tended to confirm the suitability of salt formations for this purpose.[6] They recommended that, in view of the progress made in the development of waste solidification processes, the AEC should study the effects of storing dry, packaged radioactive wastes in a salt deposit.

Following a study made in 1962 of the feasibility of carrying out such an experiment, the design and execution of Project Salt Vault was undertaken.[7] This demonstration was performed in the Carey Salt Company mine in Lyons, Kansas, with highly satisfactory results, and it led to a further study of the feasibility of establishing an actual repository for the nation's needs. We undertook a conceptual design of a repository for high-level wastes in mid-1969; however, in March 1970, the scope was enlarged to provide a dual facility capable of accepting alpha-contaminated solid wastes as well. Kaiser Engineers was selected as the architect-engineer for this project in September 1970, and we have been working with them on the conceptual design since that time. The NAS has continued its periodic reviews and endorsements of this work, the most recent having taken place in mid-1970.[8]

1.6 The Disposal Concept

Figure 1.2 shows the cross section, at the mine level, of one quadrant of a 1-square-mile conceptual repository for high-level wastes. This concept, developed in the early 1960s, is still applicable in all important respects. The waste containers, or cylinders, are lowered through a shaft from the surface into a motorized carrier which moves out along a peripheral tunnel to the current disposal area, a room perhaps 50 by 300 ft in cross section and 15 to 20 ft high, where each cylinder is lowered into a hole in the floor and the hole is then backfilled with salt. The cylinders would be spaced, depending on their power levels and subsequent decay characteristics, so that the temperatures of the salt and overlying formations do not exceed acceptable levels. When filled with waste containers, the room is backfilled with salt and disposal begins in a newly

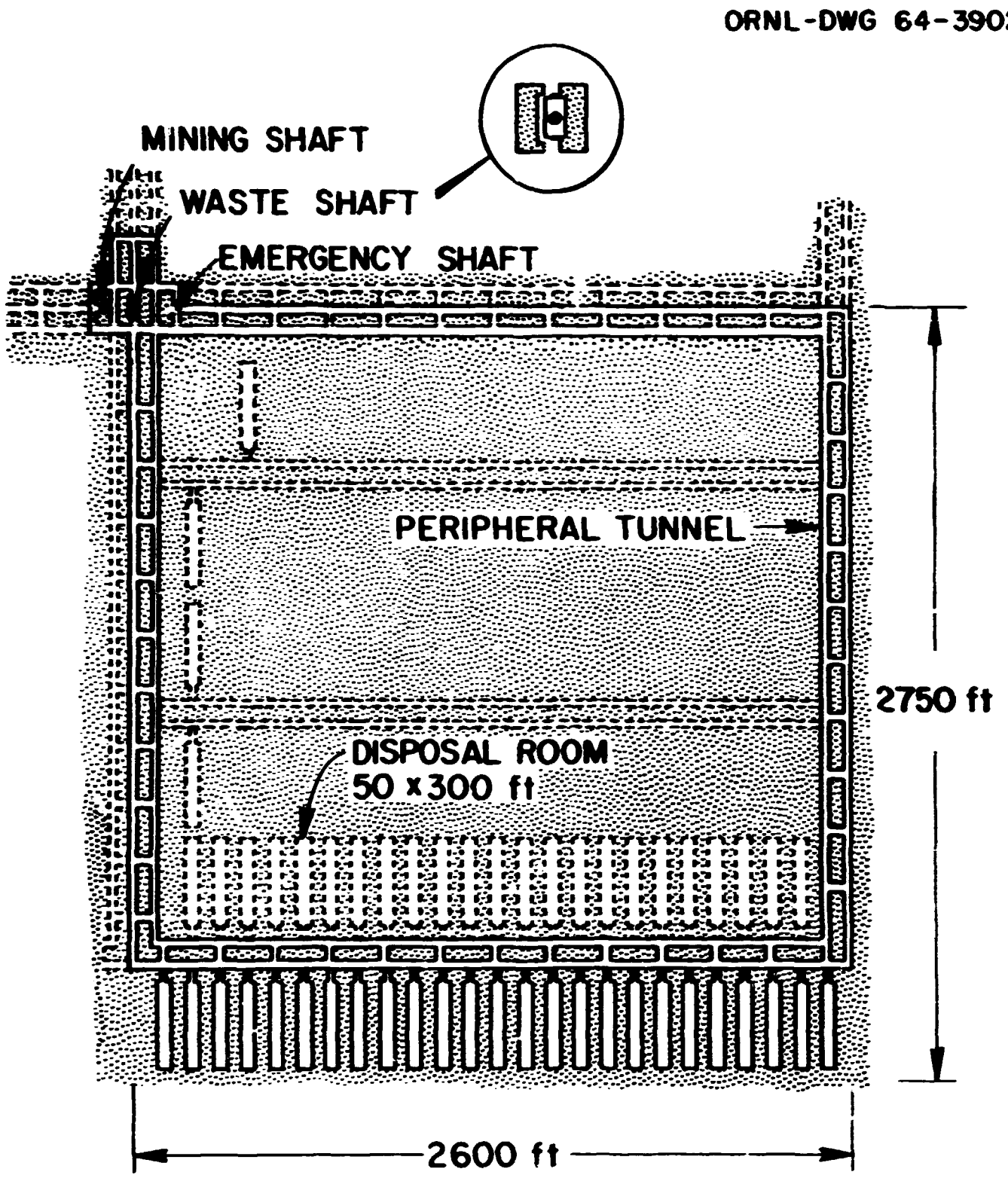

Fig. 1.2. Quadrant of 1-Square-Mile Concept Mine.

mined room. The corridors are likewise backfilled with salt as the rooms are utilized. A most important feature of this concept is that, as the temperature rises, the deformation of the solid salt throughout the area causes reconsolidation and recrystallization of the crushed salt. After several decades, when this process is completed, the wastes are completely isolated from any contact with the biological environment.

1.7 Project Salt Vault

A field-scale experiment called Project Salt Vault, referred to earlier, was carried out in the Carey mine at Lyons in the mid-1960s to demonstrate the feasibility and safety of the disposal-in-salt concept, to demonstrate the equipment and techniques for handling packages of highly radioactive solids, and to obtain data for the design of an actual disposal facility (Fig. 1.3). Fourteen irradiated fuel assemblies from the ETR, two each in seven containers, were used to simulate solidified wastes. These were placed in arrays of holes in the floor of the mine. Electrical heaters were used to raise the temperature of a large quantity of salt in the central pillar in order to obtain information on its in situ structural properties.

A total of about 4 million curies of fission-product activity, in 21 containers, was transferred into and removed from the mine without incident. During the 19-month course of the experiment, the average dose delivered to the salt at the walls of the array holes was about 8×10^8 rads, with a peak dose of 10^9 rads. In spite of these rather high doses, there was no measurable radiolytic or structural effects in the salt. Much useful information was gathered with respect to thermal stresses, migration of brine-filled cavities, and salt-flow characteristics as a function of temperature.

The PSV transporter, which was positioned in the mine to receive the radioactive canisters from the surface, consists of a standard diesel-powered tractor and a specially designed two-wheel trailer with a power-positioned lead-shielded cask. It can be maneuvered to spot the shielded cask within 1 ft of any fixed point on the floor of the mine, and the cask

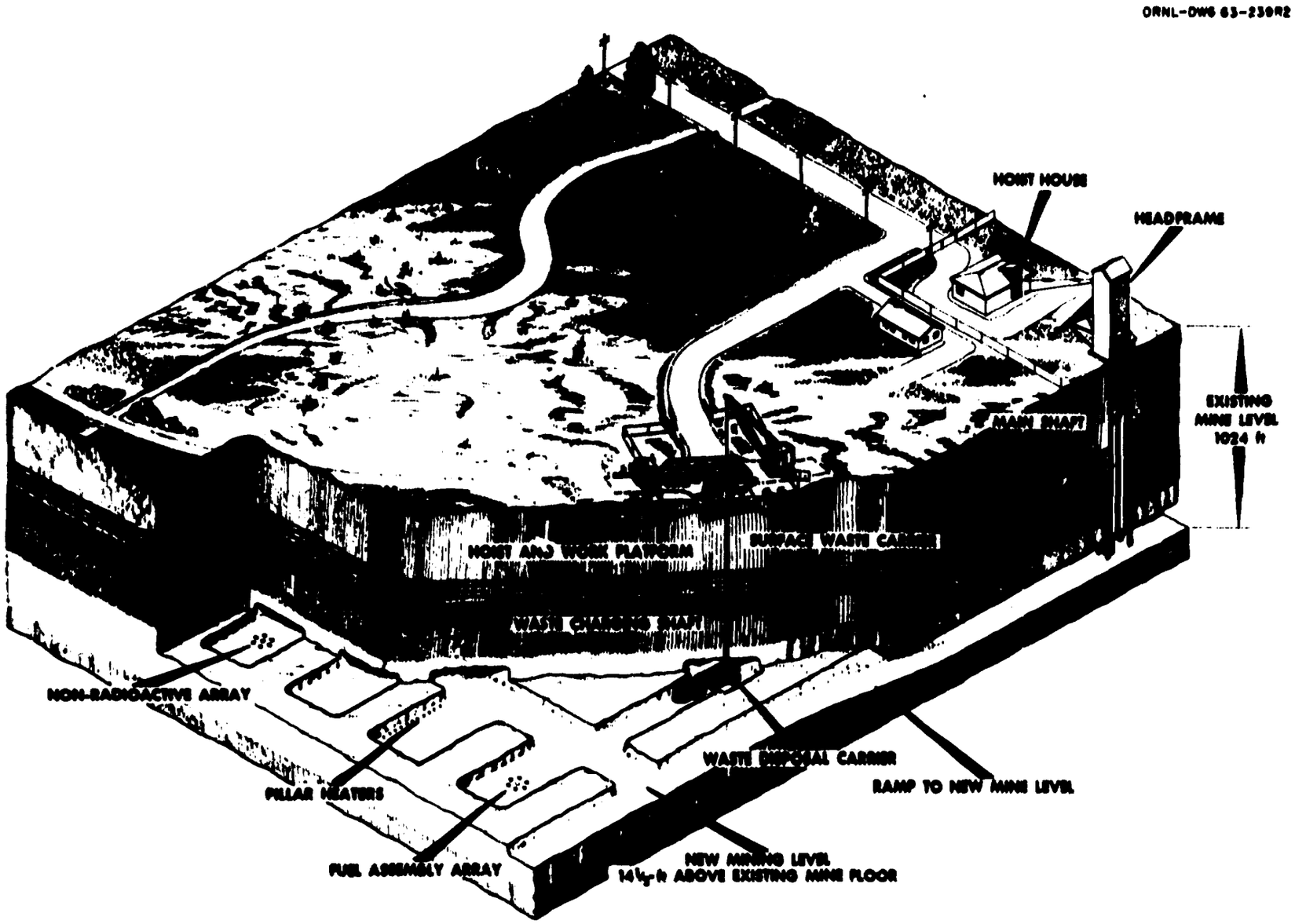

Fig. 1.3. Demonstration of Radioactive Solids Disposal in Salt.

can then be indexed to within ±1/16 in. of any predetermined point within range. The shield weighs 25 tons. The entire machine was lowered into the mine in parts and assembled there.

1.8 Major Siting Considerations

In selecting the most suitable site for the first waste repository, certain requirements (mainly of a geologic nature) consistent with considerations of long-term isolation and the efficiency of operations were established. We thought that the salt should be of the bedded type because the future stability of bedded salt formations is easier to predict than that of more highly disturbed formations such as domes and anticlines. The formation should not be less than 500 ft deep and 200 ft thick to provide for adequate heat dissipation, as well as to ensure isolation above and below the disposal horizon. The depth of the formation should not be greater than 2000 ft because of the increased difficulty and cost of operating at greater depths. The formation should have a considerable horizontal extent amounting to at least several tens of miles to provide adequate isolation from adjacent geologic structures. The site should be situated in a zone of tectonic stability. An existing mine is highly desirable in order to expedite construction and reduce the overall costs. Any facility designed to receive and accumulate large inventories of long-lived radionuclides could not be realistically considered at this time for siting near large population centers and their related high land values. Finally, accessibility by rail and motor freight and acceptance by public officials and private citizens of the area are other important requirements of the site.

We found that salt deposits in three general areas meet the geological requirements: a large area in central Kansas; a smaller area in west-central New York; and a still smaller area in southeastern Michigan (in general, underlying metropolitan Detroit). An evaluation of the geologic aspects of these sites indicated that, while all three might be suitable, the Kansas area is the most favorable. The advantages that can be attributed to central Kansas are that the depth to the salt disposal horizon is generally less

than the other sites; the thickness and areal extent of the deposit are greater; and the area is in a zone of slightly greater tectonic stability. Furthermore, the Lyons mine of the Carey Salt Company appears to be uniquely suitable in that it is the only available, accessible, nonproducing mine in any of the three geologically suitable areas; we possess much detailed information on the mine and its environs from having performed a 3-year-long experiment there; and we were confident of receiving a reasonably favorable reception from local and state officials and private citizens.

The proposed site is situated in the northeast outskirts of the city of Lyons (Fig. 1.4), which has a population of about 4300 and is located in the center of Rice County in central Kansas. It is approximately 240 miles west and slightly south of Kansas City by highway, and 65 miles northwest of Wichita. The nearest population centers are Hutchinson, 30 miles to the southeast, and Salina, about 45 miles to the northeast. Lyons is served by the Missouri-Pacific, Frisco, and Santa Fe Railroads, and is accessible via U.S. Highway 56.

1.9 References

1. "Siting of Fuel Reprocessing Plants and Related Waste Management Facilities," Federal Register 35, No. 222, 17530 (November 14, 1970).

2. U. S. Atomic Energy Commission, News Release N-102, June 17, 1970.

3. H. W. Godbee and J. P. Nichols, Sources of Transuranium Solid Waste and Their Influence on the Proposed National Radioactive Waste Repository, ORNL-TM-3277 (January 1971) (Official Use Only).

4. R. S. Dillon, J. J. Perona, and J. O. Blomeke, A Model for the Economic Analysis of High-Level Radioactive Waste Management, ORNL-4633 (Nov. 1971).

5. Disposal of Radioactive Wastes on Land, Publication 519, National Academy of Sciences-National Research Council, Washington, D. C., 1957.

6. "Minutes of the Meeting of December 7-8, 1961," National Academy of Sciences-National Research Council, Division of Earth Sciences, Committee on Geologic Aspects of Radioactive Waste Advisory to the U. S. Atomic Energy Commission.

7. R. L. Bradshaw and W. C. McClain (Eds.), Project Salt Vault: A Demonstration of the Disposal of High-Activity Solidified Wastes in Underground Salt Mines, ORNL-4555 (April 1971).

8. Disposal of Solid Radioactive Wastes in Bedded Salt Deposits, Committee on Radioactive Waste Management, National Academy of Sciences-National Research Council, Washington, D.C., November 1970.

ORNL DWG 70-11023

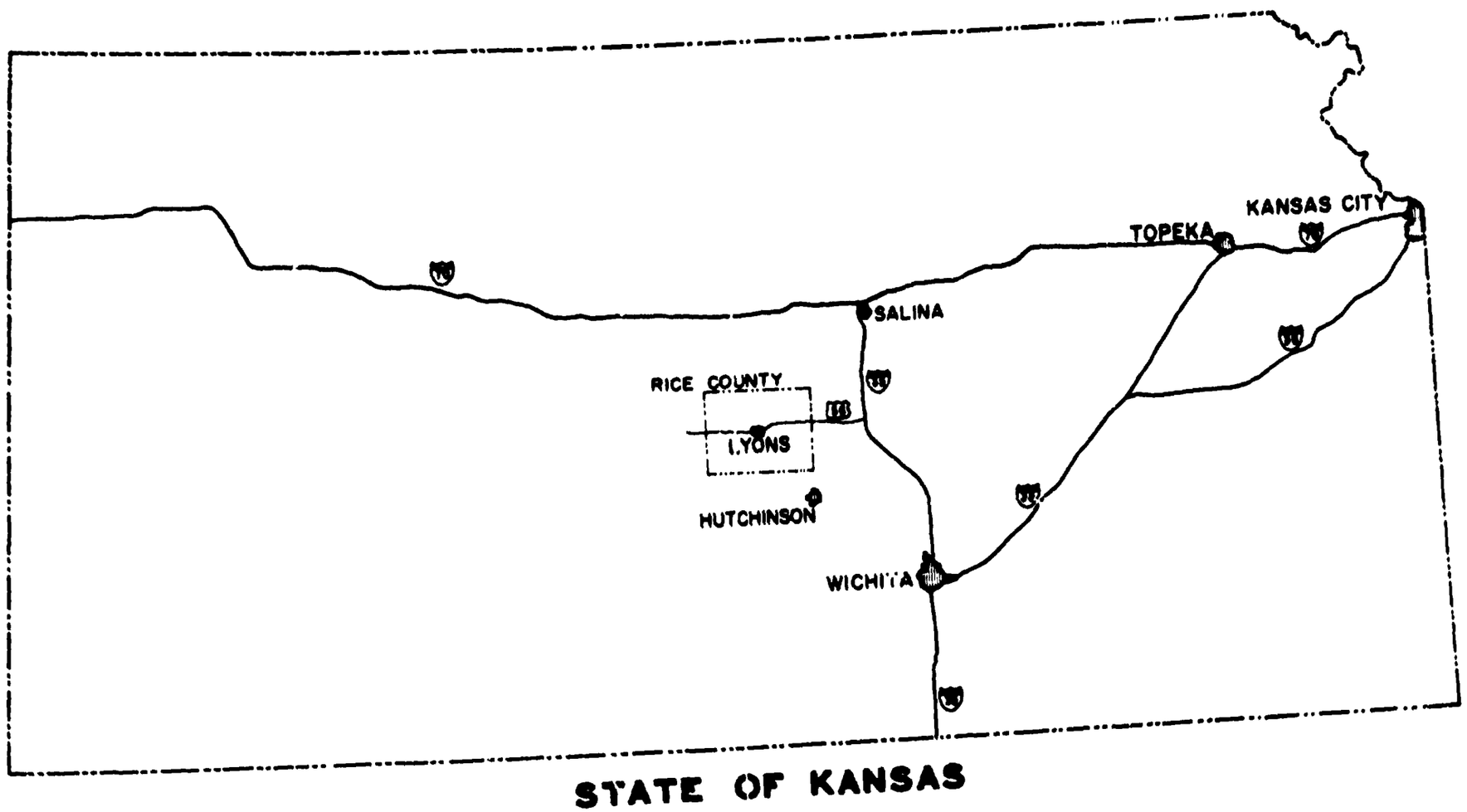

Fig. 1.4. Geographical Location of the Site of the Proposed Repository.

2. GEOHYDROLOGICAL CHARACTERISTICS OF THE PROPOSED SITE AND CONSIDERATIONS OF NATURAL CONTAINMENT OF THE WASTES

T. F. Lomenick

2.1 Geohydrological Characteristics of the Proposed Site

An investigative program that includes surface mapping, core drilling, auger and rotary drilling, geophysical well logging, hydrologic testing, and measurements of the physical, chemical, and thermal properties of the rocks has been initiated to determine and define the geological and hydrological conditions at the site of the proposed Repository and its immediate surroundings. To date, two core holes about 1300 ft deep have been completed at the northeast (test hole 1) and southeast (test hole 2) corners of the site. In addition, four 300-ft hydrologic test holes have been drilled at the approximate corners of the site, and a series of approximately 45 auger borings has been made within a 9-square-mile area centered on the Repository site to aid in delineating the unconsolidated surface sediments and in appraising the shallow groundwater aquifers. Data from this test program, coupled with the available and pertinent information obtained from existing mine shaft logs, mine workings maps, oil and gas well logs, and previous geologic and hydrologic studies of the county, will provide, when complete, the necessary knowledge to establish the suitability of the site for the safe operation of the facility and for the long-term confinement of the radioactive waste.

2.1.1 Stratigraphy

The stratigraphic section at the site, as revealed by the first two core holes, is shown in Fig. 2.1. The uppermost material in each hole (71 ft in test hole 1 and 35 ft in test hole 2) consists mostly of lean, stiff, moist, light-brown clay that is occasionally silty and contains sporadic nodules of caliche or calcium-cemented silt. According to Angino,[1] this material blankets the surface of the Repository site and much of the surrounding area (Fig. 2.2). The rather wide variation in the thicknesses of the aeolian or wind-blown sediments is not unexpected since the underlying Cretaceous rocks were subjected to a long period of erosion that created an irregular topographic surface prior to the time

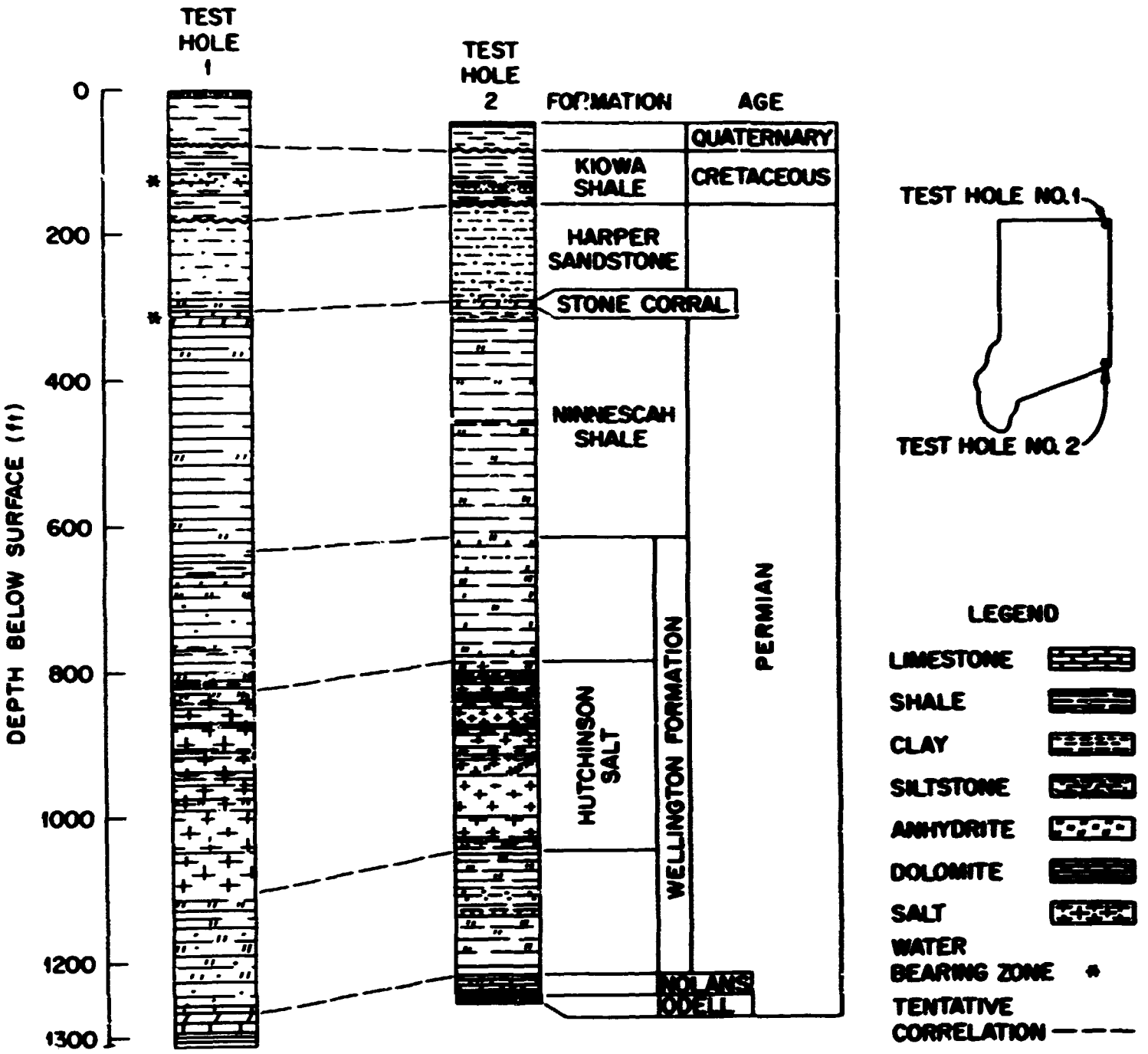

Fig. 2.1. Generalized Stratigraphic Sections at Test Holes 1 and 2. Data obtained from cores and logs of core borings performed for USAEC by U.S. Army Corps of Engineers, August-November 1970.

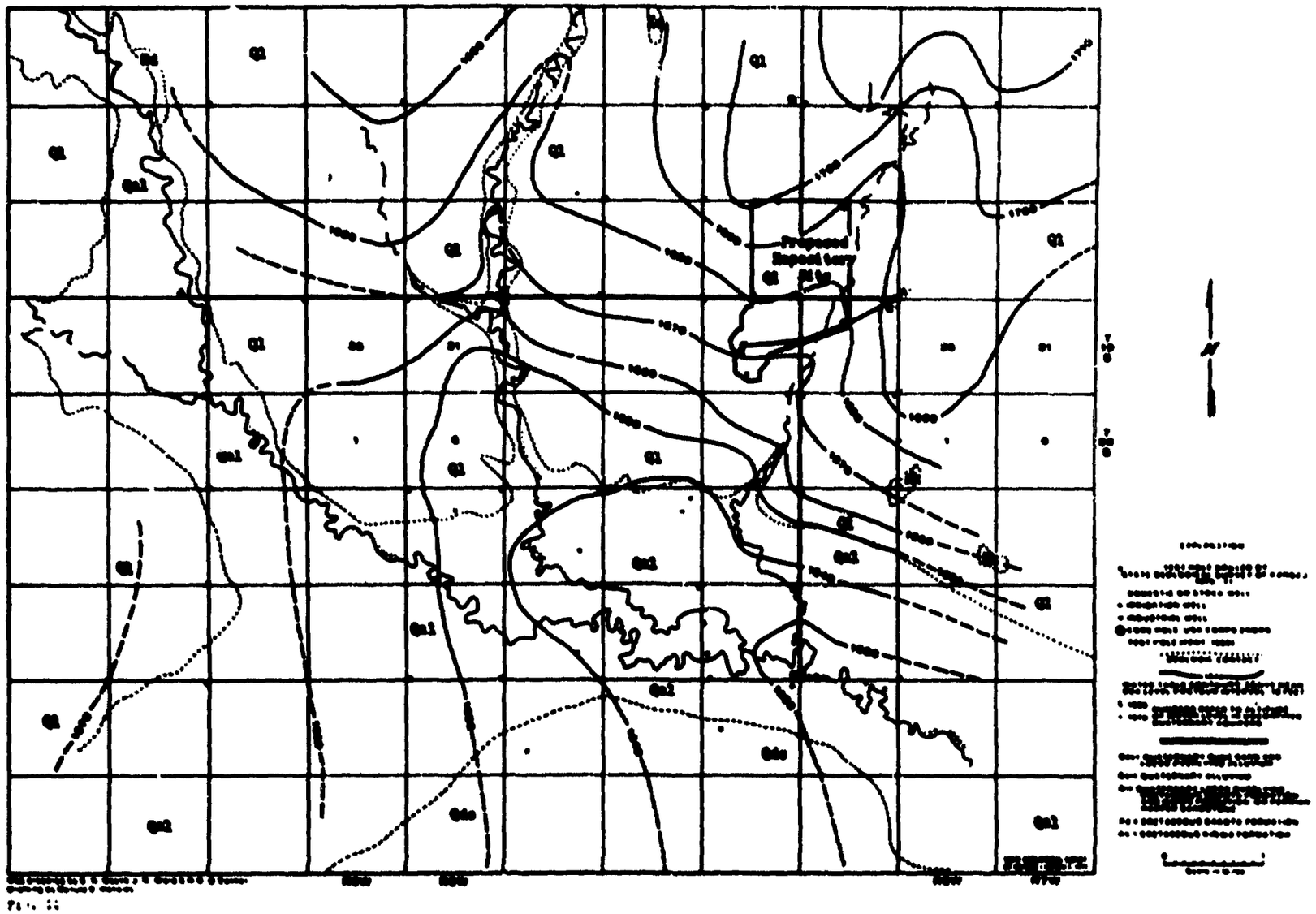

Fig. 2.2. Preliminary Geologic and Hydrologic Map of the Proposed Repository Area, Lyons, Kansas (After Charles K. Bayne et al., "Surface Geology and Groundwater Hydrology," Chapter 2 in Preliminary Report on the Geology and Hydrology of the Lyons, Kansas, Radioactive Waste Repository Site, prepared by the State Geological Survey of Kansas and the University of Kansas Center for Research, Inc., for the USAEC and the Union Carbide Corporation, November 1970).

that the Pleistocene deposits were laid down. This old erosional surface was found by Angino to consist of a thin zone of clay mixed with residual gravels and a thin layer of caliche. Outside the boundaries of the Repository in the valleys of Cow Creek and Little Cow Creek, the Pleistocene deposits consist of fluvial or water-lain materials of clay silt, sand, and gravel (Fig. 2.2). These unconsolidated sediments range from a few feet in thickness to about 180 ft and are, by far, the most important water-bearing deposits in the general area.

The Kiowa formation of Cretaceous age underlies the Pleistocene deposits at the site and is the youngest consolidated rock encountered. It consists primarily of weathered, light-brown, fissile, clay shale that contains occasional nodules of phosphate in the upper part and generally dark-gray clay shale with a few thin beds of fossiliferous limestone in the lower part. Low- to high-angle fractures with slickenside surfaces are common throughout the formation. One of the most outstanding features of the Kiowa is the occurrence of water-bearing sandstone lenses that may range from a few inches to tens of feet in thickness. In test hole 1, a 7.5-ft-thick sandstone bed with another 11 ft of underlying interbedded shale and sandstone occurs near the middle of the 100-ft-thick section of the Kiowa formation. In test hole 2, where the formation is about 74 ft thick, an 8-ft-thick section of shale and interbedded sandstone was encountered near the bottom of the formation. An oscillating shoreline during Kiowa time was probably instrumental in the development of the highly variable sandstone beds of the formation. The variable thickness of the Kiowa throughout the area is accounted for by the irregular nature of its pre-Pleistocene erosional surface at the top and by the similarly uneven erosional surface of the underlying Permian rocks at its base. The Kiowa does not outcrop at the Repository site, being completely covered by alluvium; however, surface exposures of the formation occur 1 to 2 miles southeast of the site (Fig. 2.2). Although the Kiowa persists over the Repository site, it is not present a few miles to the west, beneath the bed of Little Cow Creek, or to the south in the alluvial valleys of Cow Creek and the Arkansas River. It was eroded completely, probably during the Pleistocene, by these down-cutting streams. Toward the north of the

site, the Kiowa formation is complete (approximately 150 ft thick) and is underlain by the Cheyenne sandstone of Cretaceous age and overlain by the Dakota formation, also of Cretaceous age.

Permian-age rocks underlie the Kiowa shale formation at the site (Fig. 2.1). Here, as well as throughout the Permian Basin, these rocks reflect the conditions prevailing during this time period. In general, the sequence of beds encountered in test holes 1 and 2 include (from the top) red beds, salt, anhydrite, and limestone and shale (Fig. 2.1). The Harper siltstone formation is the youngest Paleozoic-age rock present at the site. This formation is the lowermost member of the Nippewalla group of rocks in Kansas, which is progressively more complete toward the western part of the state. At the close of the Permian Age, uplift, followed by a long period of erosion, removed most of the Upper Permian rock section from this part of the state, leaving only the Harper in the Nippewalla group. The Harper was found to be about 125 ft thick in each test hole. The formation is predominantly reddish, massive siltstone and reddish silty to clayey shale except for the uppermost shales and siltstones, which are generally soft and gray in color from weathering. The Harper is undoubtedly present beneath the entire Repository site; however, it extends only about 10 miles farther to the east before being beveled by pre-Cretaceous erosion.

Underlying the Harper siltstone is the Stone Corral formation. This well-known "market" bed, which is easily identified in well samples and on electric and radioactivity logs, is seen to be about 18 ft thick in test holes 1 and 2. It is mainly white- to light-gray anhydrite and dolomite, with a few thin beds of varicolored clay shale. The formation contains numerous gypsum-filled vugs and fractures throughout and, in the upper half, some open fractures. The Stone Corral is probably consistent in thickness and lithology beneath the Repository, although some changes occur in the formation throughout its extent in western Kansas. It is the uppermost formation of the Sumner Group of rocks in Kansas, which, like the Nippewalla Group mentioned above, consists mainly of red beds and evaporites. The Ninnescah shale and the Wellington Formation comprise the two remaining formations of the Sumner Group.

Red beds of the Ninnescah Formation unconformably underlie the Stone Corral Formation and conformably overlie the Wellington Salt Formation at the Repository site as well as throughout south central Kansas. As seen in Fig. 2.1, the formation is about 300 ft thick in test holes 1 and 2. The Ninnescah shale here is predominantly reddish silty shale that frequently shows red and green mottling. Fracture fillings of gypsum, as well as bands, partings, and thin beds of gypsum, anhydrite, and dolomite, are numerous throughout the formation. In some places the bedding is nondistinct and the shale is massive in appearance. Although all fractures appear to be filled or tightly sealed, slickenside surfaces are present in some parts of the formation.

The Wellington Formation is the lowermost member of the Sumner Group of rocks and consists, in general, of a gray and red shale sequence at the top with rock salt beds in the middle and anhydrite and shale at the base. These members are approximately 185, 260, and 170 ft thick, respectively, at the site as revealed by test holes 1 and 2 (Fig. 2.1). The upper member of the formation consists largely of silty gray shales at its top and base, separated by a rather prominent red shale zone. Thin beds and partings of anhydrite occur frequently in the lower shales but are less common in the upper gray shales, which also contain some blue clays, and in the red shales. Fractures in the upper gray shale and the red shale zone are usually filled with gypsum, while fracture fillings in the lower shale consist of anhydrite, except in the area near the contact with the underlying salt beds where salt-filled vugs and fractures exist.

Rock salt, interbedded with clay shale and anhydrite stringers, comprises the rock section from a depth of 755 to 1084 ft below the land surface in test hole 1 and for an approximately comparable depth in test hole 2. Owing to the complexities of the depositional environment of the rock salt deposit, both vertical and horizontal, persistence of the salt and its interbedded impurities is difficult to assess, even over the relatively small area of the Repository. However, from the available data, it appears that the section of salt being considered for burial of the wastes is perhaps the least variable within the entire column of salt. A comprehensive discussion of the salt rocks at the site is available below.

The predominantly anhydrite rocks that lie immediately below the rock salt comprise the basal member of the Wellington Formation. Test holes 1 and 2 have shown that, for the most part, the anhydrite is light to dark gray in color and contains numerous inclusions and partings and clay shale with some interbedded siltstone and dolomite members. The thickness of the member is about 170 ft in test holes 1 and 2 (Fig. 2.1) and is believed to be rather consistent in thickness beneath the entire site.

In contrast to the Sumner Group of evaporitic rocks described above, the underlying Chase Group consists of a sequence of alternating beds of carbonate rock and shale. Only the upper part of this group (the Nolans limestone and the Odell shale) was encountered in test holes 1 and 2 (Fig. 2.1). The Nolans was found to be about 35 ft thick and, for the most part, consists of interbedded dolomite and shale beds in the upper part with a dense, gray limestone bed at its base. Only about 10 ft of Odell shale was penetrated in test holes 1 and 2, and it was observed to consist of variegated, calcareous, hard, and massive shales.

2.1.2 Structure

The rocks beneath the proposed Repository site have been subjected to a long and complex history of deformation; the older formations show, as would be expected, a more complicated regime than successively younger beds. Local movements along the Central Kansas uplift have been instrumental in fabricating the existing structure, while the inclinations of the rocks at the site have also been affected by broad regional warping of the earth's crust. The Repository site lies on the western flank of the Geneseo uplift, which extends beneath a large part of the eastern half of Rice County and into the southern tip of Ellsworth County and the southwestern corner of McPherson County (Fig. 2.3). This egg-shaped structure is separated on the west from the genetically related, but semidetached, main lobe of the Central Kansas uplift by a rather sharp syncline, and on the east and northeast by another synclinal structure. As seen in Fig. 2.3, several north-south trending anticlinal structures, some of which have associated oil and gas fields, are superimposed on the uplift along its western edge. One of these, the Lyons Gas Field structure, is centered

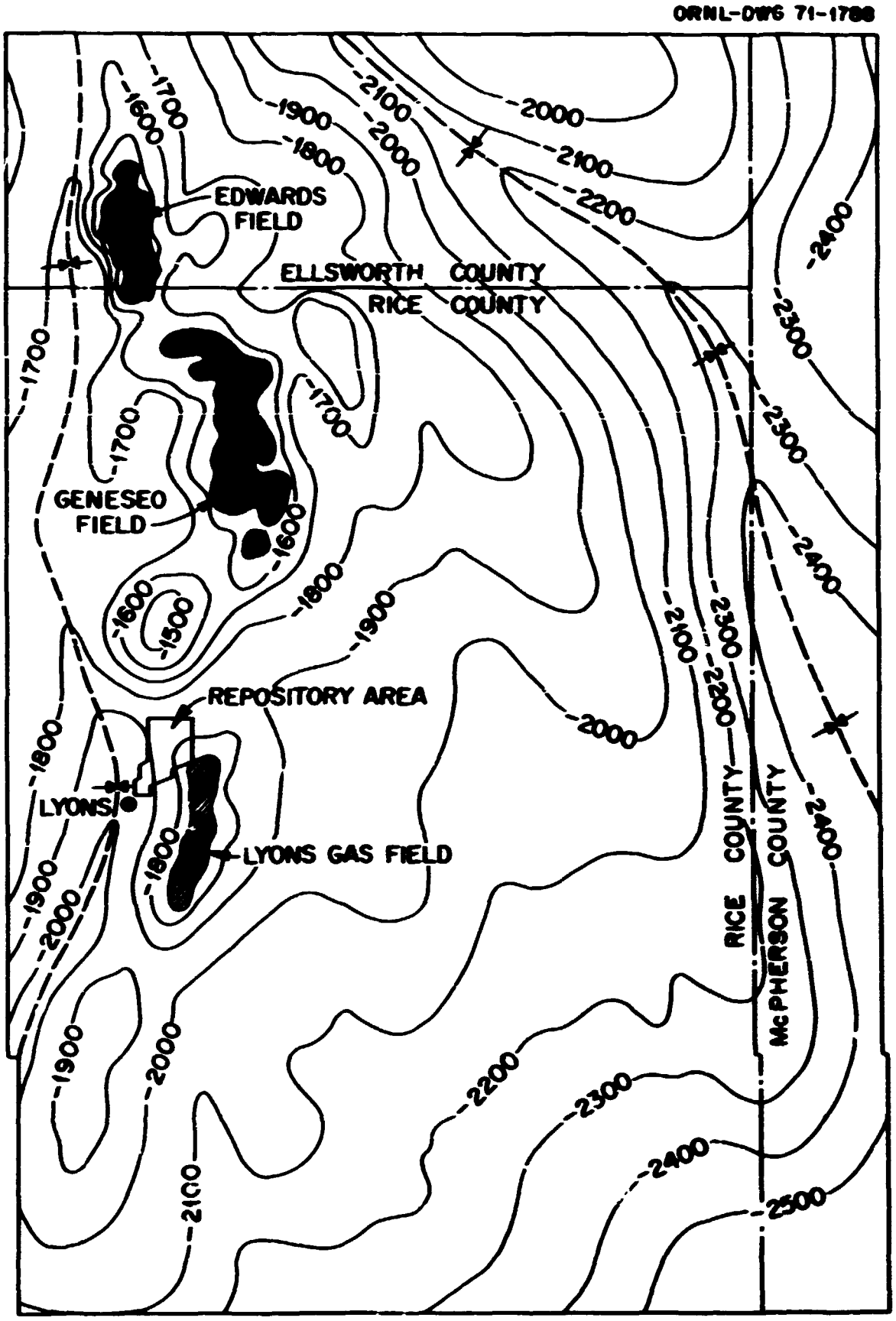

Fig. 2.3. Structural Contour Map of the Geneseo Uplift (After Stuart K. Clark et al., "Geneseo Uplift, Rice, Ellsworth, and McPherson Counties, Kansas," in Structure of Typical American Oil Fields, a Symposium, Volume III, edited by J. V. Howell, published by the AAPG, Tulsa, Oklahoma, 1948).

a short distance east of the Repository site and has been instrumental in establishing the present configuration of the rocks at the site. A generalized east-west cross section through the site and the adjoining Lyons Gas Field structure is shown in Fig. 2.4. From this section it appears that, during Arbuckle, Simpson, Viola, and Maquoketa times, the area was relatively stable. Some uplift of the Lyons Gas Field structure may have occurred after deposition of the Maquoketa section; however, the greatest deformation unquestionably occurred between Mississippian and Pennsylvanian deposition, as evidenced by the erosion of the entire Mississippian section along the crest of the anticline. This structural high remained topographically high during the deposition of succeeding beds, which, along with recurrent uplifts, account for the persistence of the structure upward through the geologic column. Structural contour maps of the Nolans limestone below the salt body and the Stone Corral above the salt at the Repository site reflect the underlying structure (Figs. 2.5 and 2.6). The regional dip of the pre-Pennsylvanian sediments within the area is southeast, while the Pennsylvanian and Permian beds are west and the Cretaceous rocks are northward. Regional tilting accounts for this discordance in the direction of dip of the various rocks within the area.

2.1.3 Rock Salt Deposits

The rock salt column beneath the site of the proposed Repository consists generally of a succession of layers of rock salt intercalated with shales and occasionally anhydritic beds. As seen in Fig. 2.7, the principal salt zones can be traced laterally from the northeast corner to the southwest corner of the site, although some irregularities in thickness and in lithology occur. In general, lateral consistency in the column is greatest in the lower to middle part of the columns and least at the extreme bottom and upper part of the formation. As seen in Fig. 2.8, the salt deposit at Lyons lies in a marginal portion of the Permian Basin. In addition, the site lies on the northwest flank of the Lyons Gas Field anticline (Fig. 2.3). With these conditions, some variations in the thickness and lithology of the entire salt sequence, as well as in individual beds over the site area, would be expected. In Fig. 2.9

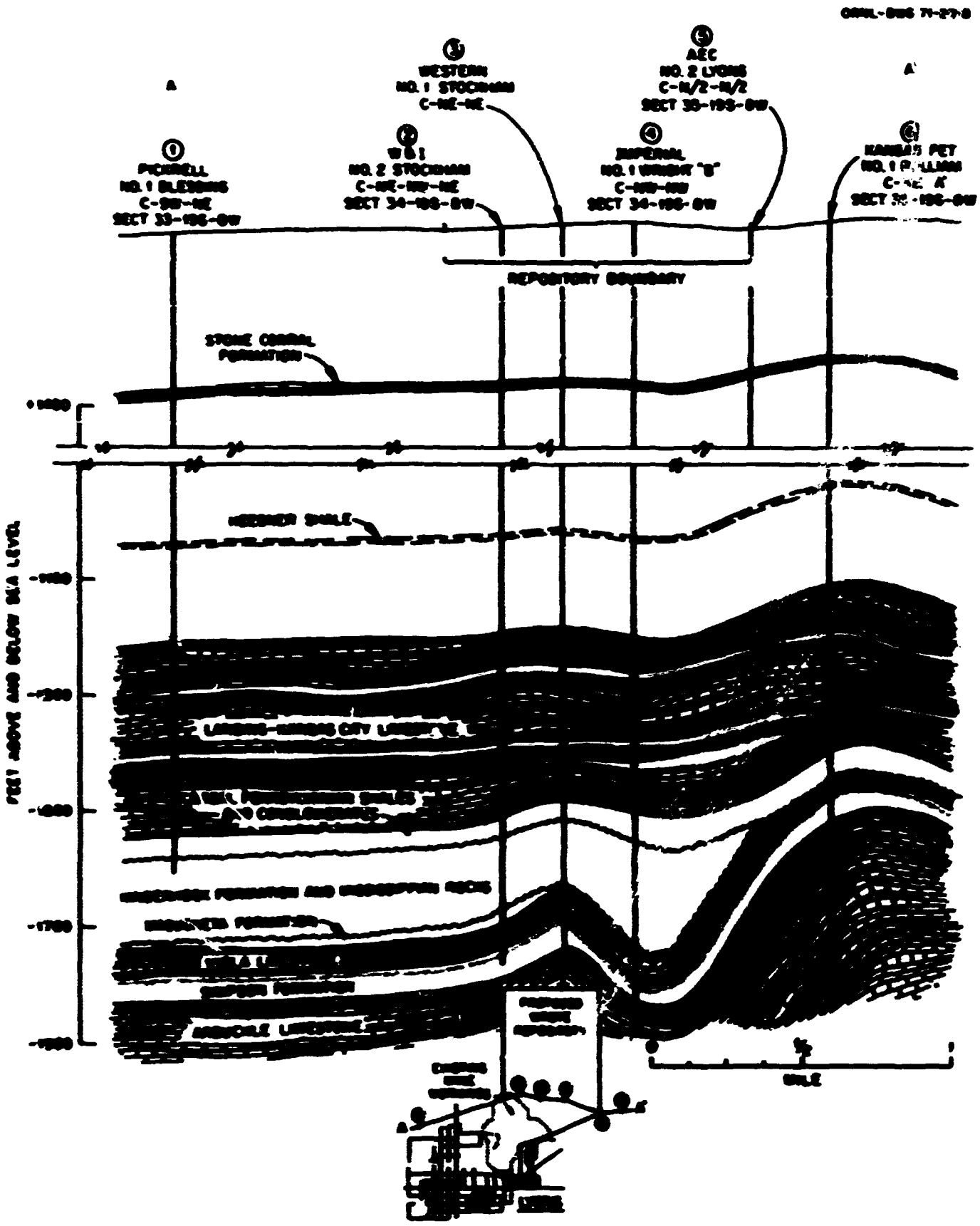

Fig. 2.4. Generalized Geologic Cross Section at the Proposed Repository Site.

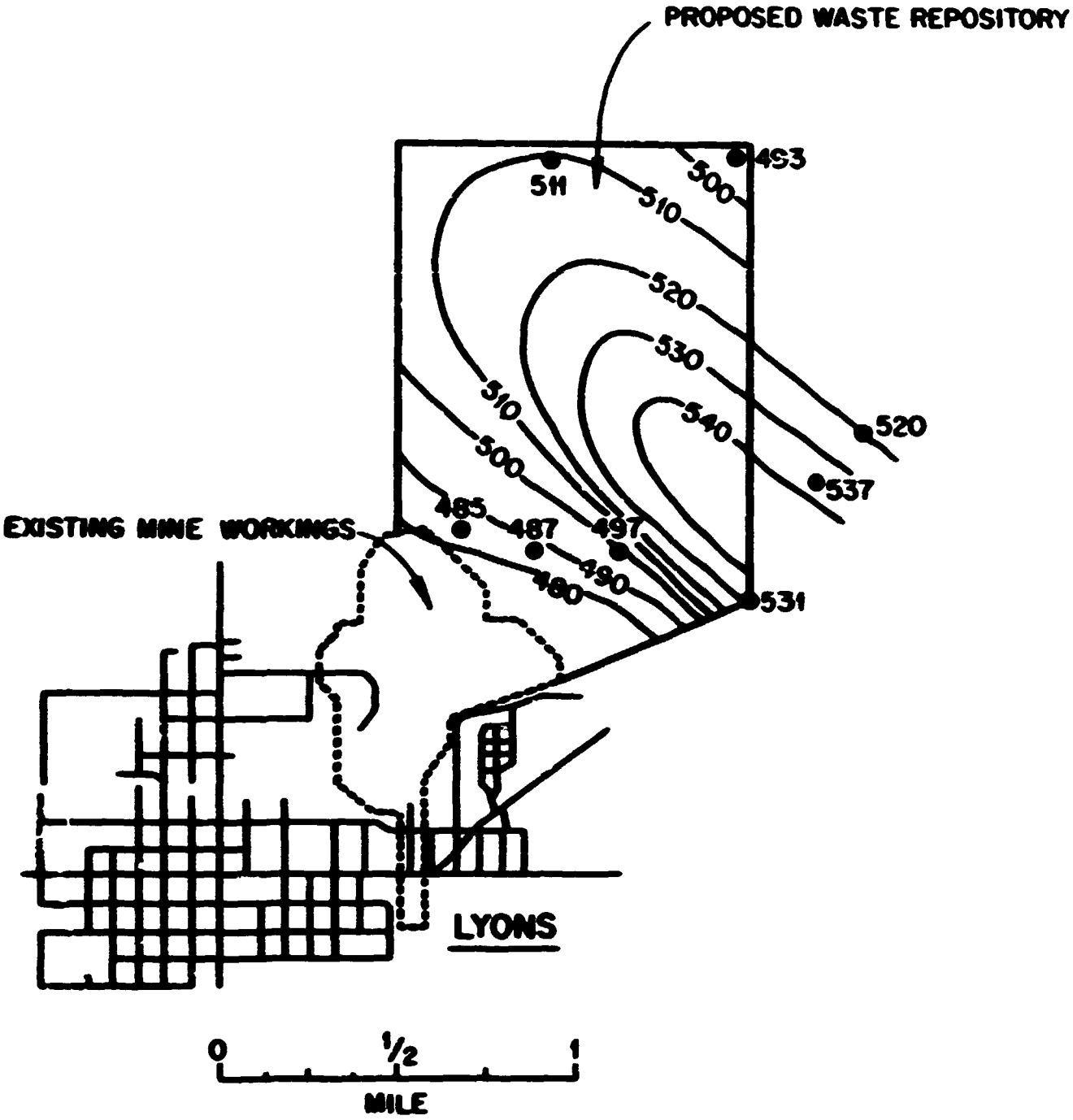

Fig. 2.5. Structural Contour Map of the Nolans Limestone.

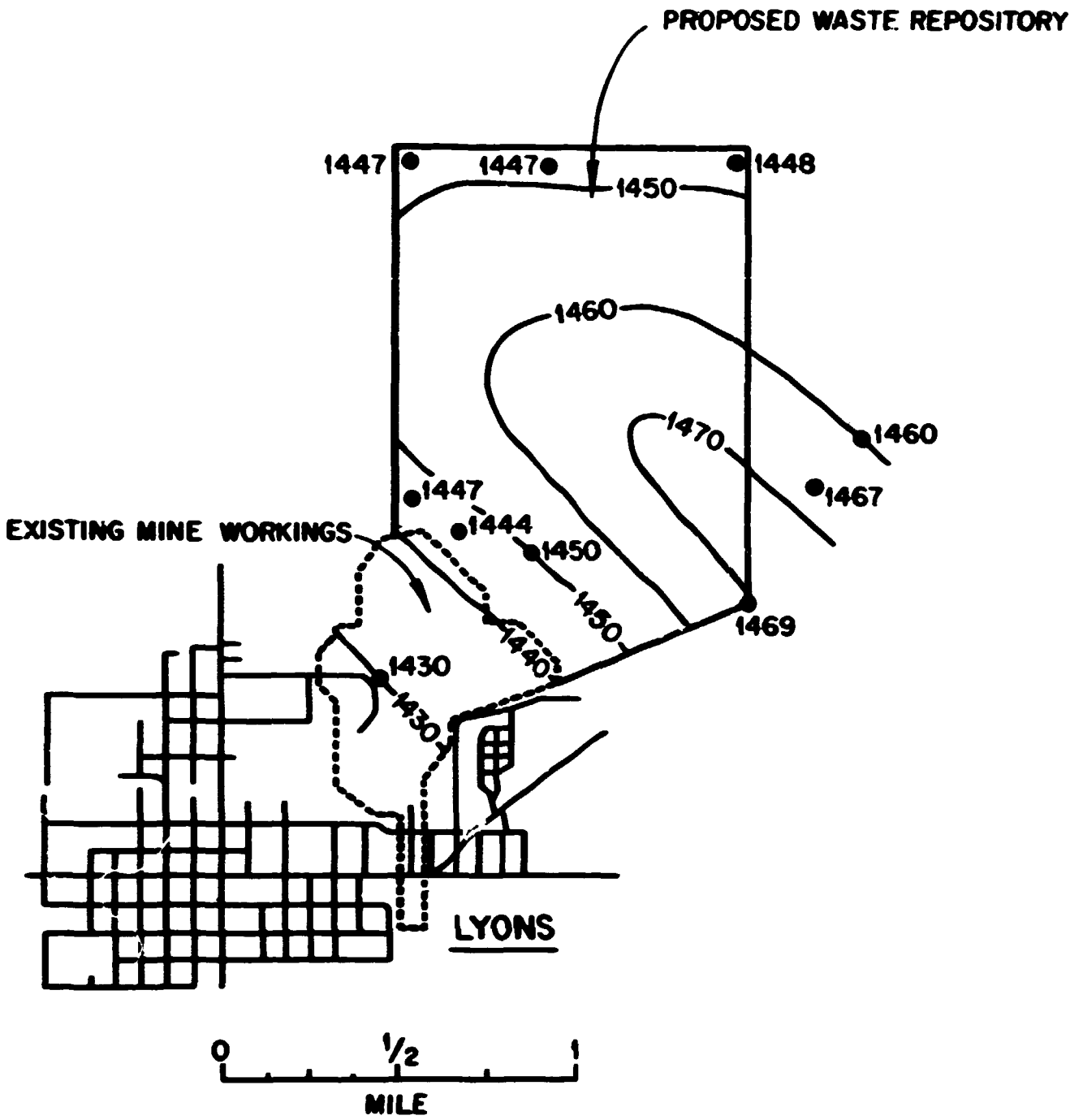

Fig. 2.6. Structural Contour Map of the Stone Corral Formation.

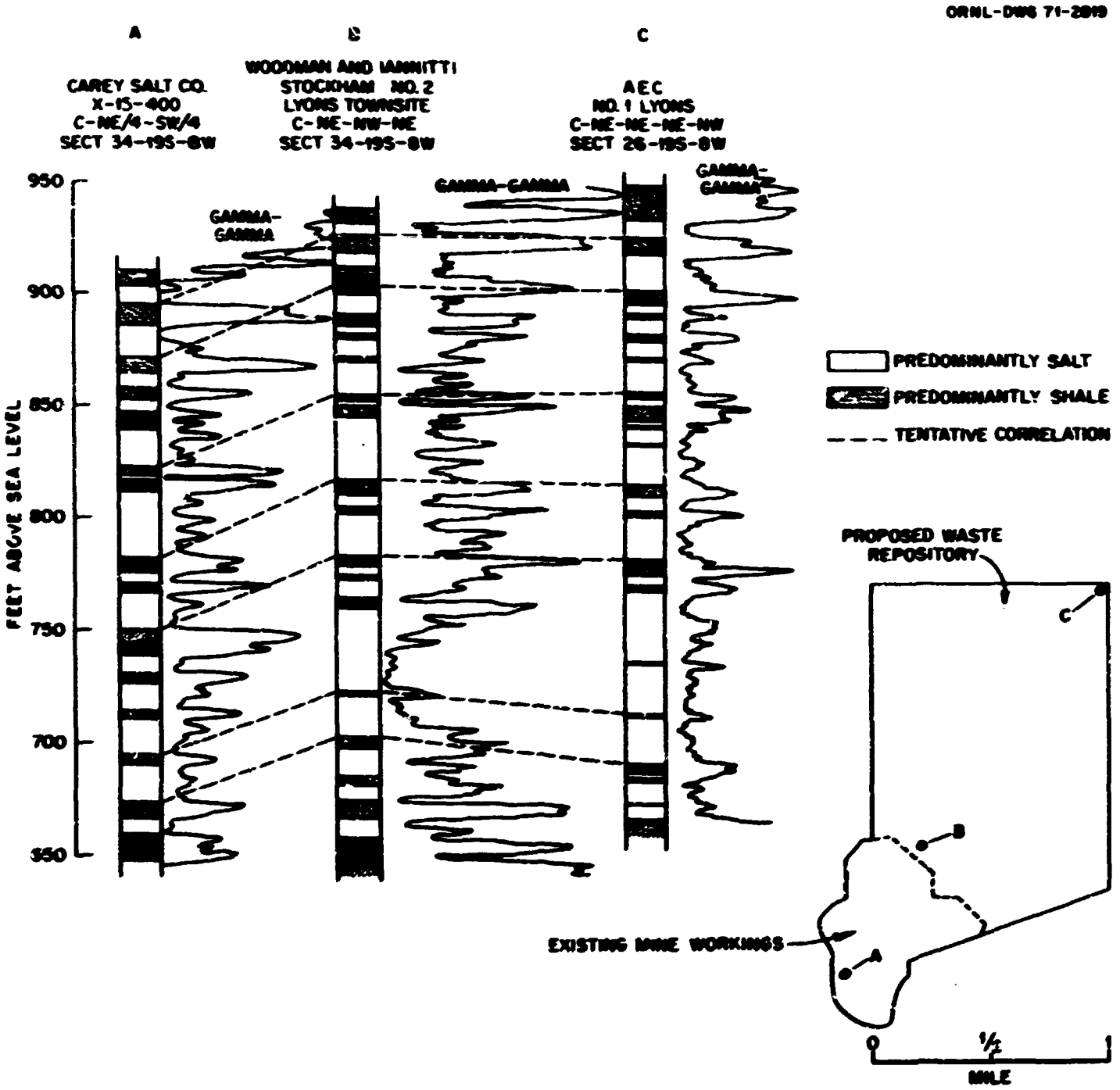

Fig. 2.7. Cross Section of the Salt Rocks at the Proposed Repository Site.

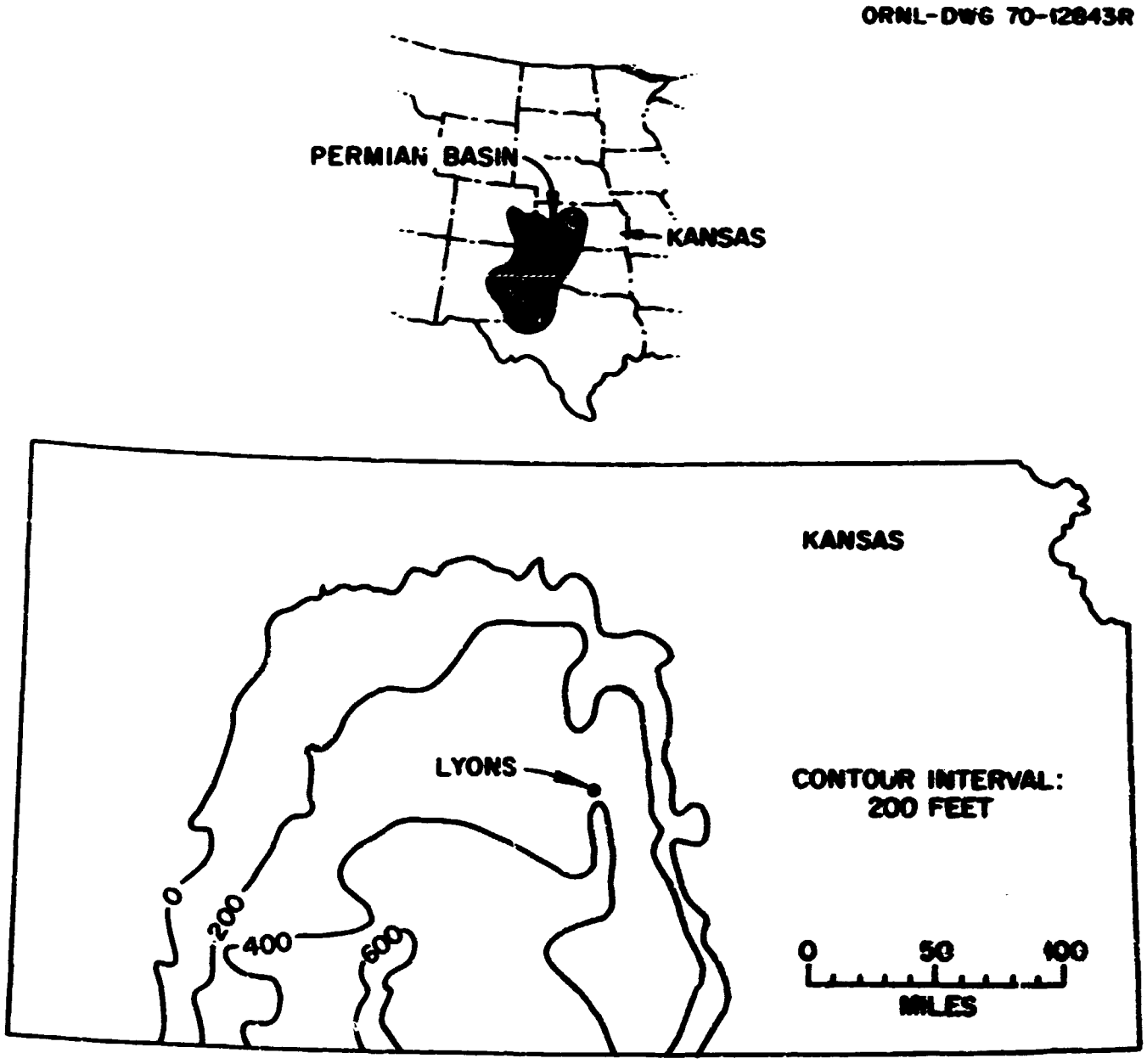

Fig. 2.8. Map of Kansas, Showing Area and Thickness of the Hutchinson Salt Member of the Wellington Formation.

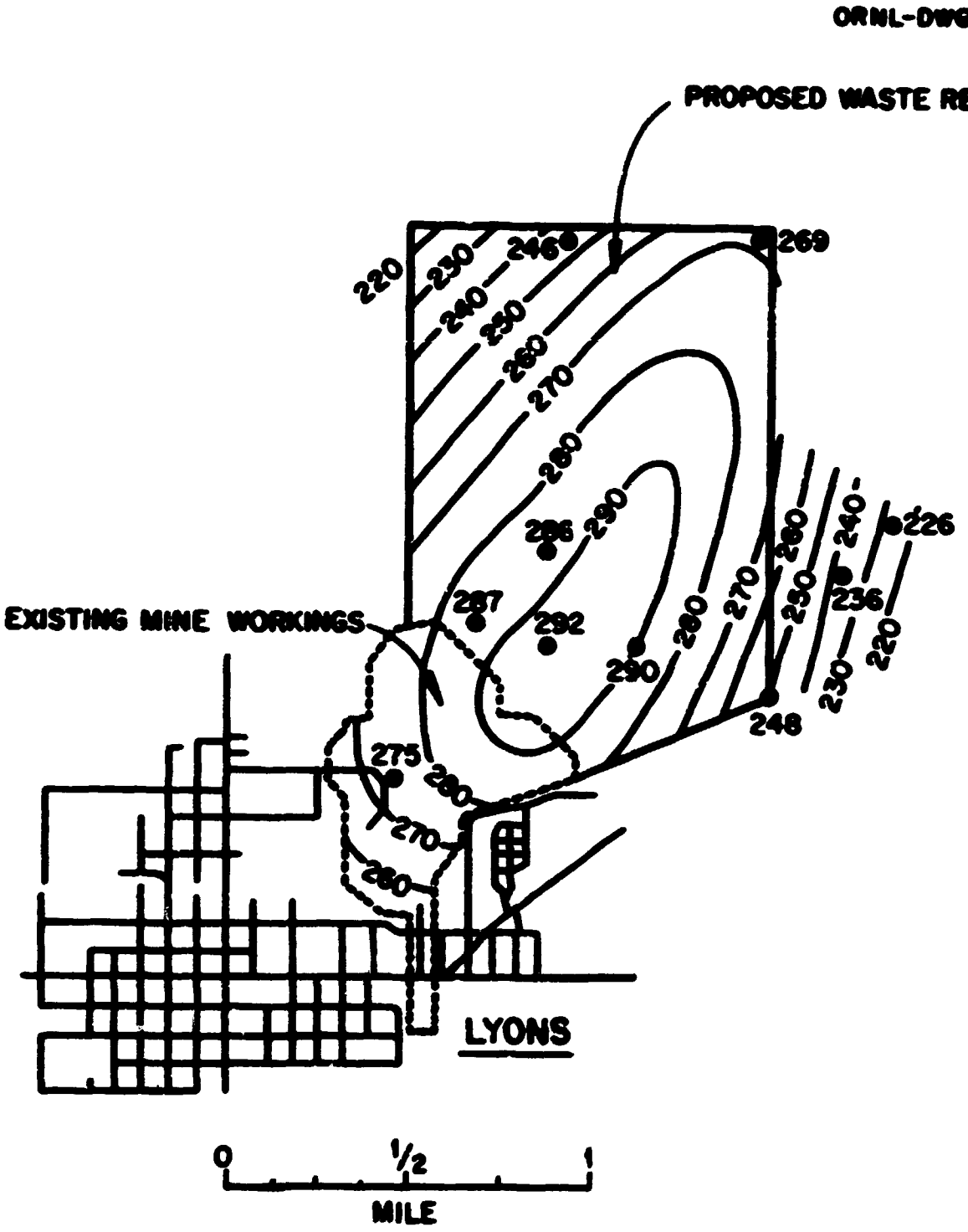

Fig. 2.9. Map Showing the Thickness of the Salt at the Proposed Repository Site.

it is seen that the salt is thickest in the south central part of the site. The principal uplift associated with the Lyons Gas Field anticline occurred in Late Mississippian to Early Pennsylvanian time or long before the deposition of salt in the Permian Age. Nevertheless, through recurrent uplift movements during the deposition of the evaporites or through the prevailing topographic relief at the anticlinal structure during Pennsylvanian and Permian times, some local thickening and thinning of the salt rocks occurred. This explanation as the cause for the measured thinning of the salt is strengthened further by the absence of any observed solutioning and collapse of the overlying shale in the top parts of the salt sections in cores from test holes 1 and 2, which, if present, could account for gross thinning of the salt column.

In the marginal areas of the evaporitic Permian Basin, such as at Lyons, it is apparent that the precipitation and deposition of salt was periodically interrupted by the influx of clay-bearing waters from nearby land masses. These local intrusions not only created irregularities in the thickness and the composition of the sediments but may also have created solution channels and slump features at various stratigraphic levels in the previously deposited salt section. It is likely that the discontinuous zones of brecciated salt observed in test holes 1 and 2 were formed in this manner. Irregularities in the salt section may also be due, in part, to periodic subaerial exposure of some areas of the salt resulting from a fluctuating water level within the basin.

The thickest and most persistent salt zone is seen in Fig. 2.7 to occur in the bottom half of the column at a distance of between 673 and 710 ft above sea level in the Project Salt Vault $(PSV)^2$ charging shaft. A 9-ft-thick bed in the lower part of the zone comprises the mined unit at The Carey Salt Company's workings at the Repository site and also at the American Salt Corporation's mine a short distance south of the site. This bed of salt is unquestionably the most uniform and the highest quality of the entire sequence; therefore, it is the desired location for burial of the wastes.

Within the mined unit at the Carey mine, 1- to 6-in. layers of relatively pure sodium chloride are separated by clay and shale laminae that

are usually less than 1 mm in thickness. These laminae constitute the major impurity in the salt and are characteristic of most bedded salt deposits. Shale beds, several inches in thickness and separated by about 15 to 18 ft of salt, lie above and below the mined unit and thus limit the vertical extent of mining. The mine floor was usually cut within a few inches of the underlying shale bed, while the roof is normally several feet below the overlying shale bed. The least contaminated salt, and thus the source of most of the former production in the mine, lies in a 9-ft-thick section that extends from the top of the shale below the floor upward to a thin (~1/16 in. thick) shale parting. Another prominent shale parting lies about 3-1/2 ft above the 9-ft roof. In some parts of the mine, this section was also mined. However, the additional excavation has resulted in a weak roof that buckles and fractures and frequently allows a 3-ft section of overlying impure salt to fall.

Two 2-in.-diam, 30-ft-deep core holes were drilled in the floor of the mine in entry 9 (Fig. 2.10), while two cores, approximately 20 ft long, were obtained from the roof of the mine at the same locations. These cores, along with the log of a third hole drilled previously in entry 7,[3] were used to construct a geologic cross section of a portion of the salt section from the northwest end of entry 7 to the southwest end of entry 9 (Fig. 2.11).

Considerable quantities of shale and some anhydrite are included in the salt section from the floor down to a depth of about 115 in. in entry 9 and to a depth of approximately 135 in. in entry 7 of the mine. The shale, which is noncalcareous and greenish gray to black in color, commonly occurs in beds that are 1 in. to as much as 15 in. thick and usually contain a few crystals of clear-to-orange halite and some stringers of fine-grained anhydrite. As seen in Fig. 2.11, these beds thicken and thin considerably over relatively short distances. Frequently, the beds grade, both laterally and vertically, into salt that contains many pods and irregularly shaped lenses of shale. This unit of the section is underlain by about 80 to 125 in. of relatively pure salt. The salt consists essentially of medium to coarsely crystalline, clear-to-brownish halite, that contains disseminated blebs and inclusions of dark-colored clay, which, in places, give the salt a dark, smoky appearance.

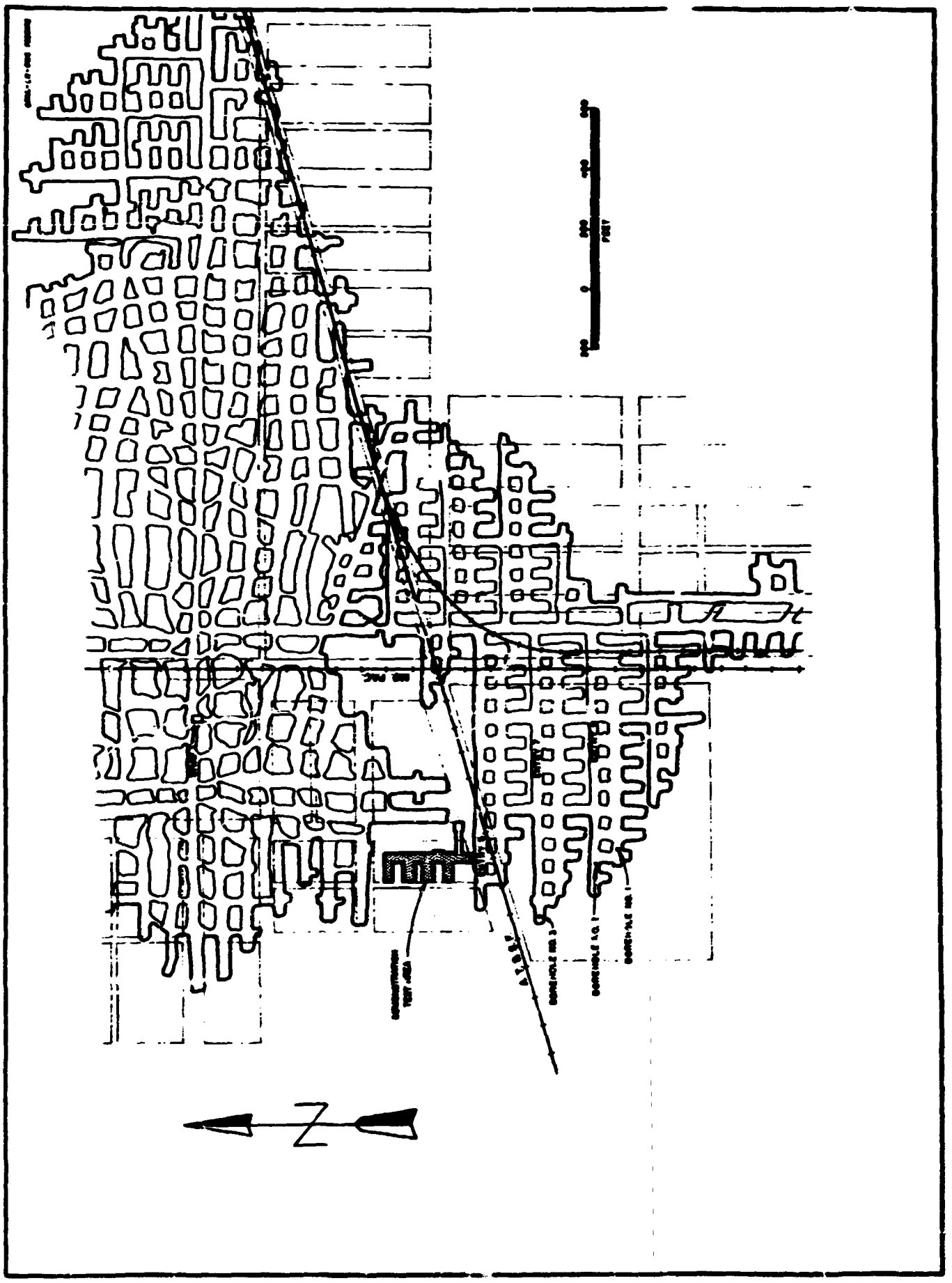

Fig. 2.10. Map of a Part of the Mine of The Carey Salt Company, Lyons, Kansas, Showing Location of Boreholes and FSV Demonstration Test Area.

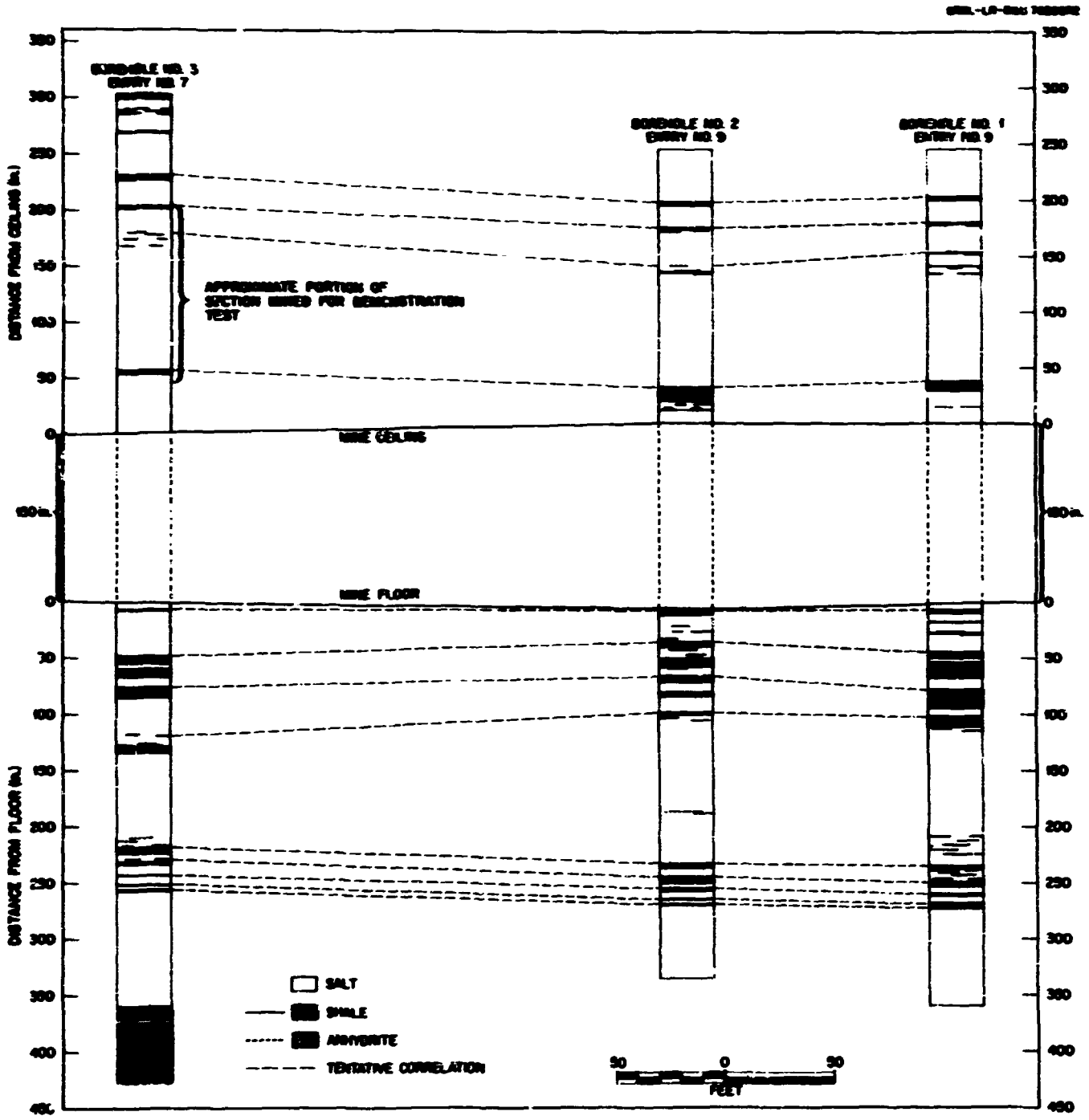

Fig. 2.11. Generalized Geologic Cross Section of a Portion of the Hutchinson Salt Member of the Wellington Formation in the Mine of The Carey Salt Company, Lyons, Kansas.

A second zone of interbedded salt, shale, and anhydrite, about 40 to 50 in. thick, lies beneath the relatively pure salt sequence. The shale and anhydrite are similar to that described higher in the section, but the shale beds are thinner, and a larger amount of anhydrite in the form of layers and lenses is present. For the remaining part of the section in entry 9, which was cored to a depth of about 360 in. below the mine floor, the cores show a relatively pure salt sequence like that described above. In entry 7, the same salt is interbedded with thick shale and anhydrite beds at a depth of about 360 in. It is likely that the same thick shale and anhydrite unit would have been intercepted in entry 9 if the drilling had proceeded a few feet deeper.

The sediments above the ceiling of the mine, up to about 250 in., consist of a relatively pure salt sequence that is interbedded with four separate shale zones. These shales, like those below the mine floor, are greenish gray to black in color and frequently contain lenses and crystals of clear-to-orange halite and stringers and lenses of anhydrite. The thickest of the shale beds lies at a minimum distance of about 20 in. above the present roof of the mine. (In the PSV demonstration test excavation, this shale bed lies about 2-1/2 ft above the mine floor.) The bed was approximately 12 in. thick in borehole 2, entry 9, but it had thinned to about 3 in. in the core from entry 7 of the mine. The other shale zones, as shown in Fig. 2.11, lie between about 130 and 230 in. above the roof. (The shale bed at about 180 to 200 in. comprised the ceiling in the demonstration test area.) The salt from the ceiling cores is composed mainly of medium-to-coarse grained, clear-to-brownish halite crystals, which contain, in places, many blebs and irregularly shaped masses of clay that give the material a smoky appearance. In addition, from about 70 in. above the mine roof to the end of the cored section, the salt contains many scattered blebs of an orange-to-red-colored microcrystalline mineral that has been identified as polyhalite.

In summary, the salt unit that has been mined in the Lyons Mine consists of relatively pure salt containing minor inclusions of clay and shale. The first 115 to 135 in. of the section below the floor in the westernmost portion of entries 7 and 9 contains between 20 and 40% shale.

The shale is present in beds that vary greatly in thickness over relatively short distances and may grade vertically and laterally into zones of salt that contain many pods and irregularly shaped lenses of shale and anhydrite. A second shale zone, approximately 40 to 50 in. thick, is present, generally from about 220 to 235 in. below the floor. Four separate shale zones occur in the first 250 in. of section above the mine roof. The thickest shale bed lies at a minimum distance of about 20 in. above the ceiling of the mine, while the other less prominent zones of shale lie between about 130 and 230 in. above the roof. These zones are usually only a few inches thick and contain, in addition to shale, lenses and stringers of anhydrite and salt.

The proposed area to be mined will lie at a level of about 20 ft above the preexisting mine floor and extend upward a distance of about 15 ft (see Fig. 2.11). The floor of the newly mined area will be rock salt, while a thin shale parting will mark the roof. A prominent shale bed that varies from a few inches to more than 1 ft in thickness will lie approximately 2-1/2 ft below the floor. Several easily distinguishable shale beds that are about 1/2 in. to 1/4 in. in thickness will probably persist in the walls of the mined area at distances of about 6-1/2, 7, 10, and 12 ft above the floor. The salt in the proposed excavation area contains numerous blebs of polyhalite that are commonly concentrated along bedding, giving the salt a banded appearance.

Because of the structural attitude of the rocks at the proposed site, some variation in the levels of individual salt and shale beds is apparent. A measure of this level change is seen in Fig. 2.12, which is a structural contour map of the prominent shale bed that exists as the "high top" or "17-ft" shale in the Carey mine workings and which will lie a few feet below the floor of the proposed working area. This shale bed, which is easily identifiable in cores as well as recognizable in the geophysical logs from the noncored borings, is observed in Fig. 2.12 to be about 10 ft higher in test hole 1, and 40 ft higher in elevation in test hole 2, than in the vicinity of the PSV charging shaft. Thus, a constant rise in the mining level will be experienced from the southwest corner of the site to the southeast corner, while there will be essentially no change in the

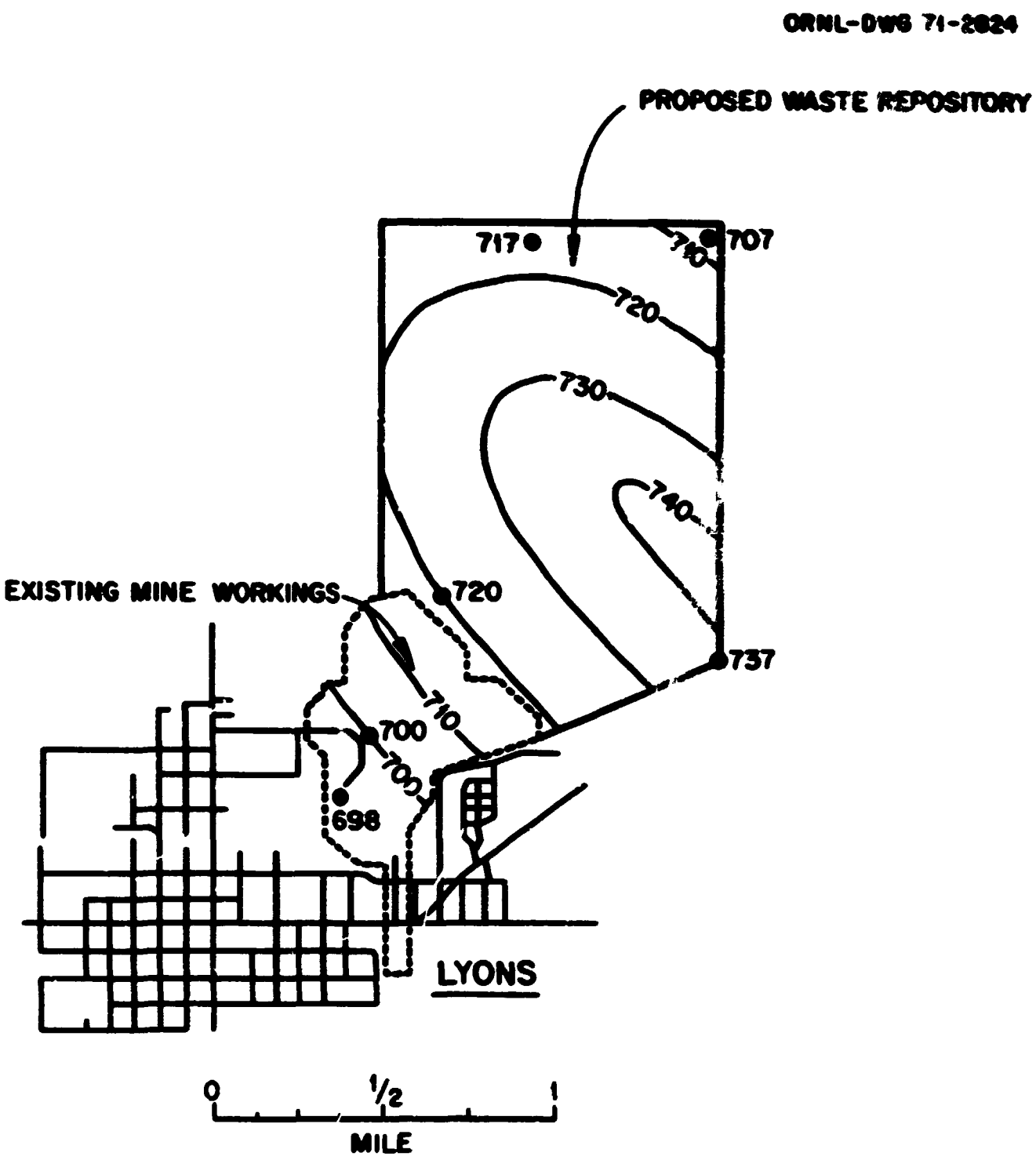

Fig. 2.12. Structural Contour Map of the "17-ft Shale Parting" in the Salt Column.

mining level along the western boundary of the site. From the southwest corner to the northeast, the mining level will rise constantly to the apex of the fold and then show a gradual decrease.

2.1.4 Surface Water

As seen in Fig. 2.13, the proposed Repository site is drained by Owl Creek and an unnamed tributary of Cow Creek. These intermittently flowing streams originate a few miles to the north of the site and flow southwestwardly through it before joining Cow Creek a few miles to the south. These streams would be expected to flow and thus carry runoff from the site only during periods of heavy rainfall, which occur most frequently during late spring and early summer. Flow measurements of Cow Creek at Lyons, as recorded over a period of 18 years, show an average flow rate of 68 cfs, with a maximum flow of 12,000 cfs and extended periods of no flow in 1938 and 1946.[4] Downstream, Cow Creek flows generally parallel to the Arkansas River before joining that stream about 50 miles southeast of the site. Flow measurement records of the Arkansas River compiled at Hutchinson for 6 years and at Wichita for 31 years show an average discharge for the stream of 652 cfs and 1074 cfs.[4] The Arkansas River has its source near the summit of the Rockies in central Colorado and flows eastward into Kansas along its westward border. The volume of the river increases toward the east throughout its mountainous area; however, as the stream emerges onto the Great Plains, its flow gradually diminishes and often ceases altogether in western Kansas during the summer months. In Kansas the stream maintains its eastward course for a distance of about 150 miles before establishing a northeastward course that diverts the stream as far north as southern Barton County and southwestern Rice County. The stream then maintains a southeastern course, flowing past Hutchinson and Wichita before leaving the state along its southern border.

2.1.5 Groundwater

Figure 2.14 is a map of Kansas showing the general availability of groundwater in the various regions of that state. The greatest quantities of water are found in the gravel- and sand-filled valleys of the larger streams. Less productive areas include the valleys of the smaller streams

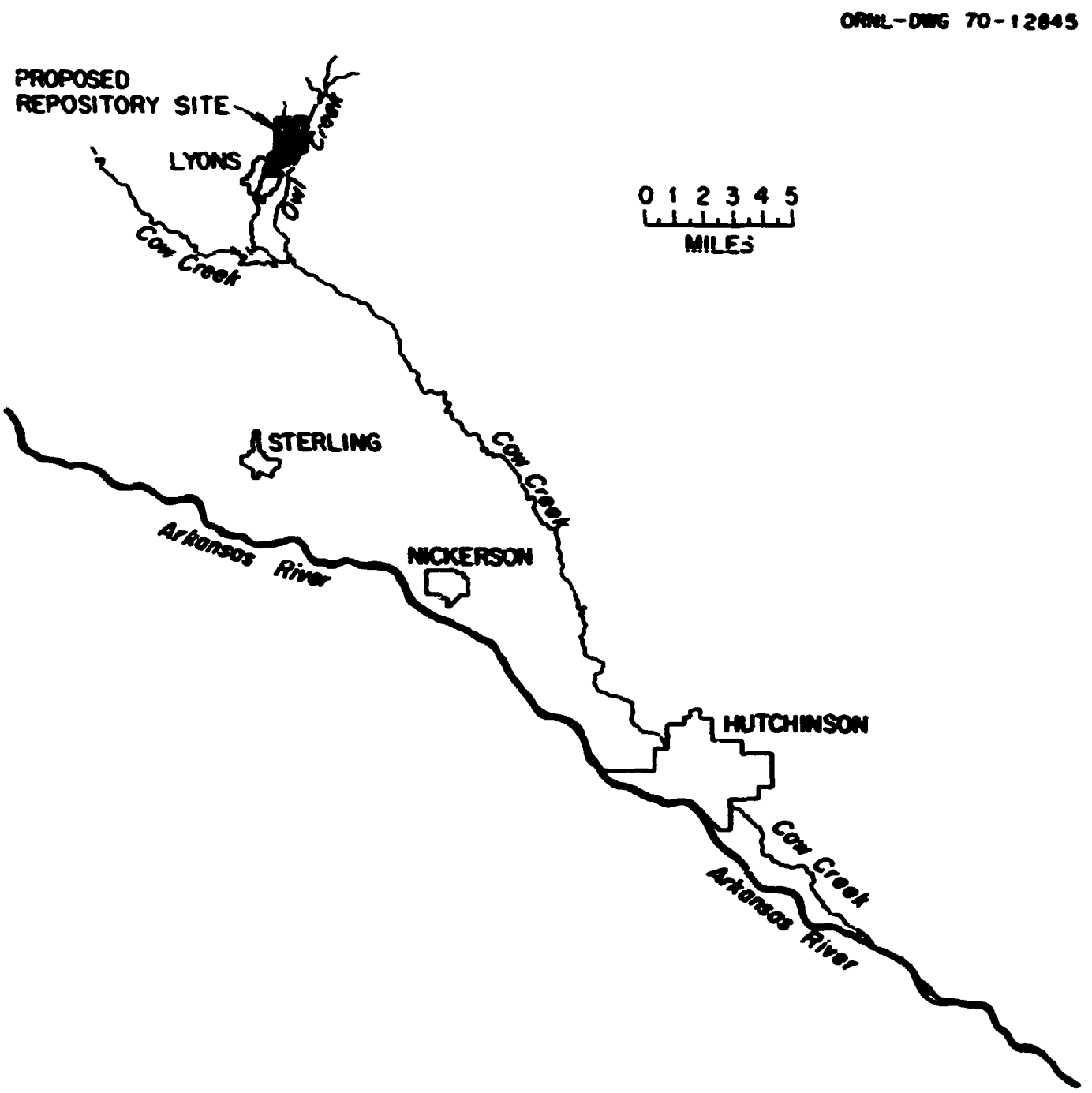

Fig. 2.13. Surface Drainage at the Proposed Repository Site.

ORNL DWG 70-11042

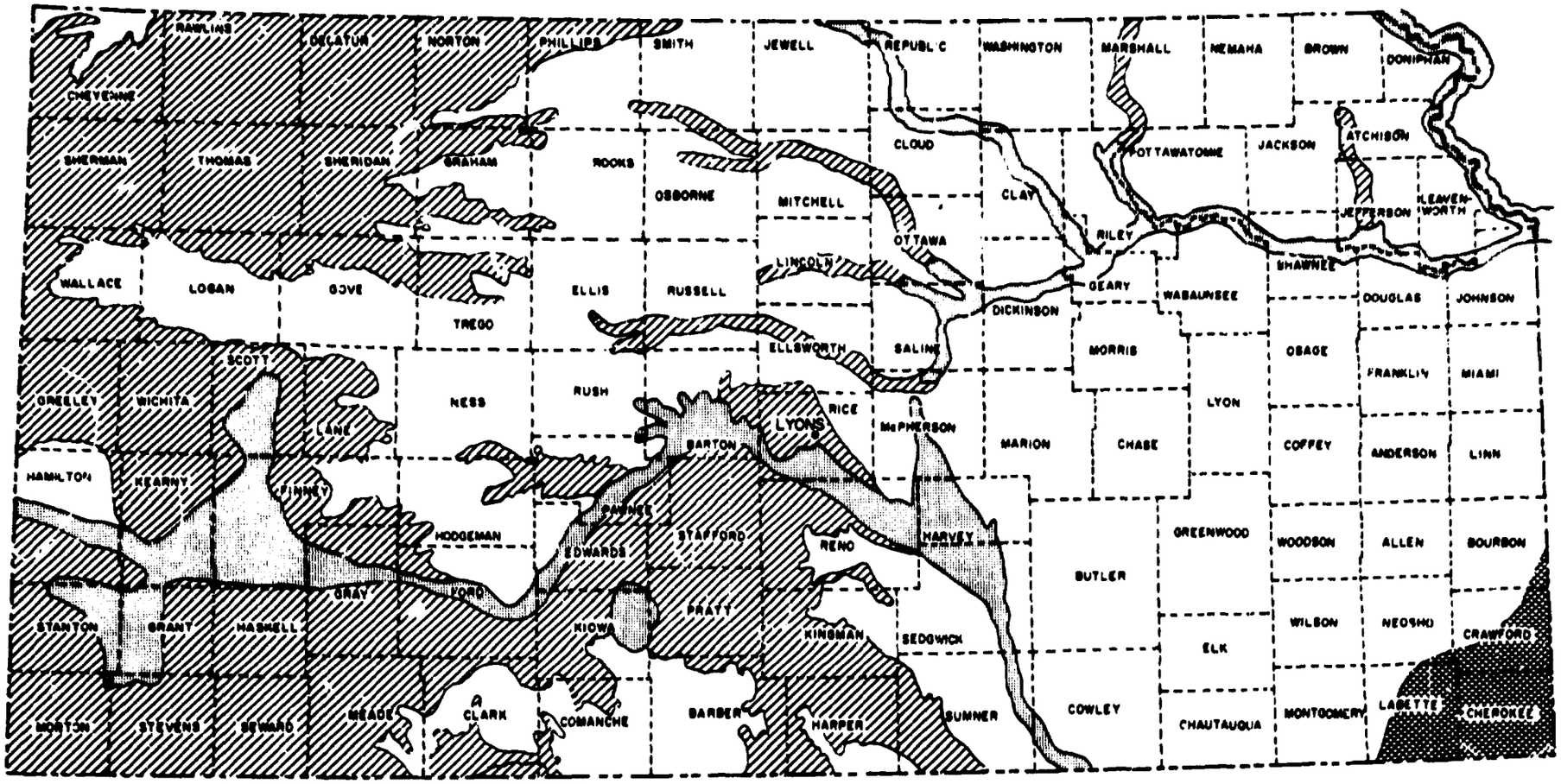

Fig. 2.14. Map of Kansas Showing General Availability of Groundwater (After S. W. Lohman et al., in Ground-Water Supplies in Kansas and Available for National Defense Industries, University of Kansas Publications, State Geological Survey of Kansas, Bulletin 41, Lawrence, Kansas, April 1942).

and areas underlain by thick deposits of Tertiary and Quaternary deposits. Moderate supplies of groundwater may also be obtained from deep water-bearing rocks in the extreme southeastern corner of the state. Generally, small supplies of groundwater are available in those areas of the state where Pennsylvanian-, Permian-, or Cretaceous-age bedrocks exist at or near to the surface.

In the general region of the Repository site, the thick deposits of gravel and coarse sand that fill the large stream valleys are the source beds for the principal supplies of groundwater (Fig. 2.14). Perhaps the most important source bed is found in the Great Bend region of the Arkansas River Valley, which lies a few miles to the south of the site. This region is underlain mostly by sand and gravel deposits of Tertiary and Quaternary age. These deposits may be as much as 300 ft thick. Overlying sand dunes provide an excellent surface for recharge. Depth to groundwater within the area is generally less than 100 ft. Supplies in excess of 1 million gallons per day from these deposits are commonly developed.

The city of Lyons obtains its water supply from several wells in alluvial deposits located about 2-1/2 miles south of the proposed site. The towns of Sterling (about 10 miles south of the site) and Chase (about 10 miles west of the site) also obtain public water supplies from alluvial deposits in the Arkansas River Valley.

Within the immediate vicinity of the site there are several wells extending to the Cretaceous-age sandstones from which water is drawn for domestic or stock uses. The yields from these wells or from deeper wells would be insufficient for industrial, irrigation, or public water supplies.

In general, the rocks below the salt bed contain numerous porous beds that contain salt water and perhaps some oil and/or gas. Fresh water is confined essentially to the uppermost 300 ft of the rock column. The Stone Corral, which lies between about 270 and 285 ft, is the deepest known freshwater aquifer at the site. It may yield water at the rate of about 1 to 3 gal per min. The Cretaceous-age sandstones (45 to 120 ft below the surface) are capable of yielding water at the rate of about 20 gal per min, while the overlying unconsolidated silts (0 to 45 ft below

the surface) may yield water at the rate of about 5 gpm. The average depth to groundwater at the site is about 25 ft.

2.1.6 Hydrological Characteristics of the Rocks in the Vicinity of the Site

Except in the incised valleys of Cow and Little Cow Creeks (which are located south and west of the Repository site, respectively), where thick deposits of water-bearing gravels, sands, and silts have accumulated, the Pleistocene surface sediments in the immediate vicinity of the site consist mostly of a thin blanket of eolian silts that have a low permeability and may yield little or no water to wells. According to Angino,[1] the loess deposits probably would not yield more than 10 gpm to wells anywhere within the area, while the fluvial deposits in the stream valleys will yield quantities of water to wells in excess of 1000 gpm. Consequently, there are no known usable wells that penetrate only the loess deposits in the area; however, there are several domestic, stock, and even municipal and irrigation wells in the thick valley fill deposits. In general, the depth to groundwater at the site is about 25 ft, rising somewhat in the wet winter months and falling slightly in the dry summer months. The direction of groundwater movement is from northeast to southwest across the site toward the buried valley of Cow Creek and then generally southeastward (Fig. 2.2). Indeed, the depth to groundwater and the direction of movement as determined recently by Angino[1] is similar to that as determined by Fent[5] approximately 20 years earlier in a more general study of the geology and groundwater of Rice County.

Cretaceous rocks in the vicinity of the site include the Cheyenne sandstone, the Kiowa shale, and the Dakota formation. However, only the Kiowa shale is present directly beneath the site; the other two pinch out a few miles to the north. In general, the Cheyenne consists mostly of low-permeability siltstone that yields no water to wells. In contrast, the Dakota formation, which consists of clay, shale, siltstone, and highly permeable channel sandstones that yield water at the rate of 30 to 70 gpm to several industrial wells in the southwestern part of the county, is a prolific water bearer.[5] Except for a thin rubble zone at its top, which may yield, locally, moderate amounts of water, the only water-bearing

zones in the Kiowa are the sandstone members. At the site the sandy beds, which may occur at several stratigraphic horizons, vary in thickness from 30 to 50 ft in the southeastern portion of the area to thin beds of alternating sandstone and shale in its western part.[1] Yields to wells in these areas are reported to be 50 to 100 gpm and 10 to 20 gpm, respectively.[1]

The Harper sandstone at the site of the Repository consists mostly of silty shale and siltstones that are apparently non-water-bearing. Only very small quantities of water have been found in the uppermost weathered zone, which is probably the most active water-bearing part of the formation. Some potential for storing and transmitting water through the formation may exist in the unsealed fractures observed in the core of the Harper from test hole 1. Additional studies have been initiated to define further the nature and extent of the fracturing and to determine the significance of it with regard to the hydrologic regions of the area.

The deepest freshwater-bearing rocks encountered in borings at the site are those of the Stone Corral formation. This thin sequence of anhydritic, dolomitic, and shaly beds contrasts sharply with the overlying silty beds of the overlying clay shale of the Ninnescah Shale formation and is consequently easily identifiable in subsurface borings at the site as well as in surface exposures to the east. The dolomitic and anhydritic beds in the upper half of the formation are vuggy and often fractured, and thus provide the principal paths of water movement through it. The aquifer is probably capable of yielding water only at the rate of a few gallons per minute and hence is not known to supply water to any wells within Rice County.

The Ninnescah shale, the Wellington formation (which includes the Hutchinson salt member), the Nolans limestone, and the Odell shale lie successively below the Stone Corral at the site and apparently are all non-water-bearing rock formations. It is especially significant that no voids, open fractures, permeable zones, or measurable quantities of water were found through observations of the core in test holes 1 and 2 in the salt column and at the interface or contact between the salt and the overlying and underlying rocks.

Hydraulic tests have been conducted in test holes 1 and 2 by the U.S. Geological Survey and in four shallower borings at the four corners of the site by the U.S. Geological Survey and the State Geological Survey of Kansas. Preliminary data from these tests indicate that the sandstone members of the Kiowa shale are the principal freshwater-bearing aquifers above the salt and that the Stone Corral formation contains and transmits only limited quantities of water. Also, it was concluded that neither the rocks above the salt and below the Stone Corral nor the rocks below the salt (to the extent of the penetration of the borings into the Odell shale) contain significant quantities of water. Furthermore, it was concluded that the waters in the Kiowa and the Stone Corral exist under some artesian pressure, which causes their levels to extend somewhat above their stratigraphic positions but still maintain decreasing potentials with depth. This means that the unrestrained water level or piezometric surface in the Kiowa shale will rise into the lower part of the overlying alluvium but not up to the elevation of the water level of that aquifer. Similarly, the unrestrained water level in the Stone Corral will extend upward into the Harper sandstone but not up to the hydrostatic level of the Kiowa aquifer.

The direction of flow of water in the Kiowa is from northeast to southwest across the site, or in the same general direction as that in the overlying loess deposits.[1]

Chemical and radiochemical analyses of water samples from many of the borings and wells on and near the site are being performed by the State Geological Survey of Kansas and the State Department of Health. To date, the results indicate that the groundwaters in the unconsolidated sediments and the Kiowa formation are hard and high in calcium and bicarbonate.[1] Dissolved solids range generally from 250 to 750 ppm; however, a few samples taken near salt mines and oil wells, where salt brines have been discharged into the soil, show considerably higher concentrations. Trace-element analyses of samples indicate that, with one exception, these elements are found in concentrations which are within the limits established for potable water in the United States.[1]

Preliminary results of the hydraulic tests conducted in test holes 1 and 2 by the U.S. Geological Survey indicate that the rock column in the interval below the Stone Corral formation has low permeability.[6,7] In test hole 1, an inflatable packer was set against the side walls of the hole just below the top of the salt at a depth of 802 ft. The isolated interval (802 to 1300 ft) was then charged instantaneously with a quantity of fluid, and measurements were made of the reaction of the water level to this stress. From these measurements the transmissivity of the isolated interval was estimated to be 1×10^{-4} m^3 day^{-1} m^{-1}. By assuming that the contributing interval was that of the 38-ft-thick Herington limestone (1252 to 1290 ft below the land surface), the hydraulic conductivity was estimated to be 2×10^{-5} m^3 day^{-1} m^{-2}.[6] The relative specific capacity of the interval was estimated to be about 1.8×10^{-3} m^3 per day per meter of drawdown, and the static water level in the hole was estimated to be about 330 ft below land surface.[6] In test hole 2, the packer was set at a depth of 296 ft or just below the Stone Corral, and the remaining portion of the hole (to a depth of 1216 ft) was tested as a single hydrologic unit. From the injection test conducted in the isolated interval (296 to 1216 ft), the transmissibility was estimated to be 1.8×10^{-4} m^3 day^{-1} m^{-1}, and the hydraulic conductivity was estimated to be 6.4×10^{-7} m^3 day^{-1} m^{-2} (assuming that the thickness of the producing interval is the entire isolated interval). The hydraulic potential for the tested interval was estimated to be 315 ft, and the relative specific capacity estimated to be 2.5×10^{-4} m^3 per day per meter of drawdown.

2.2 Natural Containment of the Wastes

The geohydrological characteristics of the site have a direct bearing on the natural containment of the salt formation, and investigations have been undertaken of the natural processes which could lead, in the future, to a gross disturbance of the salt by dissolution or by any other mechanism. A number of such processes have been identified, as follows.

1. The salt formation at the site, as well as throughout Kansas, is protected from dissolution by the overlying impermeable zones. These rocks are subject to normal erosional processes. An estimate of the maximum future erosion rates has been made by compiling data on the rates of erosion in regions which are similar in climate to that which has existed in Kansas in the past. Based on these data, it is estimated that, in the next million years, the maximum amount that the surface at the site may be lowered is about 450 ft, with a total potential for local stream incision of about the same depth. This depth is not sufficient to breach the overlying rocks, thereby permitting dissolution of the salt.

2. Somewhat along the same lines, there is evidence to suggest that the eastern boundary of the salt deposit (Fig. 2.15), about 25 miles east of the Lyons site, has been slowly dissolved (and, in fact, is still being dissolved) by groundwater. Since the subsidence of the overlying rocks into the void controls, to a certain extent, the location of river channels which are subsequently filled with alluvium as the channel migrates, it is possible to date the progress of the retreating salt front. Such observations indicate that the maximum rates of westward migration of the eastern edge of the salt are on the order of 2 to 5 miles per million years. These results will be verified and refined by ^{14}C and other methods of dating of peat deposits, the locations of which are similarly controlled by the subsidence resulting from the dissolved salt.

3. The third mechanism is related to the oil and gas test wells which have been drilled through the salt section in the area (Fig. 2.16). It is estimated that perhaps 50,000 such holes exist in the area of central Kansas underlain by the salt deposit. In four known instances, freshwater has flowed into the well from the surface aquifers, circulated past the salt section dissolving it, and been discharged into the lower permeable zones, principally the Arbuckle. The removal of the salt

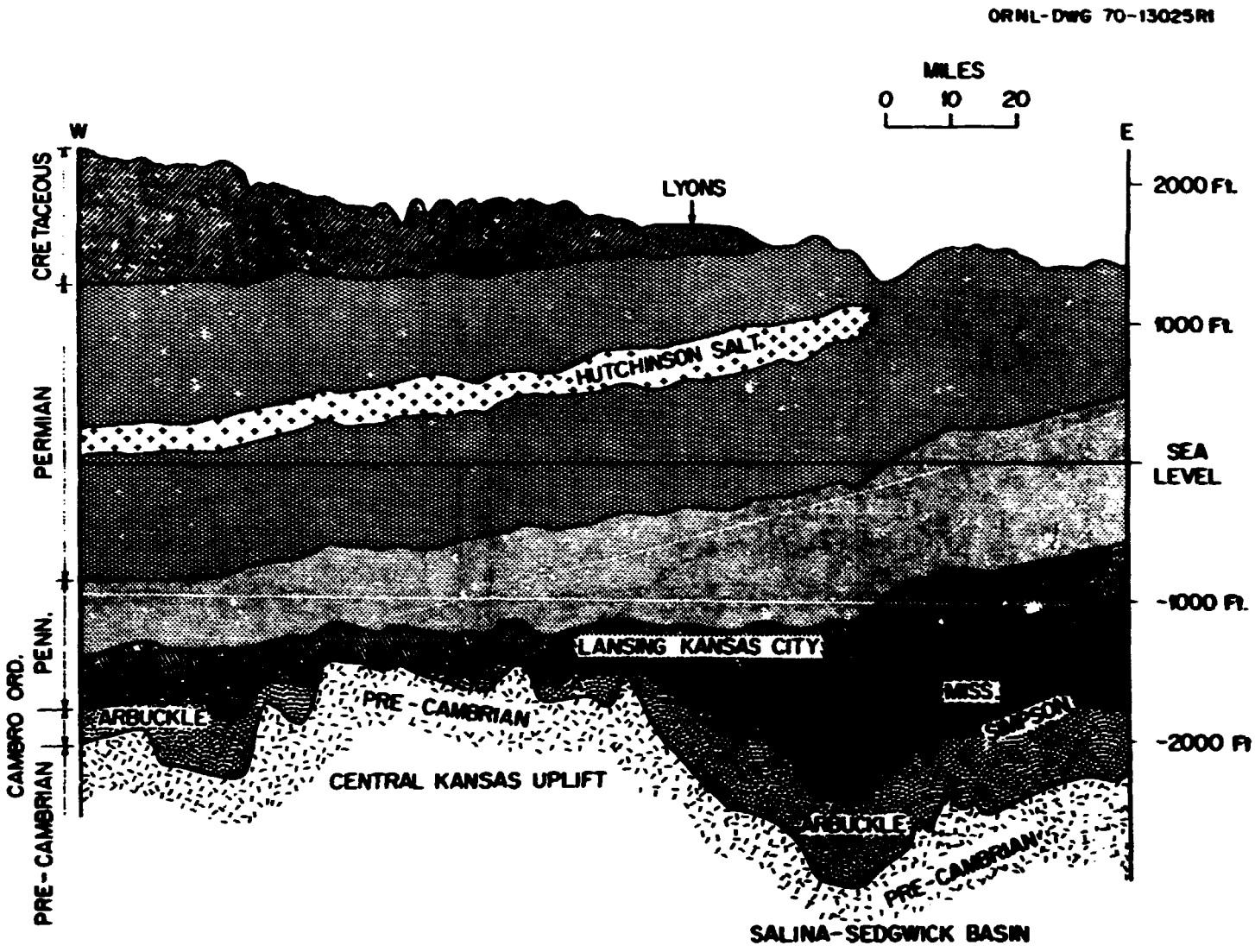

Fig. 2.15. Geologic Cross Section of a Portion of Central Kansas.

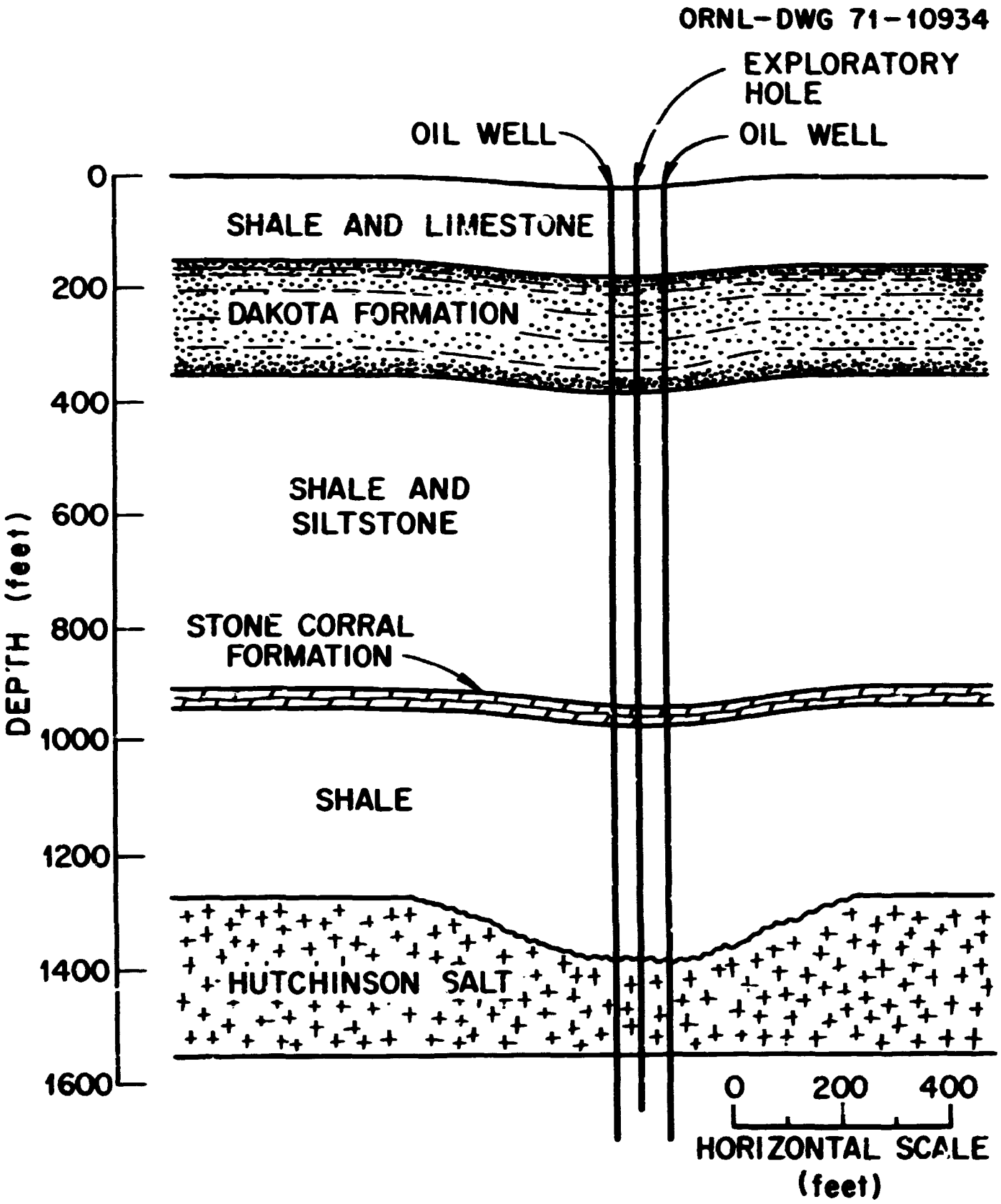

Fig. 2.16. Crawford Sink Area – Russell County, Kansas.

causes the collapse of the overlying rocks and subsidence of the surface. One of these areas is traversed by Interstate 70, where the subsidence occurs at the rate of about 0.7 ft per year. In another case, the collapse was very sudden, creating a small lake almost overnight. Preliminary investigation of the four known and documented cases indicates that they have the following in common: (1) access to a shallow aquifer yielding copious quantities of water (several hundred gallons per minute), (2) a well whose history suggests the possibility of a casing break in the salt zone, and (3) a connection with a highly permeable underlying zone. Investigation of these four cases is continuing to clarify further the necessary conditions and the phenomenology, especially the apparent rates of dissolutioning.

Twenty-nine oil and gas wells are known to have been drilled on and within 1 mile of the Lyons site (Fig. 2.17). In a few cases these holes were plugged to meet the requirements of the salt miners, and the plugs are probably satisfactory. However, most of the holes will have to be reopened and replugged permanently. Work concerned with this problem is currently in progress in two areas: (1) the collection of detailed information for each of the wells (such as location, size, casing configuration, depth and zones penetrated, and quality of present plug) so that the requirements of the permanent plug can be determined; and (2) development of materials (such as special sulfate-resistant or plastic cements, and sand-clay mixtures) for designing plugs to meet those requirements.

4. The fourth mechanism for possible dissolutioning of the salt bed also concerns man's activities — in this case, instances where freshwater has been pumped into the salt formation either to produce brine or to create a large cavity for the storage of liquefied petroleum gases. More than 350 individual cavities of this latter type are in existence in central Kansas. Although some of these will be studied for information related to unintentional dissolutioning, all of the cavities are more than 20 miles from Lyons and, therefore, not of immediate interest.

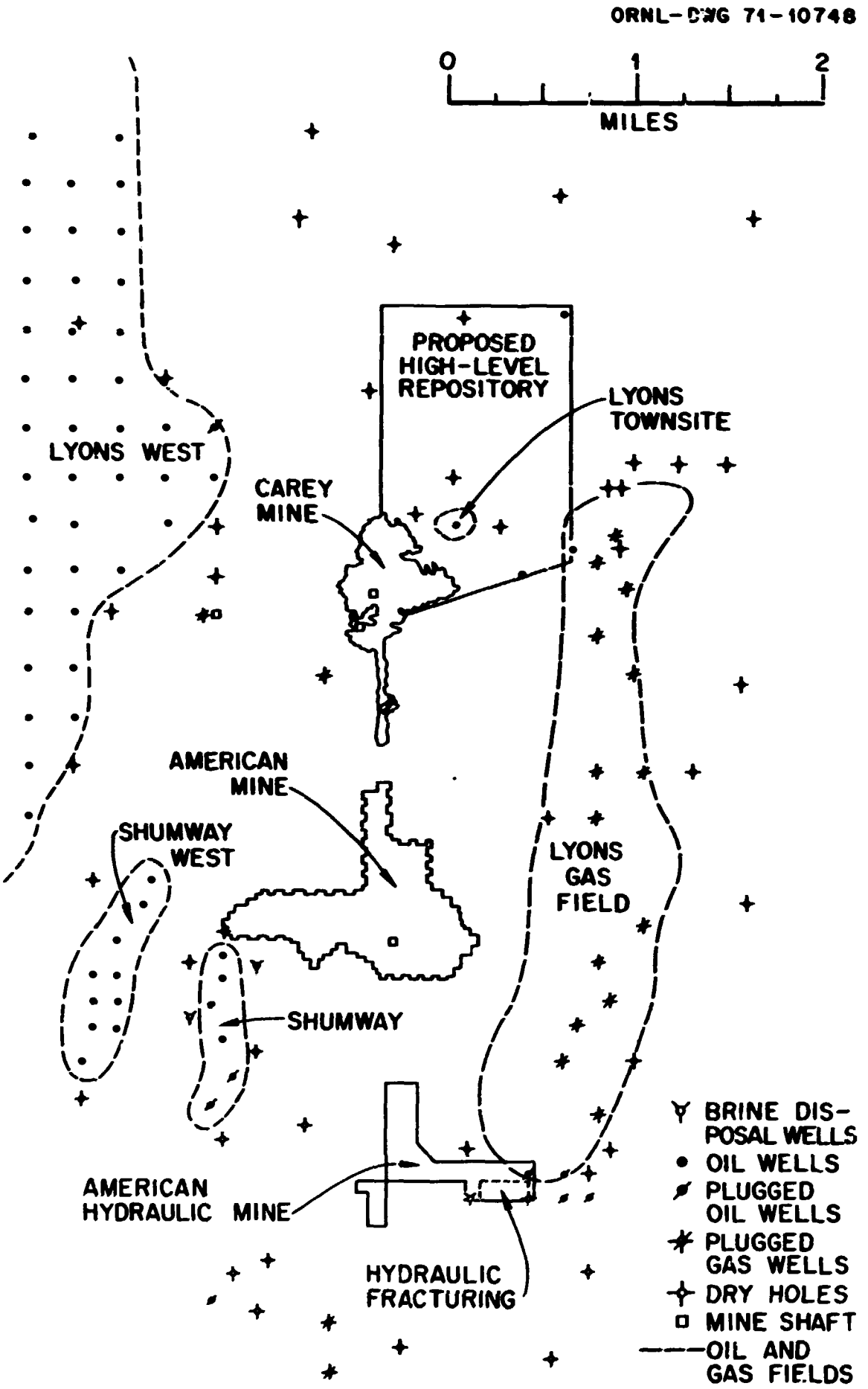

Fig. 2.17. Map of Lyons Area Showing Underground Workings, Oil and Gas Fields, and Deep Boreholes.

However, hydraulic mining operations are currently being conducted at the American Salt Corporation plant near Lyons (Fig. 2.17), and these are of some concern since they represent a situation where water is known to be present in the salt formation. This water is separated from the proposed Repository by three-fourths of a mile of intact salt, and by a distance of about 3 miles overall. We are currently investigating both American Salt Corporation's hydraulic mining operations, especially some anomalous hydrologic data, and the long-term stability of solution cavities, in general, in order to evaluate the potential threat to the integrity of the salt formation at the Repository from these operations.

The existing oil wells and the American Salt Corporation's hydraulic mining activities represent the most serious technical objections to the Lyons site. Although the investigation and evaluation are not yet complete, neither of these is considered sufficient to render the site unsuitable at this time.

2.3 References

1. E. Angino et al., Preliminary Report on the Geology and Hydrology of the Lyons, Kansas, Radioactive Waste Repository Site, prepared by the State Geological Survey of Kansas and the University of Kansas Center for Research, Inc., for the U. S. Atomic Energy Commission and Union Carbide Corporation, November 1970.

2. R. L. Bradshaw and W. C. McClain (Eds.), Project Salt Vault: A Demonstration of the Disposal of High Activity Solidified Wastes in Underground Salt Mines, ORNL-4555 (March 1969).

3. W. B. Heroy, Lithology of the Salt Section in the Mine of The Carey Salt Company, Lyons, Kansas, Technical Report No. 62-9, The Geotechnical Corporation, Dallas, Texas, 1962.

4. Surface Water Supply of the U. S. 1961-65, Part 7, Lower Mississippi River Basin, Vol. 2, Arkansas River Basin, Geological Survey Water Supply Paper 1921, U. S. Government Printing Office, Washington, D. C., 1969.

5. O. S. Fent, Geology and Ground-Water Resources of Rice County, Kansas, Kansas Geological Survey Bulletin 85, 1950.

6. S. W. West, Research Hydrologist, USGS, letter to T. F. Lomenick, "Concerning Results of Hydraulic Testing in USAEC Test Hole No. 1," October 26, 1970.

7. S. W. West, Research Hydrologist, USGS, letter to T. F. Lomenick, "Concerning Results of Hydraulic Testing in USAEC Test Hole No. 2," December 4, 1970.

3. THERMAL ANALYSIS

R. D. Cheverton and W. D. Turner

Heat is generated in high-level waste as the result of radioactive decay. After this solidified waste is buried in the mine, the heat from radioactive decay is dissipated in the salt and surrounding formations and eventually flows to the surface of the earth, where it is transferred to the atmosphere and flowing groundwater. A consequence of the subsurface heat release is an increase in the temperatures of the mined area and its environs. These temperatures gradually increase and then finally decrease since the heat generation rate in the waste is continuously decreasing. Eventually the heat source will completely decay, and the temperatures will return to normal. However, the time scale is thousands of years.

Factors which influence the allowable heat release rate include: (1) thermal instability of the solidified waste; (2) release and migration of brine contained in small cavities in the salt; (3) structural integrity of the mine during operation; (4) structural integrity of the overlying formations; (5) temperature rise in freshwater aquifers; (6) heating of the earth's surface; and (7) temperature increases beyond the boundaries of the mine.

The high-level solidified waste will be enclosed in steel containers, and these packages will be placed in vertical holes in the salt 8 ft beneath the floors of rooms mined out of the salt formation. The general scheme for a typical case is shown schematically in Fig. 3.1. Alpha waste will be received in steel boxes and/or drums and will be placed in existing rooms.

3.1 Characterization of the Wastes

Basically, two types of waste must be considered in the thermal analysis. One of these, which is referred to as high-level waste, is comprised of concentrated fission products and thus emits high-level gamma radiation. The other is alpha waste, which consists primarily of miscellaneous materials that have been contaminated with alpha emitters. Since each waste is made up of many different radioactive nuclides, its decay curve consists of sums of many exponential terms.

ORNL DWG 71-6182

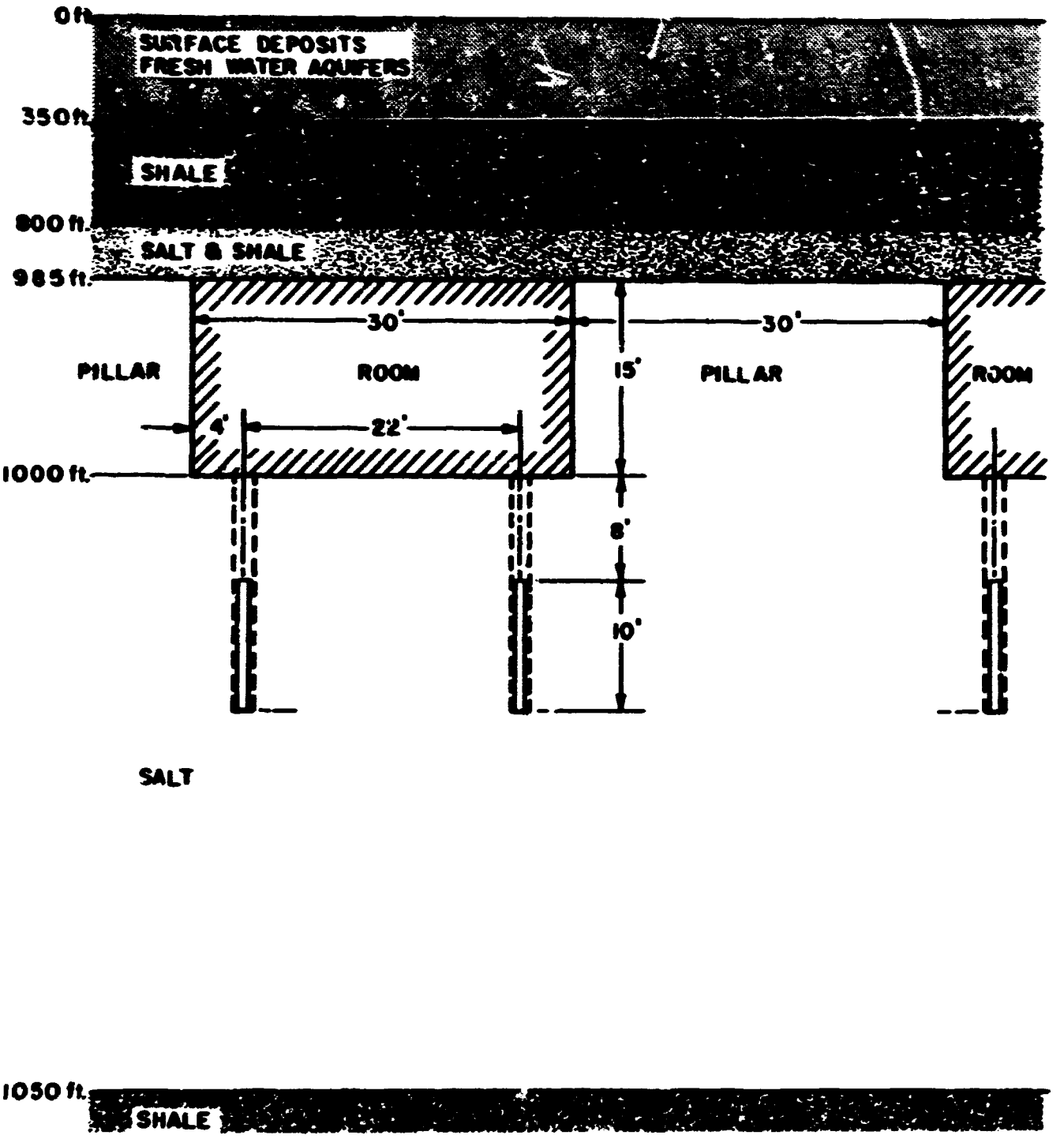

Fig. 3.1. Schematic of the National Radioactive Waste Repository: Vertical Cross Section of Typical High-Level Mine.

For the high-level waste, the volumetric heat generation rate in a particular concentrate at the time of waste burial will depend upon the fuel enrichment, the rate and degree of fuel burnup, and the length of time from reactor discharge to burial. A typical fuel from a light water reactor will experience a burnup rate of 30 MW per metric ton and a total burnup of 33,000 MWd per metric ton. Besides the fission products, the wastes generated by reprocessing the fuel will contain about 0.5% of the uranium and plutonium originally in the fuel. Waste obtained by reprocessing fuel of this irradiation history is presently referred to as Diablo Canyon waste. Federal regulations restrict the time between fuel reprocessing and burial of the wastes to a maximum of 10 years. Deferring burial for this period of time appears to offer an economic advantage. However, because it is possible that wastes much younger than 10 years will be buried, they must also be considered in the thermal analysis.

The high-level waste can also be characterized by the chemical and physical form of the solidified product. Oxides, glasses, powdered, and solid products are among the variations being considered. Accompanying these variations are significant differences in thermal properties and maximum permissible storage temperatures.

3.2 Criteria Related to Thermal Analysis

Criteria are required to facilitate interpretation of the results of the thermal analysis. These criteria are derived from studies that consider the effects of temperature increases on the seven factors mentioned earlier. As the calculations associated with the various studies are refined, new criteria are fed back for use in the thermal analysis. A set of tentative criteria for the high-level waste and mine is listed below.

3.2.1 Dimensions and Temperatures of the Waste Container

The dimensions of the waste container have tentatively been specified as 10 ft in length and 6 to 14 in. in diameter. The maximum permissible temperature of the waste is presently specified as the maximum temperature that existed during the waste solidification process. It appears that this temperature will range between 1100 and 2000°F.

3.2.2 Dimensions of the Mine

Dimensions of the rooms, pillars, and corridors are dependent on many factors in addition to thermal considerations. Eventually the dimensions will be optimized for safety and economics. For the present, a reasonable range of dimensions appears to be as follows:

Room and corridor height = 15 ft
Corridor width = 30 ft
Room-pillar width combinations = 15-25 to 50-50 ft
Room length = 500 ft

3.2.3 Location of Waste Containers

The waste containers must be positioned at least 4 ft from the walls of the room (hole drilling and waste container loading restrictions), and the distance between the top of the can and the floor of the mine is tentatively specified as 8 ft.

3.2.4 Formation Temperatures

Previous thermal and rock mechanic studies indicate that, in order to prevent excessive migration of brine to the containers, ensure stability of the mine during operations, and avoid undesirably high temperatures in adjoining formations and overlying freshwater aquifers, the following restrictions should be placed on the salt temperatures:

(1) The volume of salt having a temperature above 482°F in the area that surrounds the waste container and is confined within a unit cell outlined by horizontal planes at the ends of the container and by the usual vertical planes of symmetry shall constitute less than 1% of the unit cell volume.

(2) The volume of salt having a temperature greater than 392°F in the above unit cell shall constitute less than 25% of the unit cell volume.

Other limiting temperatures are: earth's surface temperature rise, 1°F or less; temperature rise in the geologic formation at the edge of the Repository buffer zone, 1°F or less; and stagnant aquifer temperature rise at a depth of 300 ft below the earth's surface, 50°F or less.

3.3 Calculational Techniques and Models

The thermal analysis of the Repository requires solution of the heat conduction equation for a very complicated geometry and combination of materials. For a problem of this type it is desirable to use finite difference numerical analysis in conjunction with a large and fast computer. The particular finite difference methods being used are the Classical Explicit Procedure (CEP),[1] the CEP with Levy's modification[2] applied so as to remove the restriction on the size of the time step, and the Alternating Direction Implicit (ADI) technique.[3] The latter is much faster than the others and is used for the three-dimensional problems. The ORNL version of ADI has the capability for updating thermal properties at each node and time step.

The calculational models must be selected with care so that the computer is not overtaxed and yet accurate results are obtained. A three-dimensional model that considers a unit cell of the mine, as shown in Fig. 3.2, is used to obtain local temperatures in the burial area of the mine. The cell contains room, pillar, and waste container detail and extends to a few hundred feet above and below the room floor level. Temperatures in this area peak in about 50 years, and the calculations are restricted accordingly. Nearly the same model can be constructed in two dimensions, as shown in Fig. 3.3. Since a two-dimensional model requires less computer time, greater physical detail and longer periods of time from time of burial can be considered.

A cylindrical-geometry two-dimensional model, as shown in Fig. 3.4, is used for temperatures outside the immediate burial area and extending to the earth's surface, hundreds of feet below the mine level, and well beyond the edge of the mine. The model does not include details of the mine but, rather, considers a homogenized source zone. This simplification is justified for the intent of the calculation and permits the consideration of very long times after burial. Such a feature is necessary since periods up to several thousand years are required for temperatures to peak at positions quite some distance from the heat source.

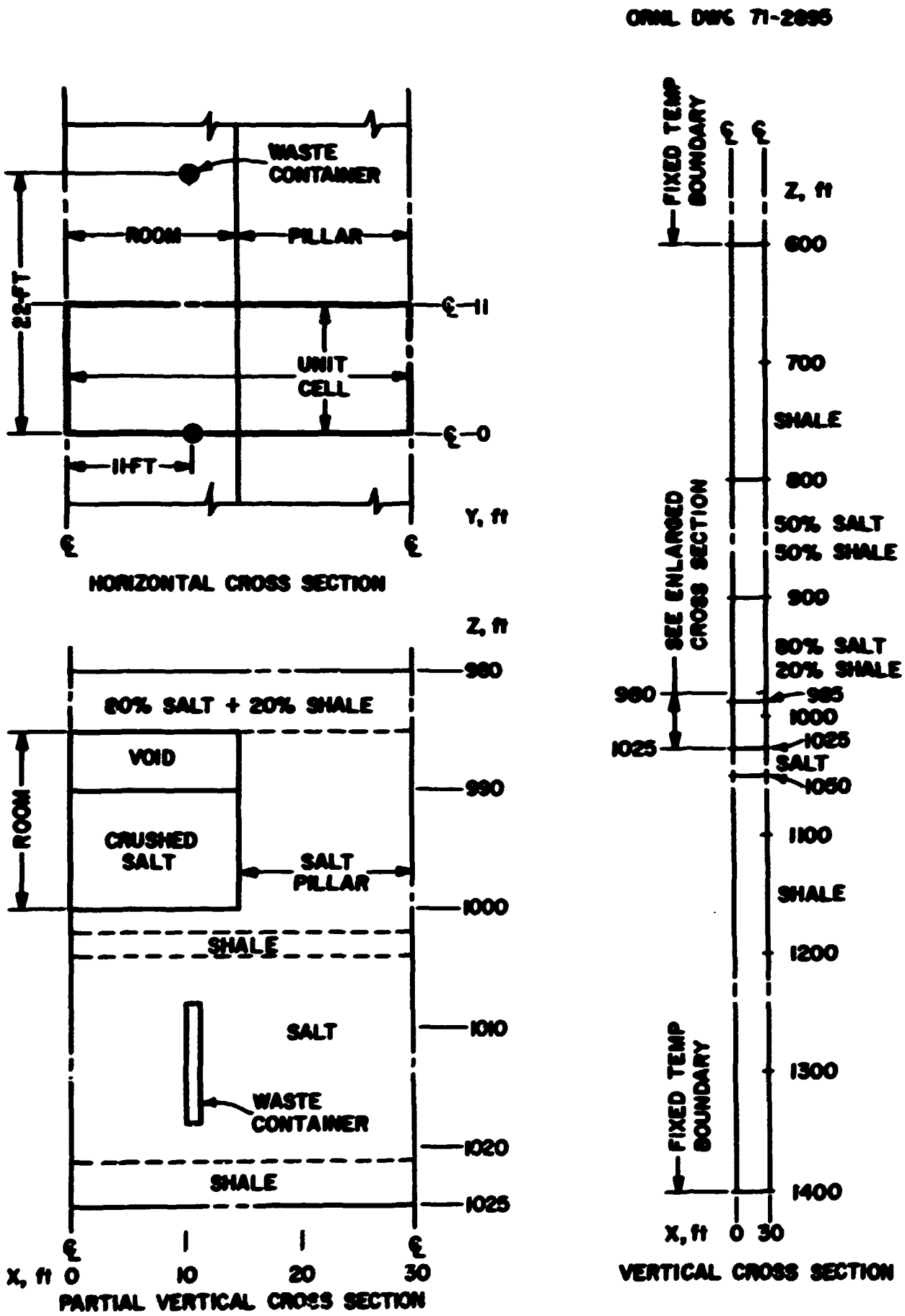

Fig. 3.2. Three-Dimensional Model of a Unit Cell of the High-Level Mine.

ORNL DWG 71-29HRI

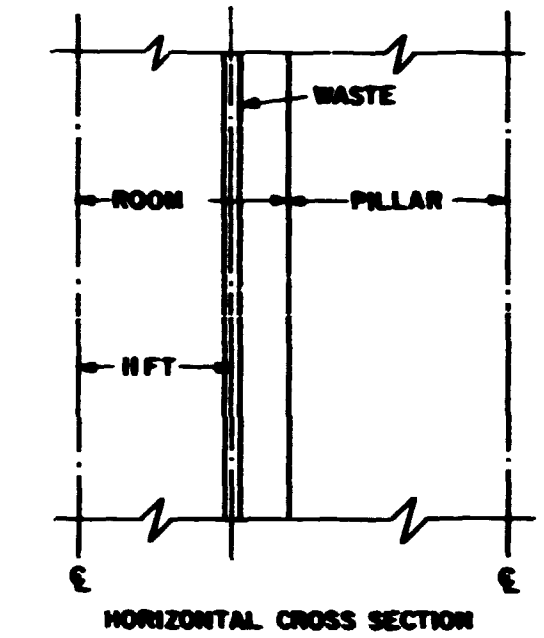

HORIZONTAL CROSS SECTION

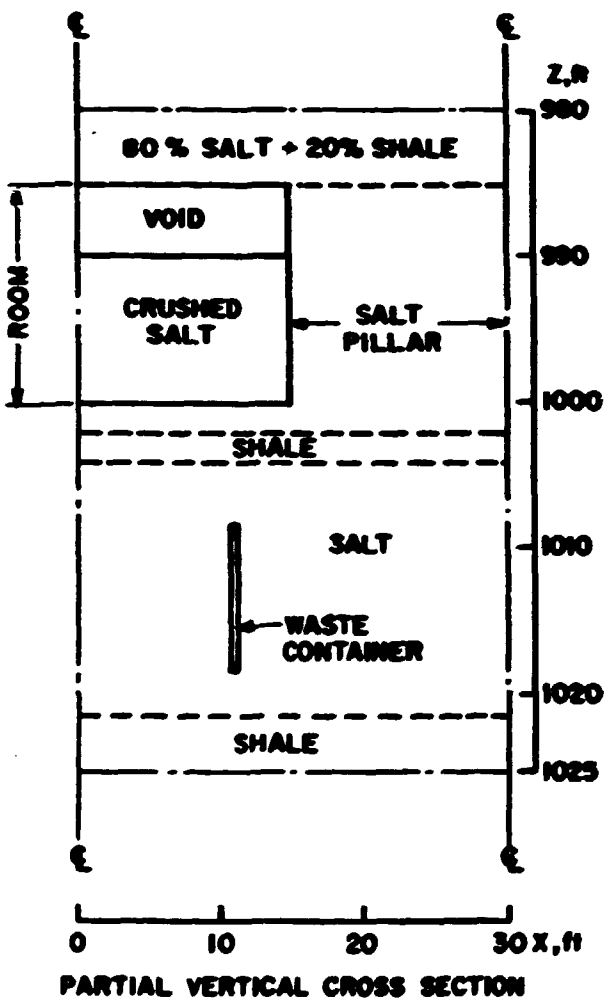

PARTIAL VERTICAL CROSS SECTION

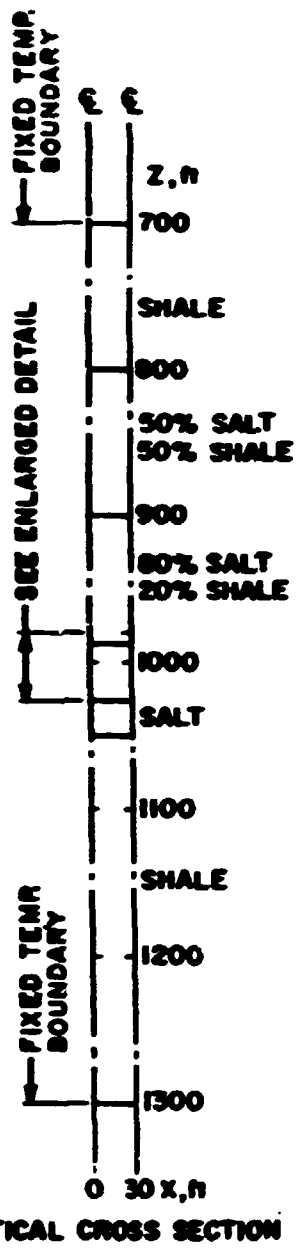

VERTICAL CROSS SECTION

Fig. 3.3. Two-Dimensional XZ Model of a Unit Cell of the High-Level Mine.

ORNL DWG 71-2901

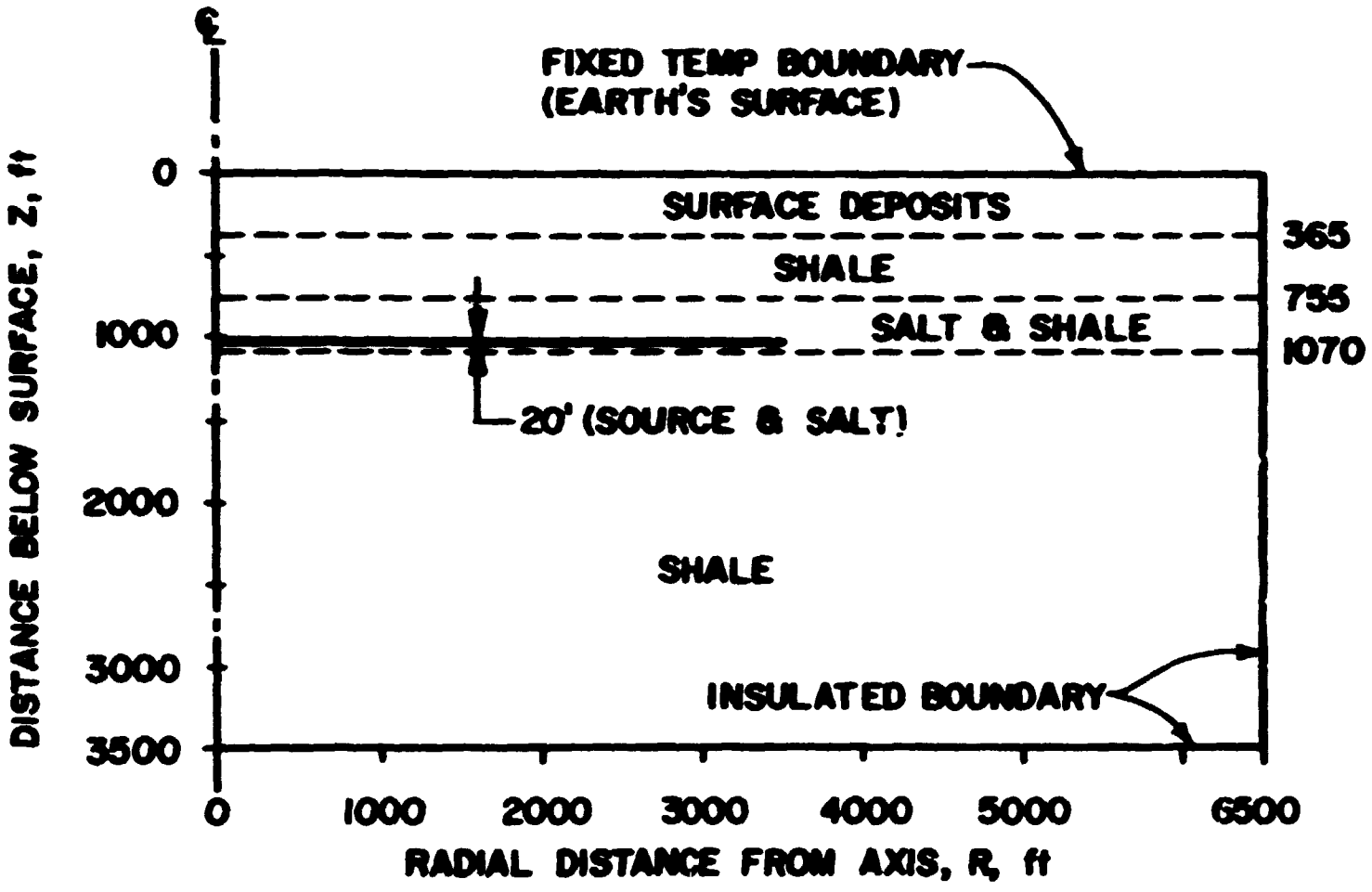

Fig. 3.4. Two-Dimensional Cylindrical Model of the High-Level Mine.

The accuracy of the calculations is continually checked by conventional means and can generally be increased at the expense of computer time. An important means for checking on the accuracy of the overall numerical analysis is an independent study. Such an effort is under way on a small scale and will be amplified in the near future.

3.4 Typical Results Obtained from Thermal Analysis

Power densities in the alpha waste are so low that, even with a compaction factor of 10, the heat removal problem is negligible as compared with that for the high-level waste. For this reason, all further discussions of results are confined to the high-level waste.

Thus far, high-level waste calculations have been made primarily for the purpose of demonstrating feasibility and examining the sensitivity of the results to variations in the calculational models, stratigraphy, thermal properties, and solidified waste characteristics. The results indicate that the temperatures in the geologic formations some distance from the local burial area are essentially independent of room, pillar, and waste detail, and even reasonable variations in thermal properties and stratigraphy, provided that the temperature criteria in the burial area are met. The important independent variable is the average initial power density in the mine and thus the initial total power when considering a specific repository size. With regard to temperatures in and close to the waste containers, there is a greater dependence on local detail. However, it appears that the criteria can always be satisfied by varying room, pillar, and waste container dimensions, waste burial arrays, and initial power per container.

A typical case considered burial of 10-year-old waste generated by reprocessing Diablo Canyon fuel. This case is further characterized by the dimensions and stratigraphy indicated in Figs. 3.2 and 3.4. In addition, the diameter of the waste container was 6 in., and the solidified waste was a calcine-type, which tends to have relatively low thermal conductivity and relatively low permissible temperature. The corresponding three-dimensional model stratigraphy and backfill characteristics were

selected so as to result in conservatively high temperatures in the local salt formation. Thermal properties used in the two-dimensional (RZ) calculation were selected to give conservatively high temperatures at the earth's surface and in the aquifers. Furthermore, it was assumed that all of the waste in the mine was identical and that all of it was buried at the same time.

3.4.1 Temperature Distributions in Space and Time

Temperatures in the Vicinity of the Mined Area. - Figure 3.5 shows, for the above typical case, the effect of time on the temperature rise at various points of interest in the mined area close to the waste package. As indicated, the temperature at the center of the waste peaks in about 12 years, reaching a temperature rise of 540°F as compared with a minimum limiting value of 1000°F. At a position 8 in. from the edge of the container (nearly equivalent to the 1% area criterion), the temperature peaks in about 30 years, and the corresponding temperature increase is 365°F as compared with a limit of 410°F. Midway between the containers (nearly equivalent to the 25% area criterion), the temperature peaks at 40 years, with a temperature rise of 328°F. This is essentially the same as the permissible value of 320°F. The power per container corresponding to these temperatures is 2000 W.

Temperatures Outside the Immediate Mine Area. - Temperature increases outside the immediate mine area for the above typical case are shown in Figs. 3.6-3.8. Each of these figures represents vertical temperature-rise profiles extending from the surface of the earth to about 2500 ft below the waste container. Results of the analysis indicate that the radial temperature distributions above and below the mine area are essentially flat to within about 500 ft of the edge of the mine several years after the entire disposal area is full. Figure 3.6 shows the vertical temperature profiles for this area.

The peak temperature increases in the region containing freshwater aquifers (down to 300 ft below the surface) are in the range less than 1°F to 30°F, assuming that the aquifers are stagnant. Because of the very low heat flux in this region, only a small aquifer flow rate would

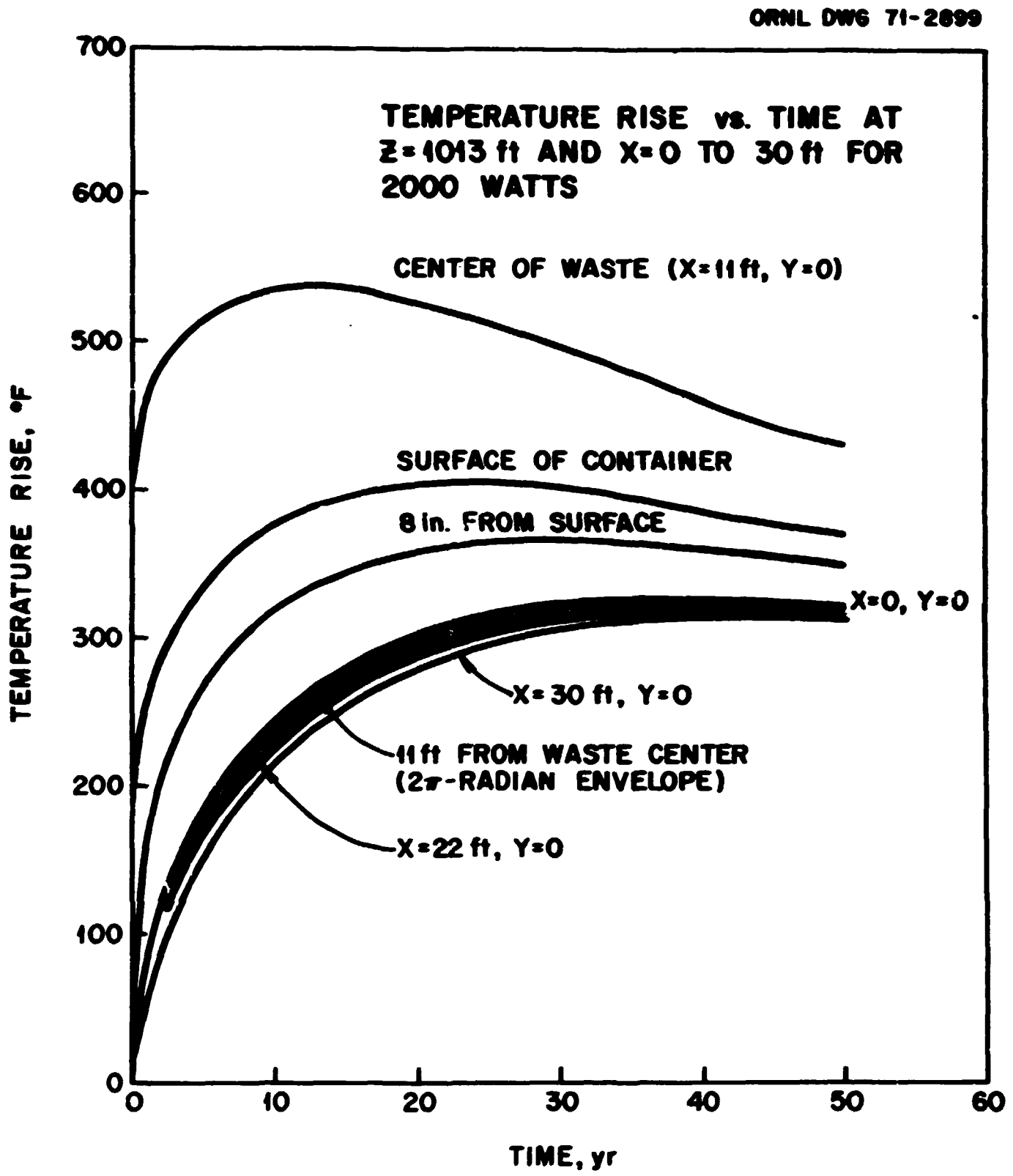

Fig. 3.5. Temperature Rise vs Time at Z = 1013 ft and X = 0 to 30 ft for 2000 W.

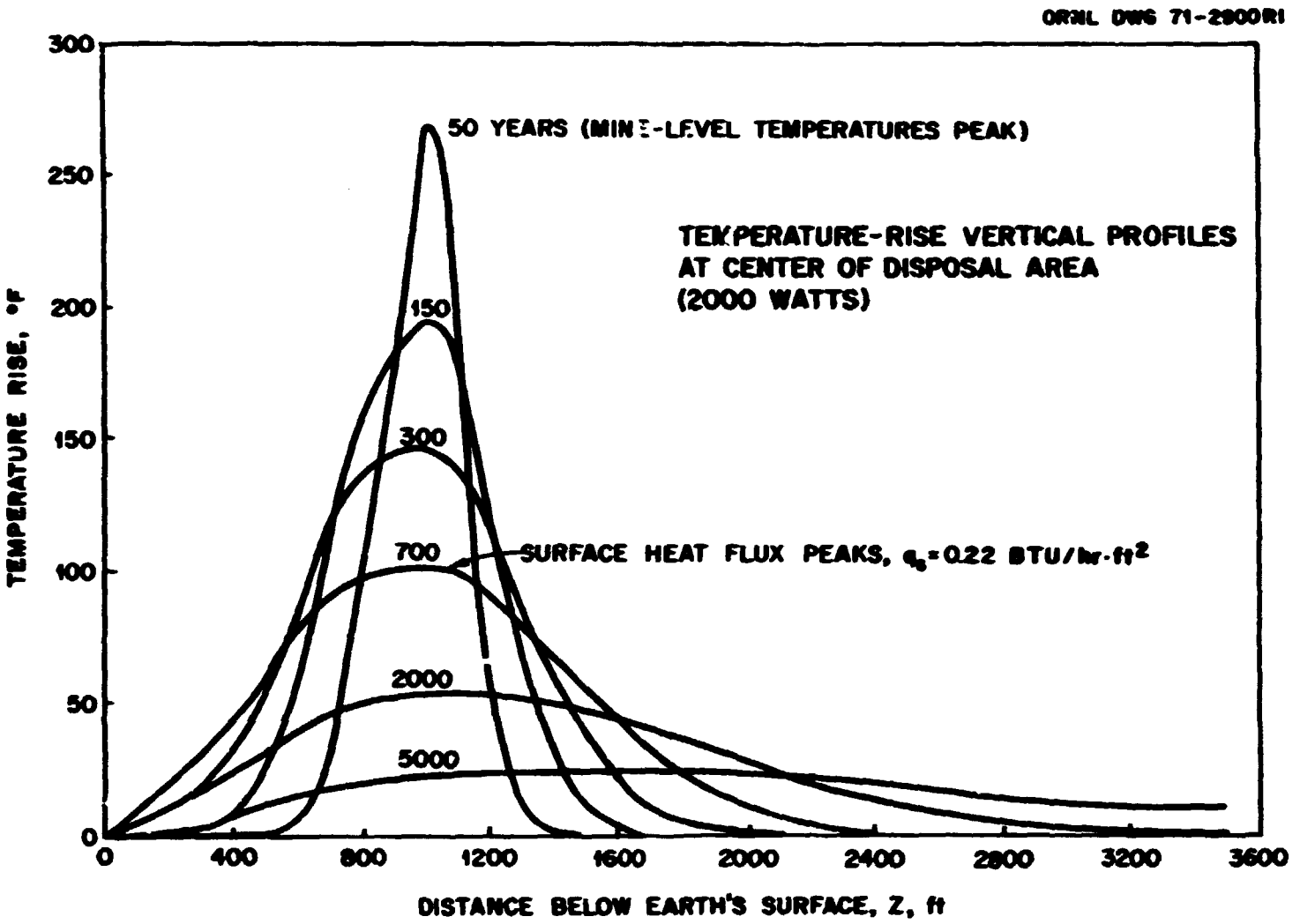

Fig. 3.6. Temperature-Rise Vertical Profiles at Center of Disposal Area (2000 W).

ORNL DWG 71-2902

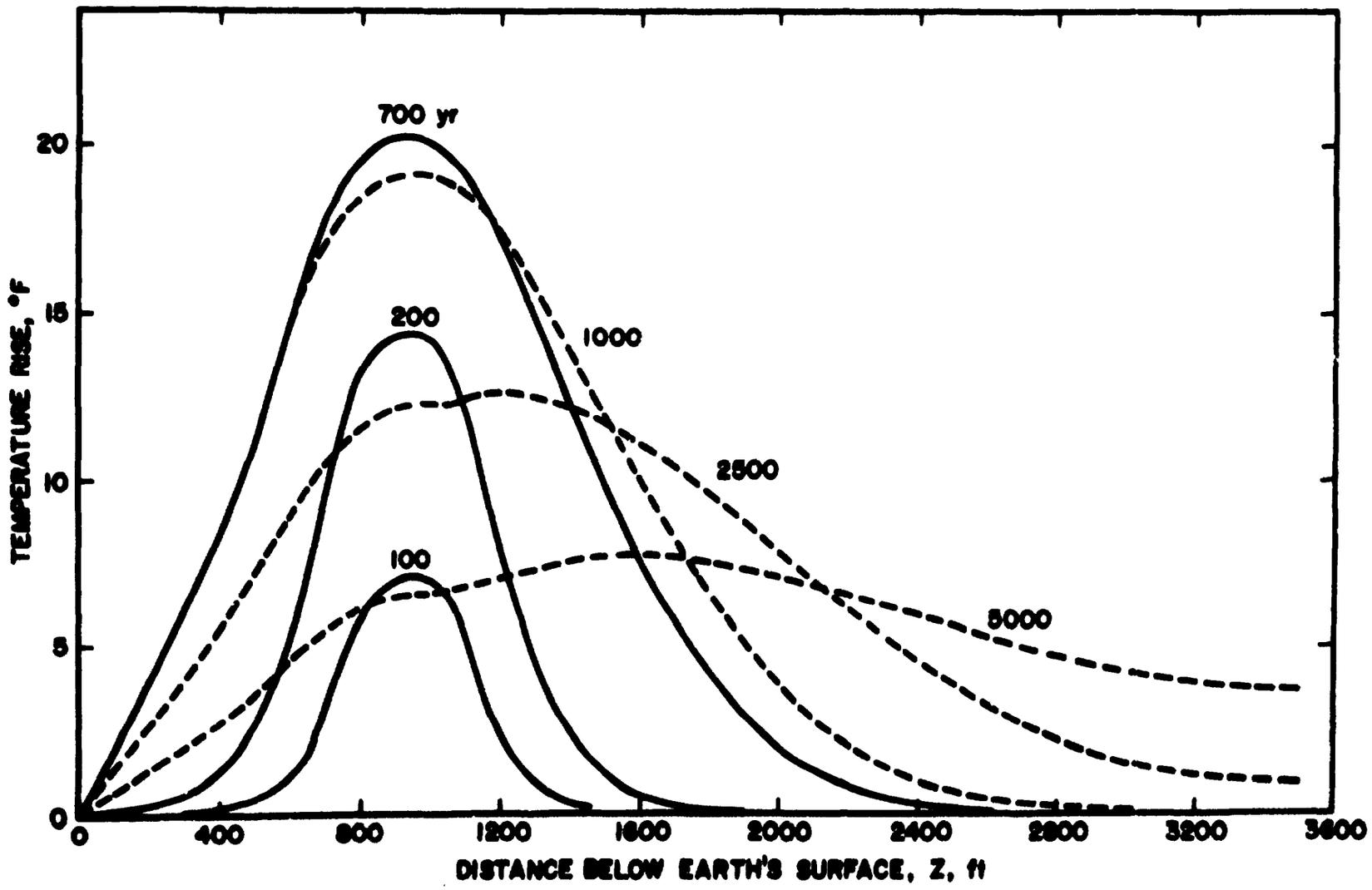

Fig. 3.7. Temperature-Rise Vertical Profile 500 ft Beyond Edge of Mine (2000 W).

ORNL DWG 71-2903

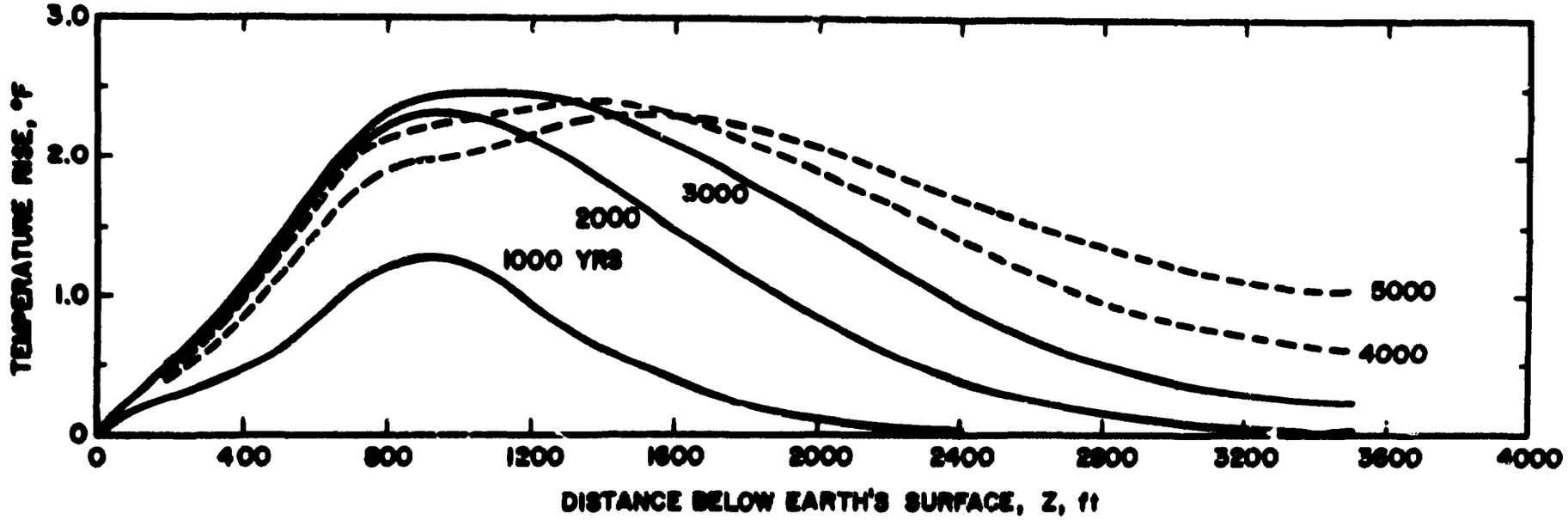

Fig. 3.8. Temperature-Rise Vertical Profile 1750 ft Beyond Edge of Mine (2000 W).

be required to essentially eliminate the temperature rise in this region. It is observed that a perceptible temperature increase in a stagnant aquifer requires 100 years and attainment of the peak requires 700 years.

Figure 3.7 shows the vertical temperature profiles 500 ft from the edge of the mine. The shortest peak time is about 700 years, and the corresponding temperature rise is about 20°F. At 1750 ft from the edge of the mine (Fig. 3.8), the minimum peak time is about 3000 years and the corresponding temperature increase is 2.5°F. A peak temperature rise of 1°F occurs at about 3000 ft from the edge of the mined area.

Referring again to Fig. 3.6, it is observed that the surface heat flux peaks in about 700 years. Its value is estimated from the slope of the temperature curve to be 0.22 Btu hr^{-1} ft^{-2}. As indicated in Fig. 3.9, about 100 years is required for a noticeable calculated addition; however, after the peak value is reached in 700 years, it persists for hundreds of years. Figure 3.10 shows how the peak surface heat flux varies with radial distance from the center of the mine. A short distance (500 ft) beyond the edge of the mine the peak value is decreased by a factor of 5.

The surface temperature rise associated with the added surface heat flux has been calculated to be about 0.2°F. It is of interest to note that the "waste" peak heat flux at the surface is about 12 times the geothermal heat flux (2.0×10^{-2} Btu hr^{-1} ft^{-2}) and about 500 times less than the solar heat flux.

From an economics point of view, three important parameters are the power per gross area of the mine, power per net area of the mine (based on room floor area, which is proportional to the amount of salt that must be mined), and the power per waste package. Maximum permissible values of these parameters, consistent with the waste and salt temperature criteria, are shown in Figs. 3.11-3.13 as a function of pitch (distance between waste packages along the length of the room) for 10-year-old waste and for the indicated different room sizes and burial arrays. The results are from three-dimensional calculations that included thermal-property temperature dependence. Figure 3.11 pertains to the 15-ft room with a single row of packages and shows the limiting values of power per

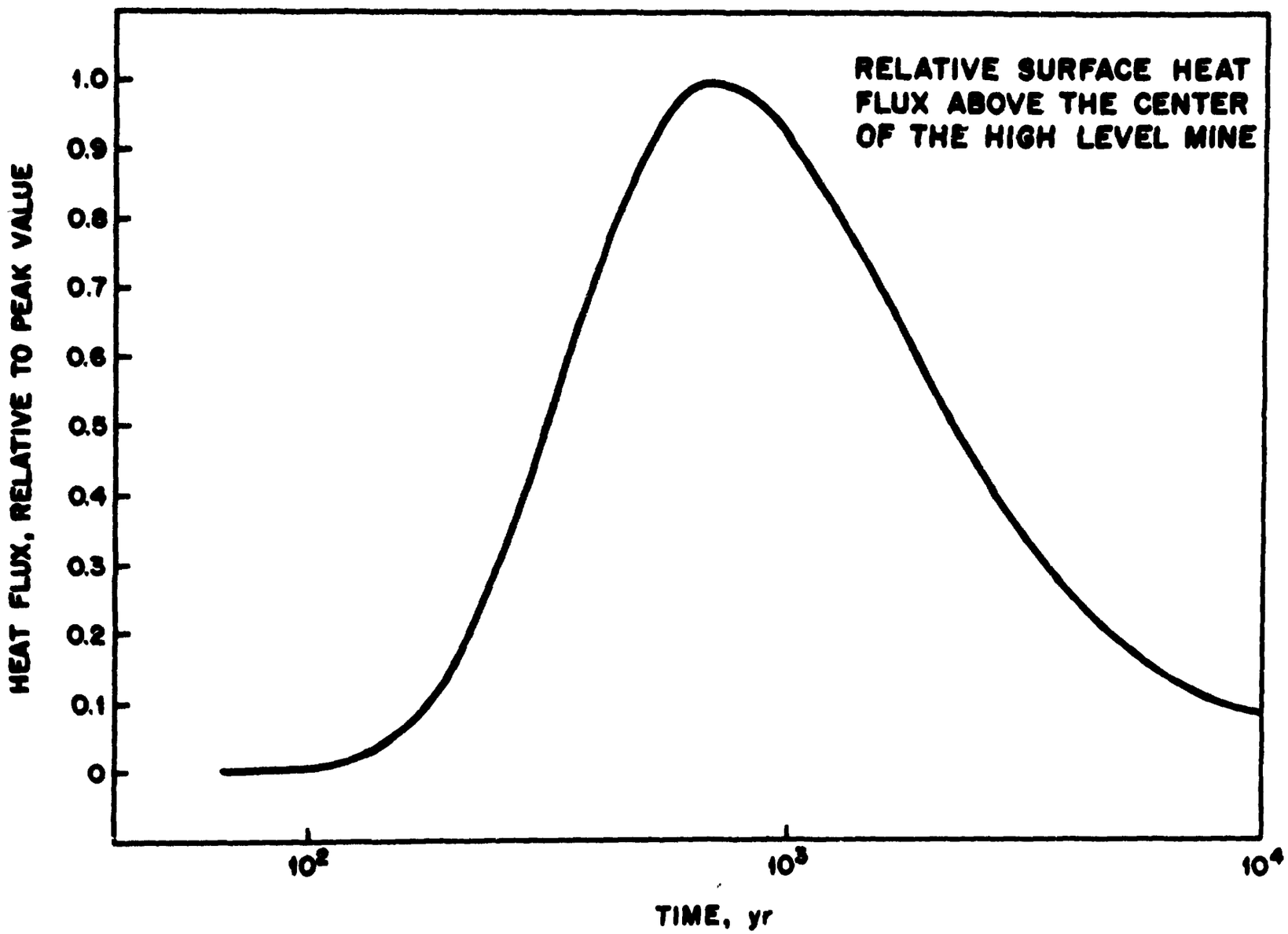

Fig. 3.9. Relative Surface Heat Flux Above the Center of the High-Level Mine.

ORNL DWG 71-2898 R1

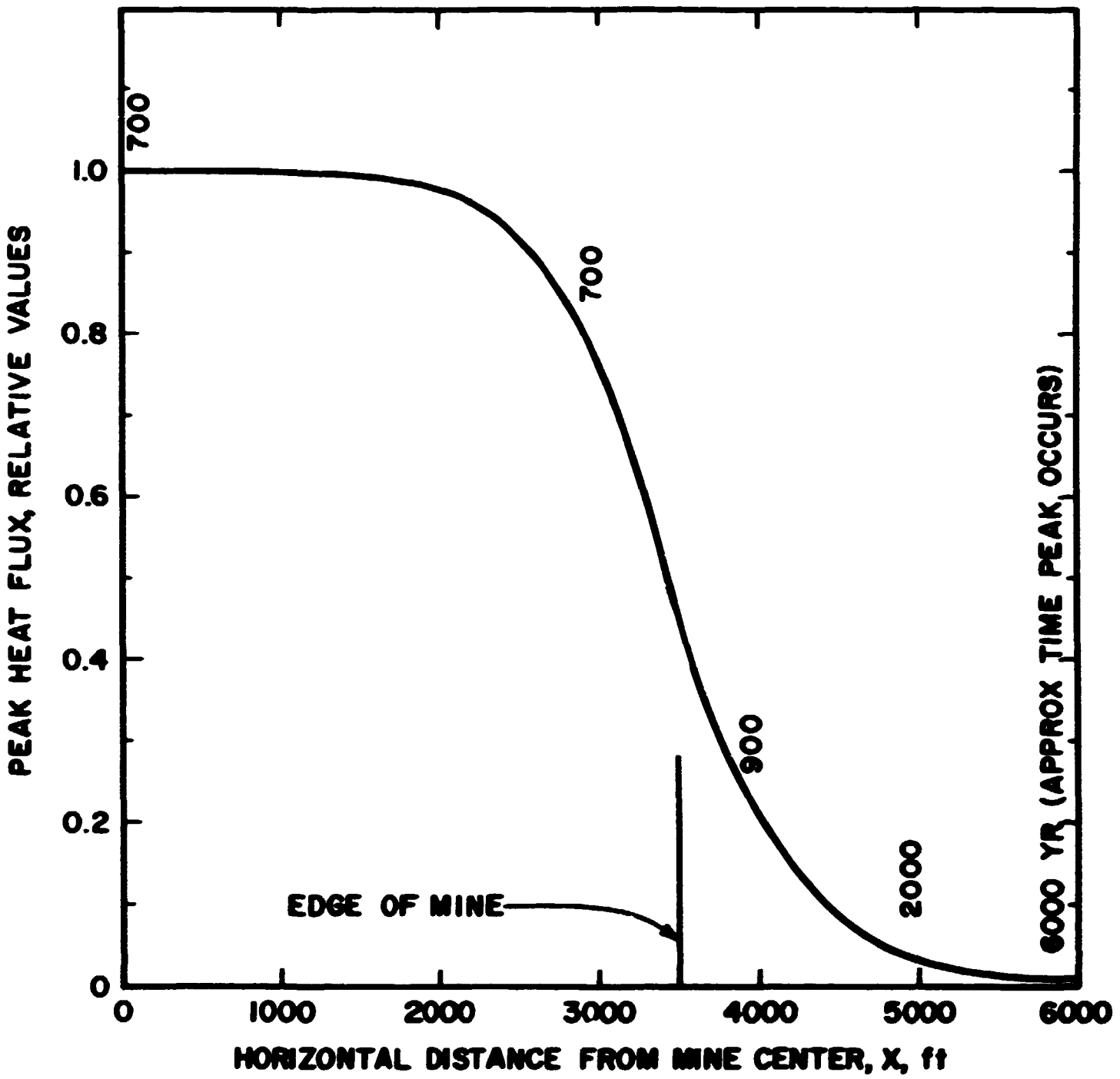

Fig. 3.10. Peak Surface Heat Flux as a Function of Horizontal Distance from the Center of the Mine.

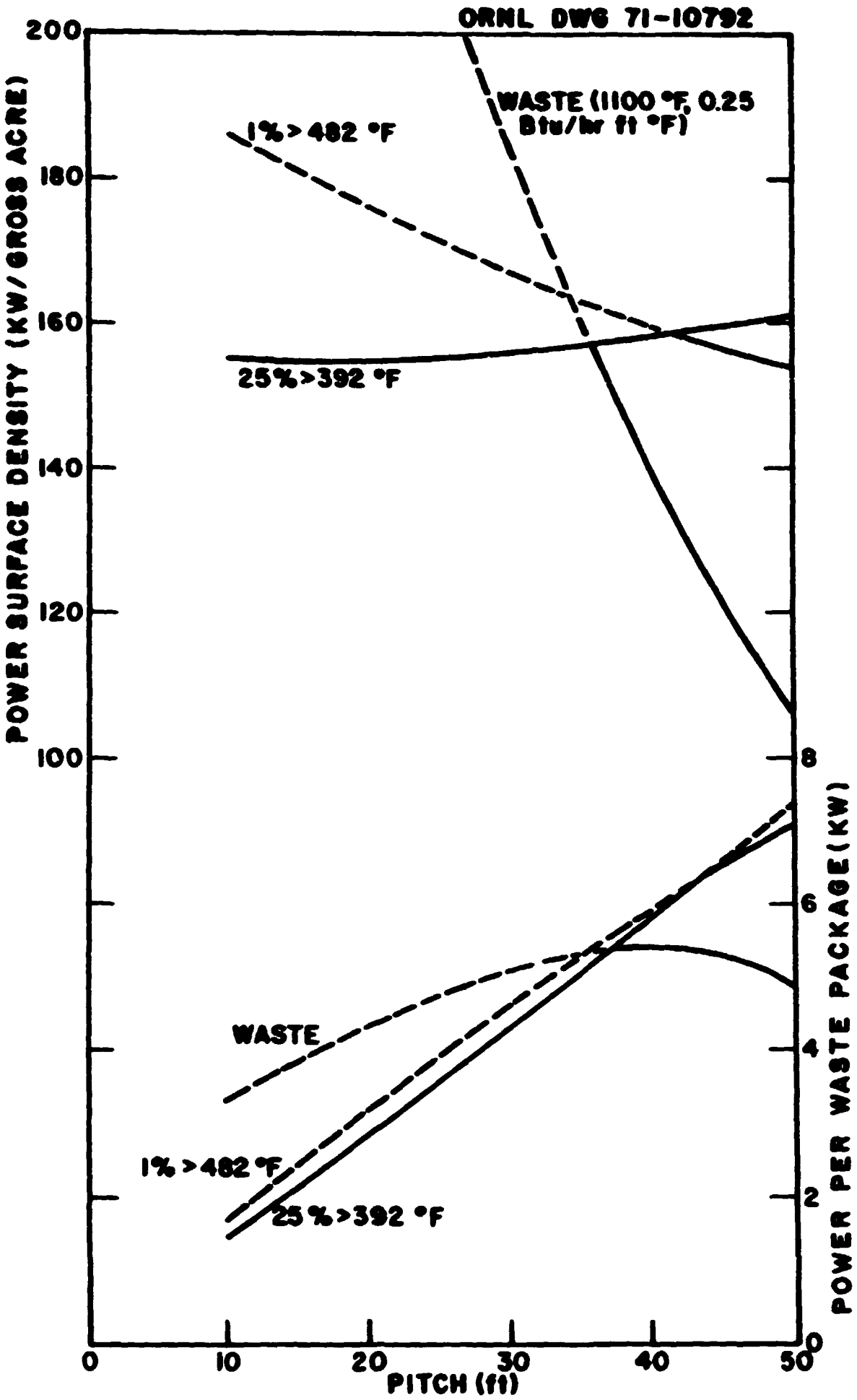

Fig. 3.11. Maximum Permissible Power and Power Surface Density for a 15-ft Room with a 25-ft Pillar, a Single Row of 6-in.-diam Cans, and 10-year-old Waste.

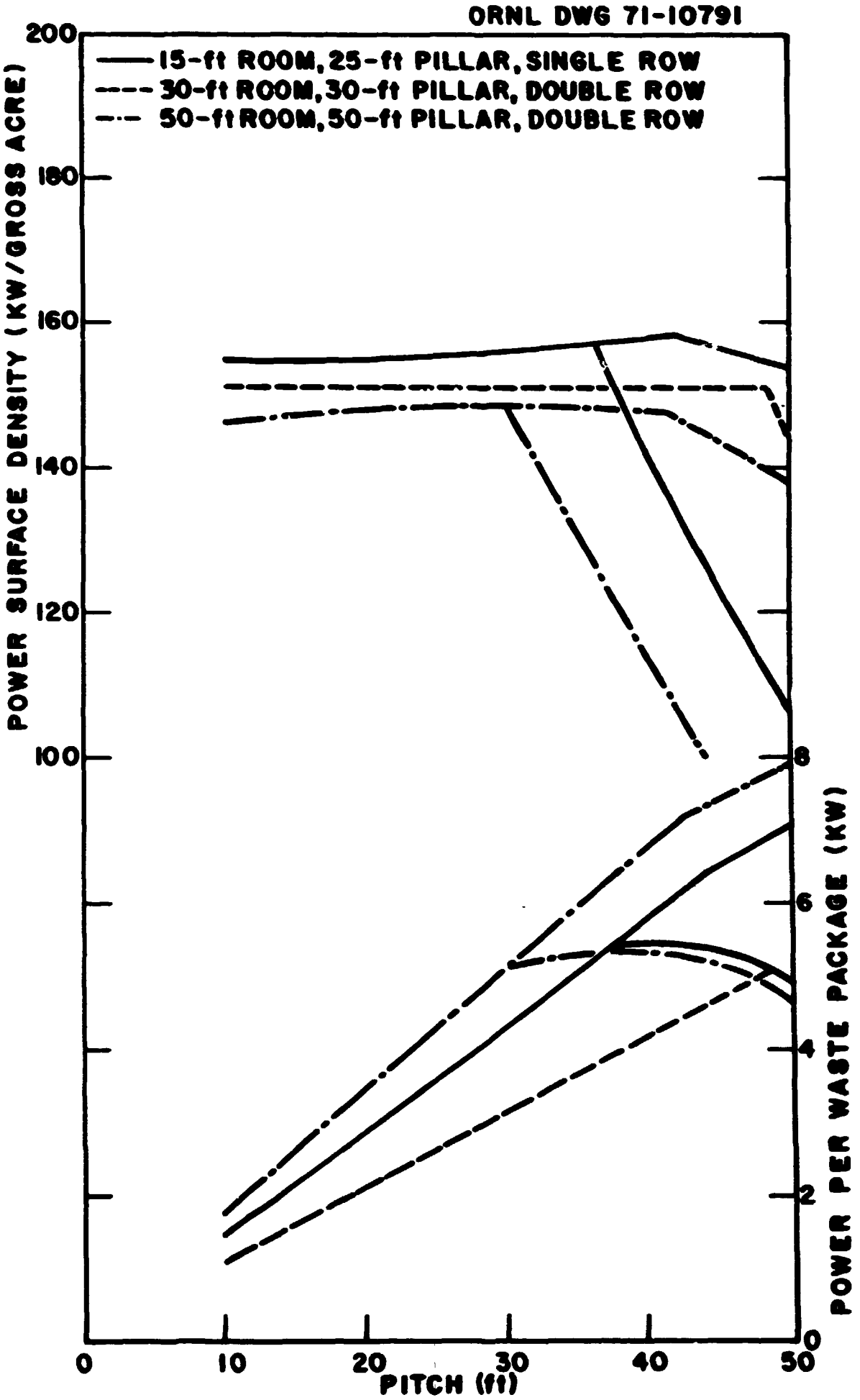

Fig. 3.12. Comparison of Maximum Permissible Power and Power Surface Densities for Different Room Sizes, 6-in.-diam Cans, and 10-year-old Waste.

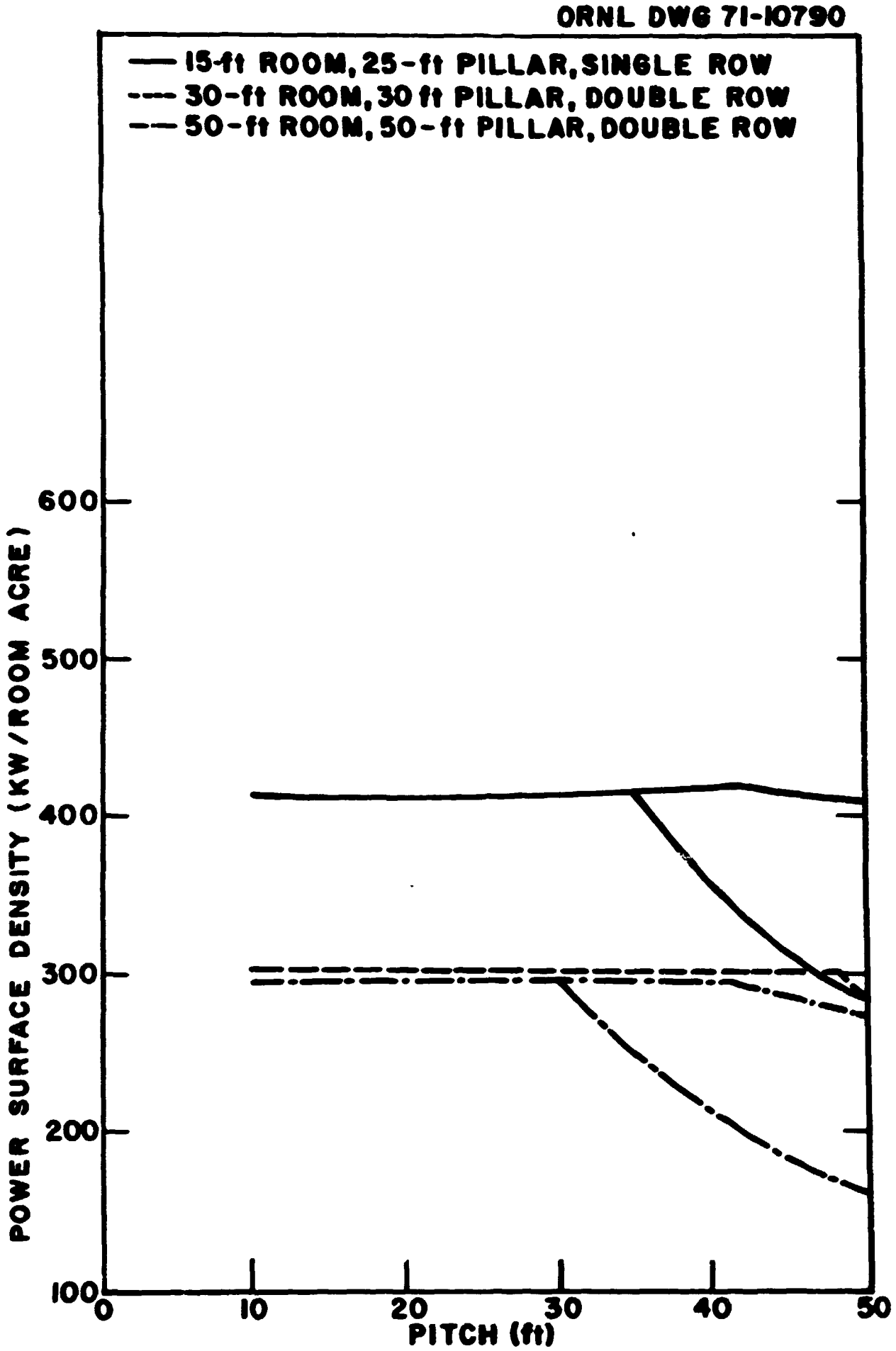

Fig. 3.13. Comparison of Maximum Permissible Power Surface Density Based on Room Floor Area for Different Room Sizes, 6-in.-diam Cans, and 10-year-old Waste.

gross acre and power per package. The particular waste under consideration has a maximum permissible temperature of about 1100°F and a thermal conductivity of 0.25 Btu hr^{-1} ft^{-1} $(°F)^{-1}$, the lowest values for any of the proposed wastes. It is observed that this waste can be quite restrictive for powers above 5 kW per package. One of the "better" wastes would remove this restriction for power levels up to 7 kW. Even without the removal of this restriction, a power surface density of 150 kW/acre can be achieved for power levels up to 5 kW.

Figures 3.12 and 3.13 show a comparison of results for 15, 30, and 50-ft rooms, the latter two having two rows of packages and the former a single row down the middle. It is observed that there is not much difference in power per gross acre for a particular power per package; the 15-ft room is slightly better than the 30-ft room, which is, in turn, somewhat better than the 50-ft room. There is a greater fractional difference in power levels, with the 50-ft room being better than the 15-ft room and the 15-ft room being better than the 30-ft room.

Figure 3.13 shows that, based upon the amount of salt that must be mined, the 15-ft room is about 30% better than the other two rooms.

The above results pertain to a 10-year-old waste. The shorter effective thermal-power half-life of younger waste allows a greater power surface density. For instance, a one-year-old waste has a permissible loading of about 350 kW/acre, but the amount of waste required to produce this higher power level is only one-third that of 10-year-old waste. Therefore, it appears more economical to put off burial to the 10-year limit. If all waste is 10 years old at burial, the proposed 1000-acre site will accommodate the amount accumulated through the year 2000.

3.4.2 Results of the Sensitivity Study

Sensitivity studies have thus far considered perturbations in the following parameters: (1) shale layer thickness above and below the waste package (see Fig. 3.2), (2) room content (crushed salt and void, bedded salt and void, all bedded salt), (3) backfill around waste container, (4) mine loading sequence, and (5) thermal conductivity (temperature, anisotropy, radiation damage, and general uncertainty effects).

The existence of shale layers close to the waste package causes some concern since these layers tend to insulate the enclosed region (because of the low thermal conductivity of shale as compared with that of salt). The layer thicknesses used for the typical case are considered to be maximums. Removal of one or both layers nas little effect on the temperatures; the maximum change in the salt temperature is only 9°F (2%).

Variations in room content have a somewhat greater effect. The most severe condition expected with regard to temperatures near the waste package is that used for the typical case. With time, the void will be replaced with salt and the crushed salt will recrystallize, thereby improving the thermal conductivity substantially. If this condition existed from the outset, the peak temperature at the container surface would be about 30°F (8%) lower; and, at the point of maximum positive difference, which is located a few feet above the pillar, the peak temperature would be about 14°F (6%) higher as compared with the typical case.

When the waste package is placed in the salt, there will be an annular clearance around the container that must be backfilled with some reasonably good thermal conductor. If crushed salt, which has been proposed for this purpose, is used, the thickness of the annulus might be about 2 in. The thermal conductivity of typical crushed salt is much less than that of bedded salt. If the lower value persisted, the peak temperature rise in the waste would be about 870°F, and it would occur at about 5 years. This condition, although more severe, appears to be acceptable. Actually, based on experiments in the Lyons salt mine,[4] it is expected that the crushed salt will revert to bedded salt within a few months as a result of temperature and pressure effects. Under these conditions, the waste temperature rise would peak even sooner but at a value less than 870°F.

A mine loading sequence was simulated in a two-dimensional (RZ) calculation by adding, at two-year intervals for a total of 26 years, concentric equal-radial-width annuli to make up the disk source shown in Fig. 3.4. This accelerated loading-rate scheme resulted in very little difference in temperatures as compared with the instantaneous loading scheme used in the typical case. Although further loading sequence studies must be performed, it appears that the anticipated sequences will not have a significant effect.

The thermal conductivities used in the typical-case two-dimensional (RZ) calculations presumably should be increased by about 50%, based on recent geothermal flux measurements.[5] This was done in one calculation. Peak temperatures adjacent to and near the center of the disk source were 42°F (16%) less but occurred at about the same time. At a distance from the source the temperatures peaked sooner, but the percentage differences were smaller.

Thermal conductivity anisotropy in shale was included in a two-dimensional (RZ) calculation, assuming that the ratio of horizontal to vertical thermal conductivity was 1.5. Based on results of recent experiments,[6] the ratio might be this high at 74°F; however, at the higher temperatures that will exist, the ratio is expected to be less.[7] The results of the calculation indicate a peak temperature rise of 3.3°F at a position 1750 ft from the edge of the mine as compared with 2.5°F without anisotropy. Temperatures close to the source and near the center of the mine all the way to the earth's surface were essentially the same. Thus, it appears that anisotropy effects are negligible.

Gamma radiation of salt will presumably reduce the thermal conductivity, perhaps by a significant amount. However, at present, it is believed that migration of the brine through the irradiated salt will reduce the radiation damage by a large factor. Preliminary estimates indicate that the net change in thermal conductivity will not present a significant problem.

3.5 Future Studies

The various studies conducted thus far in connection with the Waste Repository indicate that the concept is technically feasible with regard to containment capability. Future studies will be aimed at increasing the detail and improving the accuracy of the models and methods of analysis so that waste storage economics can be optimized while maintaining the required high level of confidence in the containment. Containment integrity analyses will be continued after operation of the mine commences. These studies will make use of experimental data obtained from the site to

determine whether the actual temperatures, displacements, etc., are in satisfactory agreement with predicted values.

The overall thermal analysis program for the next several years can be divided into the following general categories: (1) improvements in the modeling of the Repository, (2) improvements in the numerical solution, (3) development of more precise criteria, (4) sensitivity studies, (5) parametric studies, and (6) development of a mine-management computer program.

3.6 References

1. W. D. Turner and M. Siman-Tov, HEATING3 - An IBM 360 Heat Conduction Code, ORNL-TM-3208 (February 1971).

2. S. Levy, Use of Explicit Method in Heat Transfer Calculations with an Arbitrary Time Step, (General Electric Technical Information Series), 68-C-282 (1968).

3. J. Douglas, "Alternating Direction Methods for Three Space Variables," Numer. Math. 4, 41 (1962).

4. R. L. Bradshaw and W. C. McClain (eds.), Project Salt Vault: A Demonstration of the Disposal of High Activity Solidified Wastes in Underground Salt Mines, ORNL-4555 (April 1971).

5. Preliminary data, not for public inspection or quotation. Transmitted by Robert Schneider, U.S. Department of the Interior, Geologic Survey, to R. L. Bradshaw, Jan. 15, 1971.

6. J. H. Sass, letter to W. C. McClain, March 22, 1971.

7. Personal communication with W. H. Diment, U.S. Geological Survey, Rochester, N.Y., Apr. 5, 1971.

4. ROCK MECHANICS ANALYSIS

W. C. McClain

In the case of the Repository, it is the salt formation and the surrounding rocks, especially the thick overlying shales, which ensure long-term containment of the wastes. In Sect. 2, some of the natural conditions and processes that could lead to a breach of containment were discussed. As a direct result of the operation of the Repository, the rocks in the immediate vicinity will also be subjected to certain conditions that they have not previously experienced. Of course, these induced effects must be examined in considerable detail and evaluated for any situation which could potentially lead to a breach of containment. The first of such effects is the thermal transient, the fairly long-term (but still transitory) increase in temperature around the Repository, which was described in Sect. 3. The second effect is the mechanical deformation of rocks, which is discussed here.

The salt formation and the surrounding rocks, especially those overlying the Repository, will experience a sequence of transient and permanent displacements and strains. These deformations will result from the combined effects of (1) the designed closure of the mine openings, where the plastic creep deformation of the support pillars, accelerated by the elevated temperatures, allows the room ceilings to rest on the backfill salt, eventually reconsolidating and recrystallizing it; and (2) the bulk thermal expansion and induced thermal stresses caused by the transient elevation in temperature.

4.1 Preliminary Estimates

In an effort to quantify these effects, primarily for the purpose of scoping the required analysis, a series of preliminary calculations was made. With respect to the mine closure, the underground mine pattern and layout have not been finalized; however, the maximum permissible extraction ratio will be 50% – possibly it will be somewhat less. Although no experience with regard to complete backfilling of mine space with crushed salt exists, we feel confident that at least half of the excavated material

can be utilized. For these conditions, a 15-ft mining height was assumed; and, after the backfilled salt reconsolidates to 100% of its original density, the maximum mine closure would be 3-3/4 ft. The rate of this mine closure was estimated, based on extrapolation of the Project Salt Vault pillar deformation measurements, and is shown on the solid line in Fig. 4.1. This curve, which was based on a maximum closure of 4 ft instead of 3-3/4 ft, shows that the first foot of closure occurs about 2 years after the waste has been deposited; slightly more than half occurs during the first 10 years, while 100 years is required for the closure to be 95% complete. The surface subsidence behavior for this type of mine geometry and mine closure can be predicted from experience in the mining industry, especially in coal mines. If the mine closure were the only effect, and if the mine were completely filled with waste at one time rather than over a 20-year period, a very broad, flat, saucer-shaped subsidence basin (i.e., a basin with respect to the original ground elevation, not an actual closed depression on the surface) would be created over the Repository site. The center of this subsidence area would be flat, and there would be a transition zone, perhaps 1500 ft wide, all the way around the entire Repository site. The rate at which this surface subsidence formed would be about the same as that shown on Fig. 4.1, and the maximum subsidence in the flat central portion would be very nearly equal to the mine closure. The effects of the individual pillars would extend, at most, a few tens of feet vertically above the mine level; beyond this area, the rocks would settle uniformly.

The thermal expansion effects can be estimated by integrating the predicted temperature profiles and applying the coefficient of thermal expansion of the various rock types. The result of this calculation, which must be considered very preliminary because complete data on thermal expansion coefficients at this site are not yet available, is shown as the dashed line on Fig. 4.1. Neglecting all other effects as before, the thermal expansion of the entire rock column above and to a considerable depth below the mine would cause the ground surface to first rise gradually, reaching a maximum of a little over 5 ft after about 200 years, after which the surface would very slowly return to its original elevation as the heat

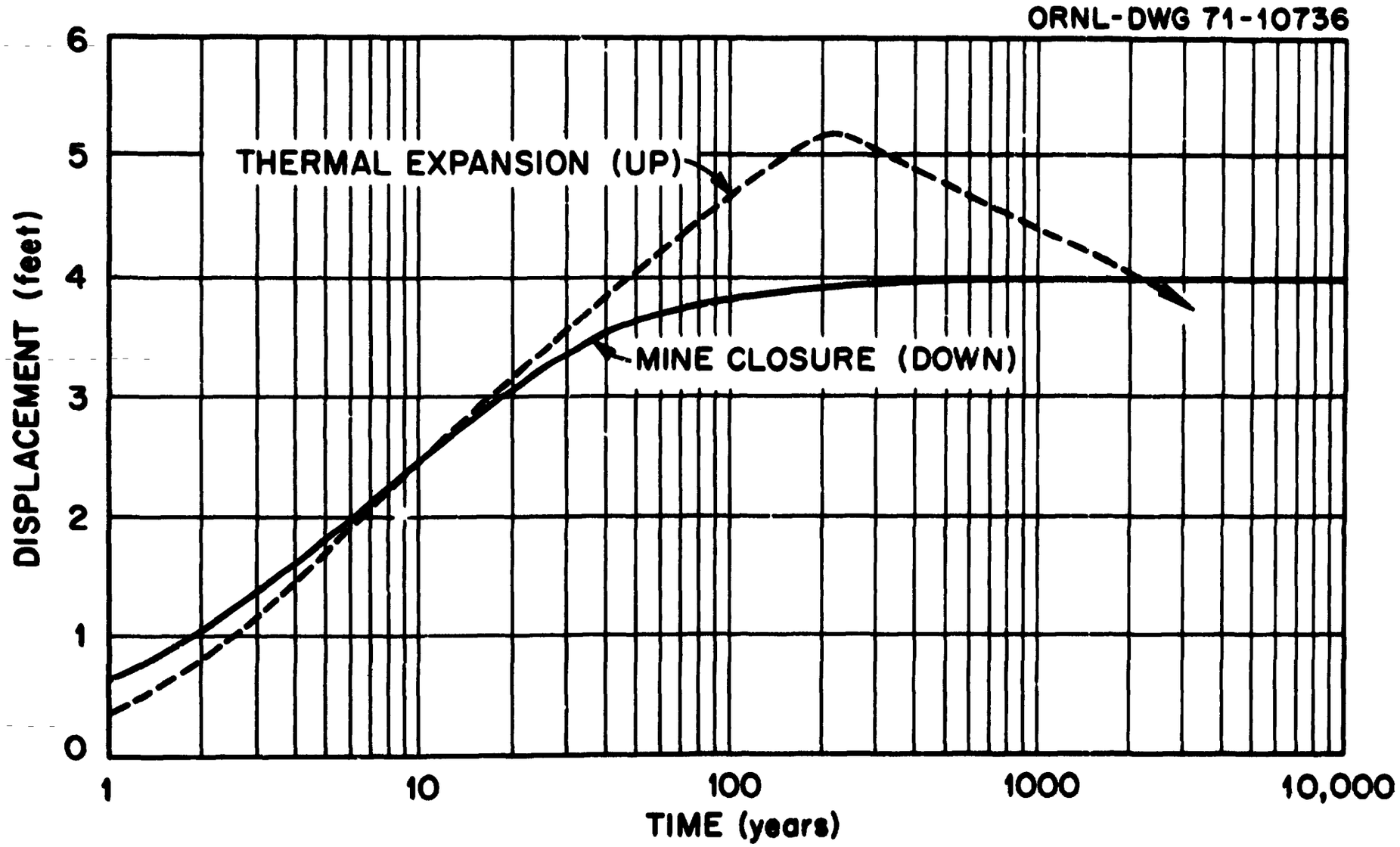

Fig. 4.1. Comparison of Mine Closure and Thermal Expansion.

load is dissipated. This process would require more than 15,000 years to complete.

The actual behavior of the ground surface will be the combination of the two effects. Using the two curves of Fig. 4.1, it can be seen that the downward subsidence is almost exactly canceled out by the upward thermal expansion for the first 30 to 40 years. Thereafter, the expansion effects exceed the subsidence, producing a net uplift of the surface which reaches a maximum of about 1 ft slightly over 200 years after initial operation of the Repository. Following this maximum, the surface will very slowly subside, pass through its original position, and, eventually (thousands of years later) reach a final position perhaps 3-1/2 ft below its original elevation.

4.2 Consequences

It is difficult to believe that the development of a broad, slight subsidence at such a slow pace as that just described would create any adverse situation on the surface. The topographic relief over the site amounts to over 50 ft, and even the groundwater table exhibits a relief greater than 25 ft. The principal factor, however, is the very slow rate of deformation and, consequently, the time available for adjustments to take place. For example, the average rate of subsidence is only about three times greater than the estimated rate of current surface lowering due to natural erosional processes. The groundwater relationships in the area (that is, structure of water table, direction of flow, etc.) may be slightly influenced by this slow subsidence, but probably by an amount less than that resulting from natural causes. Certainly, no swamp or lake will be created over the Repository. The possible effects of subsidence on groundwater relationships and surface structures, especially the long linear structures such as pipelines, railroads, etc., which are particularly susceptible to subsidence damage, will be evaluated in detail as a part of the on-going rock mechanics analysis program.

The primary concern with regard to the rock deformations does not include the consequences of the small and slow surface movement, but

chiefly involves the displacements and strains that must be absorbed by the overlying shales, principally in the transition zone above the boundaries of the Repository. Specifically, we are interested in whether those deformations, in combination with the increased temperatures and any physical alteration resulting therefrom, represent a potential mechanism whereby the integrity of the barrier provided by shales can be breached. For instance, is it possible that a throughgoing fracture which would connect water in the Stone Corral or other near-surface aquifers with the salt formation could be developed, or will the vertical permeability of the shale be increased by the development of a large number of small fractures? A rough calculation, based on the surface deformations just described, indicates that the possibility of such fracturing is extremely remote. The maximum strain rates in the shale will occur during the initial 200-year uplift period and will be on the order of 5 μ-strain per year. The maximum net strain, which will amount to about 0.5%, will not be reached until the subsidence is completed. There is evidence from the mining industry to suggest that in-situ shales can easily absorb strains of at least this magnitude even when applied over time spans of a few months. Furthermore, over long time spans such as the thousands of years available in this case, shale rocks are capable of slow plastic deformation, which further drastically reduces the potential for widespread fracturing.

In order to define more rigorously the conditions to which the shale, as well as the salt and other rocks, will be subjected and to evaluate the behavior of the rock system and the potential for fracturing, a fairly extensive rock mechanics analysis program will be carried out using the most sophisticated techniques currently available.

4.3 Plan of Investigation

The rock mechanics analysis will be carried out in two principal parts. The first part, which is already in progress, is called the semi-empirical analysis. It consists of a series of computer models, the first of which is a detailed three-dimensional simulation of the mechanical behavior of the Project Salt Vault experimental area. This analysis is similar to, but considerably extends, the two-dimensional analysis

completed as a part of the experiment[1] that was the basis for the preliminary estimate. The technique is to establish the in-situ mechanical and deformational properties of salt and the underground mine structure by correlation of the model results with the deformations actually measured in the mine during the experiment – hence the name "semiempirical." Once the behavioral properties of the salt have been determined, this computer program will be modified and extrapolated to simulate the closure of the entire high-level mine, including the effects of backfilling in the rooms with crushed salt, the anticipated mine pattern, and the schedule of utilization. This calculation will provide a mine closure curve, similar to the closure curve shown in Fig. 4.1, for each small (200-ft-square) segment of the Repository and a considerable portion of the surrounding area. These mine closure curves will then be used as input into yet another model; in this case, some standard subsidence calculation, such as Salamon's frictionless laminated model[2] would be used. The effects of thermal expansion will also be included in this calculation, using temperature data from the thermal analysis program and coefficients of thermal expansion obtained in tests of rock properties. The results of this calculation will provide a considerably improved estimate of the surface displacements, both uplift and subsidence, over the entire area as a function of time. From this, the subsurface zones (especially in the shale) that experience the maximum strains or maximum strain rates can be identified and those strains and strain rates can be estimated. Furthermore, it is anticipated that some parametric studies will be undertaken in order to determine whether a different mining pattern, layout, or schedule would significantly reduce the deformations in the overlying rocks.

As mentioned earlier, work on this "semiempirical" portion of the rock mechanics program is currently under way. The three-dimensional analysis of the Project Salt Vault experiment has been completed, and the program for modeling that behavior has been prepared. The model is presently being correlated with the measured deformations, a process that can become tedious at times. Since both the extrapolation of model to the Repository area and the subsidence calculation programs are straight-

forward, we expect this portion of the analysis to be completed by about the end of 1971.

The semiempirical approach suffers from several deficiencies that are primarily related to the subsidence model. In general, these models use only average rock property data for the entire rock column. This means that the predictions made regarding underground strains and displacements are not very accurate. However, such models (and Salamon's is one of the best) were developed for predicting surface subsidence in mining operations and have met with considerable success in that area. Another major theoretical deficiency in this approach is that the mechanical effects and the thermal effects are simply superimposed and are not coupled in any way.

For the reasons given above, the second part of the rock mechanics program, the "finite-element analyses," will be undertaken. These analyses will consist principally of two-dimensional finite-element calculations for the zones of maximum strain or strain rate defined in the previous analysis. The "models," in this case, will incorporate specific geological units with physical property parameters for each unit determined from laboratory tests on fresh specimens obtained from the next core hole to be drilled at the site (No. 3). Both thermal plastic-elastic and thermal viscoelastic analyses will be used with the temperature data coupled in one direction; that is, the thermal effects on the physical properties will be included, but the mechanical effects on the thermal properties will be omitted since they are considered to be insignificant at this time – a point which will be confirmed as a part of the rock testing program. A limited amount of three-dimensional finite-element work will be done to confirm the validity of the plane-strain assumptions of the two-dimensional calculations. In addition, it may be advantageous to undertake a simplified and large-node-spacing three-dimensional calculation of the entire Repository area; this would serve as an independent check on the semiempirical analysis. The results of this finite-element portion of the program will provide detailed histories of the displacements, stresses, and strains in the zones of interest and in the rocks of interest – the shales.

Detailed discussions were recently held with a group of consultants concerning this portion of the program, and a formal proposal is expected in the very near future. We should then be able to start the work by December 1, 1971. It is estimated that both the analyses and the rock testing associated with it could be completed in about 18 months, or by May 1973.

4.4 Evaluation of Fracture Potential

The results obtained from the rock mechanics analysis will be interpreted and evaluated in terms of the possibility of a breach of the long-term containment by the creation of a throughgoing fracture or by any other mechanism, by comparing the predicted strains with appropriate failure criteria. These criteria will be established first as a portion of the rock testing program, using standard testing techniques to determine failure envelopes for the various rock types and, in this case, as a function of temperature and for time-dependent deformations. Unfortunately, there is, in general, very few data available concerning the effects of deformations of rocks between the mining level and the surface. However, an effort will be made to correlate the laboratory-determined failure criteria with in-situ field conditions, or perhaps to derive additional criteria by first thoroughly examining the published literature and querying potential sources of unpublished data, such as the U.S. Bureau of Mines, for any relevant information. It is quite likely that this search will turn up a few instances that are particularly applicable to the analysis of the Repository; for example, cases in which similar rocks have been subjected to similar deformations would be reviewed. These few cases will be examined in detail by site visits, interviews in which the investigators are involved, and possibly ever additional on-site investigations.

This general plan for the rock mechanics analysis and investigations has been reviewed by a group of advisors who felt that it would provide an adequate basis for evaluation of the effects of the operation of the Repository. Similar reviews will take place periodically as the investigations proceed.

4.5 References

1. W. C. McClain and A. M. Starfield, "Analysis of Combined Effects," pp. 291-316 in Project Salt Vault: A Demonstration of the Disposal of High-Activity Solidified Wastes in Underground Salt Mines, ed. by R. L. Bradshaw and W. C. McClain, ORNL-4555 (April 1971).

2. M. G. D. Salamon, "Elastic Analysis of Displacements and Stress Induced by the Mining of Seam or Reef Deposits," J. South African Inst. Min. and Met. 64(4), 128-149 (November 1963).

5. ROCK PROPERTY TESTING

T. G. Godfrey and D. L. McElroy

The various analyses of the behavior of the salt mine Repository and the evaluations of the geologic containment require both a general knowledge of and specific quantitative data on the physical and mechanical properties of the rock formations involved. Some of this information has been obtained using specimens from the cores of holes 1 and 2 at the site, which were drilled primarily for geologic correlations. However, most of the testing will be carried out using specimens from the next hole (No. 3), which will be designed and drilled primarily to obtain proper specimens for these programs.

Table 5.1 summarizes the types of tests completed to date on specimens from cores 1 and 2. Standard core analyses, including porosity, permeability, density, moisture content, and thermal dehydration, all at various depths, were performed by Core Laboratories, Incorporated, of Dallas, Texas.[1] Thermal conductivity determinations at various depths were carried out at room temperature by U.S.G.S. Menlo Park.[2,3] Thermal expansion measurements and uniaxial compression tests at room temperature and at 150°C were made by U.S. Bureau of Mines personnel at Minneapolis.[4] The results obtained from these test programs are summarized below.

Figure 5.1 is a plot of the percent porosity vs depth from the surface for cores 1 and 2. This porosity is open porosity since the specimens will acquire and lose nearly the same percentage of water.[1] As shown by the figure, the porosity remains near 20% until one reaches the bedded salt level. Within the bedded salt level, it is generally less than 2%; below the salt, it rises to the indicated values.

The densities of these samples were measured and found to be in the range 2.16 (salt) to 2.95 g/cm^3.[1] Measurements of the air permeability, using a Hassler cell for sample confinement, yielded values that were quite low.[1]

After these tests had been completed, the samples were placed in a retort to measure the water of hydration and crystallization and the temperature at which water is first released. Figure 5.2 illustrates

Table 5.1. Summary of the Types of Tests Performed on Cores from AEC Test Holes 1 and 2

	No. of Samples	
	Core 1	Core 2
Standard Core Analysis vs Depth		
Porosity	43	15
Permeability	43	15
Density	43	15
Water saturation	43	15
Water release-temperature	43	15
Thermal Conductivity vs Depth		
Wet	82	25
Dry	28	4
Anisotropy	10	
Thermal Expansion at ~795 ft	2	
Uniaxial Compression at ~795 ft		
25°C	7	
150°C	5	

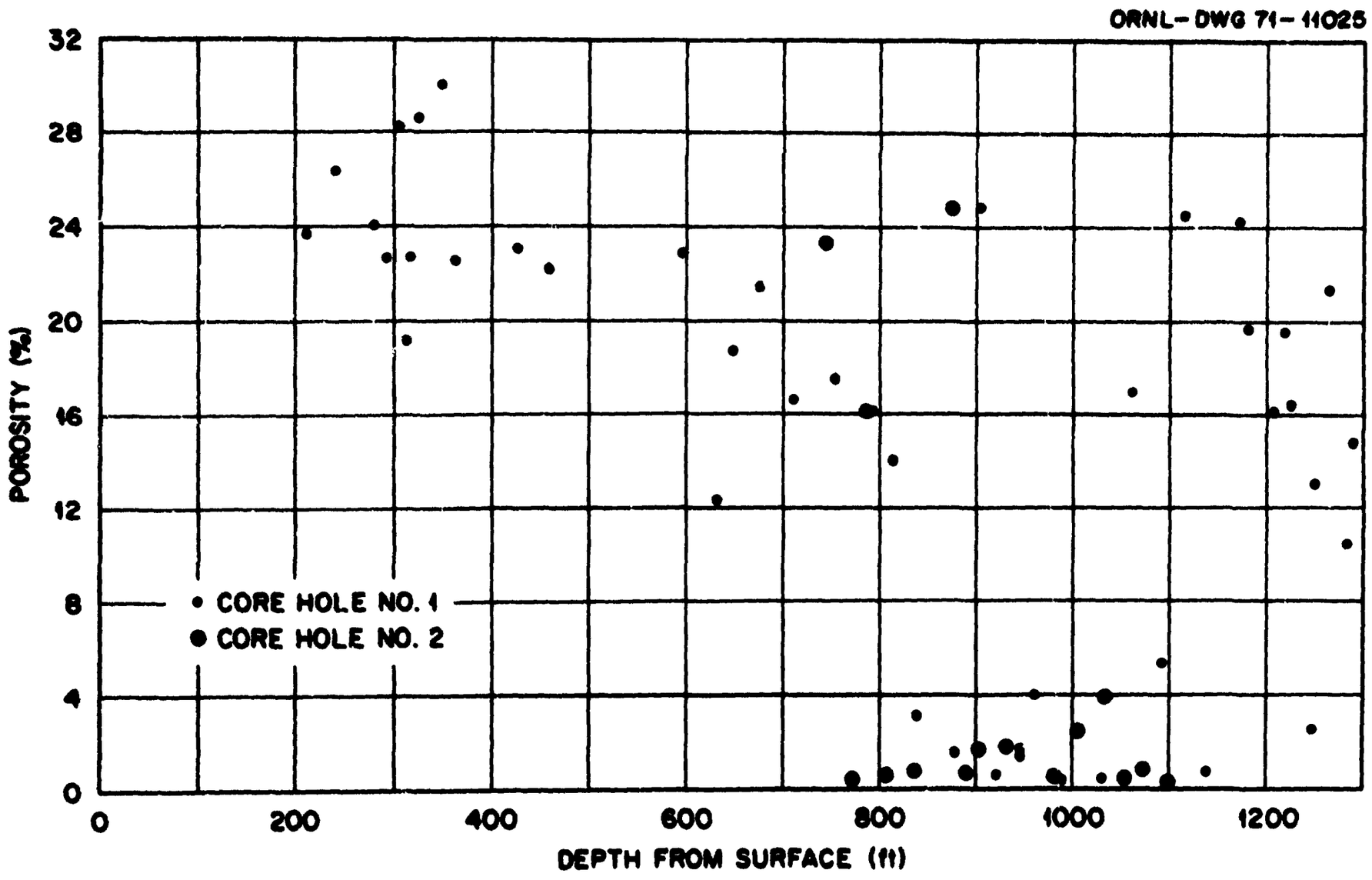

Fig. 5.1. Percent Open Porosity vs Depth from the Surface for Core 1 and Core 2.

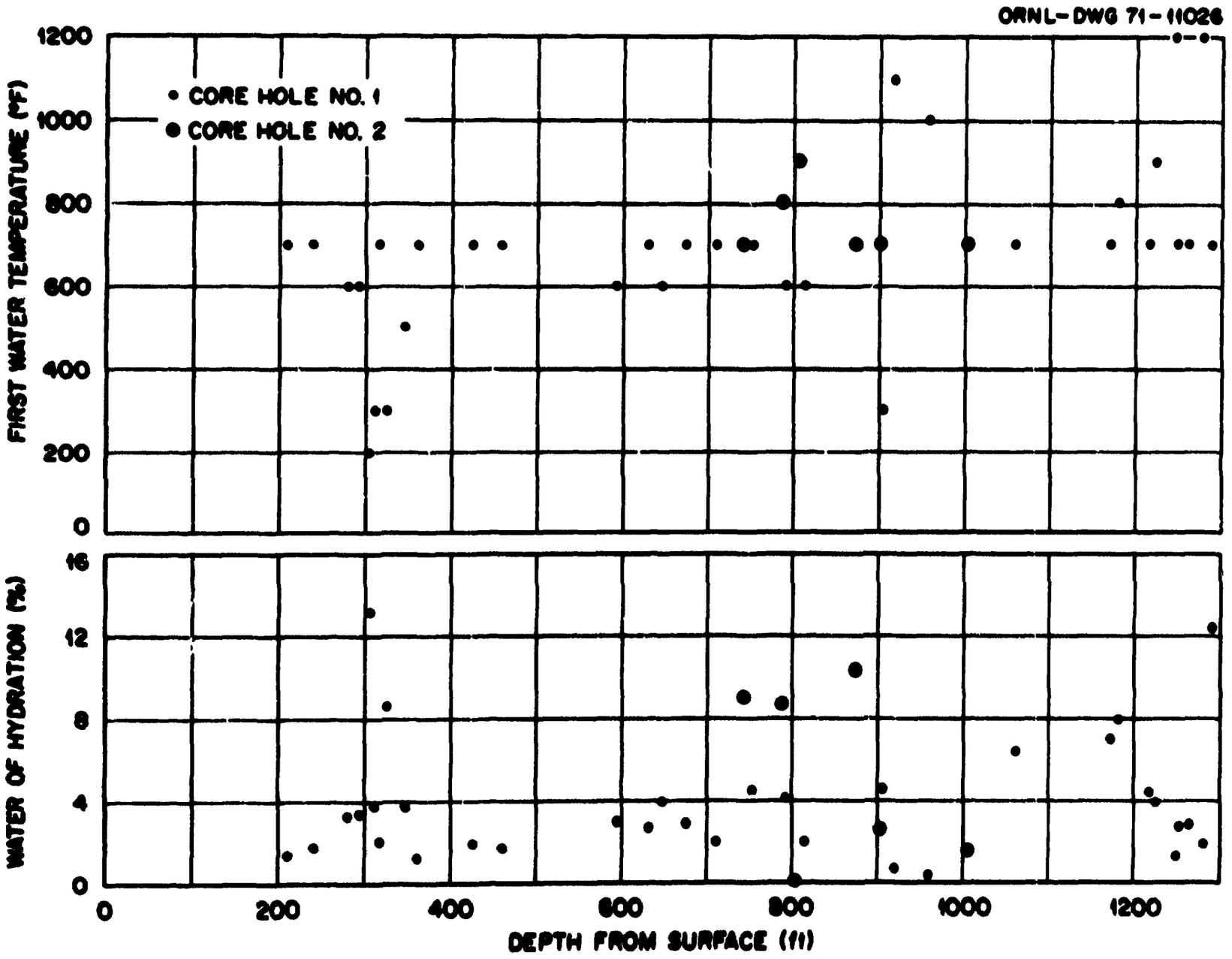

Fig. 5.2. Water of Hydration and Temperature of Initial Release vs Depth from the Surface for Core 1 and Core 2.

these results as water of hydration and temperature of the initial water release, both vs depth from the surface. In the shale region, the water of hydration was generally less than 4% with a release temperature near 700°F. An exception occurred in the Stone Corral formation, where larger water levels at lower temperatures were noted. Very low water contents were found in the salt region, and only then at high temperatures.[1]

Figure 5.3 shows values of the thermal conductivity, λ, at room temperature for wet samples vs depth from the surface for both cores.[2] The thermal conductivity units are watts per centimeter-degree. (For these units, copper has a λ of 4 and UO_2 has a λ of 0.08). Core 1 values are the open symbols, and core 2 values are the circled symbols for the salt and shale; "other" includes siltstone, dolomite, gypsum, anhydrite, or limestone. As one proceeds down core 1, the λ for shale seems to increase and then decreases; the average value is near 0.025 W/cm-deg but has a large spread. The λ of the salt is high, averaging 0.053 $\pm$ 22% for core 1. Core 2 was only tested below 700 ft but yielded similar average λ values: 0.058 $\pm$ 12% for the salt, and 0.023 $\pm$ 21% for the shale. The λ value for each core below the salt level is similar to that of its upper region. Though not shown here, the thermal conductivities for dry rock samples are 5 to 30% less than those for wet rock sample values.[2]

The λ values for the shale in the range 300 to 700 ft are for radial heat flow in the core – that is, for heat flow perpendicular to the core axis or parallel to the bedding planes. These radial values are plotted in Fig. 5.4. The line probe was also inserted along a core radius to obtain the axial λ values of this plot.[3] In every case, the axial values are lower. The ratios of the radial values to the axial values of λ are shown in the lower portion of Fig. 5.4. These ten measurements yield an average anisotropy factor of 1.38.

We have observed a similar effect for λ measurements made on Conasauga shale samples taken from 115 ft in the well Joy No. 1 at Oak Ridge.[5] Figure 5.5 shows comparative heat flow results for this material as a function of temperature and direction. These results confirm that anisotropy is a common feature of shales.

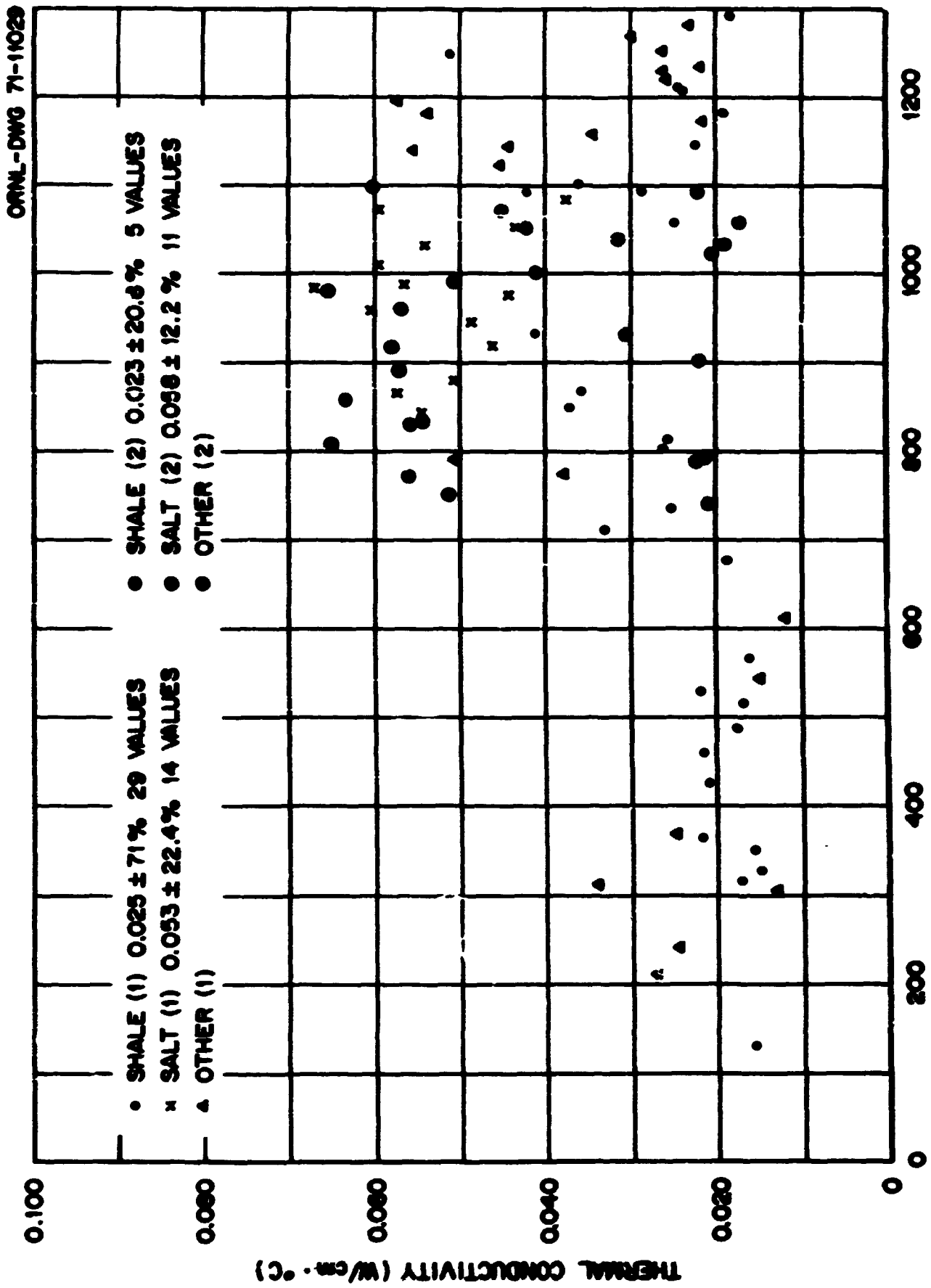

Fig. 5.3. Thermal Conductivities of Wet Samples of Core 1 and Core 2.

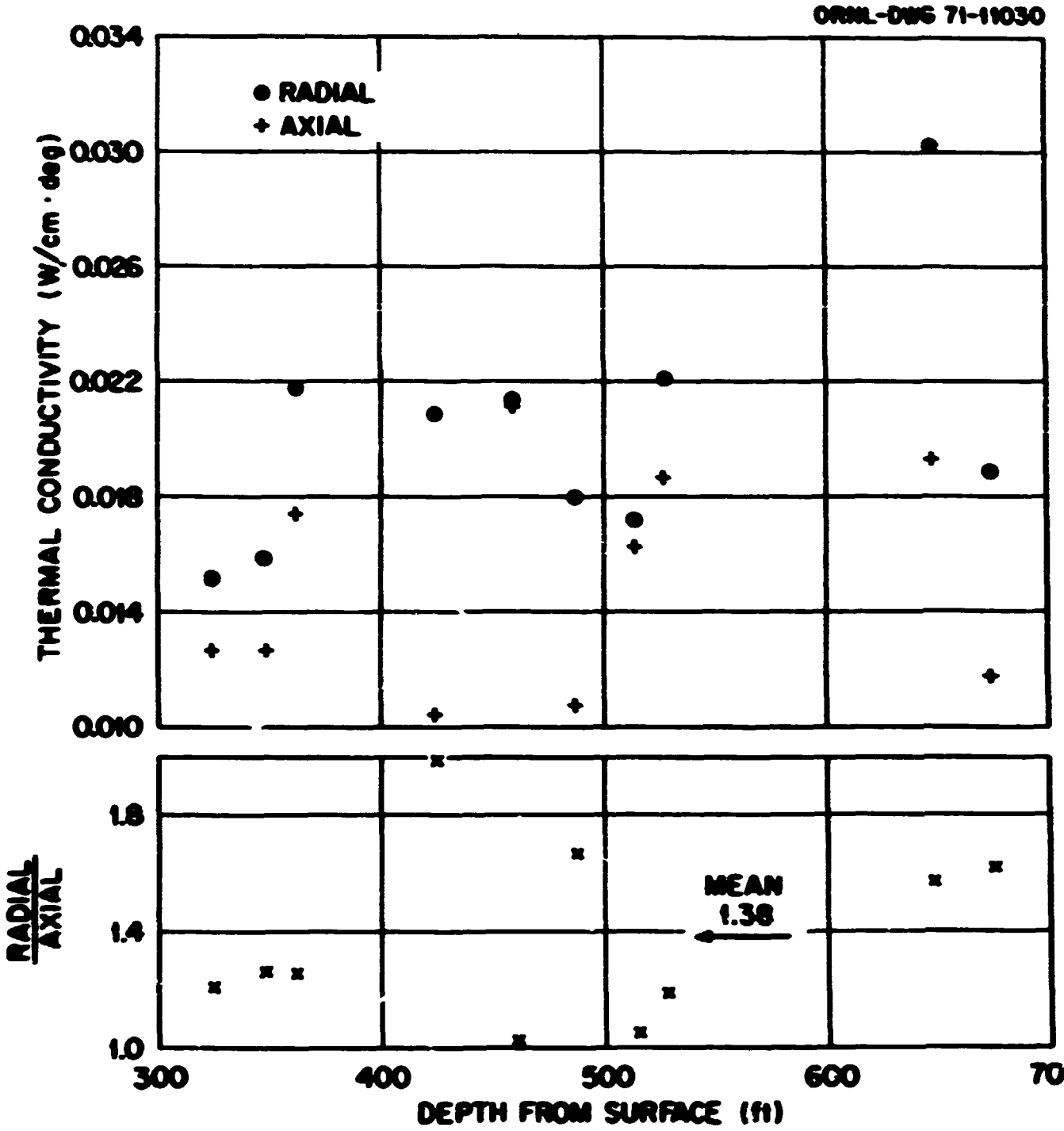

Fig. 5.4. Radial and Axial Thermal Conductivities of Wet Core 1 Samples Taken 300 to 700 ft Below the Surface.

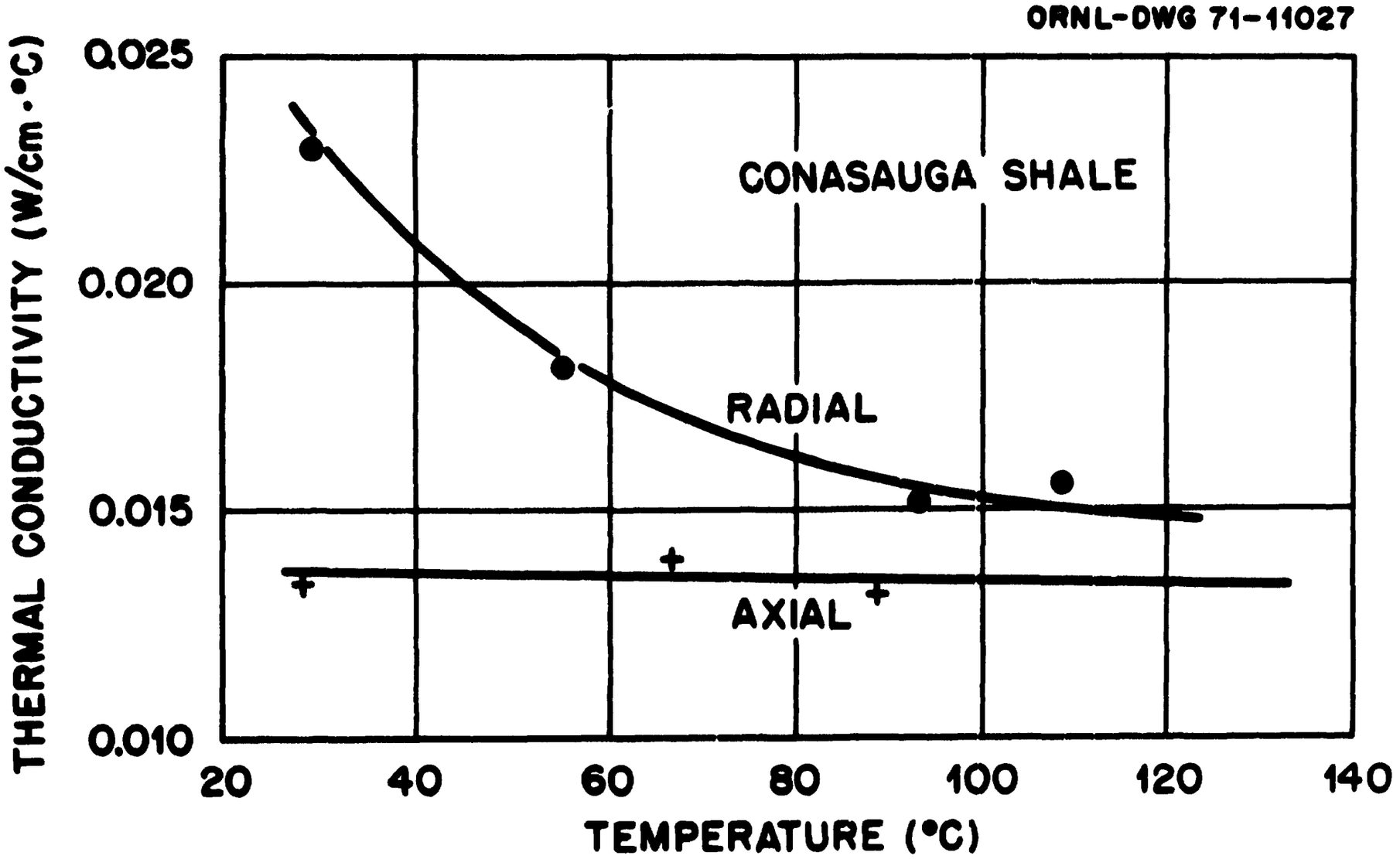

Fig. 5.5. Thermal Conductivity of Conasauga Shale as a Function of Temperature and Direction.

Figure 5.6 shows the percent thermal expansion vs temperature for two samples of shale from near the 795-ft level.[4] The expansion was measured in a quartz push-rod dilatometer with a differential transformer for length displacement detection. One of the specimens fragmented during heating above 225°C. The other specimen exhibited a slope change in this region. These data suggest an increasing coefficient of thermal expansion with increasing temperature. Below 200°C the coefficient is near 1.58×10^{-5} per °C.

In addition to these tests on the shale, several compression tests were conducted at room temperature and at 150°C. The diameter of the sample was 1 in., and 1- and 2-in. lengths were used. Figure 5.7 shows a typical stress-vs-strain plot for a test at room temperature. This particular specimen had a compressive strength of 12,300 psi and a Young's modulus of 3.6×10^6 psi. This figure shows the average values obtained at the two temperatures for these properties. The individual results exhibited considerable scatter and, for all intents and purposes, there were no significant differences in the deformation behavior at the two temperatures. However, it should be pointed out that these results may not be typical since the specimens were obtained from only one location and portions of the core had been degraded by drying and by several freeze-thaw cycles.

In addition to the standard core analyses, four specific series of tests are currently planned using specimens from core hole 3. It is quite likely that other tests will be added to this plan before the hole is drilled. In each of these programs the entire rock column down to several hundred feet below the salt section will be tested, although the major emphasis will be on the shales immediately overlying the salt (and included within it) and the anhydrite immediately below. The test areas are: thermal properties, mechanical properties, failure criteria, and mineralogical and geochemical changes.

1. Thermal Properties (Thermal conductivity, heat capacity, and coefficient of thermal expansion tests in the range 0 to 200°C). Where appropriate, anisotropic relations will also be included. This series will be performed by ORNL, and our present plan is

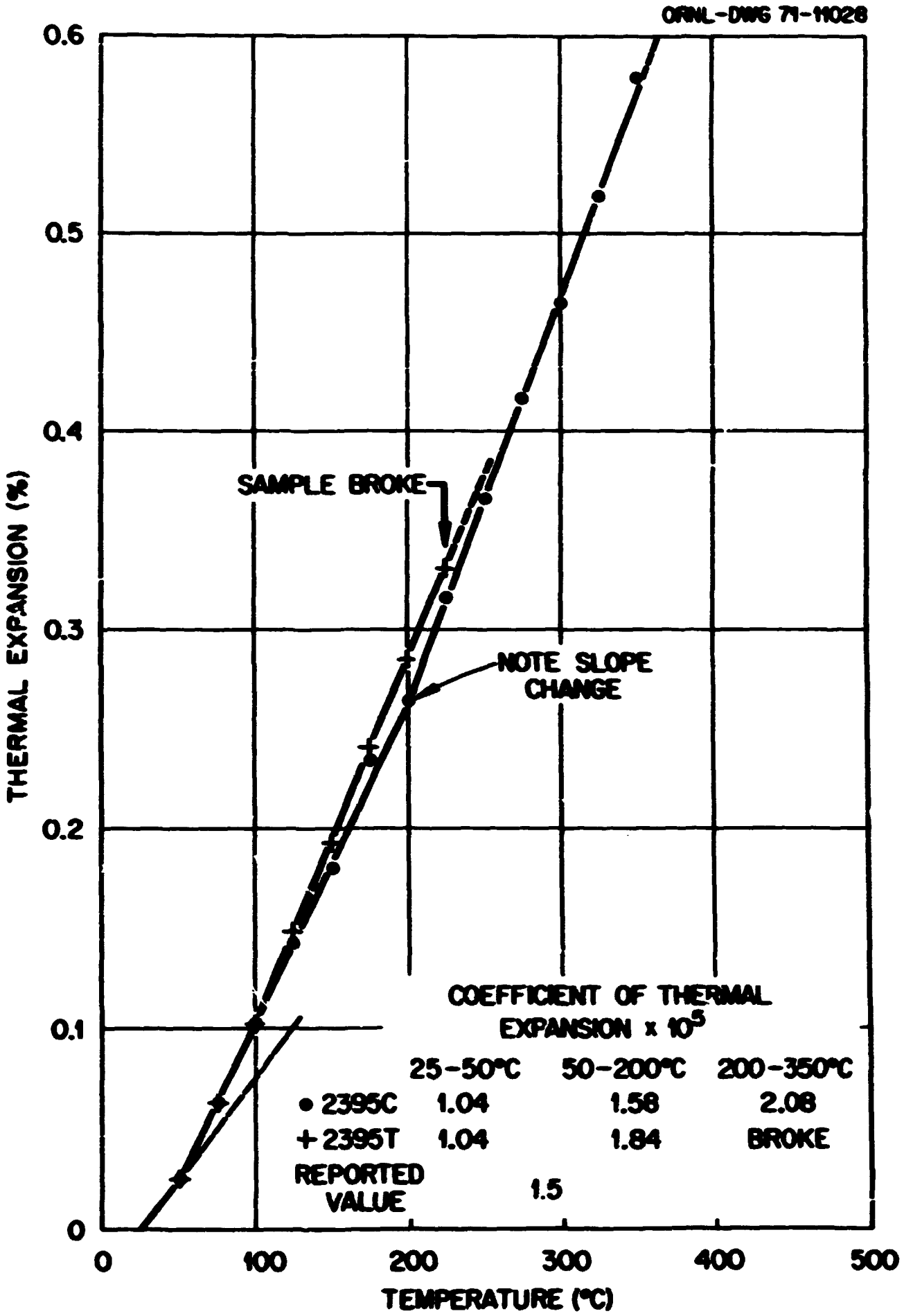

Fig. 5.6. Percent Thermal Expansion vs Temperature for Two Shale Specimens Taken from Near 795 ft in Core 1.

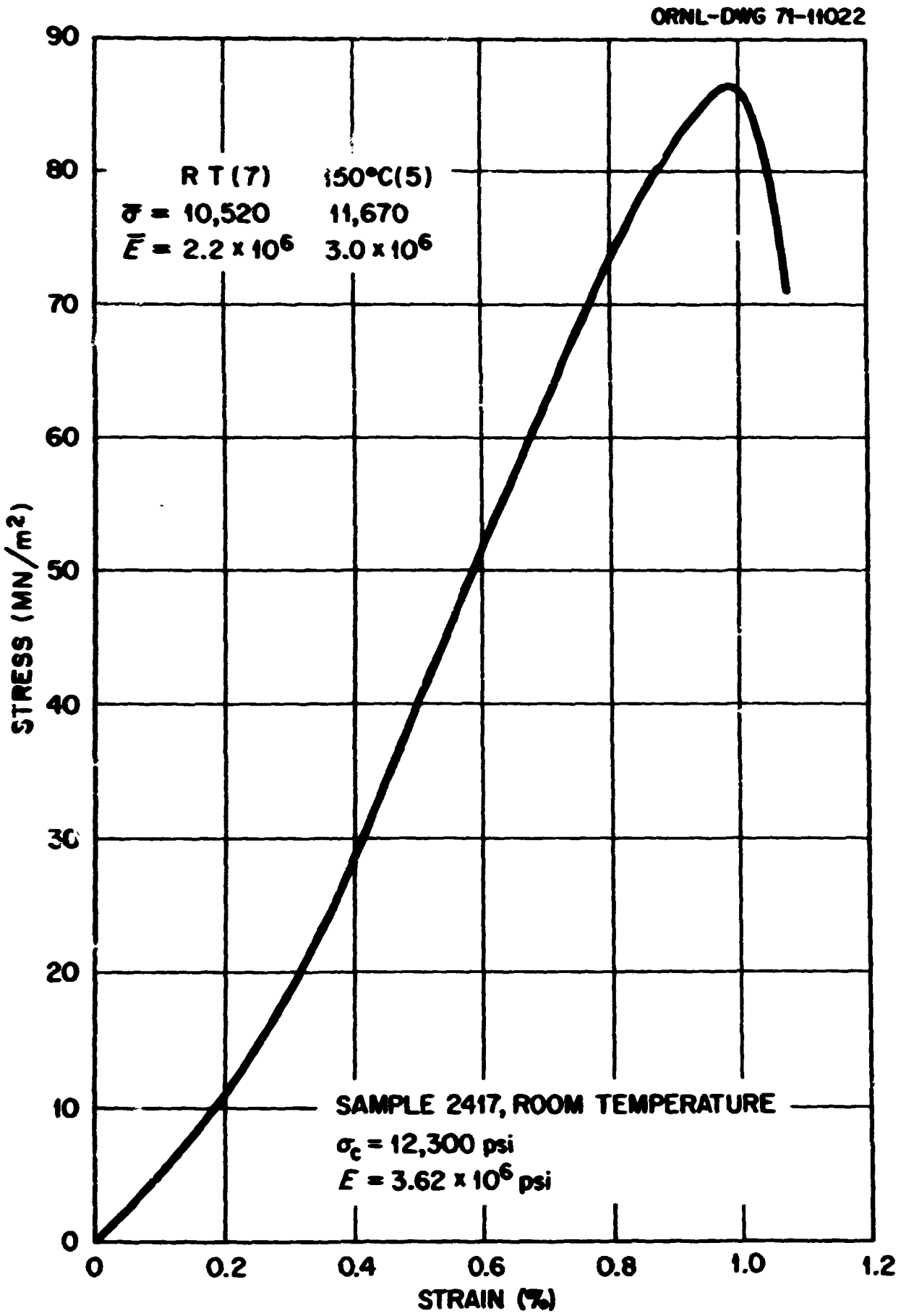

Fig. 5.7. Typical Compressive Stress-vs-Strain Results at Room Temperature for a Shale Specimen Taken from Near 795 ft in Core 2.

to use large bulk specimens (4 x 12 in.) to provide more appropriate input data to the rock mechanics analyses programs.

2. Mechanical Properties [Elastic moduli (with anisotropy), Poisson's ratio, yield stress, plastic limits, and selected creep or viscosity parameters]. These tests will also be carried out at elevated temperatures in order to establish the range of thermal effects on the properties. Tests at intermediate temperatures will be included as required, but it will not be possible to carry out replicated tests over the entire range of temperatures for each property for each rock type. These tests will provide the input parameters for the finite-element rock mechanics analysis and will be performed by the same group of consultants as part of that analysis.

3. Failure Criteria [Various strengths (shear, confined, compressive, uniaxial compressive, tensional, etc.), strain, creep-rupture strain]. Much of this testing program is simply an extension of the mechanical property testing and will be carried out at the same time as the program just described. Other parts and certain confirmatory tests will be performed at ORNL.

4. Mineralogical and Geochemical Changes (Mineral transformations, phase changes, dehydration of certain species, etc., and the secondary effects wrought by the altered hydrochemical environment resulting from these changes). This program is not yet sufficiently defined to describe in detail, but its objective is to evaluate the potential for, and consequences of, any gross change in the properties of the geologic materials due to the confining stress, induced strains, and especially elevated temperatures to which it will be subjected.

5.1 References

1. J. G. Evertson, Jr., Core Laboratories, Inc., Dallas, Tex., communication to E. E. Angino, Kansas State Geological Survey, Feb. 8, 1971.

2. Robert Schneider, U.S. Geological Survey, Washington, D.C., communication to W. C. McClain, ORNL, Mar. 15, 1971.

3. J. H. Sass, U.S. Geological Survey, Menlo Park, Calif., communication to W. C. McClain, ORNL, Mar. 22, 1971.

4. T. C. Atchison, U.S. Bureau of Mines, Twin Cities, Minn., communication to W. C. McClain, including a report by the Thermal Fragmentation Group entitled, "Some Elevated Temperature Tests of Wellington Shale," June 16, 1971.

5. J. J. Dell'Amico, F. K. Captain, and S. H. Chansky, Characterization and Thermal Conductivities of Some Samples of Conasauga Shale, ORNL-MIT-30 (Mar. 21, 1967).

6. FACILITY DESCRIPTION

B. F. Bottenfield, G. R. Renfro, and E. J. Frederick

In September 1970, Kaiser Engineers of Oakland, California, was engaged to participate, under the direction of ORNL, in a conceptual design of the Repository. That design effort was completed in April 1971, and the first draft of a "Conceptual Design and Safety Report" was issued in June with limited distribution.

Kaiser and ORNL are currently engaged in several design development studies to investigate further the feasibility of some aspects of the conceptual design.

The facility concept that will be described here may require some modifications as we progress further in engineering the facility. Such modifications are expected, at least at this time, to be minor. Future developments in the areas of public relations, safety analysis, and geologic-hydrologic investigations may also require some significant changes in the concept. In addition, detailed engineering development may impose some restrictions on the design.

6.1 General Description

The geographical relationship of Lyons to the state of Kansas is shown in Fig. 6.1. As this figure shows, Lyons is located essentially in the center of Rice County and Rice County is situated approximately in the center of Kansas. Lyons is served by three railroads. The Atchison, Topeka, and Santa Fe borders the site on the south; the Missouri Pacific penetrates the site near the western border (running north-south); and the St. Louis and the San Francisco serves Lyons on the south and west, although it does not adjoin the proposed Repository site. U.S. Highway 56 borders the site on the south.

The principal components of the Repository are as follows:

(1) Alpha-operations facility
    (a) Alpha waste receiving building
    (b) Mine operations building
    (c) Alpha mine (existing)

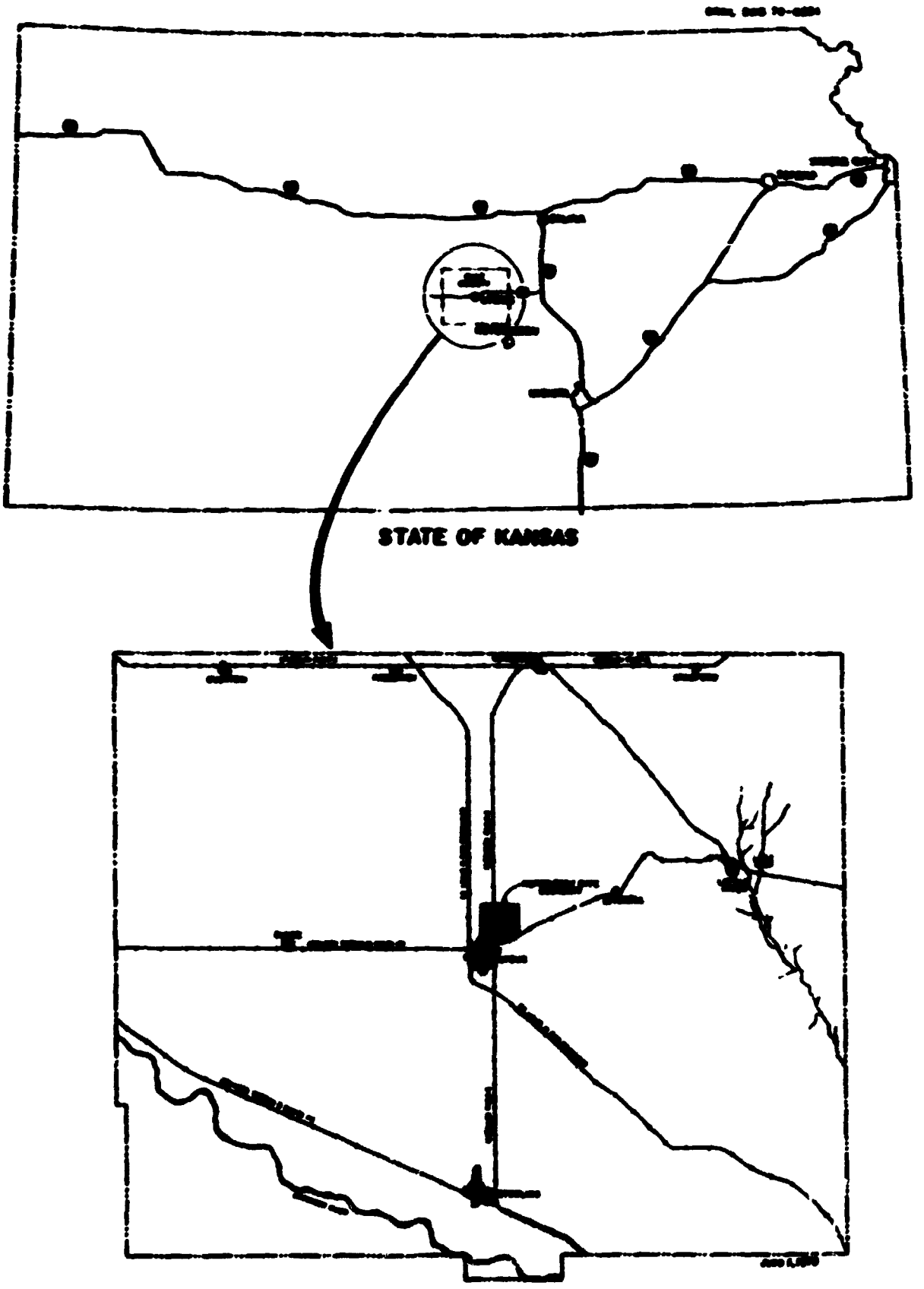

Fig. 6.1. Waste Repository in Salt: Area Location Diagram.

(2) High-level facility
    (a) High-level waste receiving building
    (b) High-level mine

(3) Support facilities
    (a) Repository administration building
    (b) Warehouse
    (c) Magazine
    (d) Utilities

The facilities and general layout are shown pictorially in the cutaway section of the Repository in Fig. 6.2. As shown, the alpha-operations facility is located in the southwest corner and the high-level facility is located in the northeast. The alpha waste receiving building will contain all the operations that are involved in receiving, unloading, inspecting, and conveying the alpha wastes to the mine for storage.

The alpha-M/M (men and materials) shaft will be approximately 18 ft in diameter and divided into three compartments, each separated from the others by a solid concrete divider. Half the shaft will be used to house the 12-ton M/M hoist and its cage for transporting men and materials into and out of the mine. Provisions will be included, as required, for future installation of salt hoisting capability in the M/M compartment. The other half is divided into two compartments; one will contain the 5-ton alpha waste hoist and cage for transporting the waste to the mine level, and the other will be used as a plenum for the introduction of approximately 62,000 cfm of ventilation air into the mine.

Separate stations will be provided at mine level for the alpha and the M/M compartments. Each of these stations will be isolated from the mine by air locks. At the base of the alpha-M/M shaft, the air supply stream will be divided for distribution to the alpha and the high-level mines.

The alpha mine consists of the existing workings of The Carey Salt Company mine; these workings will be cleaned up and used for the burial of alpha waste and storage of part of the salt from cleanup and further excavation.

The mine operations building will be located adjacent to the alpha waste receiving building and will provide space for changeroom, toilet,

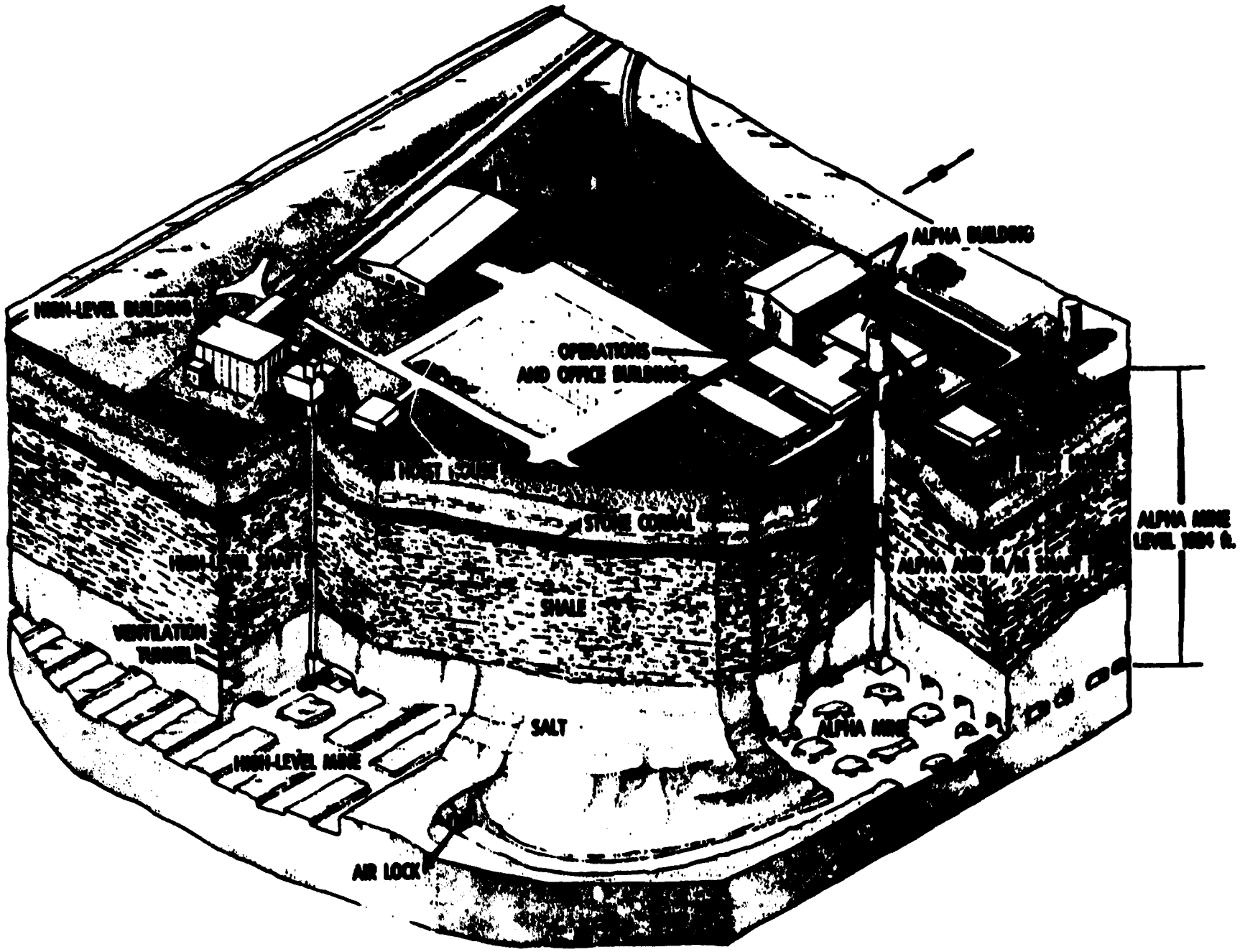

Fig. 6.2. Federal Repository.

and shower facilities for mine personnel, a personnel check station, offices for mine supervisors, a dispensary, a miners' lantern storage and repair shop, and a materials and equipment receiving and storage room with direct access to the alpha-M/M shaft. A full basement will be provided under the mine operations building to house the mechanical equipment serving the alpha-operations facility and for the Repository main switchgear, standby electrical power generation, and the central control and monitoring station. The floor space provided in this building, including the basement, will total approximately 10,700 ft^2.

The high-level waste receiving building will contain all the operations involved in receiving, cooling, and handling the loaded shipping casks; unloading the waste cans from the cask; and lowering the waste cans to the mine for burial.

The high-level shaft will be a 4-ft-diam concrete-lined shaft used for transferring the waste cans from the surface facilities to the high-level mine. The shaft will be equipped with a 10,000-lb-capacity hoist. Twin hoisting cables will be utilized to support the mine shaft cage to ensure that the load will not be dropped in the event a cable breaks. The high-level waste shaft will be an extension of the transfer cell confinement system. A shielded mine-level receiving station is located in the mine at the lower end of the shaft. The high-level waste will be buried in newly mined salt north and east of the existing Carey workings.

Support facilities, including the Repository administration (office) building, a materials warehouse, parking facilities, and a water storage tank are also shown. The location of the mine exhaust facilities is indicated in Fig. 6.3. A 6-ft shaft will serve as a duct for exhausting ventilation air from the mine to the surface for cleanup through high-efficiency filters and discharge to the atmosphere. The locations of the existing Carey mine shaft and the Project Salt Vault charging shaft are also shown. The Carey shaft, which can be used for initial access to the underground workings until additional shafts are sunk, will be used for emergency egress from the mine when the Repository is in operation.

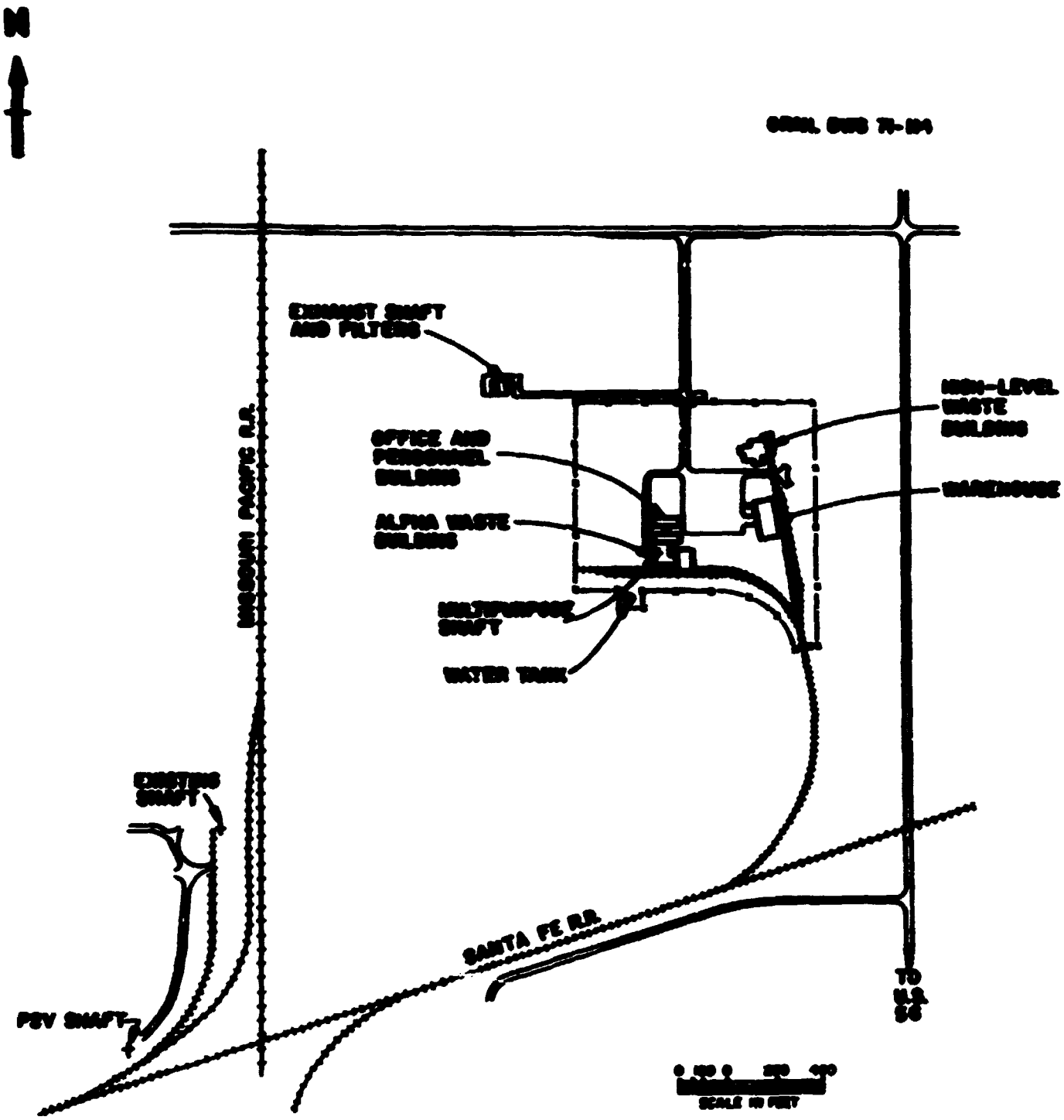

Fig. 6.3. Waste Repository Site Plan.

A railroad spur from the Santa Fe Railroad is one alternative for moving rail cars into the two waste receiving buildings. An alternate method is to take a spur off the Missouri Pacific track north of the facilities. At peak capacity it will probably be necessary to have both, but only one is being considered in the initial job scope. The two roads bordering the facilities on the north and east (Fig. 6.3) are existing county roads.

The relationship of the alpha and the high-level facilities and the existing Carey mine workings to the total Repository is shown in Fig. 6.4. The area outlined contains approximately 1030 acres, which will be purchased in fee simple. A buffer strip of approximately one mile, in which mineral rights will be obtained, will be established.

6.2 Alpha Facilities

Alpha wastes are characterized by little, if any, penetrating radiation; therefore, direct handling techniques are appropriate. Alpha waste burial units will be palletized on expendable, noncombustible pallets; they will be no larger than 4 x 6 x 6 ft high and will weigh less than 5 tons. Typically these will be of two general types. The first is a metal box secured to a pallet. The second is a number of drums banded tightly together and secured to a pallet, as shown in Fig. 6.5. Approximately four or five of these 4 x 6 x 6 ft burial units will be contained in an 8 x 8 x 20 ft long cargo container. Two such cargo containers will be shipped in an ATMX 600 series car specially constructed to provide containment of the wastes as well as to protect against fire and collision damage during transit. The ATMX car is top-loading, as indicated by Fig. 6.6.

The alpha-operations facility will be an integrated facility complex designed for a capacity of 1,000,000 ft^3 of alpha waste per year, based on 5-day, three-shift operation. The arrangement of facility structures, waste handling systems, and supporting operations will be designed to provide the most economical method for handling and storing alpha waste while maintaining high standards of operational safety and reliability.

ORNL-DWG 69-7122 R3

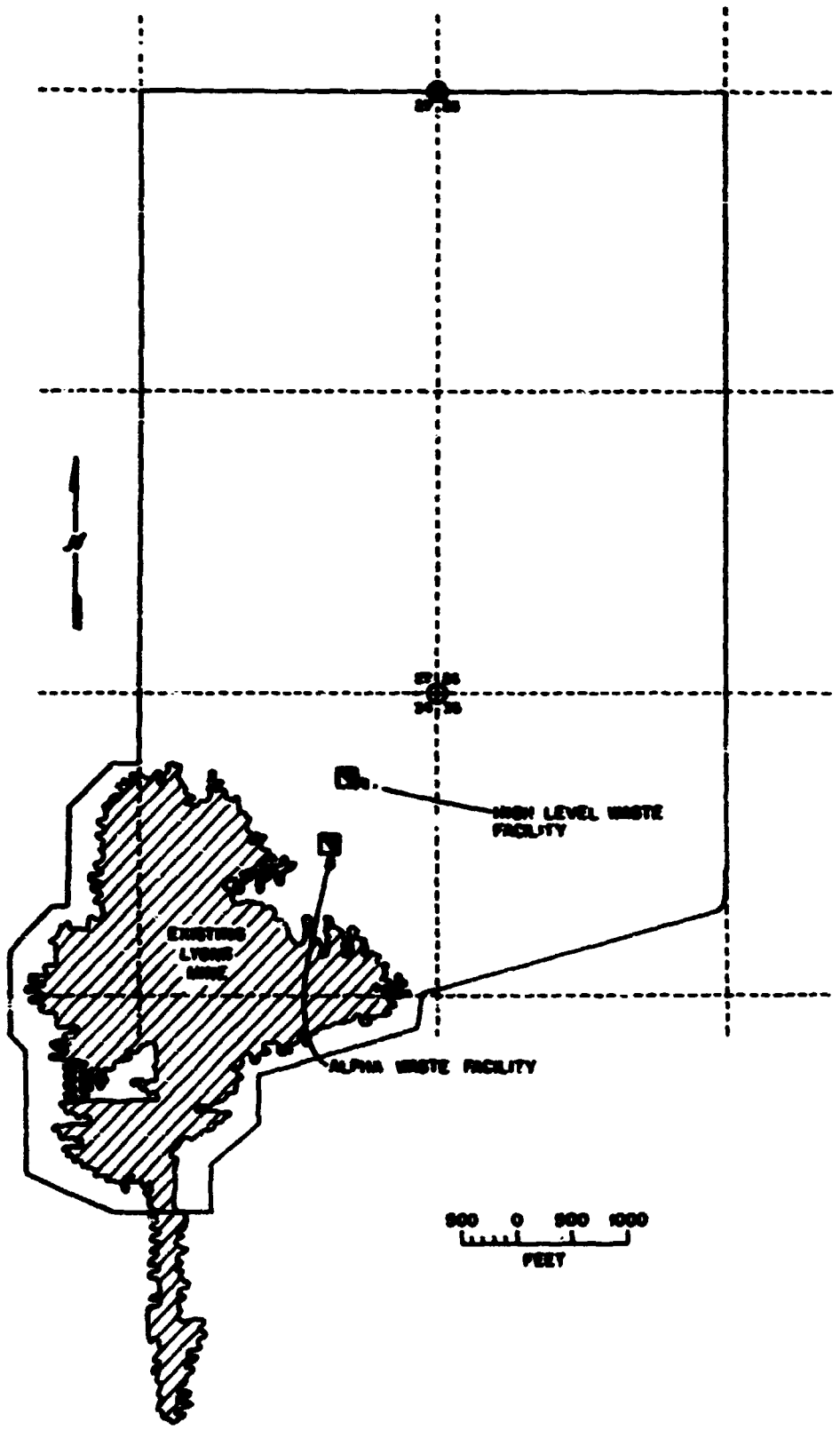

Fig. 6.4. Layout of Disposal Facility at Lyons Mine.

ORNL DWG 70-14105

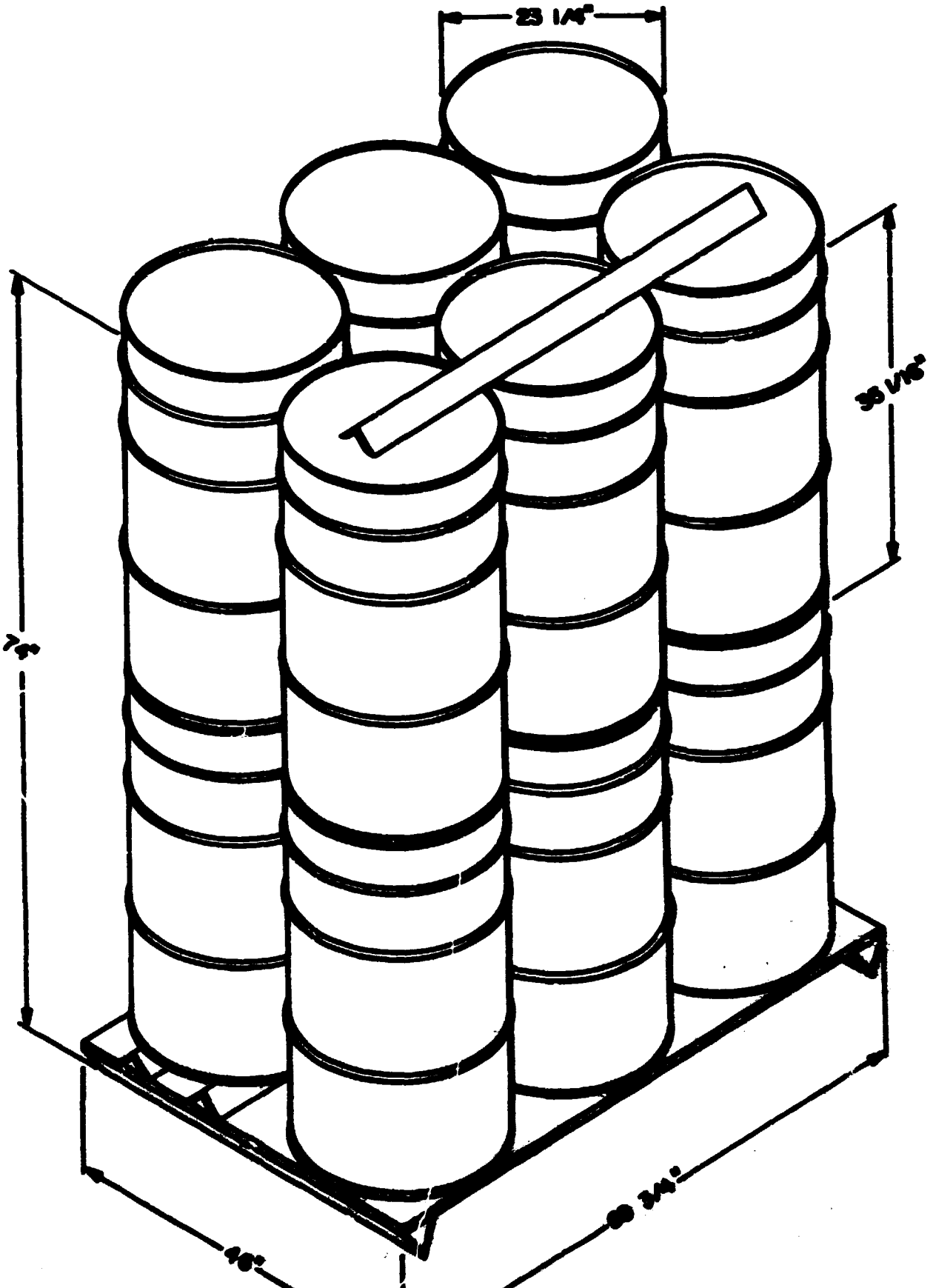

Fig. 6.5. Typical Palletized Burial Unit.

Fig. 6.6. Unloading Cargo Container from ATMX Car.

The total area of the alpha waste receiving building (Fig. 6.7) will be approximately 15,500 ft^2; and, except for the container unloading and storage area, all areas designed for handling alpha waste will be included in a confined structure. The areas within this building include:

(1) The container unloading and storage area (i.e., a weather-protected concrete working pad) in which cargo containers enclosing the alpha burial units will be unloaded from rail cars. The cargo containers will be moved on a transfer car through air locks into the unloading and decontamination rooms.

(2) Two unloading and decontamination rooms in which burial units will be unloaded from the cargo containers and checked for integrity prior to removal to the transfer room.

(3) A transfer room to provide the space for the forklift trucks to process the burial units through a weigh and nondestructive assay cycle and, subsequently, to transfer them into the alpha cage for lowering to mine level.

(4) A nondestructive assay (NDA) room used for the dual function of weighing each burial unit and monitoring its fissile material content.

(5) A waste loading compartment that will provide access from the transfer room to the sealed alpha cage. This compartment will be arranged to permit transfer of the burial unit from the transfer room to the alpha cage while maintaining the confinement integrity of the transfer room.

(6) A facility support area, located adjacent to the confined areas of this building, to house a counting room, a personnel check station, a changeroom, a maintenance and battery charge room, and a shift foreman's office.

The confined areas of the alpha waste receiving building will be of reinforced concrete construction designed to permit safe shutdown of waste handling operations without endangering the public health and safety during or following an earthquake or tornado. Confined areas will be

ORNL DWG 71-7846

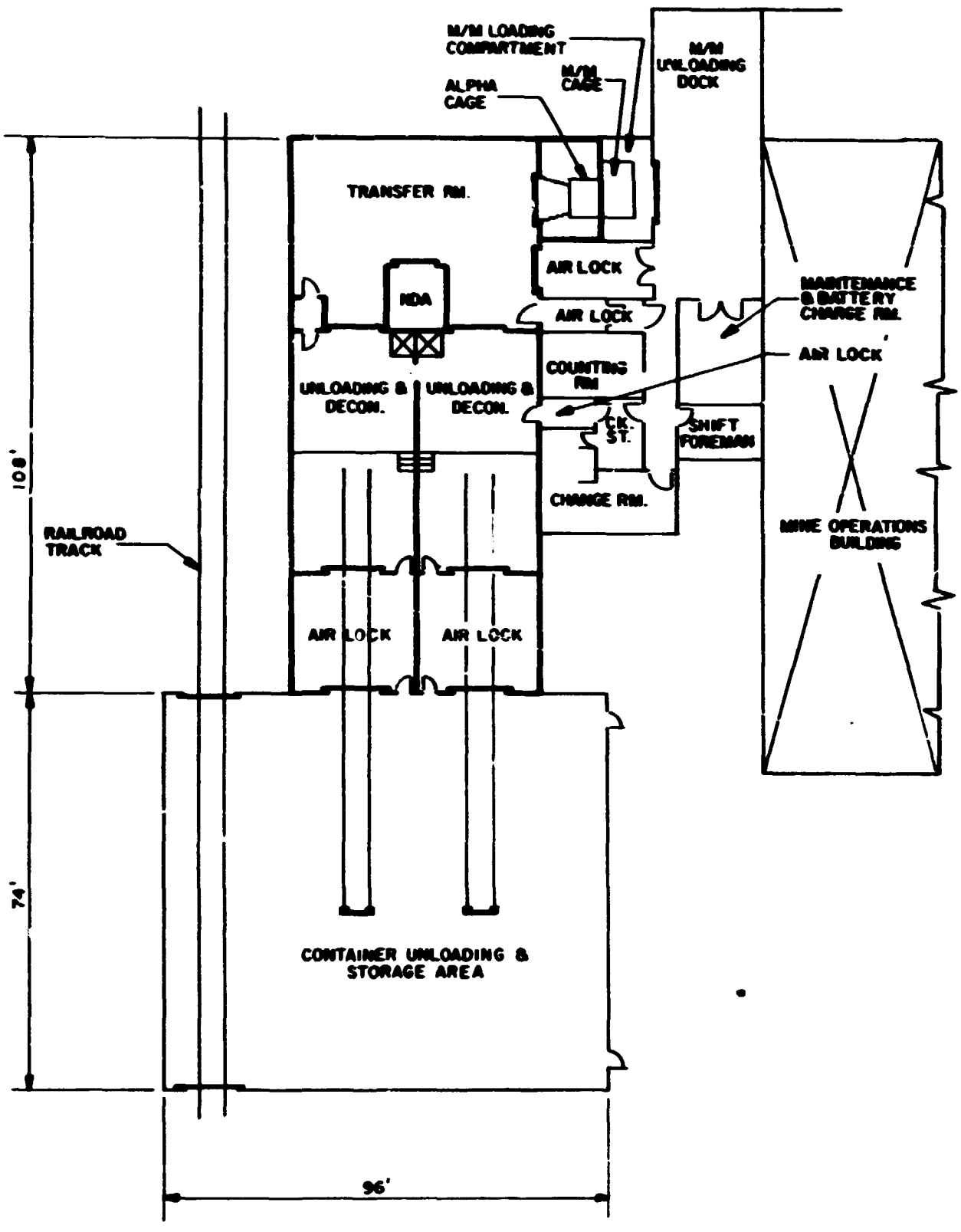

Fig. 6.7. Plan of the Alpha Building.

maintained at a negative static air pressure with respect to the outside atmosphere to ensure against any out-leakage of air (see Fig. 6.8). All exhaust air from confined areas of the building will be passed through fans and HEPA* filters located in a basement exhaust fan-filter room prior to discharge to the atmosphere through a stack. Access between confined and unconfined areas of the building will be through air locks.

The sealed burial units are lowered in an airtight cage to the mine level alpha station, where they are lifted by a battery-powered forklift and placed on a transporter. The transporter will move the burial units to the storage area, where a second forklift will unload the transporter and stack the burial units in a room. Salt will be used to backfill the rows of burial units and to fill any unused space within a room.

Supply air will enter the alpha and the high-level mines through the air supply compartment of the alpha-M/M shaft. Approximately 20,000 cfm will be directed to the alpha mine, and 40,000 cfm will be directed to the high-level mine. Within the alpha mine, temporary closures will be used to direct this ventilation flow, first, to the cleanup area and, then, to the alpha waste burial area. The filtered exhaust from the alpha waste burial area will be directed to the upcast vent shaft. In the high-level mine, a separate tunnel system located above the main entries will serve to isolate the exhaust air streams from the working areas and convey them to the base of the upcast vent shaft.

6.3 High-Level Facility

The high-level facility will provide the facilities and equipment necessary to receive and handle cans of high-level waste shipped to the Repository in shielded shipping casks. Typically, waste will be received in sealed cans up to 14 in. in diameter, up to 10 ft long, weighing up to 4000 lb, and generating 1 to 4 kW of waste heat. These cans will be shipped in casks weighing as much as 100 tons. The cans will be cooled within the casks, unloaded individually in shielded cell facilities, lowered to mine level through the high-level shaft, and then transported and buried in the salt bed using a shielded transporter. The components

*HEPA = high-efficiency particulate air filters.

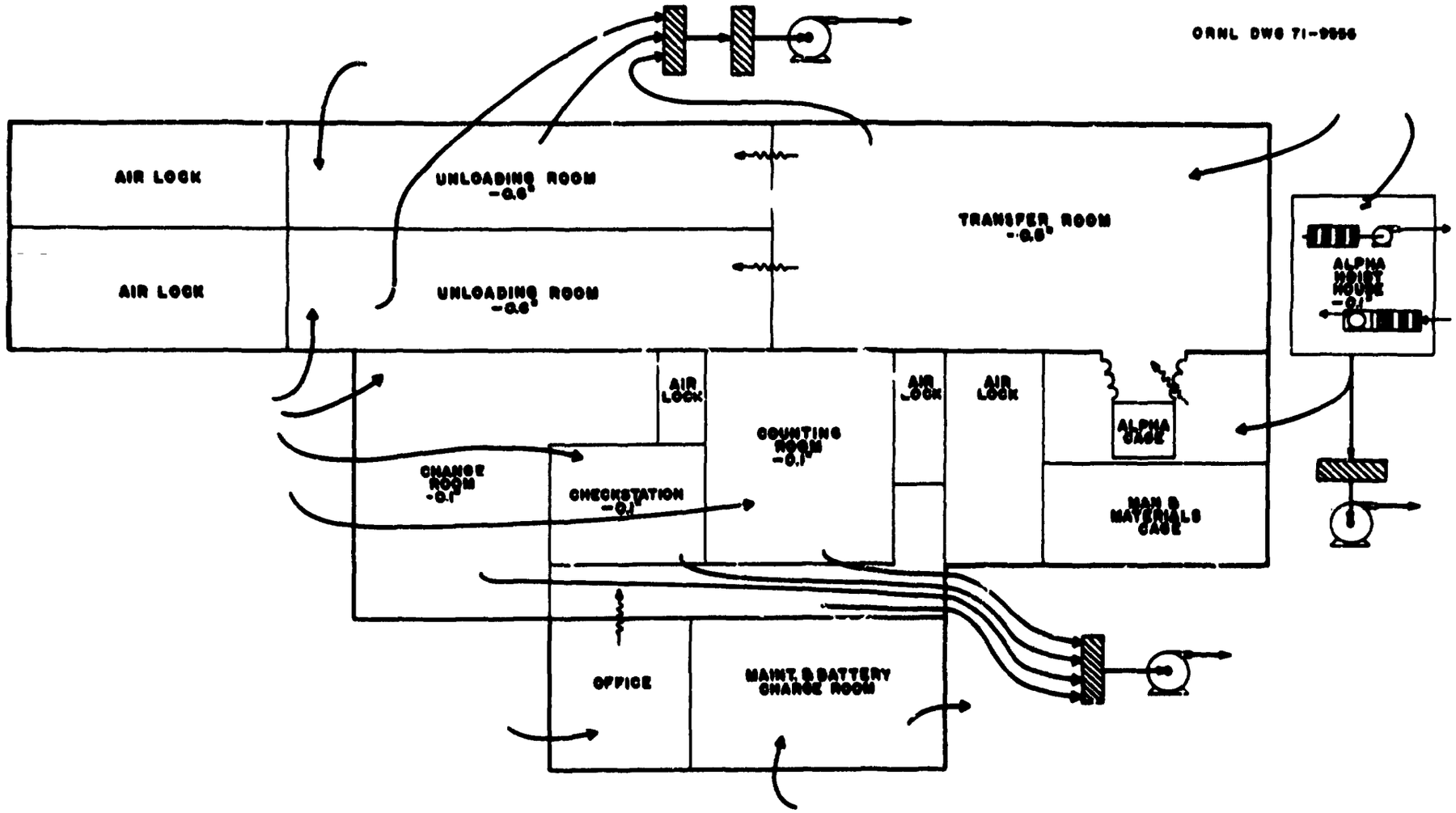

Fig. 6.8. Schematic of the Ventilation System of the Alpha-Operations Facility.

of the high-level facility will include the high-level waste receiving building, the adjoining hoist house, and the exhaust fan-filter house at surface level; the high-level shaft and the mine level receiving station; and the high-level mine with its complement of equipment to develop mine space and to transport and bury the high-level waste cans.

The high-level waste receiving building (Fig. 6.9) will receive the shipping cask on rail cars, which will pass through the rail car air lock into the cask unloading area. The cask unloading area will be a confined high bay area serviced by a 100-ton bridge crane for above-grade handling of shipping casks. A cask cooling station will be located in the cask unloading area, where the cask coolant will be sampled and the waste cans will be cooled within the cask. The cask will then be lowered into a transfer gallery through a hatch in the floor of the cask unloading area.

The basic architectural and structural guidelines used for the alpha waste receiving building will also be used for the high-level waste receiving building. Differences between the handling of high-level waste cans and alpha waste burial units will be due primarily to the presence of penetrating radiation in the high-level waste; thus, all handling operations of waste cans or opened shipping casks containing waste cans must be conducted remotely behind massive shielding. In addition, the waste cans themselves represent significant heat sources. The areas within the high-level waste receiving building whose continued integrity is necessary to permit safe shutdown of waste handling operations without endangering the public health and safety will be designed to withstand an earthquake or a tornado. Confined areas will be maintained at a negative air pressure with respect to the outside atmosphere to ensure that any air leakage will be into the building. All exhaust air from confined areas of the building will be passed through fans and HEPA filters located in an adjacent exhaust fan-filter house. These exhaust systems are shown schematically in Fig. 6.10.

The head frame for the high-level shaft will be an integral part of the high-level waste receiving building and will be constructed to provide radioactive confinement and biological shielding. As in the case of the alpha hoist, the high-level cable enclosure and hoist house will be confined areas.

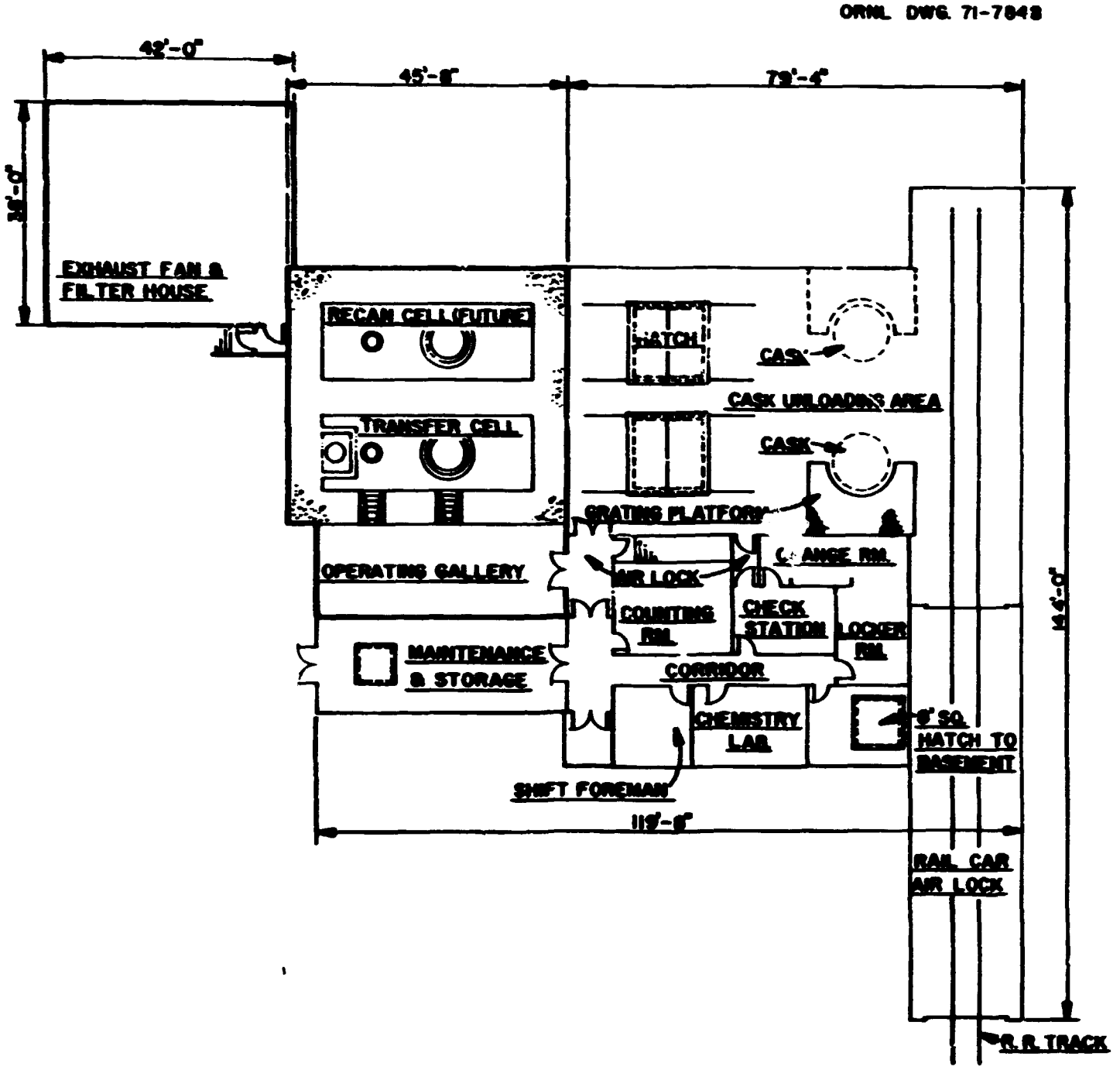

Fig. 6.9. Plan of the High-Level Building.

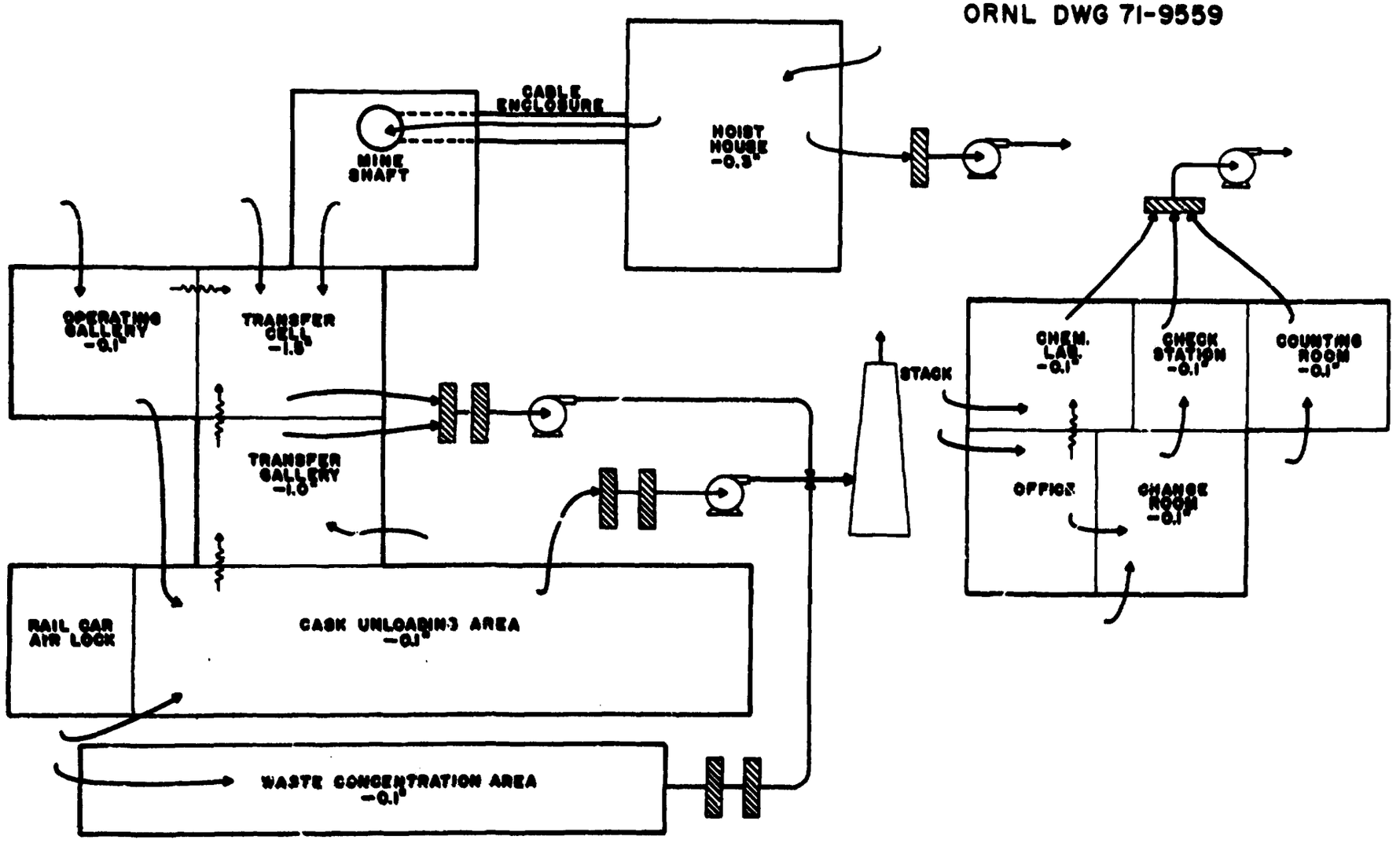

Fig. 6.10. Schematic of the Ventilation System for the High-Level Facility.

The high-level-waste receiving building, including the basement and the structure which will be provided for the future installation of a facility designed to recan high-level waste cans that have lost their initial integrity during transport to the Repository, will contain approximately 18,300 ft² of building area.

The support facilities area for this building will include a counting room, a personnel check station, a changeroom, a chemistry laboratory, a shift foreman's office, and a maintenance and storage room. Access between confined and unconfined areas of the building will be through air locks.

In the basement of the high-level-waste receiving building, space will be provided for the mechanical equipment room, boiler room, waste concentration room, decontamination equipment room, and waste casting room. The hoist house and the exhaust fan-filter house will be separate structures adjacent to the high-level-waste receiving building.

A section through the high-level building is shown in Fig. 6.11. The shipping cask is shown in three positions: on the rail car in the cask unloading area, sitting upright at the cask and can cooling station, and on a motorized dolly in the transfer gallery. The cask and dolly will be moved laterally to a location under the cask port in the shielded transfer cell, and the cask will be raised pneumatically to make a seal with the bottom of the cell (see Fig. 6.12). The cask port cover and the shipping cask shield plug will then be removed, exposing the cans and the cask interior to the cell, after which the cans will be lifted from the cask individually and lowered into the mine shaft cage, which is contained within a bottomless cage transfer car. When the transfer car is moved over the shaft by the hydraulic positioner, the waste can, contained within the mine shaft cage, will be lowered to mine level.

At mine level, the cage will be received in a station transfer car inside a shielded receiving station (see Fig. 6.13). The cage will be elevated and moved laterally to a position under a port in the top of the station, through which the waste can will be hoisted into the waiting shielded transporter. The existing Project Salt Vault transporter, with necessary modifications, will be used for initial high-level burial

ORNL DWG. 71-6585

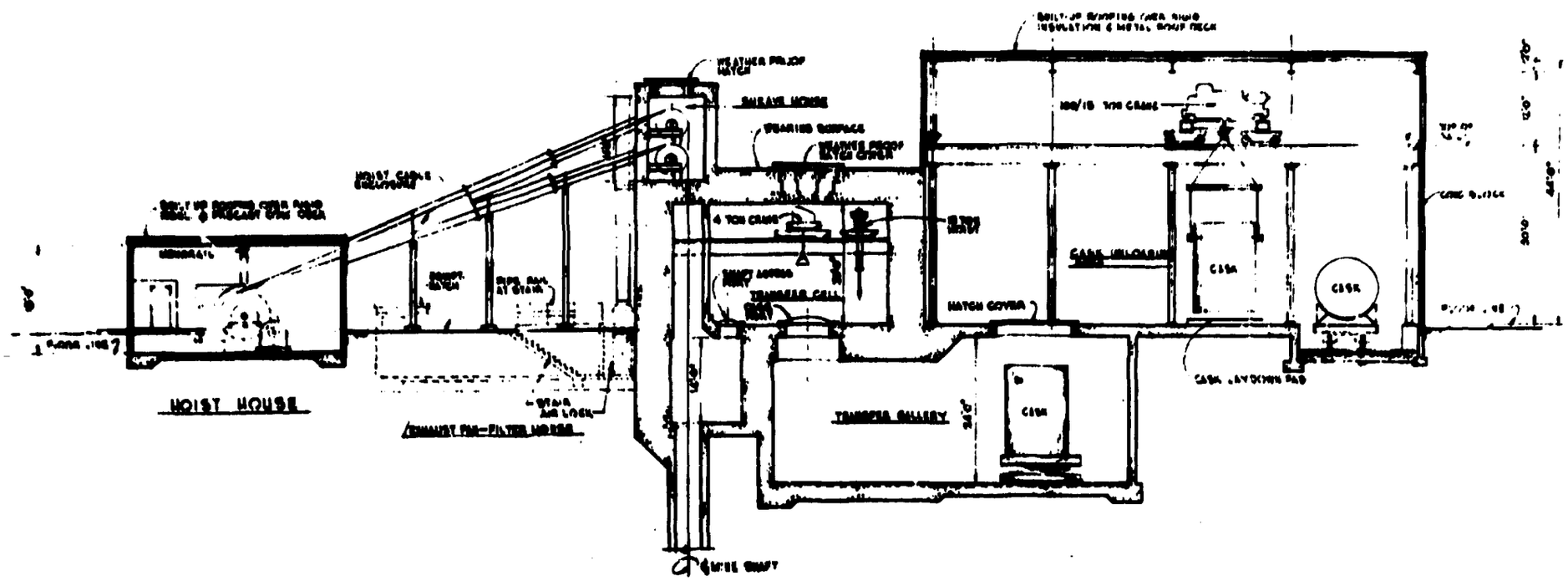

Fig. 6.11. Section Through the High-Level Receiving Building.

ORNL DWG. 71-6586

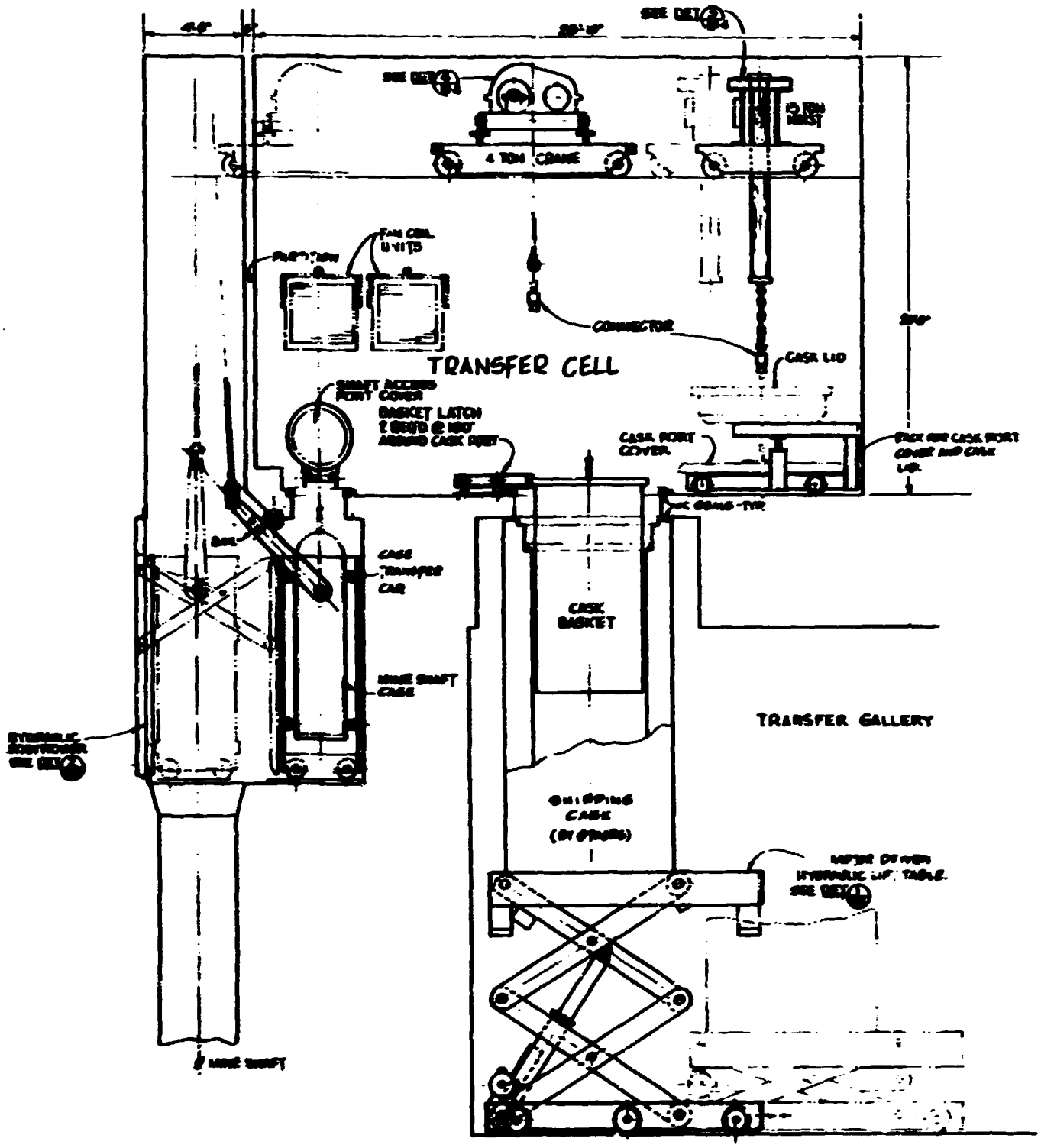

Fig. 6.12. Section Through the High-Level Transfer Cell.

ORNL DWG. 71-6588

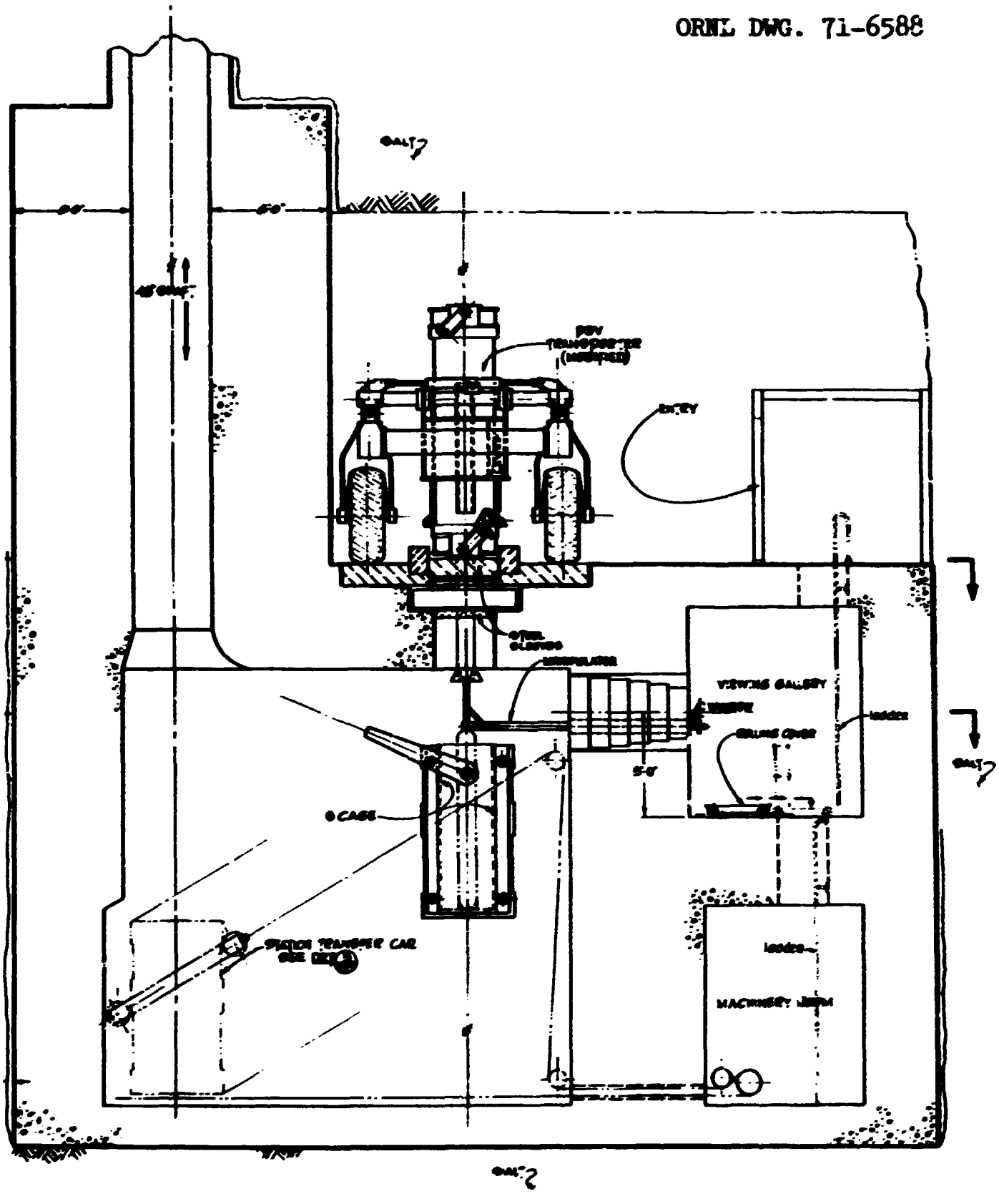

Fig. 6.13. Section Through the Mine Level Receiving Station.

operations. This transporter will receive the can at the receiving station, transport it to the burial room, deposit it in a hole that has previously been drilled in the floor, and backfill the hole with salt.

The master plan developed for the high-level mine provides for the burial of the cans containing high-level waste in accordance with projected rates of shipment to the Repository through the end of this century (Fig. 6.14). The mine layout and the sequence of salt bed utilization consider the requirements of mine ventilation, mine opening stability, heat effects, efficient use of mining and hauling equipment, and efficient use of mine space that is created. The master plan utilizes a conventional room-and-pillar layout in which the waste cans are buried in vertical holes drilled in the mine floor. The bed of salt in which the cans will be buried is the most uniform and of the best quality of the entire sequence of rock salt deposits. While the master plan is based on the concept of vertical burial, it has the flexibility to permit a change to horizontal burial at some later date if this change should prove to be technically and economically feasible.

Continuous mining machines will be utilized for the mining operations. Each mining machine will have shuttle cars associated with it as haulage vehicles. Long hauls of salt will be accomplished by the use of a conveyor. The use of continuous mining machines will eliminate any requirement for the use of explosives in the high-level mine and will preclude the shattering effect induced by explosive shock and the attendant weakening of walls and ceilings.

6.4 Confirmation Studies and Waste Retrieval

We are currently studying the types of experiments that we believe should be carried out in the mine during the early period of operation to confirm the design data. Although these experiments are not well defined at this time, they will undoubtedly include demonstration of waste handling and burial techniques and equipment; verification of calculations and laboratory studies of isotope and gas transport and diffusion phenomena; confirmation of calculated thermal and radiation effects on salt and waste;

ORNL DWG. 71-6589

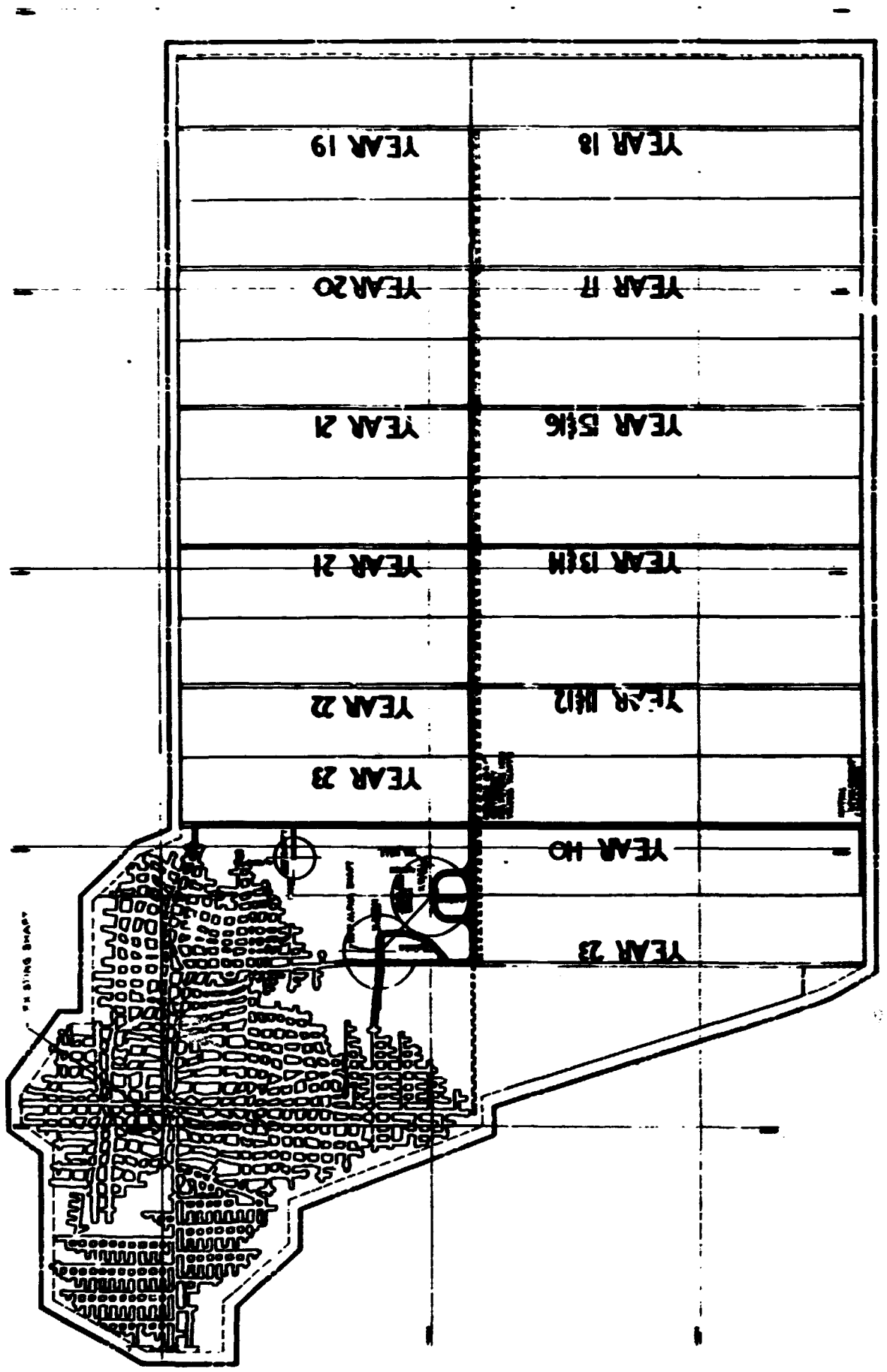

Fig. 6.14. Plan for Mine Development.

confirmation of laboratory studies of brine migration and crushed salt permeability; and others.

Figure 6.15 is a schematic version representing our initial ideas concerning design confirmation experiments in the mine. The scheme shown on the left features a system of nested components designed to give information on heat distribution, corrosive action (if any) of the waste on the waste can, and the mechanics of handling and burying waste cans in a sleeved hole in the salt. The system includes the waste can, contained and centered within a secondary containment vessel, which is, in turn, centered within an inert sleeve. The hole will be closed with a radiation shielding plug.

The second and third sketches in Fig. 6.15 indicate what we think will be the final burial method when the design confirmation studies will have been completed (i.e., direct burial in an unlined salt hole with crushed salt backfill). Our experiments will include burial of a few cans by this method, some of which we may rupture intentionally in order to determine the results of a failed can.

These experiments will be instrumented to give us as much information on the effects of gas release and flow, heat flow, and thermal and radiation effects as possible, but will involve a relatively small quantity of waste.

We have assumed that any wastes buried in the mine will be fully retrievable during the life of the mine. Concepts for retrieval of these design confirmation study wastes are in the design stage, utilizing tentative functional criteria that have been prepared recently. We will not be restricted by the facility design which we have described in the conceptual design report. Retrieval must be part of the concept, and revisions to the facility concept will be made, if necessary, to accommodate a feasible retrieval method. We have defined "retrieval" to include removal of the waste from the salt, transfer of the suitably contained waste to the surface, and loading it into a medium for transport. (A cask would be used for high-level waste and an ATMX car would be used for alpha waste.)

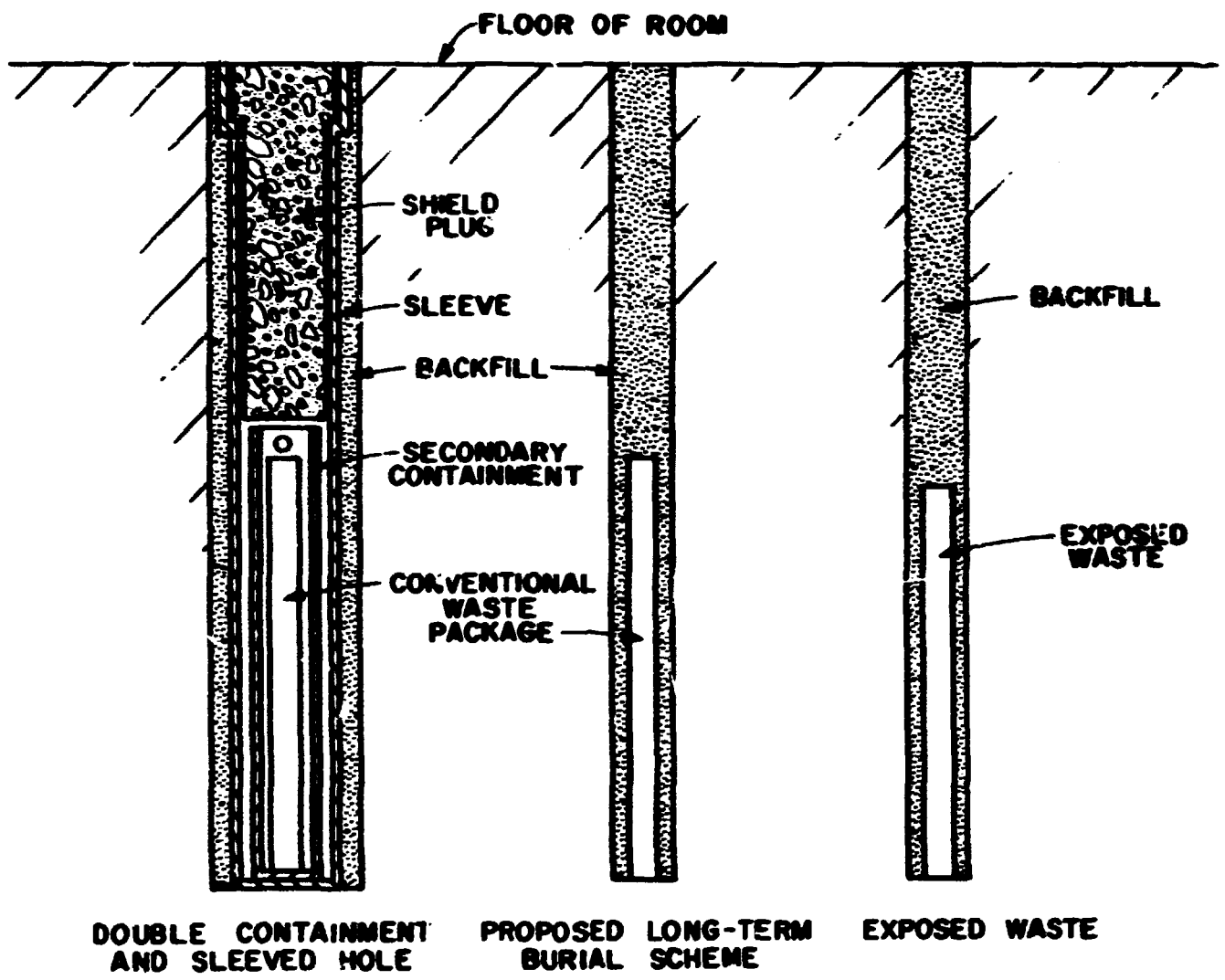

Fig. 6.15. Proposed Burial Schemes for Confirmation Period in the High-Level Mine.

6.5 Proposed Schedule

Our schedule is contingent upon a great many considerations, not the least of which are Congressional appropriations and legislation authorizing us tc proceed in certain areas. Other important considerations are, of course, the results of current and proposed research and development activities, particularly geologic-hydrologic investigations and consideration of alternative sites.

Our tentative schedule is to initiate Title I engineering in November of this year, with completion of this study to be expected in about May 1972. At the existing Lyons site, the estimated interval between Congressional authorization to proceed with construction and the start of confirmation studies at the Repository is approximately four years. At another site, this interval would be one to three years longer, depending upon the amount of investigative activity required and the presence or lack of existing mines, shafts, etc.

7. CHARACTERISTICS OF WASTES

H. W. Godbee

Detailed information concerning quantities, sizes, and descriptions of wastes that are to be stored in a waste repository is a prerequisite to the conceptual design and safety analysis of such a facility. Both plutonium-bearing wastes and fixed, canned, high-level fission-product wastes will be stored, monitored, and evaluated in the Repository.

7.1 Alpha Wastes

Solid wastes containing plutonium and other transuranium elements, frequently referred to as alpha wastes, are routinely produced during the operation of nuclear fuel production and spent fuel reprocessing plants, as well as during the operation of AEC laboratories and production facilities. The major AEC sites[1-3] and commercial installations[4] were surveyed during the past year or two to determine current and projected sources, amounts, characteristics, and practices for the disposal of these alpha wastes.

The wastes consist of a wide assortment of solid materials generated inside glove boxes during work with transuranium elements and outside the boxes during contamination control measures. They include items made of paper, cloth, wood, plastic, rubber, glass, ceramic, and metal, as well as salts and sludges that arise in the treatment of liquid waste streams and filters from cleanup of off-gas. The significant isotopes contaminating the wastes include 87.4-y ^{238}Pu, 24,400-y ^{239}Pu, 6,600-y ^{240}Pu, 14.3-y ^{241}Pu, and 433-y ^{241}Am. The transuranium-element contents of these wastes range from trace amounts to several grams per cubic foot. The densities of the uncompacted wastes vary from about 2 lb/ft^3 to as much as 200 lb/ft^3. About one-half to two-thirds of these wastes (by volume) are combustible and can be reduced via incineration by factors of about 50 and about 20 in volume and in weight, respectively; however, reliable and efficient incinerators for reducing their volumes have not as yet been developed. About one-half to three-fourths of the wastes (by volume) can

be reduced in volume by factors of 2 to 10 through compaction. The densities of the combustible wastes which are compactable generally vary from about 2 to 8 lb/ft^3, averaging about 5 lb/ft^3. Since these wastes are virtually free of penetrating radiation and evolve only a few hundredths of a watt per cubic foot, they do not require remote handling techniques. Sites in favorable geographic locations bury them on-site, whereas those in less favorable locations ship them, most frequently in wooden crates and steel drums, to commercial or AEC burial sites.

Initially, only noncombustible alpha waste will be accepted at the Repository; however, it is desirable to evaluate the feasibility of storing combustible alpha wastes packaged in proper containers in the Repository. A series of heating tests was carried out to study the oxidation and pyrolysis of typical combustible solid wastes in small wooden crates and steel drums at temperatures ranging from about 200 to 400°F for periods of time up to several hundred hours. Since most of the typical combustible alpha wastes consist of cellulosic materials (viz., paper, cloth, wood, as well as many paints and plastics), the basic mixture selected to simulate combustible solid wastes consisted of equal weights of blotter paper, cheesecloth, facial tissue, and polyethylene film. Each material was cut into 1-in. squares and packed into the containers to give a density of about 5 lb/ft^3. The temperature, pressure buildup, and weight loss on heating were recorded.

Results of these tests showed that, in the event that pyrolysis or limited combustion should occur, metal containers will ensure against the entrance of air to, or egression of smoke and fumes from, the package under conditions normally encountered; however, plywood containers proved unsatisfactory for this purpose. Among the general conclusions drawn from these results are that: (1) combustible wastes packed in combustible containers should not be accepted at the Repository, and (2) combustible wastes packed in noncombustible containers, such as metal drums or equivalents that meet DOT 17C and 17H specifications, should be acceptable at the Repository.

The noncombustible sample containers used in these studies consisted of drums with an open head, a bolt-ring closure, and a hollow neoprene gasket. They were fabricated of 0.024-in.-thick mild steel and had an

outside diameter of 5 in., a height of 9 in., and a volume of 0.1 ft^3. The "as-received" drums were modified by the addition of two electrically insulated terminals on one side so that a resistance wire (to simulate a spark or source of ignition) could be embedded in the waste; three thermocouple wells extending into the center of the drum at approximately the top, middle, and bottom; a 0.5-in.-thick machined lid; and a pressure tap on the lid. A massive aluminum block encased the drum to minimize temperature fluctuations. It was 12 in. high with a diameter of 12 in., and was machined out in the center to accommodate the drum.

The wastes were only slightly affected by heating up to 300°F, as indicated by little or no weight loss and by no obvious or only slight color change. However, as the temperature was increased above this level, the weight loss and depth of brown color increased. Speaking broadly, these observations are in accord with those expected when cellulosic and plastic materials are heated to these levels. The weight losses measured, for approximately equal heating times, ranged from about 2 wt % at 300°F to about 12 wt % at 400°F. Generally, the results show increasing weight loss as the temperature and the time at temperature are increased. In several of the runs, the Nichrome resistance wire embedded in the waste was energized and held at a red heat for several minutes. The only noticeable effect was increased charring of the waste in the vicinity of the wire. The pressures attained in the drums ranged from about 300 to 1200 in. H_2O(gage) and were about 50 to 100% greater than those expected from expansion of the air originally in the drum. Vaporization of the 5.6 wt % water adsorbed on the cellulose more than accounts for this increased pressure.

Figure 7.1 shows a representative pressure-time plot for the waste in the sealed drums. In this case, the waste was heated to 300°F and held for 135 hr. The weight loss was 2%, and the maximum pressure reached was 670 in. H_2O(gage). After about 4 hr of heating, the pressure in the drum reached 200 in. H_2O(gage) (the pressure specification of a DOT 17H drum) and the temperature was 220°F; after about 6 hr of heating, the pressure reached 400 in. H_2O(gage) (the pressure specification of a DOT 17C drum) and the temperature was 250°F. These temperatures are well beyond those normally encountered in shipping and handling such waste.

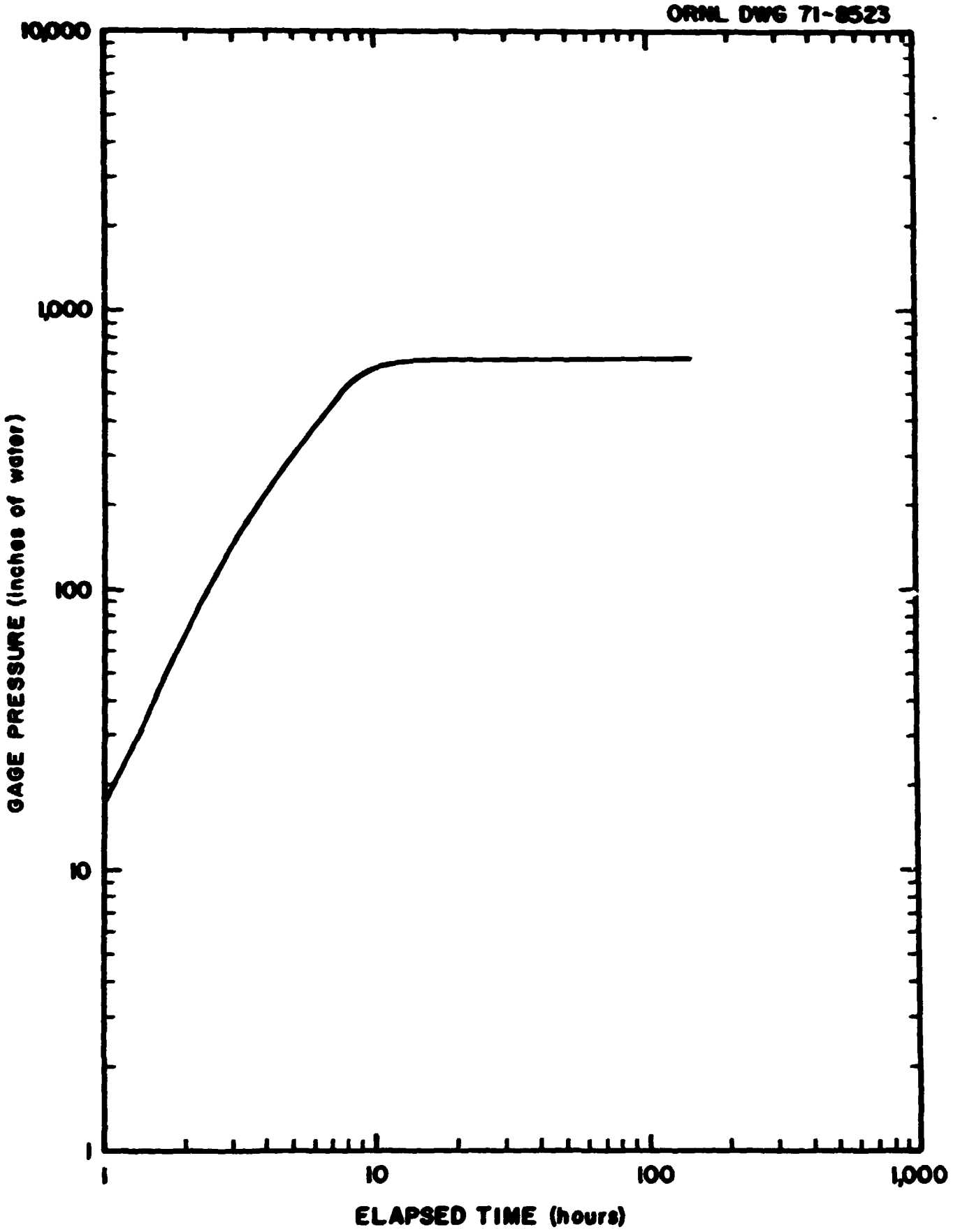

Fig. 7.1. Pressure-Time Results for Waste Mixture Composed of Equal Parts of Blotter Paper, Cheesecloth, Facial Tissue, and Polyethylene Film Held at 300°F for 135 hr.

To prevent pressure buildup in each waste drum because of gases – primarily water and carbon dioxide, but also other acidic gases – that were evolved during the thermal degradation and limited oxidation of solid combustible waste, a basic inorganic getter was added to the waste. Runs were carried out at about 400°F in which bone-dry CaO was mixed with the waste in increasing amounts to give CaO-to-waste weight ratios of 1/4, 1/2, and 1. The weight losses in these runs were only 0.2 to 0.3%, whereas the losses in comparable runs at about 400°F without a getter were about 6 to 12%. Further, the maximum pressures observed, 200 in. H_2O(gage) or less, in the runs in which CaO had been added to the waste were less than the pressure rise expected from expansion of the original air, and are below the specification pressures of DOT 17C and less than or equal to the specification pressure of DOT 17H drums. A typical pressure-time plot for waste to which CaO had been added is given in Fig. 7.2.

For the present, this work has been suspended at ORNL. However, these studies were only a small part of an on-going, in-depth AEC program concerned with collecting more information about combustible alpha wastes.

7.2 High-Level Wastes

Solutions containing fission products and small quantities of uranium, plutonium, and other heavy elements are generated during the processing of spent reactor fuels. These are generally referred to as high-level wastes because of their very intense penetrating radiation and high heat-generation rates.[5] Four processes have been developed for converting these liquid wastes to solid forms with a high degree of chemical, thermal, and radiolytic stability.[6]

The fluidized-bed waste calcining facility in Idaho (ICPP) has been operational for several years and has converted to granular solids about 2 million gallons of wastes generated by the processing of highly enriched fuels.[7] In the Waste Solidification Engineering Prototypes (WSEP) at Battelle-Northwest, the solidification of wastes from processing power reactor fuels has been demonstrated using the pot, spray, and phosphate glass processes.[8] In the course of 33 runs, more than 50 million Ci of

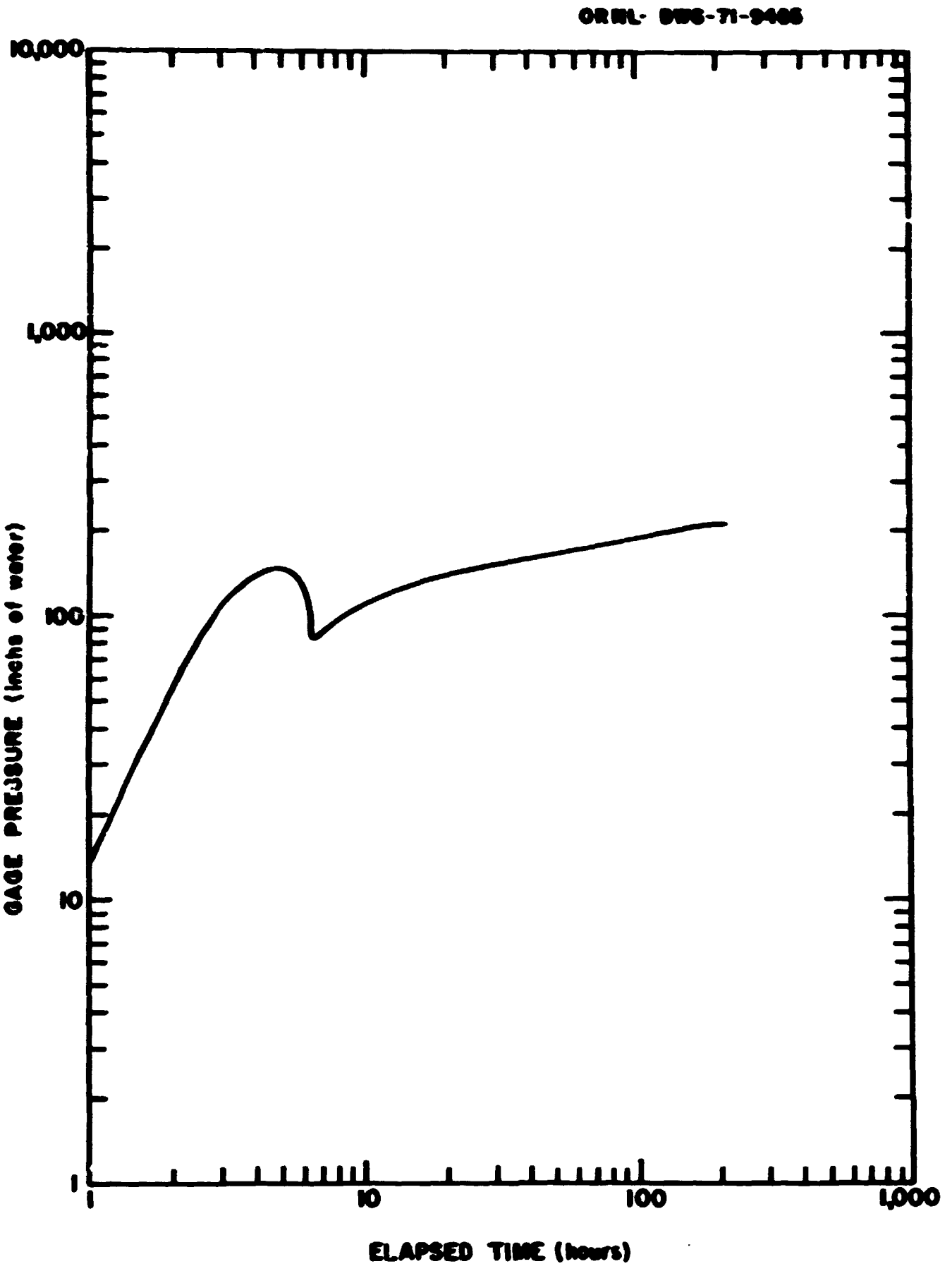

Fig. 7.2. Pressure-Time Results for Waste Mixture (Equal Parts of Blotter Paper, Cheesecloth, Facial Tissue, and Polyethylene Film) Plus One Part Calcium Oxide Held at 420°F for 205 hr.

radioactive fission products were processed in containers that were 6 to 12 in. in diameter and 8 ft long, yielding solid products with thermal power densities ranging up to 320 W/liter (Table 7.1). These processing rates and equivalent aging times are within a useful range of application.

The products from the pot calcination, spray solidification, phosphate glass, and fluidized-bed calcination processes can be described, respectively, as calcine cake, microcrystalline or rocklike material, phosphate glass, and granular solids. The pot calcination and fluidized-bed products have lower thermal conductivities and higher leach rates than do the spray solidification and phosphate glass products (Table 7.2). However, the pot calcine material is more stable at elevated temperatures. The spray melt, the phosphate glass, and the fluidized-bed product can be packaged in mild-steel containers, while stainless steel containers must be used in the pot calcination process. A more recent modification[8] of the spray and pot calcination processes is incorporation of the waste solids in borosilicate glass to produce a glassy product. The granular product from a fluidized bed may be converted to a dense solid by embedding the particles in a solid matrix or by fusing to form a glass.[9]

7.3 Preliminary Acceptance Criteria for Wastes

Alpha-waste packages that are known to contain liquids, potentially explosive chemicals, pyrophoric materials, oxidants (other than air), and sealed inner containers filled with gas under pressure will not be accepted at the Repository. These materials must be converted to stable, inert solid forms by mixing with Portland cement or an approved substitute.

High-level wastes must be converted to dry solids that are chemically, thermally, and radiolytically stable before they will be accepted at the Repository. They must be packaged in containers that will maintain their integrity for at least 90 days after they have been buried in salt.

These acceptance criteria (Table 7.3) are very preliminary and are intended only for design purposes. Additional work is continuing to substantiate both the alpha and the high-level criteria. As more information is gained, some of these criteria will probably be relaxed, some tightened, and perhaps new ones added.

Table 7.1. Present Status of Solidification Processes

Process	Status	Maximum Allowable Isotopic Power[a] (W/liter)	Isotopic Power Achieved to Date (W/liter)	Equivalent Aging Time[b] (years)	Processing Rate (equivalent tons U per day)
Fluidized-bed calcination	Operational at ICPP	70	0.55		
Pot calcination	9 runs in WSEP	82	85	1.0	0.6 to 1.0
Spray solidification	13 runs in WSEP	205	205	0.6	0.5 to 1.1
Phosphate glass	11 runs in WSEP	215	320[c]	0.2	0.3 to 0.7

[a]Based on maximum temperatures of 900°C along axis and 450°C at wall of 8-in -diam pot.

[b]Cooling time before solidification of waste from processing fuel exposed to a burnup of 20,000 MWd/ton at a specific power of 15 MW/ton.

[c]Achieved in a 6-in.-diam pot.

Table 7.2. Characteristics of Solidified High-Level Waste

	Pot Calcine	Spray Melt	Phosphate Glass	Fluidized-Bed Calcine
Form	Calcine cake	Monolithic	Monolithic	Granular
Description	Scale	Microcrystalline	Glass	Amorphous
Waste oxides, vol %	25 to 35	15 to 25	5 to 15	5 to 25
Bulk density, g/ml	1.1 to 1.5	2.7 to 3.3	2.7 to 3.0	1.0 to 1.7
Thermal conductivity, Btu hr^{-1} ft^{-1} $°F^{-1}$	0.15 to 0.25	0.4 to 1.0	0.4 to 1.0	0.10 to 0.25
Leachability in cold water, g cm^{-2} day^{-1}	1.0 to 10^{-1}	10^{-3} to 10^{-6}	10^{-4} to 10^{-7}	1.0 to 10^{-1}
Hardness	Soft	Hard	Very hard	Moderate
Friability	Crumbly	Tough	Brittle	Moderate
Volume, liters/1000 MWd (thermal)	1 to 2.5	1.2 to 3	1.5 to 5	1.5 to 5
Maximum stable temperature, °C	~900	~900	~500	~600
Container material	Stainless steel	Mild or stainless steel	Mild or stainless steel	Mild or stainless steel

Table 7.3. Preliminary Acceptance Criteria for Wastes[a]

Alpha Waste:

1. Sealed in rugged metal containers.
2. Maximum dimensions: 4 x 6 x 6 ft high.
3. Maximum weight: 5 tons.
4. Fissile isotope content: <5 g/ft^3 and <200 g/package.
5. Thermal power: <0.1 W/ft^3.
6. Penetrating radiation: <2.5 mrem/hr at 3 ft.

High-Level Wastes:

1. Thermally, chemically, and radiolytically stable.
2. Sealed in metal cylinders 6 to 14 in. in diameter and 2 to 10 ft long.
3. Maximum weight: 4000 lb.
4. Maximum thermal power: 3500 to 5000 W.
5. Fissile isotope content: <5000 g/container.

[a]Shipments conform with 49 CFR 173, 19 CFR 71, and AECM 0529.

7.4 References

1. R. D. Walton, Jr., et al., Compaction of Radioactive Solid Waste, A Report to the General Manager's Task Force on AEC Operational Radioactive Waste Management, AEC, Washington, D. C., WASH-1167 (June 1970).

2. W. L. Lennemann et al., Incineration of the Radioactive Solid Wastes, A Report to the General Manager's Task Force on AEC Operational Radioactive Waste Management, AEC, Washington, D. C., WASH-1168 (August 1970).

3. H. W. Godbee and J. P. Nichols, Sources of Transuranium Solid Waste and Their Influence on the Proposed National Radioactive Waste Repository, ORNL-TM-3277 (January 1971) (Official Use Only).

4. H. H. Van Tuyl et al., A Survey of Alpha Waste Generation and Disposal as Solids in the U.S. Nuclear Fuel Industry, BNWL-B-34 (December 1970).

5. W. K. Winegardner, Sect. 2.0, "High Level Wastes," pp. 2.1-2.18 in Waste Solidification Program, Volume 1, Process Technology - Pot, Spray, and Phosphate Glass Solidification Processes, ed. by K. J. Schneider, BNWL-1073 (August 1969).

6. K. J. Schneider, "Solidification and Disposal of High-Level Radioactive Wastes in the United States," Reactor Technol. 13(4), 387-415 (Winter 1970-1971).

7. G. E. Lohse, T. K. Thompson, and B. R. Wheeler, "In-Bed Combustion Calculation of Radioactive Wastes," Trans. Am. Nucl. Soc. 14(2), 495-96 (October 1971).

8. J. L. McElroy, A. G. Blasewitz, and K. J. Schneider, "Status of the Waste Solidification Demonstration Program," Nucl. Technol. 12, 69-82 (September 1971).

9. D. W. Rhodes, "Storage and Further Treatment of Product from Fluidized Bed Calcination of Radioactive Wastes," pp. 623-41 in Proceedings of the Symposium on the Solidification and Long-Term Storage of Highly Radioactive Wastes, CONF-660208 (February 1966).

8. ISOTOPE TRANSPORT

A. P. Malinauskas
B. K. Annis
R. B. Evans III
H. W. Godbee
J. L. Rutherford
J. Truitt
G. M. Watson

This section is a summary of the research, performed or planned, which is directed toward demonstrating that salt formations successfully inhibit isotope transport (i.e., isotope migration may be taken to be insignificant in a practical sense).

If only to provide a conservative basis on which to construct the safety analysis framework, it is desirous to regard the metal package simply as a means for the safe transport of the radioactive waste to the individual burial sites, rather than as a barrier to isotope transport once the package has been lowered into its chamber in the salt formation. Therefore, the current research program has been designed not only on the premise that a breach of the metal package is inevitable but also that it will occur shortly after burial.

Once a breach of the temporary containment occurs, the most immediate effect is an alteration of the chemical environment around the radioactive waste. Because of this circumstance, there thus exists the potential for interaction between the waste and the new environment to result in the formation of volatile species from previously nonvolatile waste. A thorough study in this regard, however, requires that we first specify the chemical aspects of this new environment. Since the study of this aspect is not yet complete, our considerations of volatile species formation have been limited to interactions of the waste with water vapor; this topic is discussed in Sect. 8.1.

Our concern with the possible formation of volatile species implies a concern for the unwanted dispersal of radioactivity via a gas transport mechanism. In addition to this form of isotope migration, two other transport phenomena must be considered; these include solid-state "bulk" diffusion, and diffusion at grain boundaries and along free surfaces. In Sect. 8.2, our investigations pertinent to gas and aerosol transport are summarized; solid-state diffusion is the subject of Sect. 8.3; and surface diffusion as a mode of isotope dispersal is taken up in Sect. 8.4.

In each of these investigations, only one phenomenon is studied. Because this is tantamount to a denial of the possibility of synergism among the various phenomena (and is, in fact, unlikely inasmuch as the transport mechanisms are concerned but cannot be dismissed relative to a consideration of the formation of volatile species), a series of experiments has been designed in which the migration of simulated waste species through crushed salt columns will be investigated. These experiments are briefly described in Sect. 8.5. Section 8.6 presents the conclusions derived from the work performed thus far.

8.1 Enhancement of Volatility of the Fission Product Oxides in the Presence of Water Vapor

Aside from the relatively inert sodium chloride, water vapor is a major component to which the waste will be exposed when the metal package is breached. This species comes from the salt itself.

In the proposed Kansas site, for example, the salt contains from 1/4 to 1/2%, by volume, brine,[1] which is partly contained within occlusions of the type shown in Fig. 8.1. This figure shows several cavities, approximately cubical in shape, which are almost totally filled with brine except for the small bubbles that appear as circular black areas within the cavities. These so-called "negative crystals" are distributed throughout the body of the salt relatively uniformly and range downward from about 2 mm in size. Grain boundaries or other crystal imperfections, on the other hand, are generally decorated with numerous smaller cavities that are more nearly spherical in shape.[2]

If a temperature gradient is maintained along a body of salt containing these negative crystals, the brine-filled cavities are observed to migrate. The accepted mechanism is one in which the sodium chloride dissolves at the hotter edge of the brine, is transported through it, and crystallizes at the colder edge.[3] As a result, the cavity itself moves up the temperature gradient (i.e., toward the heat source). In this manner, considerable quantities of the brine can be brought into contact with the waste-

Fig. 8.1. Brine-Filled "Negative Crystals" in Bedded Salt.

filled cylinder.* Two estimates of the volume of brine reaching the waste cylinder cavities as the result of negative crystal migration are plotted as a function of time since burial in Fig. 8.2. Both estimates probably represent upper limits for the respective conditions for which the calculations were made. It should be noted, however, that the brine inflow volume is estimated in terms of liters of liquid, whereas the water entering the cavity will actually be in the gaseous state. The upper curve was calculated by Jenks[4] for ten-year-old waste that is buried when the thermal power is 5 kW per container, whereas the estimate by Bradshaw and McClain is for a smaller amount of younger waste.[5] The latter estimate indicates that approximately 15 liters of brine will enter the cavity over a 20-year period, and that the inflow thereafter will be insignificant. Jenks' calculations, on the other hand, yield a total inflow of about 50 liters, occurring over a 50-year period. This would correspond to all of the brine contained within the salt along the 10-ft length of a high-level-waste-filled cylinder out to a distance of about 3 ft beyond the edge of the cylinder cavity.

Since one of the main components available for interaction with the calcined waste is water vapor, and since interactions of this type are known to result in enhanced volatility of some oxide species, a thorough study of the literature in this regard was undertaken.

Specifically, the observed enhancement in the vapor pressure of a rather broad class of oxides in an atmosphere containing water vapor is believed to result from a reaction which is usually of the form

$$MO_n(s) + H_2O(g) = MO_{n-1}(OH)_2(g) \ , \qquad (1)$$

where M denotes element. The "oxyhydroxide" that is formed appears to be stable only in the gaseous phase under the conditions in which enhancement of vapor pressure has been investigated, although the solid phase is

---

*We wish to point out that this report, in a strict sense, only considers phenomena as they affect isotope migration in the high-level facility. However, with few exceptions (e.g., combustion), the phenomena effecting radioactivity dispersal in the alpha facility are identical in kind but are of lesser significance than those in the high-level facility.

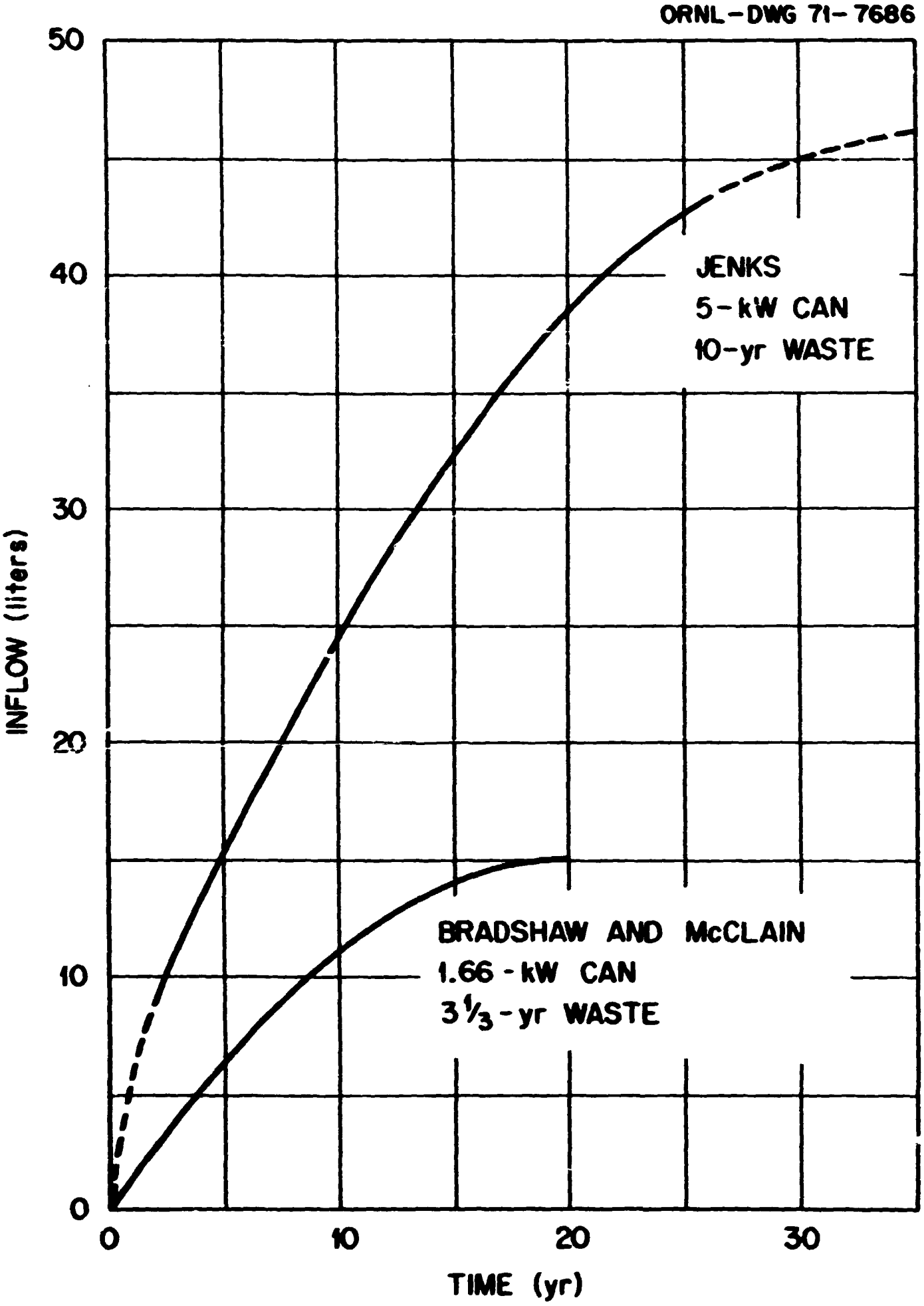

Fig. 8.2. Estimates of Brine Inflow into Waste Cylinder Cavities due to Negative Crystal Migration, as a Function of Time Since Burial.

known to be stable at lower temperatures in some cases. Moreover, in virtually every case studied thus far, the form of the species resulting from the interaction is inferred from thermodynamic considerations. This type of approach ordinarily yields necessary, but not sufficient, conditions for the existence of the chemical species in question. In short, evidence for the actual existence of the oxyhydroxide species is inconclusive, but the fact that enhancement of the vapor pressure of the oxide occurs is unassailable.

Glemser and co-workers have performed most of the research that has been performed to date regarding this phenomenon.[6-13] The most recent investigation is a report of negative results,[14] whereas the most recent detailed review is contained in a report of Malinauskas, Gooch, and Redman.[15]

Table 8.1 is a listing of vapor pressure data[6-8,14,16-20] for several oxides that were chosen either because their behavior in water vapor atmosphere has been investigated or because they are of particular interest in the context of the present report. The data are summarized through the use of the analytical representation

$$\log p\ (\text{torr}) = A - (B/T)\ , \tag{2}$$

where p represents the vapor pressure in torr at temperature T in °K. The constants A and B were generally derived from the data presented in the references cited by employing the method of least squares.

The results[7-12,14,15,18,21,22] of investigations made regarding vapor pressure enhancement are listed in Table 8.2. In this case an equilibrium constant, K, is defined which, for a reaction described by Eq. (1), takes the form

$$K = p_{\text{oxyhydroxide}}/p_{H_2O}\ . \tag{3}$$

The summary in Table 8.2 is then given in terms of the parameters that define the temperature dependence of K, namely,

$$\log K = \alpha - (\beta/T)\ . \tag{4}$$

Table 8.1. Vapor Pressure Data for Selected Oxides

Oxide	A	$10^{-3}B$ (°K)	Temperature Range (°C)	Source[a]
BeO[b]	18.50	34.23	1950-2150	16
CrO_3	20.14	10.30	175-195	6
Li_2O	10.59	19.68	900-1500	17
MgO	10.81	29.50	1500-1700	18
MoO_3[c]	18.08	18.19	600-750	7
PuO_2	11.03	29.58	1400-1800	17
Re_2O_7	13.88	6.89	150-250	8
RuO_2	<0.001 torr at 930°C			14
RuO_4	10.67	2.88	0-100	19
Sb_2O_3	3.6 torr at 600°C			14
Sb_2O_4	<0.001 torr		800-900	14
SnO_2	<0.001 torr at 930°C			14
SrO	14.88	33.64	1300-1900	17
TeO_2	12.35	13.23	400-700	20
V_2O_5	-	-	-	-
WO_3	15.76	25.57	800-1200	17
ZnO	10.32	16.37	700-1300	17

[a]These numbers designate references that are listed at the end of Sect. 8.

[b]For this case, $\log p + 2 \log T = A - (B/T)$.

[c]The predominant vapor species is a trimer.

Table 8.2. Vapor Pressure Enhancement due to Water Vapor

Oxide	α	$10^{-3}\ \beta$ (°K)	Temperature Range (°C)	Source[a]
BeO	1.93	9.28	1400-1500	21
CrO_3	6.63	5.05	150-200	9
Li_2O[b]	9.53	17.26	800-1100	22
MgO	2.87	14.50	1500-1700	18
MoO_3	5.45	7.73	600-700	7
PuO_2	-	-	-	-
Re_2O_7[c]	14.44	7.80	150-250	8
RuO_2	No effect at p_w = 350 torr, 930°C			14
RuO_4	-	-	-	-
Sb_2O_3	No effect at p_w = 350 torr, 600°C			14
Sb_2O_4	-	-	-	-
SnO_2	No effect at p_w = 350 torr, 930°C			14
SrO	-	-	-	-
TeO_2	3.28	6.63	550-700	15
V_2O_5[d]	-3.24	4.66	500-650	10
WO_3	4.10	8.73	400-1100	7,11
ZnO	10.66	22.30	1300-1400	12

[a] These numbers designate references that are listed at the end of Sect. 8.

[b] $Li_2O(s) + H_2O(g) = 2LiOH(g)$.

[c] $Re_2O_7(s) + H_2O(g) = 2ReO_3(OH)(g)$.

[d] $V_2O_5(s) + 2H_2O(g) = V_2O_3(OH)_4(g)$.

Table 8.3 is a listing of results obtained for the enhancement of the vapor pressure of selected oxides under rather conservative conditions relative to those anticipated in salt mine repositories. In this table, p_{oxide} represents the normal vapor pressure of the oxide at 500°K, whereas $p_{hydroxide}$ designates the increase in vapor pressure at this temperature due to exposure to 1-atm water vapor. In most cases, however, extrapolation considerably beyond acceptable limits has been made; thus this tabulation may amount to little more than a computational exercise. Nonetheless, the results are worthy of qualitative comparison.

It should be noted that, in every case in which the vapor pressure is negligible for practical purposes, enhancement by many orders of magnitude still renders the gaseous phase as totally insignificant. For example, it is reasonable to assume that the interaction of SrO with H_2O will not be too different from that of either BeO or MgO; and, on this basis, it seems safe to assert that the increase in vapor pressure will not exceed 10^{-10} torr at 500°K in water vapor at 1-atm pressure. Similarly, the vapor pressure of PuO_2 militates against an enhancement greater than 10^{-10} torr under the conditions cited.

In a relative sense, then, a significant enhancement in vapor pressure can result from interactions with water vapor, although, in absolute terms, the resulting vapor pressure is still completely negligible for the oxides of concern to isotope migration in the Repository. Furthermore, like the vapor pressure itself, the enhancement drops exponentially with decreasing temperature; thus there is a natural provision of an additional margin of safety. Of course, if the salt were impermeable in all respects to gaseous species, the aspect of volatility enhancement, or of volatility <u>per se</u>, would be of little consequence. This consideration is the topic of Sect. 8.2.

Table 8.3. Enhancement of Vapor Pressure as the Result of Exposure to 1-atm Water Vapcr at 500°K

Oxide	P_{oxide} (torr)	$P_{hydroxide}$ (torr)
BeO	4.4×10^{-56}	1.7×10^{-14}
CrO_3 [a]	3.5×10^{-1}	2.6×10^{-1}
Li_2O	1.7×10^{-29}	8.7×10^{-12}
MgO	6.5×10^{-49}	5.6×10^{-24}
MoO_3	5.0×10^{-19}	7.6×10^{-8}
PuO_2	7.4×10^{-49}	-
Re_2O_7	1.2	7.2
RuO_2	-	-
RuO_4 [b]	-	-
Sb_2O_3	-	-
SnO_2	-	-
Sb_2O_4	-	-
SrO	4.0×10^{-53}	-
TeO_2	7.8×10^{-15}	7.6×10^{-8}
V_2O_5	-	1.6×10^{-7}
WO_3	4.2×10^{-36}	3.3×10^{-11}
ZnO	3.8×10^{-23}	8.4×10^{-32}(?)

[a] CrO_3 melts at 196°C (according to the Handbook of Chemistry and Physics, Chemical Rubber Publishing Co., Cleveland, Ohio, 1951).

[b] RuO_4 decomposes explosively at approximately 107°C (see ref. 19).

8.2 Gas and Aerosol Transport Through Crushed and Bedded Salt

A discussion of the dispersal of radioactivity throughout the Repository by gas or aerosol transport requires a consideration of effects which cover the entire time span over which the wastes require containment. The extent to which the crushed salt backfill will retard these types of transport is of interest, with regard to immediate effects; long-term effects, on the other hand, are concerned with the permeability of the bedded and reconsolidated salt itself to gas. Between these extremes, the extent of permeability reduction of the crushed salt, as the result of reconsolidation, must likewise be considered.

At the outset, it is important to note that aerosol transport is ordinarily less rapid than gas migration, although it is possible that aerosol transport can, in some instances, actually yield a greater dispersal of radioactivity simply because the radioactive species can be more concentrated in the solid (or liquid) phase in comparison with the gas phase. In addition, there is one notable exception to the general rule that individual molecules (gas) travel faster than clusters (aerosol particles); the phenomenon in which the reverse occurs is known as "thermal diffusion," which is defined as the transport of matter resulting from a temperature gradient. (The patterns of dust on walls near radiators provide a "household" example of the thermal diffusion process.)

Unfortunately, aerosol transport studies are relatively recent, and no work appears to have been performed thus far on the thermal diffusion of aerosols through porous media. For the present, therefore, it appears prudent to regard this type of transport as just another case of gas molecule migration, subject to confirmatory tests if the situation should warrant them. (This view actually involves a fairly reasonable assumption since no "credit" is taken for the filtration capability of, for example, a crushed salt column when applied to aerosols.)

In describing gas transport through porous media, it is convenient to introduce three terms: the viscous flow coefficient, B_o; the Knudsen diffusion coefficient, D_K; and the porosity-tortuosity ratio, ϵ/q. These three parameters, in addition to various properties of the gas, are all

that are required to describe nonturbulent flow of gases through porous media, whatever the driving force (or combination of driving forces) may be. As an example, the permeability K of a porous body to a gas of viscosity η is given by

$$K = (B_o/\eta)\bar{p} + D_K \ , \tag{5}$$

where $\bar{p} = 1/2\ (p_1 + p_2)$ is the arithmetic average of the pressures at the two sides of the septum, whose inequality causes the gas flow in the first place. In physical terms, K is the rate of flow of the gas (in pressure-volume units per unit time) through a porous body (of unit area-to-length ratio) due to the application of unit pressure drop across the body. Permeability is thus a measure of the rate of passage of gas through the porous body as the result of a pressure imbalance across the body; however, circumstances exist (and are relevant to the salt mine) where transport through the body is possible even under conditions of constant pressure. These cases involve gradients in concentration; the process is called ordinary diffusion in the isothermal case and thermal diffusion in the nonisothermal situation. To describe either process, it is necessary to introduce the internal geometry of the porous septum in terms of ϵ/q. This ratio relates the rate of transport of a gaseous species through the porous medium to the rate of transport in free space under otherwise identical conditions. (A more detailed discussion of gas transport in porous media is given in refs. 23 and 24.)

Permeability and diffusion measurements were made using three columns of crushed salt which were formed by employing three different size distributions of the salt grains. The results of the investigation are summarized in Table 8.4. The salt columns are differentiated by the average grain size $\langle d_g \rangle$; thus the grains comprising the "medium" column are about six times larger, on the average, than those in the "fine" crushed salt bed. However, in each case, about 38% of the volume of the bed is free space; that is, the porosities ϵ_t are almost identically 0.38. (The porosity ϵ_t, frequently called the "total porosity," should not be confused with the porosity ϵ that appears in the quantity ϵ/q. This latter porosity is, in fact, only the part of ϵ_t that is involved in gas transport. In some cases,

Table 8.4. Gas Transport Characteristics and Physical Properties of Crushed Salt Columns at 24°C

Type	$\langle d_g \rangle$ (cm)	ϵ_t	B_o (cm²)	D_K (cm²/sec)	ϵ/q
Medium	0.313	0.375	2.44×10^{-5}	700[a]	0.37
Medium-fine	0.129	0.268	3.28×10^{-7}	161[a]	0.124
Fine	0.057	0.377	4.36×10^{-7}	119[a]	0.213

[a]Determined with helium.

and the present instance affords a good example, the two quantities may be considered identical to a fair approximation.)

The ϵ/q values which are tabulated (Table 8.4) indicate that crushed salt beds do not provide a very effective barrier to gas transport. For example, the best performance in this regard is provided by the medium-fine type, which inhibits transport by only a factor of 8 as compared with the rate that would have been observed if the column had not contained the crushed salt.

In the event that a waste package containing significant gaseous radioactivity or material which could become gas-borne loses its integrity, the dispersal of this type of radioactivity would probably not be significantly limited by the crushed salt beds. However, compaction or consolidation of the crushed salt will commence almost immediately as a result of thermal and hydrostatic stresses. Studies of the effects of closure on crushed salt beds thus appear to be desirable to assess effects which might contribute to radioactivity transport while the salt is undergoing reconsolidation; these studies will probably require <u>in situ</u> experimentation.

Another mechanism for reducing the permeability of the crushed salt backfill involves the moisture associated with the migrating negative

crystals in the bedded salt; this subject has likewise come under investigation. In these investigations, water vapor was allowed to permeate a crushed salt column, along which a temperature gradient was imposed, until permeability reduction of the column was observed. In the work performed thus far, the permeability reduction was observed to occur rather rapidly.

One of the bridges that was formed between the salt and the glass tube which enclosed the column is shown in Fig. 8.3. The area below the bridge does not appear to have been affected by exposure to the water vapor, whereas the stained region above the bridge has obtained this appearance as a result of reflux action by the water. In this particular instance, the salt-glass bridge was formed by allowing water vapor in equilibrium with liquid water at 76°C to diffuse through the column at constant total pressure for about two weeks. During this period, the temperature profile displayed in Fig. 8.4 was maintained along the length of the column. As is rather clearly illustrated in the figure, the wet bridge begins almost precisely at the expected dew point.

In the case of this particular experiment, the permeability of the column on completion of bridging decreased by about a factor of 30 from its original value. It is possible, however, that channeling resulted at the salt-glass interface; in such a case, the reduction in permeability provided by the salt within the bridge might be considerably greater. This possibility is currently being examined.

Another aspect regarding gas transport involves the permeability of the bedded salt itself. Since surprisingly little work appears to have been done in this regard, some studies with samples from the Lyons mine are planned. Reynolds and Gloyna[25] have reported results of permeability investigations on Grand Saline dome salt and Hutchinson bedded salt specimens; their work is best summarized by noting that the values they obtain for B_o range about 7×10^{-10} cm^2 for the dome salt and lie between 0 and 2×10^{-12} cm^2 for the bedded salt. Moreover, results of experiments designed to simulate overburden pressure indicated further permeability reductions with the dome salt. By comparison of their values with those listed in Table 8.4, it is quite obvious that significant reduction in permeability exists; however, one cannot, unfortunately, scale the B_o

Fig. 8.3. A Crushed Salt Column After Exposure to Water Vapor.

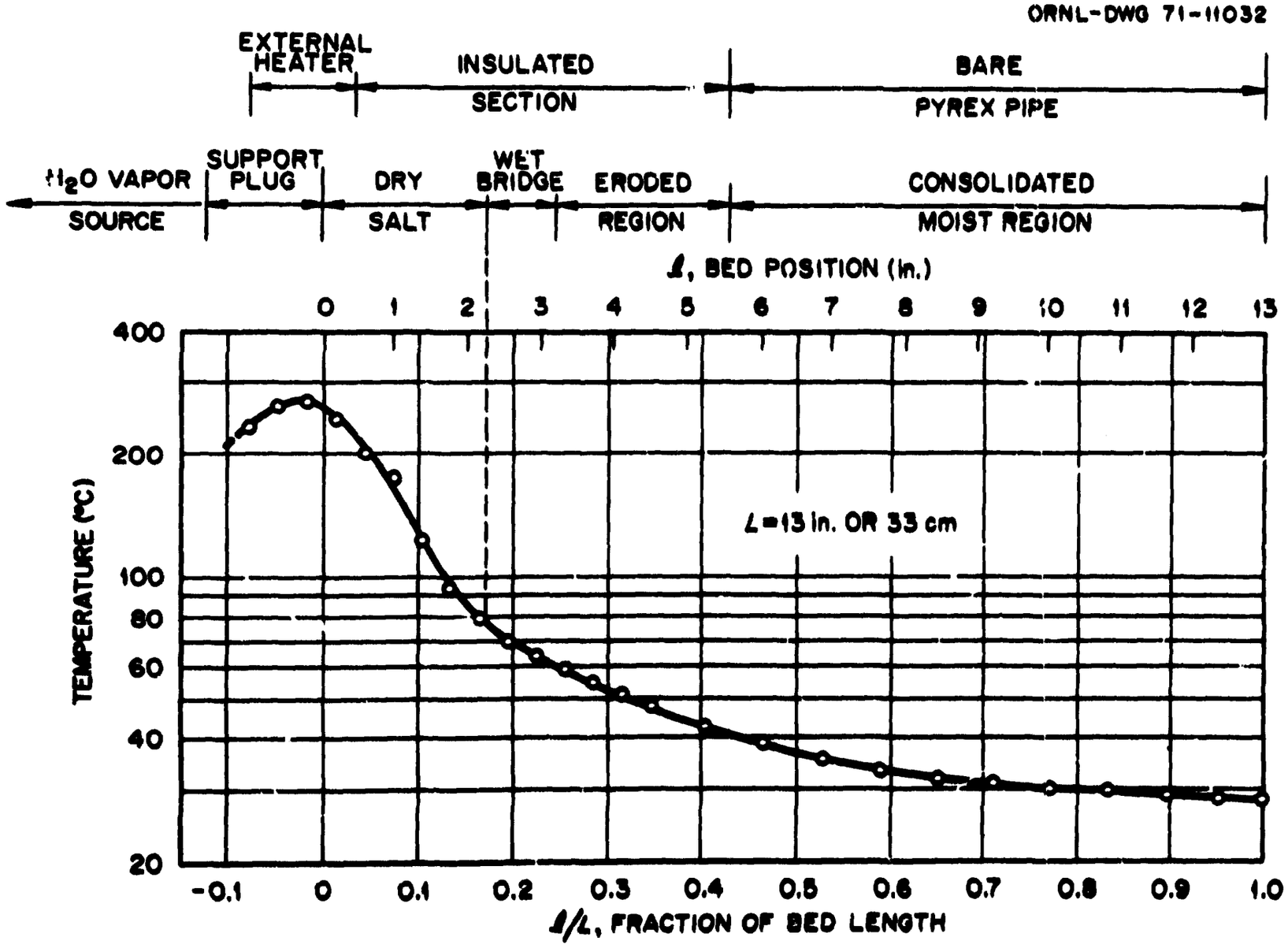

Fig. 8.4. Temperature Profile of the Crushed Salt Column.

values to estimate the ϵ/q results in a straightforward manner. For example, a graphite specimen that has been investigated in this laboratory[23] yielded $B_o = 1 \times 10^{-14}$ cm^2 and $\epsilon/q = 1 \times 10^{-3}$. Thus, further work in this area appears warranted.

Gas phase transport ordinarily provides the most rapid mechanism for the dispersal of matter. If the bedded salt should prove to be truly impermeable to gases, this mechanism would then be an operational possibility only during the relatively brief period during which reconsolidation of the crushed salt backfill occurs. In Sect. 8.3, a much slower mechanism, solid-state bulk or volume diffusion, is considered. The potential significance of this mode of transport rests solely in the extremely long time span over which this mechanism is operational.

8.3 Solid-State Diffusion of Plutonium in Sodium Chloride

In order to obtain some idea of the extent to which solid-state bulk diffusion would contribute to the dispersal of radioactivity throughout the salt formation, we have considered the results of several investigations that have been reported in the literature. These investigations include:

(1) self-diffusion of Na^+ in NaCl,

(2) interdiffusion of various metal ions in NaCl,

(3) interdiffusion of some metal ions through a similar, but larger, lattice (e.g. KCl),

(4) self-diffusion of various ions in a variety of inorganic salts,

(5) interdiffusion of metal ions in various inorganic salts.

To put the problem in some sort of perspective, we shall use, as the characteristic displacement, the rms displacement of the molecules of interest over a 1-million-year period. We chose the rms value instead of the mean displacement because the latter is necessarily zero (positive and negative displacements are equally likely). In reality, diffusion will proceed in all directions. However, our comparison of the results will be equally valid, and much simpler, if we consider diffusion only in

one direction - for example, the x direction. The case we will consider is one in which an initial amount of diffusing species is placed as a thin film or the end of a long rod of solute-free material. If a similar solute-free rod is welded to the plated end of this rod (without any diffusion occurring) and the rod is then annealed for time t, so that diffusion can occur, the concentration of solute (in moles/cm^3) along the bar will be given by the equation

$$C(x,t) = \frac{S}{2(\pi Dt)^{1/2}} \exp\left(-\frac{x^2}{4Dt}\right), \tag{6}$$

where S is the total amount of diffusing species plated on the rod (in moles per centimeter), D is the diffusion coefficient (in cm^2/sec), t is the annealing time (in seconds), and x is the distance along the rod (in centimeters) measured from the initially plated material at x = 0. The mean square displacement is obtained from the relation

$$\overline{\Delta x^2} = \frac{\int_{-\infty}^{\infty} C(x,t)\, x^2\, dx}{\int_{-\infty}^{\infty} C(x,t)\, dx} = 2Dt(\text{cm}^2), \tag{7}$$

whence the rms displacement is simply $(2Dt)^{1/2}$.

8.3.1 Self-Diffusion of Na^+ in NaCl

Mapother et al.[26] measured the rate of diffusion of radioactive $^{24}Na^+$ in sodium chloride over a wide range of temperatures (300 to 700°C). The results for the self-diffusion coefficient can be represented by the equation

$$D = D_o \exp(-Q/RT), \tag{8}$$

with D_o = 3.13 cm^2/sec, Q = 41.4 kcal for T > 550°C; and $D_o = 1.6 \times 10^{-6}$ cm^2/sec, Q = 17.7 kcal for T < 550°C. The values of the self-diffusion coefficient for Na^+ in NaCl at 400 and 350°C have been calculated and are presented, along with the rms displacements for a 1-million-year period, in Table 8.5. The magnitude of the sodium self-diffusion

Table 8.5. Self-Diffusion Coefficients for Na^+ in NaCl, and Root-Mean-Square Displacement for a 1-million-year Period

T (°C)	D (cm^2/sec)	$(2Dt)^{1/2}$ (cm)
400	2.86×10^{-11}	42
350	1×10^{-11}	25

Table 8.6. Interdiffusion Coefficients of Some Metal Ions in NaCl, Calculated from Electrical Mobilities

$$D = D_o \exp(-B/T)$$

System	D_o (cm^2/sec)	B (°K)	$D_{350°C}$ (cm^2/sec)	$(2Dt)^{1/2}$ (cm)	Reference
Cu-NaCl	0.5	12,600	0.83×10^{-9}	229[a]	27
Ni-NaCl	0.2	12,700	2.82×10^{-10}	133[a]	28
Au-NaCl	0.2	12,300	5.4×10^{-10}	184[a]	29

[a]Root-mean-square displacement for a 1-million-year period.

coefficient indicates that sodium ion would diffuse for a distance of less than 25 cm in a million years at 350°C. This is a very encouraging result.

Interdiffusion coefficients[27-29] of some metal ions in NaCl are presented in Table 8.6. At 350°C, the calculated rms displacements for interdiffusion in NaCl are somewhat larger than the self-diffusion coefficients of Na^+ in NaCl; however, they are still small to a very comfortable extent.

Some results[29,30] for interdiffusion through the larger but similar crystal lattice of KCl are presented in Table 8.7. Again, the calculated rms displacements are quite small.

Table 8.7. Interdiffusion Coefficients of Some Metals in KCl, Calculated from Electrical Mobilities

System	D_o (cm^2/sec)	B (°K)	$D_{350°C}$ (cm^2/sec)	$(2Dt)^{1/2}$ (cm)	Reference
Cu-KCl	55	15,200	1.4×10^{-9}	297[a]	29
Au-KCl	11	15,000	3.9×10^{-10}	157[a]	30

[a]Root-mean-square displacement in a million years.

It is probably pertinent to examine other cases of ionic diffusion (even if not through NaCl). Values of diffusion coefficients at selected temperatures,[31-48] along with the corresponding rms displacements for a 1-million-year period, have been calculated from information in the literature and are given in Table 8.8. All of the rms displacement results given in this table are less than 40 m with the exception of four: Ag^+ in β-Ag_2S, Ag^+ in α-Ag_2S, Ag^+ in β-AgI, and Cu in Cu_2S. These systems have displacements of 49, 330, 350, and 250 m, respectively.

Table 8.8. Diffusion Behavior of Some Ions in Solid Inorganic Compounds

System	T (°C)	D (cm^2/sec)	$(2Dt)^{1/2}$ (cm)[a]	Reference
Ag–β–Ag_2SO_4	350	1.3×10^{-9}	290	31
Ag–AgBr	300	1.0×10^{-7}	2,500	32
Ag–β–Ag_2S	179	3.8×10^{-7}	4,900	33
Ag–α–Ag_2S	350	1.7×10^{-5}	33,000	33
Ag–α–AgI	300	2×10^{-5}	35,000	34
Ba–BaO	1,080	1×10^{-9}	250	35
Bi–NaBr	500	1.9×10^{-12}	11	36
Ca–CaO	900	3.3×10^{-16}	0.14	37
Ni–NiO	1,000	1×10^{-10}	70	38
Co–CoO	800	2×10^{-10}	100	39
Fe–FeO	700	2.5×10^{-8}	1,300	40
Fe–FeS	700	3.2×10^{-8}	1,400	40
Hg–α–$AgHgI_4$	127	5×10^{-8}	1,800	41
Pb–PbS	400	3.2×10^{-16}	Negligible	42
S–β–Ag_2S	179	3.6×10^{-13}	4.7	34
Zn–ZnO	800	1.5×10^{-15}	Negligible	43
Mg–MgO	1,400	1.2×10^{-11}	27	44
O–CdO	640	4.5×10^{-16}	Negligible	45
O–$UO_{2.002}$	550	5.5×10^{-15}	Negligible	46
O–$UO_{2.063}$	500	8.4×10^{-12}	23	46
Cu–Cu_2S	400	1×10^{-6}	25,000	47
Be–BeO	1,200	1.4×10^{-12}	9.4	48

[a] At t = 1 million years.

The rapid diffusion in systems such as silver in Ag_2S is explained on the basis of electron transfer. That is, the mobility of electrons is much greater than the mobility of silver ions. Variability in the Ag/S ratio in a salt like Ag_2S can greatly affect the electrical conductivity and the diffusion behavior of the salt. When there is a gradient of the metal/nonmetal ratio, metal ions and electrons migrate in the same direction, electrons having a tendency to move faster than silver ions. This gives rise to an electrical potential gradient, which decelerates electrons and accelerates silver ions so that the actual volume element remains essentially electrically neutral. In Ag_2S, the concentration of excess electrons is substantially lower than the concentration of disordered ions; however, conduction is preponderantly electronic because the mobility of an excess electron is much greater than the mobility of an interstitial ion or an ion vacancy. This situation is encountered not only in Ag_2S but also in Cu_2Se,[49-51] Cu_2Te,[52] AgI,[34] and in KCl[49,52] having an excess of potassium.

Under the influence of radiation, the possibility exists that NaCl will acquire an excess of sodium, which will result in some enhancement in diffusion rates. Although this problem is not considered serious, it should be kept in mind with the idea of checking it experimentally. Some additional results for interdiffusion of ions in various salts that appear pertinent[53-55] are listed in Table 8.9. Values for the rms displacement for a 1-million-year period are also given.

High results were again obtained for a few nonstoichiometric systems that have an excess metal, such as Cu in AgI, Ag in CuI, Cu in Ag_2S, Ag in Cu_2S, and Ag in CuBr. The same explanation as that given above for Ag_2S appears pertinent, although this behavior is not expected in sodium chloride unless radiation alters the picture.

The diffusion behavior of PuO_2 and of Pu_2O_3 should also be considered. In postulating their behavior, however, the possible mechanisms of diffusion of PuO_2 and Pu_2O_3 through NaCl need to be considered. There may be several possibilities concerning the diffusing particles. These could include the following diffusing species: (1) PuO_2 molecules; (2) Pu_2O_3 molecules;

Table 8.9. Coefficients for Interdiffusion of Ions in Various Pertinent Salts

System	T (°C)	D (cm^2/sec)	$(2DT)^{1/2}$ $(cm)^a$	Reference
Cu–AgI	321	2.47×10^{-5}	4.0×10^4	53
Ag–CuI	412	1.56×10^{-5}	3.1×10^4	53
Ag–γ–CuI	254	7×10^{-9}	6.6×10^2	53
Cu–Ag_2S	330	6.3×10^{-6}	2.0×10^4	53
Ag–Cu_2S	313	7.3×10^{-6}	2.1×10^4	54
Na–AgCl	300	2.1×10^{-10}	1.1×10^2	53
Cu–AgCl	238	2.4×10^{-7}	3.9×10^3	53
Na–AgBr	300	2.3×10^{-9}	3.8×10^2	55
Li–AgBr	300	7.6×10^{-8}	2.2×10^3	53
Ag–CuBr	245	5.1×10^{-5}	5.7×10^4	53
Se–Cu_2S	571	1.1×10^{-9}	2.6×10^2	54
Cl–AgI	180	$<1.1 \times 10^{-10}$	0.8×10^2	55

[a]For t = 1 million years.

(3) atoms of Pu° and O°; (4) Pu^{4+}, Pu^{3+}, and O^{2-} ions. The crystal structures of PuO_2, Pu_2O_3, and NaCl are discussed briefly below.

Plutonium dioxide has a face-centered cubic structure with a unit cell of 5.396 Å on an edge.[56] The volume of the unit cell is $(5.396)^3$, or 157 $Å^3$.[57] Each unit cell has an equivalent of four molecules of PuO_2; accordingly, the volume of one PuO_2 molecule is about 39 $Å^3$.

Plutonium sesquioxide has a hexagonal structure with an "a" dimension of 3.84 Å and a "c" dimension of 5.957 Å.[58] The volume of the unit cell is given by $(0.866\ a^2c)$, or $(0.866)(3.84)^2(5.957) = 76\ Å^3$. Each unit cell has an equivalent of one molecule; hence the volume of one Pu_2O_3 molecule is 76 $Å^3$.

Sodium chloride consists of two interpenetrating face-centered cubic lattices composed of sodium and chloride ions, respectively.[59] The radius of the sodium ion is 0.96 Å, and the radius of the chloride ion is 1.83 Å. In the lattice, each sodium ion is surrounded by six chloride ions and each chloride ion is surrounded by six sodium ions. Diffusion through the NaCl lattice could take place via a vacancy or an interstitial mechanism. For interstitial diffusion, the diffusing species must be of such size as to fit interstitially in the NaCl lattice and must be able to pass through the interionic spaces of the lattice without causing an undue amount of strain. For vacancy diffusion, the diffusing species will have to be of a proper size that will not cause large strains in the NaCl lattice. Sizes of various species of interest[56,58,60,61] are given in Table 8.10.

Clearly, the sizes of the Pu_2O_3 and PuO_2 molecules rule these two species out of contention for interstitial (and vacancy) diffusion through the NaCl lattice, which consists of Na^+ ions (0.96 Å) and Cl^- ions (1.83 Å). The same can be said about the atomic diffusion of plutonium, which has an atomic radius in the range of 1.7 to 1.86 Å. Furthermore, because of the large stability of the PuO_2 and Pu_2O_3 molecules (ΔF° = -237 kcal/mole[62] and -418 kcal/mole,[63] respectively), the likelihood of dissociation into atoms is negligible. Although the stabilities of Pu_2O_3 and PuO_2 prevent their dissociation into ions, it would appear that, from the standpoint

Table 8.10. Molecular Atomic and Ionic Radii of the Species of Interest (Ionic charges given in parentheses)

Species	Metallic Radii (Å)	Ionic Radii (Å)	Molecular Radii (Å)	Reference
Pu_2O_3			3.8	58
PuO_2			3.1	56
Pu	1.86	1.00 (+3); 0.90 (+4)		60
Cu	1.27(0)	0.96 (+1); 0.70 (+2)		61
Ni	1.24(0)	0.69 (+2)		61
Au	1.40(0)	1.37 (+1)		61
Na	1.86	0.96 (+1)		61
K	2.23	1.33 (+1)		61
Cl	1.05	1.83 (-1)		61
O	0.60	1.32 (-2)		61

of size alone, either Pu^{3+} or Pu^{4+} would be a good candidate for diffusion through NaCl. However, if by some unforeseen phenomenon, Pu^{4+} and Pu^{3+} ions were to become available, it is most improbable that their diffusion rates could be faster than the self-diffusion of Na^+ ion. In order to justify this statement, at least qualitatively, the mechanism of diffusion of Na^+ in NaCl should be considered briefly and it should be extrapolated to the case in which Pu^{4+}, Pu^{3+}, and O^{2-} exist.

From a random-walk analysis,[64] the diffusion coefficient of Na^+ in NaCl is given by:

$$D_v = \frac{1}{6} \Gamma_v \alpha , \qquad (9)$$

where α is the length of the jump and Γ_v is the frequency of the jumps. Since α is determined by the lattice through which diffusion occurs (the NaCl lattice), the length of the jump should be the same for Na^+ and plutonium. The frequency of jumps is related to the universal molecular frequency of vibration (kT/h) and the probability that vacancies exist for the atom to jump to a neighboring site. Both Na^+ and plutonium ions will have the same vibrational frequency at the same temperature. The probability of vacant sites suitable for Na^+ occupation appears to be not less than the corresponding probability for plutonium ion, and is probably higher in the case of Na^+ since the valence does not change. That is, when a sodium ion leaves a vacancy, that vacancy is exactly right for occupation by another sodium ion. On the other hand, trivalent or tetravalent plutonium ions will probably not find these vacancies completely suitable for occupation relative to size, and certainly not with regard to electric charge. Furthermore, in the case of self-diffusion of Na^+ in NaCl, no accommodation problem exists relative to the Cl^- ions. On the other hand, if the diffusing species are Pu^{3+}, Pu^{4+}, and O^{2-}, the additional problem of accommodating the O^{2-} exists. For these qualitative reasons, it appears quite reasonable to contend that the diffusion of plutonium and oxide ions through NaCl would tend to proceed no faster than the self-diffusion of Na^+; on this basis, migration by solid-state bulk diffusion appears to be completely negligible. This is particularly true for strontium and cesium since, in these cases, a diffusion time interval of 1 million years is unrealistically conservative (by at least three orders of magnitude).

Additional, usually more rapid, mechanisms do exist; however, these involve transport through the salt body either because of microscopic irregularities in the crystal lattice (grain boundary diffusion) or because of macroscopic irregularities (surface diffusion). Progress in these two areas is described in Sect. 8.4.

8.4 Migration on the Surface of Sodium Chloride

At this point, only grain boundary diffusion and transport along free surfaces remain to be considered as contributory mechanisms for the dispersal of radioactivity through the salt formation. Of these, the latter is ordinarily the more rapid. Hence, although the time interval over which this mode of transport may proceed may be limited to the period over which recrystallization occurs, diffusion along free surfaces can be regarded as a special, probably more rapid, form of grain boundary transport. It is with this view in mind that we consider solid-state, grain boundary diffusion and surface diffusion to be identical.

Mass transport along the surface of a solid is one of the least understood of the many forms of diffusion phenomena. Two factors are primarily responsible for the ambiguity. The first invokes the concept of a solid surface. For example, processes occurring on the surface of a polycrystalline material may be expected to behave quite differently from those on the surface of a single crystal face. While the latter case would appear to represent the most controllable type of surface, considerable latitude for uncertainty still exists. The orientation of the crystal face, the possibility of structural defects such as valleys and terraces, and the presence of contaminants such as nitrogen and water vapor can affect experimental reproducibility and complicate the formulation of realistic mathematical models for surface movement.

The second source of ambiguity arises from the manner in which the diffusing component is distributed upon the surface. This aspect of the problem has two facets. One is concerned with the amount of surface area occupied by a single layer of atoms, while the other involves the vertical distribution, or the possibility of a multilayer deposit, of the diffusing

species. Barrer,[65] in a review of the early work on surface diffusion, stresses the importance of the first type of concentration dependence and indicates that differences in the diffusion coefficient of one to two orders of magnitude may occur due to the distribution over the surface. Unfortunately, the possibility of a concentration-dependent diffusion coefficient can render the mathematical analysis of a diffusion problem intractable; consequently, it would appear that this aspect has been largely ignored in subsequent investigations.

Somewhat more progress has been made on the question of vertical distributions. Langmuir and Taylor[66] have hypothesized that the ratio of the heat of adsorption for an atom in a monolayer to the activation energy for migration in the first layer of cesium on tungsten remained constant as additional layers were deposited. The diffusion coefficient characteristic of the second layer was estimated to be approximately six orders of magnitude larger than that for the first layer at room temperature. Experimental evidence for such an effect may be found in the measurements of Arnikar and Mehta,[67] who investigated the self-diffusion of I^- on copper for monolayers and for films composed of approximately 100 layers. The multilayer diffusion coefficient was larger by a factor ranging from 3 to 10.

Similar evidence comes from an investigation of the migration of H_2, CO, and O_2 over tungsten by Gomer.[68] He observed that deposits of approximately a monolayer or less were essentially immobile; however, when the coverage was in excess of a monolayer, spreading occurred with a sharp boundary. This was interpreted as the result of atoms in the second (or higher) layer skating with relative ease over the primary layer, falling off the edge, and becoming chemisorbed on the substrate.

Discussion of a somewhat similar problem may be found,[69-73] in which the existence of a layer extending into the substrate and characterized by a higher diffusivity than that of the bulk material has been postulated. Such a concept necessitates the introduction of an additional parameter, corresponding to the layer thickness, into an analysis of the concentration distribution of the diffusing component. At the present time, estimates of this thickness range from one atomic layer (10^{-8} cm) to 10^{-6} cm.

In view of the numerous experimental and conceptual difficulties, it is not surprising that numerical values for surface diffusion coefficients, particularly those related to NaCl, are sparse. Only one direct measurement appears to have been made. Nikitine and Goltzene[74] reported a tentative value of 2×10^{-8} cm^2/sec at 423°K for the diffusion of Cu^+ over RbBr. The Cu^+ originated in a layer of CuCl deposited on the crystal surface. No diffusion of CuCl was observed.

The remaining studies were primarily directed toward an investigation of the nucleation of adsorbed molecules being deposited on a surface. Such studies provide a value for the activation energy of migrating molecules from which the diffusion coefficient can be inferred through the use of the relation[75]

$$D = a^2 \nu \exp(-Q_D/RT) , \qquad (10)$$

where "a" is the distance between absorption sizes, ν is the atomic vibration frequency, and Q_D is the activation energy. Sumner[75] suggests values of 4 Å and 7×10^{12} sec^{-1} for "a" and ν, respectively; and these were used to compute the diffusion coefficients in Table 8.11.[75-79] In the case of In-NaCl,[76] values for the mean diffusion length λ_s and the lifetime on the substrate τ were reported; the diffusion coefficient can then be estimated from

$$\lambda_s^2 = D\tau . \qquad (11)$$

Unfortunately, comparison of these computed values with a direct measurement does not appear to be possible. However, it is worth noting that, in the case of silver on mica, a direct measurement[80] of D, using ^{110}Ag as a tracer, yielded an activation energy approximately an order of magnitude larger than that obtained by studying the nucleation process.[81]

Another factor influencing the reliability of the values in Table 8.11 is the necessity of using a theoretical model to explain the nucleation process. In the case of Pt-NaCl, two different analyses of the data have been made with quite different results.

A final study that indicates the possibility of rather divergent evaluations of a surface diffusion coefficient is found in the work of

Table 8.11. Surface Diffusion Coefficients for NaCl and Related Systems

System	T (°K)	Q_D (kcal/mole)	D (cm^2/sec)	$(2Dt)^{1/2}$ $(cm)^a$	Reference
Au–KCl	473	2.77	6×10^{-4}	2×10^5	77
	673		1.4×10^{-3}	3×10^5	
In–NaCl	293	-	2×10^{-2}	1×10^6	76
Ag–NaCl	473	<4.61	8×10^{-5}	7×10^4	78
	673		3.6×10^{-4}	1.5×10^5	
Pt–NaCl	473	4.15	1.3×10^{-4}	9×10^4	75
	673		5×10^{-4}	1.8×10^5	
Pt–NaCl	473	10.4 ± 1.1^b	1.8×10^{-7}	3.4×10^3	79
	673		4.7×10^{-6}	1.7×10^4	

[a]Root-mean-square displacement after a 1-million-year period as ascertained from a one-dimensional random walk model.

[b]Reinterpretation of data in ref. 75 by Lewis (ref. 79).

Geguzin et al.[82,83] The authors present a theoretical and experimental analysis of the coalescence of islands of gold deposited on an NaCl crystal and obtain a value of 10^{-16} cm^2/sec at 573°K. Admittedly, this is an anomalous result, and the discrepancy may stem from the possibility of charges on the gold.

Since no reliable estimate of surface migration of radioactive waste species was available on the basis of the existing data, an experimental program was initiated. Much of the work performed to date has been primarily concerned with the development of an appropriate experimental technique. The most promising method investigated thus far involves depositing the species of interest on an NaCl crystal using electron beam deposition and, after subjecting the specimen to a diffusion anneal procedure, determining the concentration profile of the deposited species with an electron microprobe. The results of a trial experiment are displayed in Fig. 8.5.

The data plotted in Fig. 8.5 were obtained by depositing La_2O_3, which is being used as a substitute for highly toxic PuO_2, on an area of NaCl to a depth of about 100 monolayers, then heating the sample at 200°C for approximately two days, and finally scanning the surface with an electron microprobe. In this figure, the concentration relative to the concentration in the bulk part of the deposit is plotted as a function of distance from an arbitrary point within the nondiffused area of the deposit. The data have been matched at the point $2C = C_o$ with two theoretical profiles: one corresponding to a diffusion coefficient of 10^{-10} cm^2/sec, and a second characteristic of $D = 10^{-8}$ cm^2/sec. Aside from the inexplicably long "tail" exhibited by the data, the results appear to indicate that surface diffusion (and hence grain boundary diffusion as well) proceeds acceptably slowly relative to the salt-mine applications. However, it is important to emphasize that this experiment only suggests the appropriateness of the techniques employed; the profile may, in fact, be the result of experimental artifacts produced by the method employed to mask the sample during deposition of the La_2O_3. These aspects are currently under investigation.

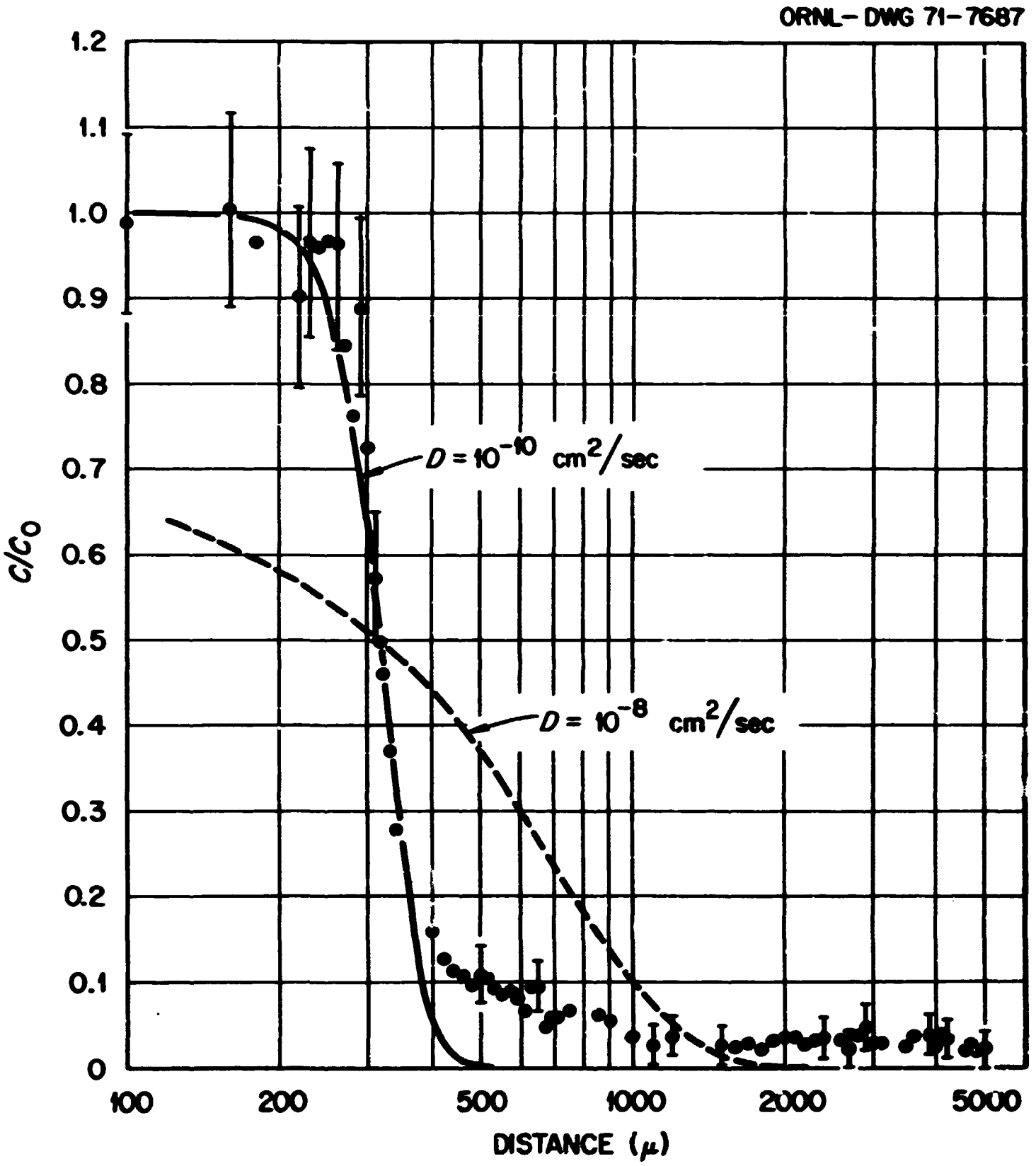

Fig. 8.5. Relative Concentration Profile of La_2O_3 Deposited on an NaCl Surface.

8.5 "Integrated" Experiments for the Investigation of Isotope Migration

All of the work discussed above has considered specific mechanisms for the dispersal of radioactivity through the Repository without regard to the possibility of synergism among the various phenomena. Although a set of circumstances that yields an apparent synergistic effect with regard to an interaction of the transport mechanisms per se can be concocted, a true synergistic effect in this sense is highly improbable. However, the situation is not quite so straightforward relative to the possible formation of volatile species. In addition, this problem affords an investigation of an almost endless number of possible chemical combinations to yield volatile compounds; thus a systematic theoretical approach appears to be prohibitive.

Because it seems advisable to design experiments that simulate the actual situation as closely as possible, a series of so-called "integrated" experiments has been planned. Simulated waste material which is tagged with appropriate radioactive tracers will be used in these experiments.

A schematic diagram of the apparatus that will be employed in this work is presented in Fig. 8.6. In the initial experiments, simulated calcined waste, containing ^{137}Cs in one series and ^{106}Ru in another, will be positioned at about the midplane of a crushed salt column; and the column, in turn, will be positioned within a furnace. Once the crushed salt bed has been brought to the desired temperature, the column will be exposed to air or air-water vapor mixtures, and transport of the waste, both upstream and downstream relative to the gas flow, will be monitored by scanning the column for the cesium and ruthenium. In later experiments, both the purge gas composition and the tagged species will be changed as circumstances dictate.

In a related experiment, the migration of plutonium will be investigated. A view of the apparatus involved, which requires glove-box operation, is shown in Fig. 8.7. This experiment is identical in concept with the integrated experiments discussed above, except in this case the salt bed will be contained within a stack of Plexiglas plates for purposes of later sectioning the column for plutonium analysis. The initial experiments will

ORNL DWG 71-9867

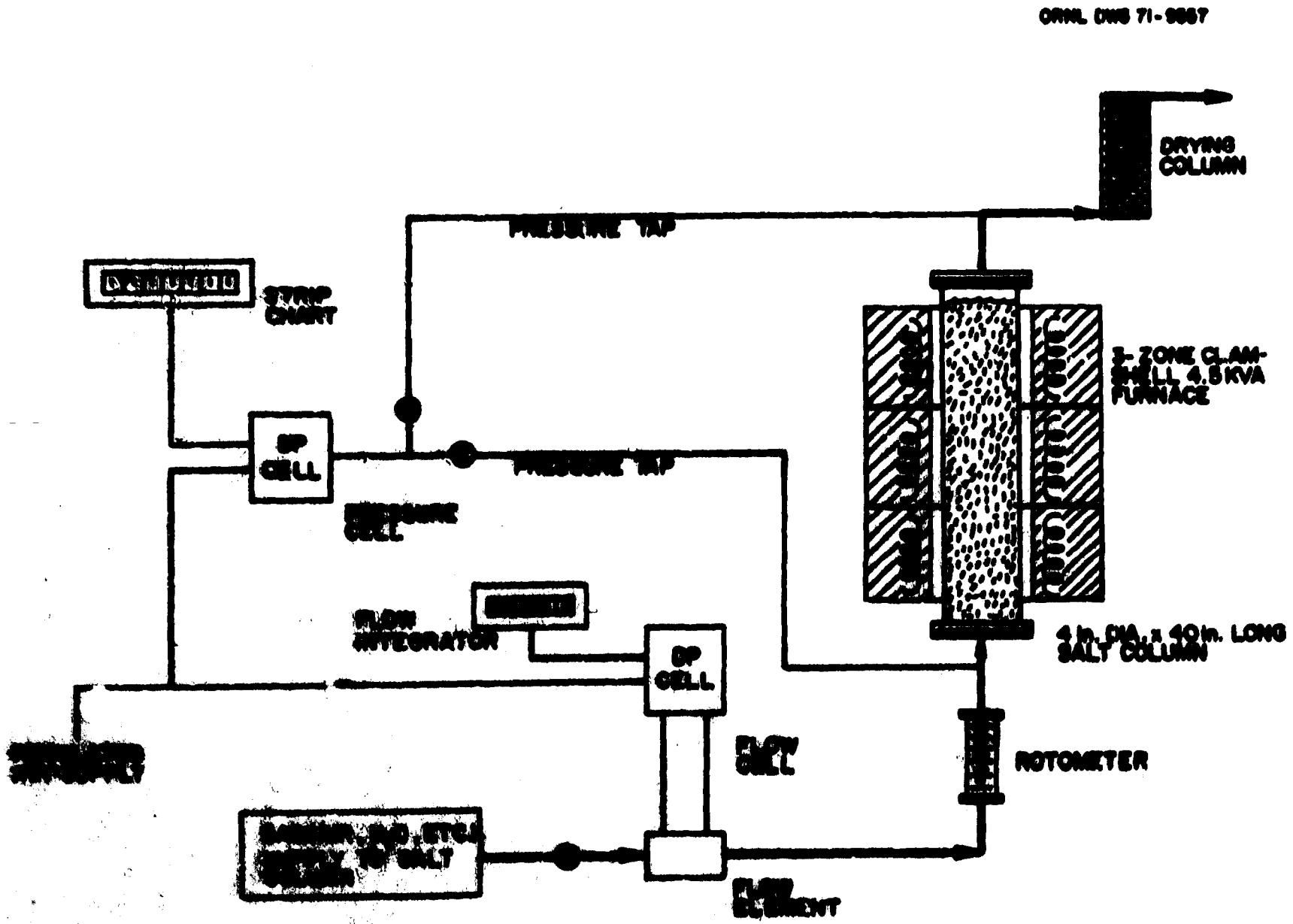

Fig. 5.6. [illegible] of Apparatus for Studying Movement of [illegible]

Fig. 8.7. Apparatus for the Investigation of Plutonium Migration in a Crushed-Salt Column.

be performed at room temperature, and the plutonium that will be suspended at about the midplane of the crushed salt bed will result from the previous evaporation of a plutonium nitrate solution on some of the salt comprising the bed.

8.6 Conclusions Regarding Isotope Migration in the Salt-Mine Repository

The information obtained to date regarding isotope transport within the Repository has not revealed any concrete causes for concern. However, the investigations have uncovered several areas in which definitive data are simply nonexistent; and, in these cases, experimental programs have been initiated.

It is most unlikely that volatile species of any consequence can result from the interaction of water vapor with the oxide wastes, but it is not yet clear whether noncxide species can be released through a similar type of interaction. Also, no consideration has been given thus far to reactions between the waste and the products of the radiolysis reactions which will occur within the brine inclusions. Such effects will be investigated in the integrated experiments.

Gas transport characteristics of crushed salt beds, as determined in the present study, clearly indicate that such beds are virtually ineffective in retarding gas migration. Hence, if significant amounts of gaseous or gas-borne activity are involved, it is imperative that the waste cylinder maintain its integrity until reconsolidation processes reduce the permeability of the salt. On the other hand, in view of estimates of hydrogen production (see Sect. 10), it may be desirable to inhibit reconsolidation to avoid the possibility of forming voids of high hydrogen content in the salt. With regard to gas transport, it is likewise pertinent to point out the necessity of obtaining additional data on the permeability of the bedded salt itself. This information will be obtained shortly.

Although no data describing solid-state bulk diffusion appear to have been obtained for systems of direct application to the salt mine, the work which has been done leaves little doubt that this mechanism yields negligible transport, except possibly in certain cases in which radiation may induce

space charges within the crystal. Even this effect appears remote when one considers that some of the experimental data were obtained using radiotracer techniques.

Whereas solid-state bulk or volume diffusion has been investigated sufficiently well to permit meaningful inferences to be drawn from published data, quite the reverse is true of grain boundary and surface transport. Not only is there a paucity of data, but even a cursory examination of what is available indicates gross inconsistencies. An experimental program to investigate these phenomena has been initiated.

Although the studies described above are ultimately concerned with demonstrating that salt formations provide excellent encapsulation facilities for the long-term storage of radioactive wastes, only in situ experimentation can provide unassailable evidence in this regard. Hence these laboratory investigations ought really to be considered as parametric studies in the sense that the results obtained in the laboratory will provide the information to properly instrument and conduct the in situ experiments planned for the early, demonstrational phase of the Repository operations.

8.7 References

1. R. L. Bradshaw and W. C. McClain (Eds.), Project Salt Vault: A Demonstration of the Disposal of High-Activity Solidified Wastes in Underground Salt Mines, ORNL-4555 (April 1971), p. 170.

2. Ibid., p. 4.

3. Ibid., pp. 164-67.

4. G. H. Jenks, ORNL, private communication. See Sect. 10 of this report.

5. Reference 1, pp. 170-72.

6. O. Glemser, A. Müller, and U. Stöcker, Z. Anorg. Allgem. Chem. 333, 25 (1964).

7. O. Glemser and R. v. Haeseler, Z. Anorg. Allgem. Chem. 316, 168 (1962).

8. O. Glemser, A. Müller, and H. Schwarzkopf, Z. Anorg. Allgem. Chem. 334, 21 (1964).

9. O. Glemser and A. Müller, Z. Anorg. Allgem. Chem. 334, 150 (1964).

10. O. Glemser and H. Ackermann, Z. Anorg. Allgem. Chem. 325, 220 (1963).

11. O. Glemser and H. Ackermann, Z. Anorg. Allgem. Chem. 325, 281 (1963).

12. O. Glemser, H. G. Volz, and B. Meyer, Z. Anorg. Allgem. Chem. 298, 311 (1957).

13. O. Glemser and H. G. Wendlandt, Adv. Inorg. Chem. Radiochem. 5, 215 (1963).

14. D. A. Furey and E. W. Bloore, Effect of Water Vapor on the Volatility of Fission Product Oxides, Ballistic Research Laboratories Memorandum Report No. 2022 (February 1970).

15. A. P. Malinauskas, J. W. Gooch, Jr., and J. D. Redman, Nucl. Appl. Technol. 8, 52 (1969).

16. N. D. Erway and R. L. Seifert, J. Electrochem. Soc. 98, 83 (1951).

17. M. S. Chandrasekhariah, in Appendix B of the Characterization of High Temperature Vapors, ed. by J. L. Margrave, Wiley, New York, 1967.

18. C. A. Alexander, J. S. Ogden, and A. Levy, J. Chem. Phys. 39, 3057 (1963).

19. A. B. Nikol'skii, Russian J. Inorg. Chem. 8, 541 (1963).

20. A. P. 'alinauskas, Vapor Pressure of Tellurium Dioxide, ORNL-4300 (September 1968).

21. W. A. Young, J. Phys. Chem. 64, 1003 (1960).

22. J. Berkowitz, D. J. Meschi, and W. A. Chupka, J. Chem. Phys. 33, 533 (1960).

23. A. P. Malinauskas, J. L. Rutherford, and R. B. Evans III, Gas Transport in MSRE Moderator Graphite. I. Review of Theory and Counter-Diffusion Experiments, ORNL-4148 (September 1967).

24. E. A. Mason, A. P. Malinauskas, and R. B. Evans III, J. Chem. Phys. 46, 3199 (1967).

25. T. D. Reynolds and E. F. Gloyna, Reactor Fuel Waste Disposal Project Permeability of Rock Salt and Creep of Underground Salt Cavities, TID-12383 (December 1960).

26. D. Mapother, H. Crooks, and R. Mauer, J. Chem. Phys. 18, 1231 (1950).

27. S. A. Arzybyschew and N. B. Borissow, Phys. Z. Sowjetunion 10, 44 (1936) and 10, 56 (1936), cited by W. Jost in Diffusion in Solids, Liquids and Gases, p. 202, Academic, New York, 1960.

28. I. A. Parfianovitsch and S. A. Schipizyn, Acta Physicochim. USSR 6, 263 (1937), and Pogodaev, Khim. Ref. Zhur. 4, Nr 4, 12 (1941), both cited by W. Jost in Diffusion in Solids, Liquids, and Gases, Academic, New York, 1960.

29. W. J. Bogomolowa, Acta Physicochim. USSR 5, 161 (1936), cited by W. Jost in Diffusion in Solids, Liquids, and Gases, Academic, New York, 1960.

30. S. A. Arzybyschew, Compt. rend-Acad. Sci. USSR (N.S.) 8, 157 (1935), cited by W. Jost in Diffusion in Solids, Liquids, and Gases, Academic, New York, 1960.

31. A. Murin and Ju. Tausch, Dokl. Akad. Nauk SSSR 80, 579 (1951); see, for example, J. Teltow, Z. Elektrochem. 56, 767 (1952).

32. I. Pfeiffer, K. Hauffe, and W. Jaenicke, Z. Elektrochem. 56, 728 (1952).

33. R. L. Allen and W. J. Moore, J. Phys. Chem. 63, 223 (1959).

34. D. Peschanski, J. Chim. Phys. 47, 933 (1950).

35. R. W. Redington, Phys. Rev. 82, 574 (1951).

36. H. W. Schamp and E. Katz, Phys. Rev. 94, 828 (1954).

37. R. Lindner, J. Chem. Phys. 23, 410 (1955).

38. M. T. Shim and W. J. Moore, J. Chem. Phys. 26, 802 (1957).

39. R. E. Carter and F. D. Richardson, J. Metals 6, 1244 (1954).

40. L. Himmel, R. F. Mehl, and C. E. Birchenall, Z. Metals 5, 827 (1953).

41. K. E. Zimen, G. Johansson, and M. Hillert, J. Chem. Soc. (London) 1949, 392.

42. G. Simkovich and J. B. Wagner, J. Chem. Phys. 38, 1368 (1963).

43. R. Lindner, Acta Chem. Scand. 6, 457 (1952).

44. R. Lindner and G. D. Parfitt, J. Chem. Phys. 26, 182 (1957).

45. R. Haul and D. Just, Z. Elektrochem. 62, 1124 (1958).

46. A. B. Auskern and J. Belle, J. Chem. Phys. 28, 171 (1958); J. Belle, A. B. Auskern, W. A. Bostrom, and F. S. Susko, Proc. Fourth Intern. Symp. on the Reactivity of Solids, Amsterdam, 1960, p. 83.

47. V. Wehefritz, Z. Physik. Chem. (NF) 26, 339 (1960).

48. H. J. de Bruin and G. M. Watson, J. Nucl. Mater. 14, 239 (1964).

49. C. Wagner, Z. Physik. Chem. B32, 447 (1936).

50. H. Reinhold and H. Mohring, Z. Physik. Chem. B38, 221 (1937).

51. H. Reinhold and H. Seidel, Z. Physik. Chem. B38, 245 (1937).

52. H. Reinhold and H. Braunginger, Z. Physik. Chem. B41, 397 (1939).

53. O. Stasiw, Nachrichten Gesellsch Wisenschaffen Gottingen (NF) 1, 147 (1935).

54. C. Tubandt, H. Reinhold, and W. Jost, Z. Anorg. Allgem. Chem. 177, 253 (1928), cited by W. Jost in Diffusion in Solids, Liquids, and Gases, Academic, New York, 1960.

55. H. Braune and O. Kahn, Z. Physik. Chem. 112, 270 (1924), cited by W. Jost in Diffusion in Solids, Liquids, and Gases, Academic, New York, 1960.

56. R. W. G. Wycoff, Crystal Structures, 2d ed., Vol. 1, p. 243, Interscience, New York, 1963.

57. W. Jost, Diss. Halle, 1926, cited by W. Jost in Diffusion in Solids, Liquids, and Gases, Academic, New York, 1960.

58. R. W. G. Wycoff, Crystal Structures, 2d ed., Vol. 2, p. 3, Interscience, New York, 1963.

59. Ibid., Vol. 1, p. 88.

60. Plutonium Handbook, Vol. 1, ed. by O. J. Wick, Gordon and Breach, New York, 1967, p. 331.

61. Handbook of Chemistry and Physics, 36th ed., Chemical Rubber Company, Cleveland, Ohio, 1954.

62. Plutonium Handbook, Vol. 1, ed. by O. J. Wick, Gordon and Breach, New York, Publishers, 1967, p. 340.

63. Ibid., p. 342.

64. P. G. Shewmon, Diffusion in Solids, pp. 51-54, 137-143, McGraw-Hill, New York, 1963.

65. R. M. Barrer, Diffusion In and Through Solids, Cambridge University Press, New York, 1941.

66. J. B. Taylor and I. Langmuir, Phys. Rev. 44, 423 (1933).

67. H. J. Arnikar and O. P. Mehta, J. Phys. Chem. Solids 24, 1633 (1963).

68. The Solid-Gas Interface, ed. by E. A. Flood, p. 597, Marcel Dekker, New York, 1967.

69. Ya. Ye. Geguzin, G. N. Kovalev, and O. M. Ratner, Phys. Metals Metallog. (USSR) (English Transl.) 10 (1), 45 (1960).

70. P. G. Shewmon, J. Appl. Phys. 34, 755 (1963).

71. T. Suzuoka, J. Phys. Soc. Japan 20, 1259 (1965).

72. V. A. Panteleyev and V. S. Metrikin, Phys. Metals Metallog. (USSR) (English Transl.) 23(6), 96 (1967).

73. B. Ya. Pines, I. P. Grebennik, and I. V. Gektina, Soc. Phys. Crystallography 12, 556 (1968).

74. S. Nikitine and A. Goltzene, Phys. Letters 13, 290 (1964).

75. G. Sumner, Phil. Mag. 12, 767 (1965).

76. V. M. Kosevich and S. N. Grigorov, Soviet Phys.-Solid State (English Transl.) 10, 1998 (1969).

77. V. I. Trofimov, A. E. Chalykh, and V. M. Lukyanovich, Soviet Phys.-Solid State (English Transl.) 11, 698 (1969).

78. D. Walton, T. N. Rhodin, and R. W. Rollins, J. Chem. Phys. 38, 2698 (1963).

79. B. Lewis, Surface Sci. 21, 289 (1970).

80. V. I. Solunskii and A. A. Dobrikov, Soviet Phys. "Doklady" (English Transl.) 14, 497 (1969).

81. V. S. Postnikov, V. M. Ievlev, I. V. Zolotukhin, Soviet Phys.-Solid State (English Transl.) 10, 2531 (1969).

82. Ya. E. Geguzin, Yu. S. Kaganovskii, and V. V. Kalinin, Soviet Phys.-Solid State (English Transl.) 11, 203 (1969).

83. Ya. E. Geguzin, Yu. S. Kaganovskii, and V. V. Slyozov, J. Phys. Chem. Solids 30, 1173 (1969).

9. ENERGY STORAGE[1]

E. Sonder S. Lindenbaum
J. P. Nichols R. S. Dillon*
J. O. Blomeke

Stored energy, as used in this section, refers to energy stored in irradiated solids due to the introduction of defects and other disorder which will give a negative contribution to the specific heat of the solid when the latter is warmed subsequent to the irradiation. In some cases (particularly in strongly covalent crystals in which large amounts of energy can be stored), all of the energy can be released with a relatively low initiating temperature since the initial energy release can heat the solid sufficiently to trigger energy releases at successively higher transition temperatures. In the case of long-term storage of radioactive wastes, it is important to know how much energy can be stored at saturation in the materials that will be in the radiation field and thermal environment of the Repository. (We define saturation as that level of damage at which the radiation removes as much energy by radiation annealing as it supplies by radiation damage.) The materials in question are the glass or ceramic boule containing the radionuclides, the metal container, and the surrounding salt. The temperature of the wastes and their containers will be from 600 to 900°C initially and will decrease to less than 500°C in about 10 years, while the temperature of the salt will range between 20 and 350°C, depending on its proximity to the waste and the thermal power of the source. The maximum accumulated radiation dose in salt will range from 2×10^{11} rads adjacent to the wastes to about 82 rads at a distance of 5 ft.

9.1 A Brief Review of the Literature

Most previous work has been concerned with two subjects: (1) stored energy in metals produced by irradiation at liquid helium temperatures, and (2) study of graphite irradiated at and above room temperature. In copper,

---

*Present address: AECOP, Oak Ridge, Tenn.

a typical metal, the mobility of defects, particularly interstitials, is high enough that approximately half of the stored energy is released between 30 and 50°K. Although there have been no irradiations heavy enough to approach saturation, one can estimate that if there were about 1% Frenkel pairs produced, a total energy of about 10 cal/g would be released between 30 and 50°K or that approximately a total of 20 cal/g could be stored by low-temperature heavy-particle irradiation.[2] Fairly extensive work has been done with graphite. This material, being covalently bonded and having a much higher melting point (and therefore, cohesion) than metals, will release damage at much higher temperatures, retaining some up to 2000°C. For irradiation in the vicinity of room temperature, approximately 700 cal/g can be stored; however, if the irradiation is performed at 250°C, only one-third of this amount is retained.[3]

With the exception of the above-mentioned work with metals and graphite, very few measurements have been made of stored energy in solids. Kobayashi[4] reports an energy release of 2 to 2-1/2 cal/g between room temperature and 400°C in NaCl that has been heavily irradiated with protons at room temperature. Bunch and Pearlstein[5] have compared the F-center concentration in X-ray-irradiated NaCl with the stored energy and give a value of 12.4 eV per F-center (4.7×10^{-19} cal/F-center). For a saturation concentration of 2×10^{19} F-centers/cm^3 (ref. 6), this would yield a saturation stored energy of 4 cal/g.

9.1.1 Possible Method for Estimating Stored Energy in Other Solids

It is generally agreed that, by far, the major part of energy stored in irradiated crystals stems from the creation of point defects. For every atom or ion that has been removed from a normal (minimum energy in a thermodynamic sense) lattice position, the crystal increases its energy by an amount corresponding to the energy of binding of the atom or ion in the crystal. In addition, when an atom or ion is displaced to an interstitial site, the crystal energy may be raised due to resulting strain. The total energy stored is less than the sum of these two effects since there will be some amount of binding of the displaced atoms or ions to lattice atoms or to each other.

In metals where complete relaxation of the electronic structure takes place when an atom is displaced (i.e., where no charged points can be created), both the vacancy and interstitial energies are chiefly elastic and are correspondingly small (for example, ~20 cal/g for copper containing 1% Frenkel pairs). In insulators, particularly covalent crystals, where bonds are broken and electrons are consequently left in free ion- or free atom-like states, the energy stored is much greater. We can estimate what stored energy to expect from these broken bonds by assuming that, for each vacancy created, the crystal gains energy equal to the cohesive energy of one atom or ion. The heat of sublimation, which can be measured experimentally and is tabulated in many handbooks, is closely related to the cohesive energy, and can also be used. Table 9.1 lists cohesive or sublimation energies[2-5,7-10] for a number of materials. These values give some idea of the range of energies that might be stored in various materials. The fourth column of the table lists 1% of the cohesive (or sublimation) energies. One expects 1 to 5% Frenkel pairs to be a saturation value since with such a degree of disorder the crystal either breaks up, becomes amorphous, or is healed by the radiation at the same rate as damage is created. For the case of copper and graphite this reasoning seems to lead to agreement with the measured values. For NaCl, where the saturation vacancy concentration is known to be 0.12%, agreement is also within 50%.

9.2 Experimental

9.2.1 Sodium Chloride

Rock salt samples in the vicinity of the waste containers in the Project Salt Vault experiment consist of fairly pure sodium chloride. To ascertain the purity of these samples, gravimetric chloride analyses were performed on unirradiated and irradiated (8×10^7 rads) samples from the mine. Values of 60.4 ± 0.2 and 60.6 ± 0.2% Cl were found, respectively. These values may be compared with the chloride content of pure NaCl (60.66% Cl). These analyses suggest that, for the purpose of stored energy measurements by solution calorimetry, the samples may be considered to be pure water-soluble NaCl.

Table 9.1. Estimates of Stored Energy in Various Solids at Saturation

Material	Cohesive Energy (kcal/g)[a]	Heat of Sublimation (kcal/g)	Estimated Energy Stored for 1% Frenkel Pairs (cal/g)	Measured Stored Energy (cal/g)	Ref.
Na		1.55	15		7
Cu		1.28	13	20[b]	2,7,8
W		1.14	11		7
NaCl	2.62		26	2-1/2 - 4[c]	4,5,9
MgO	6.00		60		9
Al_2O_3	6.54		65		9
SiO_2	6.66		67		10
Graphite	20 ± 4		200	700	3,10

[a]For ionic solids, the cohesive energy is calculated with respect to separated atoms.

[b]The measured value for stage 1 annealing is ~10 cal/g. It is assumed about one-half of the damage anneals in stage 1.

[c]This is for a saturation vacancy concentration of 0.12%.

Stored energy can, therefore, be measured by determining the difference between the heat of solution of the irradiated and unirradiated samples in a solution calorimeter. Samples of 0.2 g of salt were dissolved in 500 g of water in the solution calorimeter. The literature value for the heat of this dissolution for pure NaCl is 16.48 cal/g. Our measured value for unirradiated rock salt from the Lyons, Kansas, mine is 16.2 cal/g.

Two series of samples were studied by this method. The first series consisted of samples of synthetic NaCl, all cleaved from the same single crystal and irradiated with 2-MeV electrons from the ORNL electron Van de Graaff accelerator. Samples were irradiated at two different dose rates, at a number of temperatures between room temperature and 100°C, and to a number of different total doses. The results are summarized in Fig. 9.1, where different point symbols are used to indicate the different irradiation conditions. It is clear that the stored energy saturates with dose and that, even for doses up to 10^{11} rads, no more than 2 to 3 cal/g can be stored. These preliminary data suggest that stored energy behaves with respect to irradiation conditions in a fashion similar to that for F-center production. That is, the energy storage becomes greater as the dose rate is increased or the sample temperature during irradiation is lowered.[11]

The second series of samples consisted of rock salt from the Lyons mine, irradiated either with 1- to 2-MeV electrons or in the mine under "Project Salt Vault" conditions. Most of these samples were held at temperatures near or above 200°C during irradiation. It is well known that, at these elevated temperatures, vacancy defects can aggregate. In fact, the yellow color normally present and attributed to single vacancies is not observed in such samples; instead, a deep blue color, which is thought to be due to vacancy aggregates or so-called metal colloid centers, results. In Table 9.2 we list results of our preliminary measurements from which we can draw the following conclusions:

1. Samples irradiated at dose rates three or four orders of magnitude higher than the dose rate anticipated in the disposal facility, and to total doses greater than 10^{10} rads, exhibit amounts of stored energy in the range of 2 to 14 cal/g. There

ORNL-DWG 71-10705

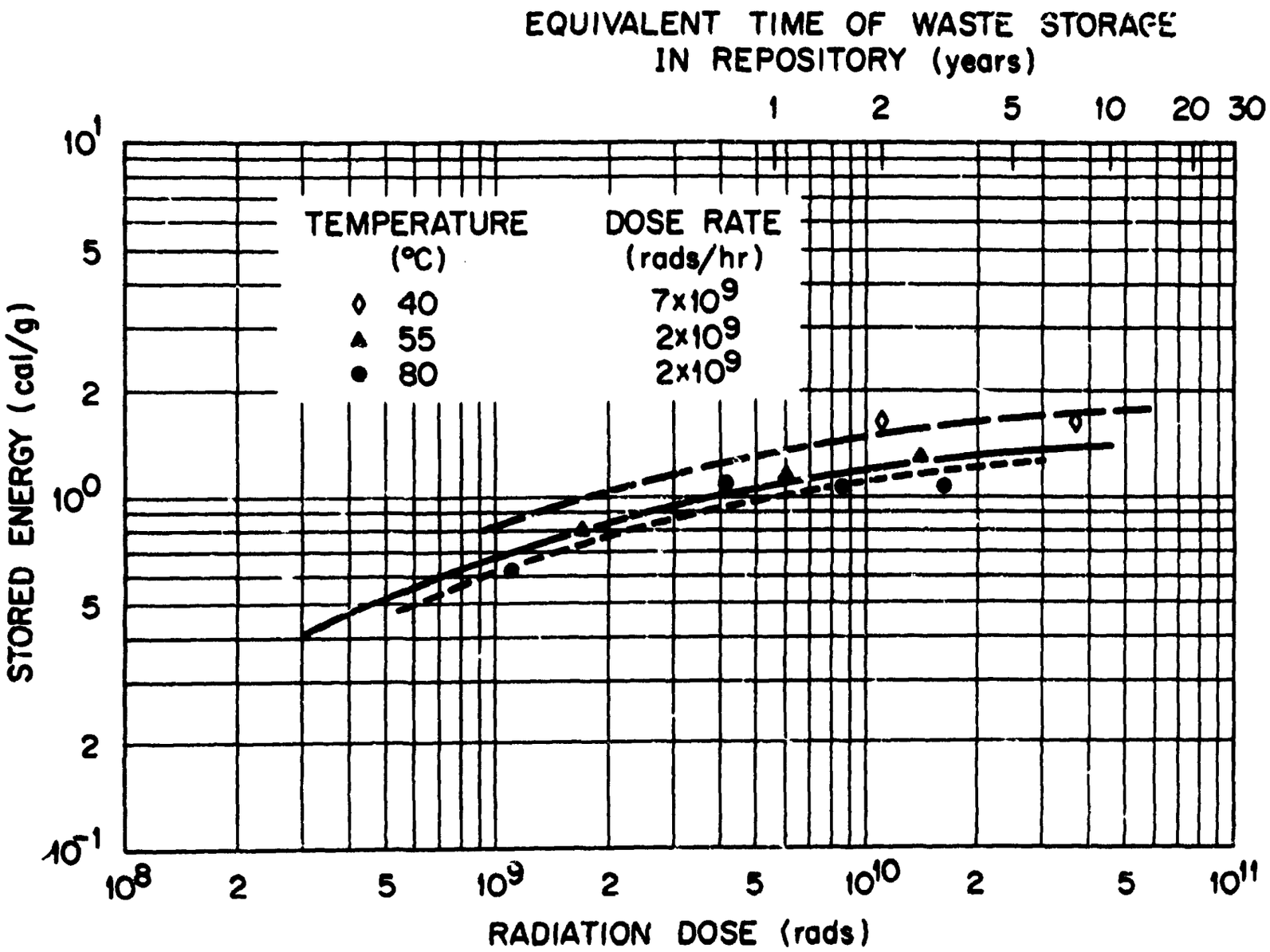

Fig. 9.1. Stored Energy in NaCl as a Function of Radiation Dose and the Temperature of Irradiation.

Table 9.2. Stored Energy Measurements in Rock Salt by Solution Calorimetry

Sample	Irradiation Temp. (°C)	Dose (rads)	Stored Energy (cal/g)
	Electron-Irradiated Samples		
V_OA	250 ± 150	10^{11}	14
V_OB	250 ± 150	10^{11}	1.6[a]
V_OC	250 ± 150	10^{11}	7[b]
V_1	225 ± 50	8×10^{10}	3.0
V_2	225 ± 50	2×10^{11}	2.1
V_3	225 ± 50	3×10^{11}	4.3
L_2	210 ± 10	2.5×10^{9}	0.6
L_3	210 ± 10	2.6×10^{10}	5.8
L_5	210 ± 10	7.2×10^{10}	7.5
L_6	210 ± 10	7.2×10^{10}	3.6
L_8	210 ± 10	7.2×10^{10}	2.6
L_8	210 ± 10	7.2×10^{10}	2.2
	Project Salt Vault Samples		
Hole 10 (7-1/2 ft depth)	125	8×10^{7}	0
Hole 4A (11 ft depth)	165-200	9×10^{8}	0
Hole 4B (9-1/2 to 11 ft depth)	165-200	9×10^{8}	0

[a]Heated at 250°C for 7 hr subsequent to irradiation.

[b]Stored at room temperature for 78 days.

is a large variation in the energy stored, even for samples irradiated under identical conditions. It is not yet clear whether this is due to the fact that different pieces of Lyons salt behave differently or whether, at these temperatures (at which vacancy cluster nucleation is undoubtedly of a determining character for energy storage), very small variations in impurity content will cause large changes in the relative rates of defect production and annealing. It is of interest that the color of these samples is not uniform; for example, a single piece of irradiated NaCl will have both nearly uncolored and very darkly colored portions.

2. Annealing of irradiated NaCl near or above the irradiation temperature of 250°C causes some of the stored energy to disappear. As shown in Table 9.2, sample V_OB (which was a piece of V_OA after irradiation) retained only 11% of the stored energy after annealing for 7 hr. This large difference is probably significant, whereas the factor of 2 decrease shown for sample V_OC (which was also a piece of V_OA after irradiation) after standing at room temperature for 78 days may be due to general scatter.

3. Samples irradiated with photons in the salt mine to less than 10^9 rads do not exhibit any significant stored energy. It should be pointed out that most of the irradiation occurred while these samples were warmed from approximately 75 to 150°C, and that only during the last few days of a 500-day irradiation did the samples reach their final high temperature. Thus it is probable that some annealing took place as a result of the final heating.

As a check on our calorimetric measurements, H. Kubota of the ORNL Analytical Chemistry Division has performed differential scanning calorimetry experiments on some of our samples. His results indicate values of 21 ± 6 and 0 ± 4 cal/g for samples V_OA and 4B respectively. We feel that these results are in substantial agreement with our solution calorimetry values. Also, samples of salt from the experimental holes of Project Salt Vault were supplied to E. J. Zeller of the Kansas State

Geological Survey, and he has reported measurements that are in reasonable agreement with ours.[12]

In view of these experimental results, we conclude:

1. At room temperature and a dose of 10^{10} rads, only small amounts of energy (~2 cal/g) are stored in rock salt.
2. At higher temperatures, the amount of stored energy may be greater. Some samples of salt irradiated near 200°C stored between 3 and 14 cal/g.
3. Stored energy is released (annealed out) slowly, even at 250°C.

Solidified Wastes. — Although no measurements of energy storage in solidified wastes have been made to date, it is quite likely that energy can be stored in some of these materials, and over a wider temperature range than is possible in salt. Zeller et al.[13] have measured up to 200 cal/g in olivine (a mineral containing about the same amount of silicate as is present in some of the solidified waste products) when it was irradiated with protons at liquid nitrogen temperatures. However, all of this energy was released below 450°C.

9.3 Analysis of the Effects of Energy Release

9.3.1 Thermal Effects

Various calculations have been made to evaluate the maximum transient temperatures in the salt that could result from an instantaneous release of stored energy. In this study, we have evaluated primarily the effect of initial age of the waste, initial thermal power, and the length of time that the cylinder has been stored in the salt. The energy storage has been conservatively overestimated as 1% of the total deposited photon-neutron energy up to a maximum saturation value of 200 cal/g in the calcined waste and 20 cal/g in the salt.

The calculations of total integrated dose as a function of distance from the waste cylinder (Fig. 9.2) were calculated with the ANISN[14] transport code using the $S_{16}P_3$ approximation, 27 energy groups for

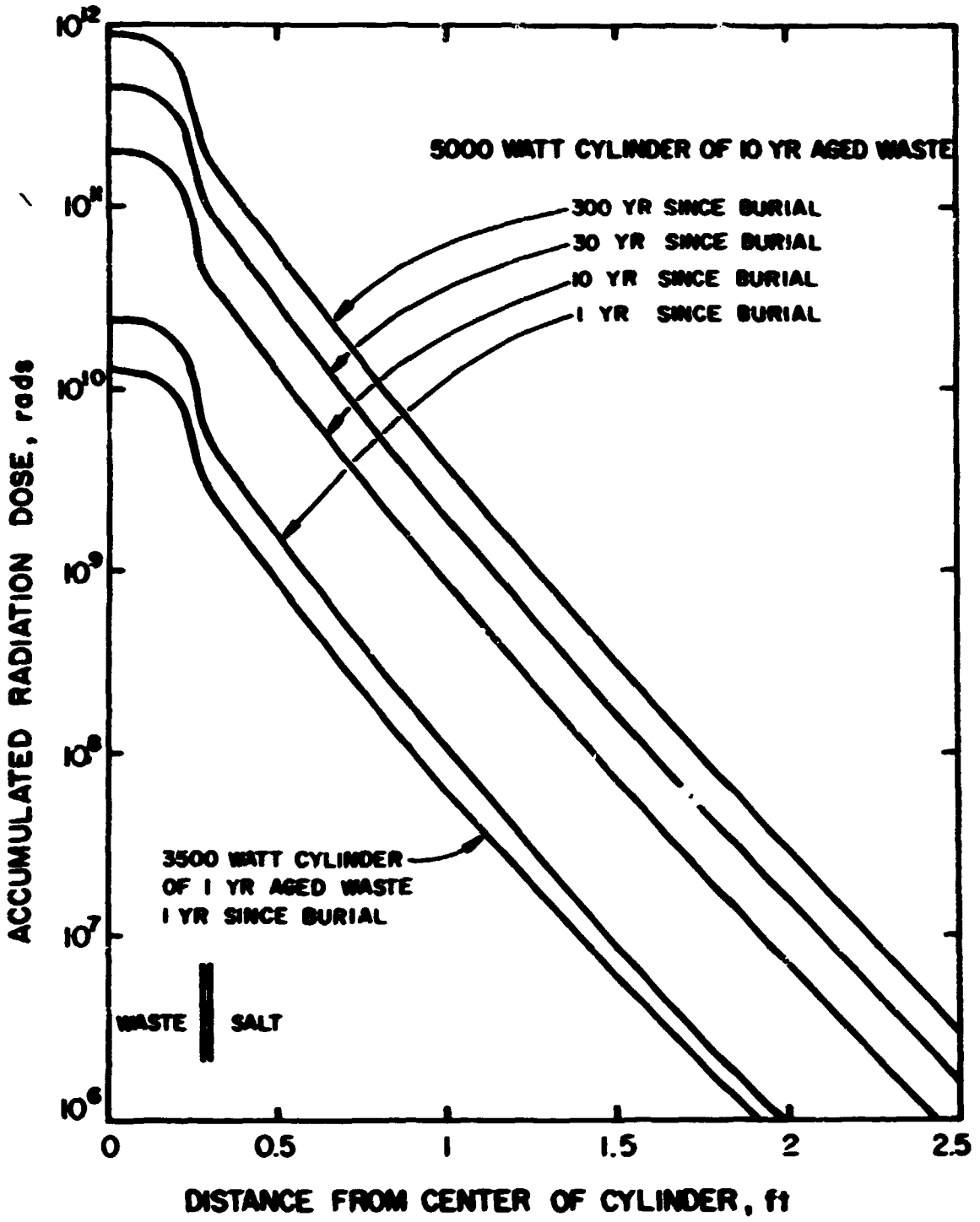

Fig. 9.2. Accumulated Photon-Neutron Dose in the Horizontal Midplane of Cylinders of Solidified High-Level Waste Buried in Salt. Each waste cylinder has an inside diameter of 6 in., a steel wall thickness of 0.25 in., and an active height of 8 ft.

neutrons, and 20 energy groups for photons. This calculation takes into account the dose from secondary gamma rays as well as that from the primary gamma rays and neutrons that are generated within the wastes. The photon and neutron sources of typical waste were computed by summing the contributions from several hundred radionuclides.

Because of the linearity of this problem, the thermal effects of an energy release can be decoupled from the decay-heat temperature gradient in the salt at the time of the release. In essence, this decoupling was accomplished by assuming that the temperature in the mine was zero everywhere before the lease, and that no heat sources existed in the mine. Then, by invoking the principle of superposition, the temperatures calculated by the procedure described below can be added to the decay-heat gradients existing in the mine at the time of release to obtain the total temperature profiles as a function of time and position.

In each of the four cases studied, a one-dimensional finite-difference calculation was made to determine the transient thermal behavior of the temperatures generated by the release. The initial temperature conditions were set to the temperature rise resulting immediately after the energy release. In addition, the boundary at a distance midway between containers was insulated from heat flow. The initial temperature inside the waste container was set at 1638°F, corresponding to an energy release of 200 cal/g in a material with a heat capacity of 0.22 Btu lb^{-1} $°F^{-1}$. The salt temperature extending from the wall of the container to a point at which 1% of the total integrated dose (Fig. 9.2) fell below 20 cal/g was set at 166°F. The heat conduction code HEATING3[15] was used to calculate nodal temperatures at various distances and postrelease times, and these temperatures were added to the decay-heat gradients. The results are summarized in Table 9.3. Of the cases studied, the maximum thermal effect of a stored energy release is associated with the assumption that a cylinder having an initial thermal power of 5000 W and an initial waste age of 10 years resulted in an energy release 30 years after burial in the salt (Fig. 9.3, Table 9.3). The effect of this release was to cause no melting of the salt and a temperature rise of less than 2°F at 13.5 ft from the center of the cylinder.

Table 9.3. Estimated Maximum Mechanical Energy Release and Temperature Increases That Could Result from Release of Stored Energy Developed by a Waste Cylinder Stored in Salt

Properties of Waste Cylinder[a]				
Initial thermal power, W	5000	5000	520	3500
Initial age of waste, years	10	10	10	1
Time of storage in salt, years	1	30	30	1
Distance between cylinders, ft	27	27	8	12
Volume Change Due to Thermal Expansion, ft³				
Waste and salt	0.12	0.36	0.13	0.08
Brine	1.53	5.62	1.79	0.88
Total	1.65	5.98	1.92	0.96
Mechanical Energy Release,[b] equivalent pounds of TNT	0.19	0.69	0.22	0.11
Maximum Temperature Rise, °F				
1 ft from center of cylinder	56	170	150	49
4 ft from center of cylinder	4	7	4	3
Midpoint between adjacent cylinders	0.9	2	4	2

[a]Cylinders are assumed to have diameter of 6 in. and active length of 8 ft.

[b]Assumes 1600 Btu of energy per pound of TNT.

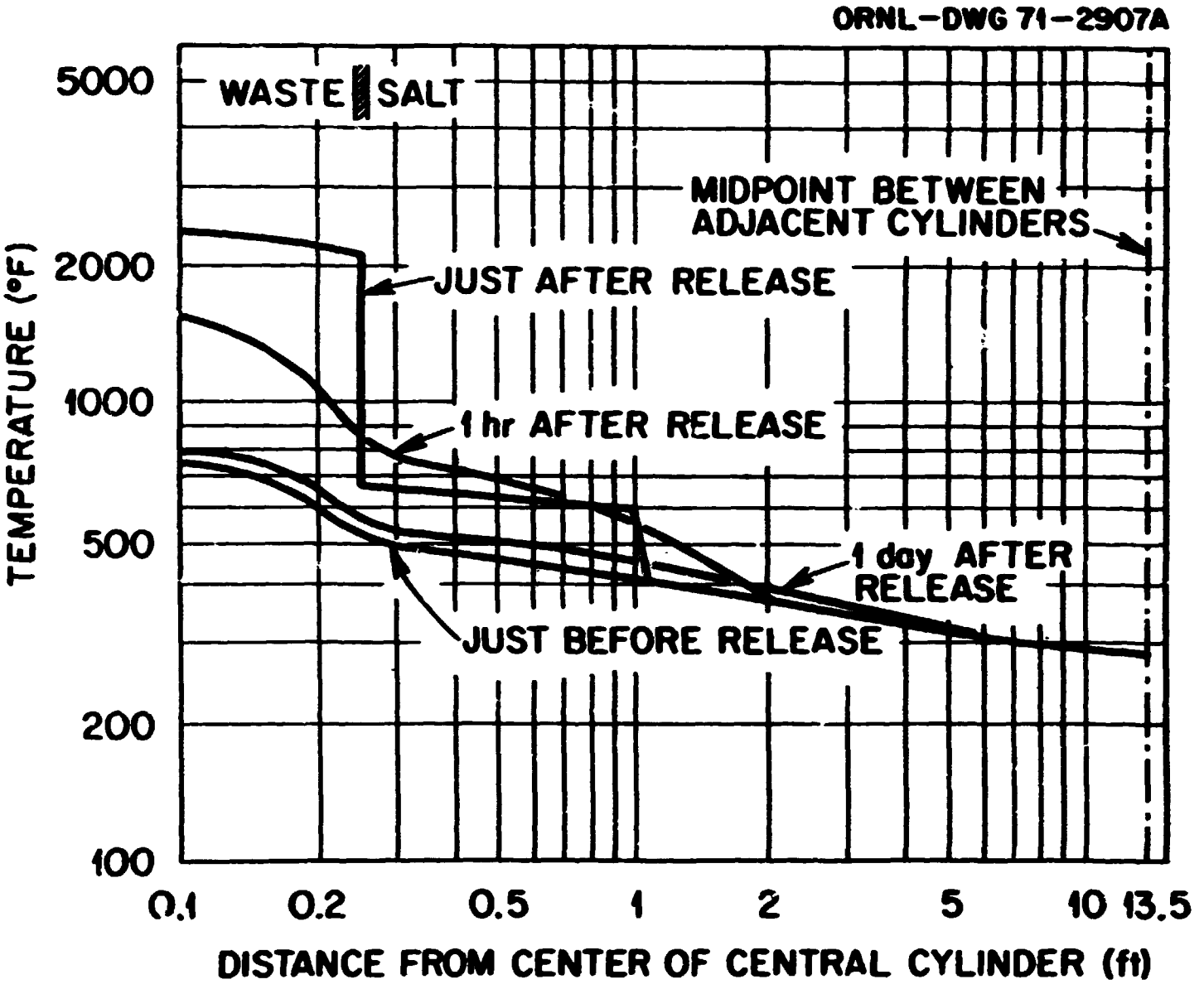

Fig. 9.3. Estimated Temperature in the Horizontal Midplane of a Cylinder Buried in Salt Just Before, Just After, and at Various Times After a Release of Stored Energy. Waste having an initial power of 5000 W and an age of 10 years since processing is assumed to have been stored for 30 years. Energy storage is assumed to be 1% of the total deposited photon-neutron energy up to a maximum saturation value of 200 cal/g in the waste and 20 cal/g in the salt.

9.3.2 Mechanical Effects

Rapid thermal expansion of the waste and the nearby salt resulting from a release of stored energy can potentially result in an explosive release of mechanical energy. An overestimate of the maximum amount of mechanical energy generated can be made by assuming that the expansion occurs reversibly against the ambient overburden of 1000 psi. Table 9.3 presents the results of estimates of maximum mechanical energy generation for several assumed conditions of mechanical energy release. Materials properties that were used for these calculations are given in Table 9.4. Thermal expansion of the brine, which constitutes 0.5% by volume of the salt, was overestimated by assuming that the brine is pure water and by using thermodynamic data from steam tables.

These estimates show that the maximum amount of mechanical energy generated is conservatively less than the equivalent of 1 lb of TNT. This amount of released energy would result in practically no deformation of the floor of the room above the waste container and would constitute no danger to personnel from missiles.

9.4 Conclusions

On the basis of the foregoing discussion, we are confident that energy storage under the conditions that will prevail in the Repository does not carry any serious implications. We expect to conclude our experimental work related to NaCl by establishing saturation values of stored energy as a function of temperature, radiation dose, and chemical purity. Also, some additional work is required to establish upper-limit values for energy storage in the solidified wastes, and the conditions under which it can be released.

Table 9.4. Assumed Properties of Calcined Waste and Salt Used for Analysis of Stored Energy Release

Calcined Waste	
Density, lb/ft^3	113
Thermal conductivity, Btu hr^{-1} ft^{-1} $°F^{-1}$	0.25
Heat capacity, Btu lb^{-1} $°F^{-1}$	0.22
Coefficient of cubical expansion, $°F^{-1}$	0.88×10^{-5}
Rock Salt	
Density, lb/ft^3	135
Brine content, vol %	0.5
Thermal conductivity, Btu hr^{-1} ft^{-1} $°F^{-1}$	1.81
Heat capacity, Btu lb^{-1} $°F^{-1}$	0.218
Coefficient of cubical expansion, $°F^{-1}$	0.67×10^{-4}
Melting point, °F	1470
Crushed Salt	
Density, lb/ft^3	95
Brine content, vol %	0.5
Thermal conductivity, Btu hr^{-1} ft^{-1} $°F^{-1}$	0.36
Heat capacity, Btu/lb	0.218

9.5 References

1. J. O. Blomeke, E. Sonder, J. P. Nichols, S. Lindenbaum, R. S. Dillon, E. D. Arnold, and H. F. Soard, An Analysis of Energy Storage and Its Effects in the Proposed National Radioactive Waste Repository, ORNL-TM-3403 (June 1971).

2. Solid State Div. Ann. Progr. Rept. Aug. 31, 1961, ORNL-3213, p. 18 ff.

3. R. E. Nightingale, Nuclear Graphite, pp. 329, 400, Academic, New York, 1962.

4. K. Kobayashi, Phys. Rev. 102, 348 (1956).

5. J. M. Bunch and E. Pearlstein, Phys. Rev. 181, 1290 (1969).

6. D. Pooley, Brit. J. Appl. Phys. 17, 1 (1966).

7. F. Setiz, Modern Theory of Solids, p. 3, McGraw-Hill, New York, 1940.

8. H. F. Wenzl, Proceedings of the International Conference on Vacancies and Interstitials in Metals, Jülich, 1968, North Holland Publishing Co., Amsterdam, 1970.

9. F. Seitz, Loc. Cit., p. 48.

10. F. Seitz, Loc. Cit., p. 61.

11. E. Sonder and W. A. Sibley, "Defect Creation by Radiation in Polar Crystals," Defects in Solids (J. H. Crawford and L. Slifkin, Eds.), Plenum Press (in press).

12. E. J. Zeller, communication to J. O. Blomeke, Oak Ridge National Laboratory, Feb. 2, 1971.

13. E. J. Zeller, G. Dreschhoff, and L. Kevan, Modern Geology 1, 141 (1970).

14. W. W. Engel, Jr., A User's Manual for ANISN, A One-Dimensional Discrete Ordinates Transport Code with Anisotropic Scattering, K-1693 (March 1967).

15. W. D. Turner and M. Siman-Tov, HEATING3--An IBM-360 Heat Conduction Program, ORNL-TM-3208 (February 1971).

10. RADIOLYSIS AND HYDROLYSIS IN SALT-MINE BRINES

G. H. Jenks

Salt deposits of the type to be used for radioactive waste disposal contain a small volume-fraction of brine inclusions (~0.5%). Some brine from these inclusions will be present on the surfaces of the crushed salt* around a given waste container at the time of its burial (Fig. 10.1) (see ref. 1). Additional brine will enter the open and unconfined spaces in the crushed salt region after burial due to the migration of the inclusions, which takes place in the presence of thermal gradients in the salt, and due to salt-fracture, which takes place at high temperatures starting at about 250°C.**

The brine, vapors, and any salts precipitated from the brine will be exposed to high gamma-ray intensities and to high temperatures (Table 10.1) (see refs. 2 and 3). Accordingly, they will be subject to radiation decomposition and to changes in composition brought about by thermally induced reactions.

We have reviewed and analyzed pertinent theoretical and experimental information, with the objectives of identifying possibly bothersome decomposition products and of obtaining estimates of rates of formation of these within the spaces around the waste container. Results of this work are summarized below.

10.1 Composition of Encapsulated Brine

Holser[4] reported experimental values (Table 10.2) for the ratios of Mg, Br, SO_4, and Ca to Cl in the brine inclusions in salt from The Carey Mine at Hutchinson, Kansas, and from a core from the Naval Air Station at

---

*Brine is released from the cavities by crushing the salt.

**The fracture of the salt at high temperature is thought to be a result of the high vapor pressure of water within the brine inclusion and of strain due to the thermal expansion of liquid within cavities.

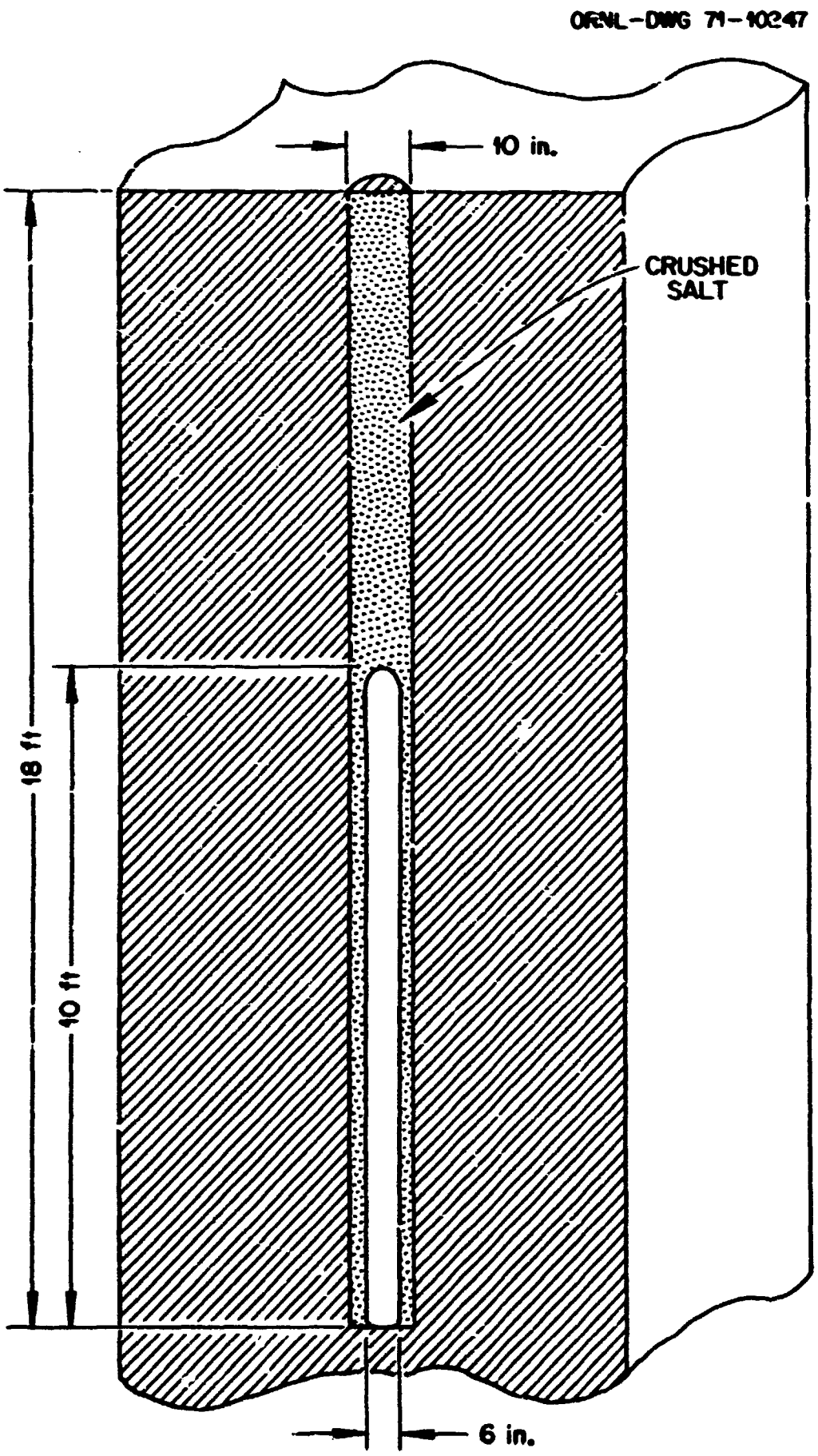

Fig. 10.1. Waste Container in Backfilled Hole (After Bradshaw et al., ref. 1).

Table 10.1. Illustrative Values[a] for Dose Rates, Doses, and Temperatures for Waste Cans Containing 10-year-old Wastes; Midplane Values

	2-kW Can	5-kW Can
Initial dose rate		
Edge of can, rads/hr	2×10^6	5×10^6
Edge of hole, rads/hr	10^6	2.5×10^6
Dose at edge of can		
30 years after burial, rads	4×10^{10}	10^{11}
300 years after burial, rads	8×10^{10}	2×10^{11}
Maximum temperature		
Edge of can, °C	≥250 (25 y)	≥340 (1 y)
Edge of hole, °C	240	≥280

[a]Values obtained from refs. 2 and 3.

Table 10.2. Reported[a] Ratios of Concentration of Ions in Brine Inclusions

	Weight Basis	Mole Basis[b]
Mg/Cl	0.231	0.333
Br/Cl	0.015	0.0067
SO_4/Cl	0.009	0.003
Ca/Cl	0	0
Mg/Br[b]	15.6	49.6

[a]By W. T. Holser.

[b]Derived from Holser's data.

the same location.* He did not report any ionic concentrations but stated that his results showed that the brine inclusions were formed by the evaporation of sea water and that the concentration factor was about 60.**

Using Holser's data and interpretations, together with data on the concentration of potassium in sea water after a sixty-fold concentration[5] and on the solubility of NaCl in solutions of $MgCl_2$ (Fig. 10.2),[6,7] we deduced that the composition of the brine is within the following range of compositions:

Ion	Molarity
Mg	2.3 to 3
K	0.4
Na	2 to 1
Cl	7 to 7.5
Br	0.05
pH	slightly basic†

10.2 Radiation Chemistry of Brine

10.2.1 Theory

Spur Diffusion Model. - The radiation chemistries of water and aqueous solutions are usually described in terms of the spur diffusion model. Several pairs of radicals or ions (primarily e^-_{aq}, OH, and H_3O^+ in pure water) are formed in small, isolated volume elements (spurs) in the initial radiation process. Species within the spurs interact as they diffuse into homogeneous distribution, and these interactions result in the re-formation of water and in the formation of other molecular products. In pure water being subjected to gamma irradiation, the decomposition products that appear in homogeneous distribution are, principally, e^-_{aq}, OH, H_2, and H_2O_2.†† The H_2O_2 and H_2 are formed, primarily, by the

---

*These deposits are thought to be substantially the same as those at Lyons, Kansas.

**Holser further stated that the brine inclusions are probably unchanged samples of bitterns left behind in Permian time.

†At room temperature.[8] The (H^+) at elevated temperatures will be several hundred micromolar due to hydrolysis of $MgCl_2$ in solution.[9]

††The number of a species which appears in homogeneous distribution in the initial radiation-decomposition per 100 eV of absorbed energy is symbolized in this section by $g'(OH)$, $g'(H_2)$, etc. Also, these products are referred to as g'-products.

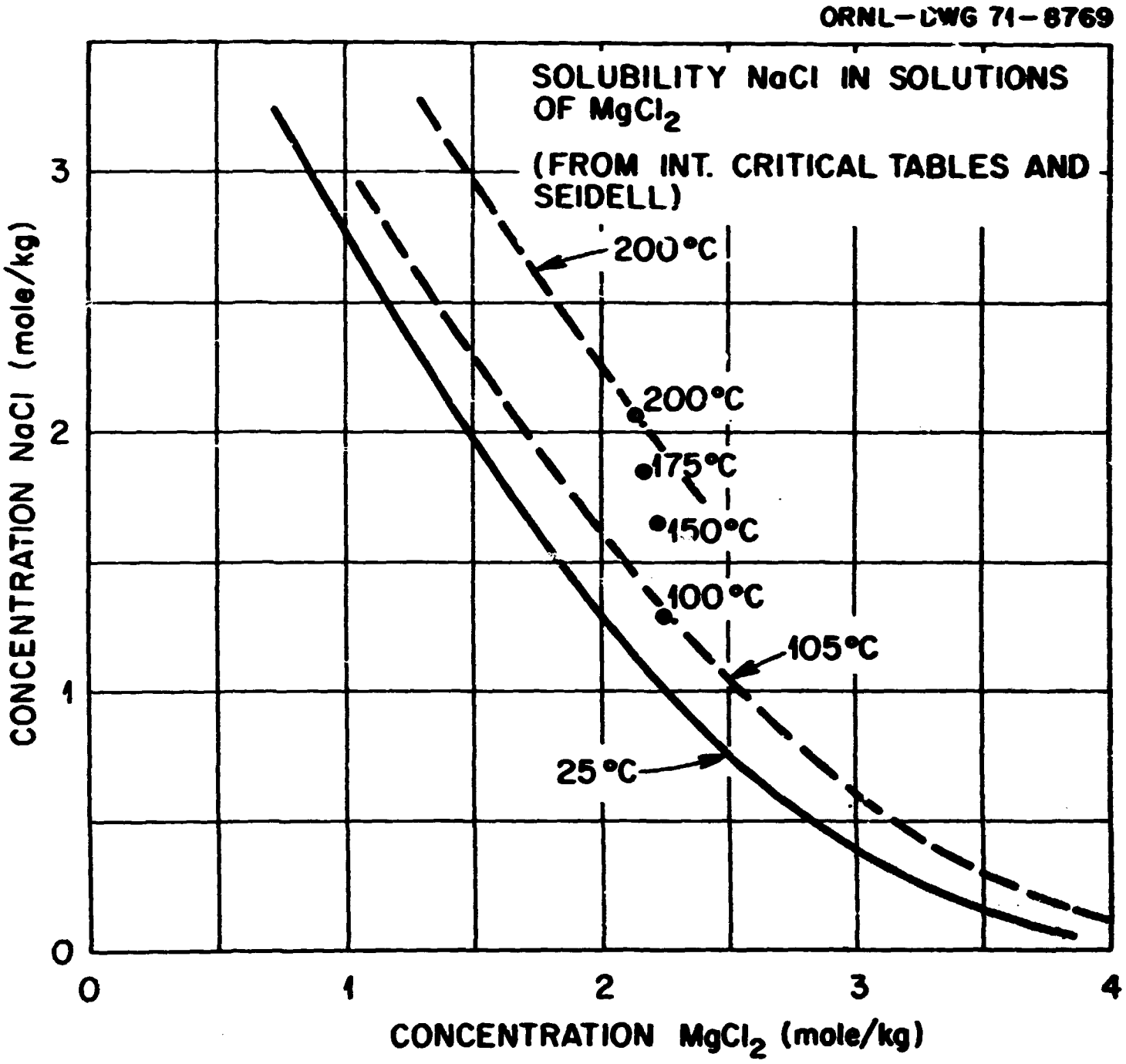

Fig. 10.2. Solubility of NaCl in Solutions of $MgCl_2$.

following reactions:

$$e^-_{aq} + e^-_{aq} + 2H_2O \rightarrow H_2 + 2OH^- \ , \qquad (1)$$

$$OH + OH \rightarrow H_2O_2 \ . \qquad (2)$$

Important water re-formation reactions are:

$$e^-_{aq} + H_2O_2 \rightarrow OH + OH^- \ , \qquad (3)$$

$$e^-_{aq} + OH \rightarrow OH^- \ , \qquad (4)$$

$$OH^- + H_3O^+ \rightarrow 2H_2O \ . \qquad (5)$$

Reactive solutes at high concentrations can react with radicals within the spurs and thus cause changes in g'-values from those in pure water and, at the same time, cause the formation of additional g'-species.

It is known that Cl_2^- is formed during gamma irradiation of concentrated neutral chloride solutions. According to the spur diffusion model, most of the Cl_2^- is formed from Cl^0, which is formed within spurs by reaction (6):

$$OH + Cl^- \ H_3O^+ \rightarrow Cl^0 + 2H_2O, \qquad k = 1.7 \times 10^{10} \ \underline{M}^{-2} \text{ at } 25°C \qquad (6)$$

The removal of OH from the spur by reaction (6) would presumably cause reductions in $g'(OH)$ and $g'(H_2O_2)$ from those in pure water. It would also promote increases in $g'(e^-_{aq})$ and $g'(H_2)$, providing that the new products of the spur reactions (i.e., Cl_2^- and possibly Cl_2) do not react as readily with e^-_{aq} as do OH and H_2O_2 in the pure water system.

Direct Action of Radiation on Solutes. - Solutes at high concentrations can be affected also by direct action of radiations; for example, reaction (7),

$$Cl^- \xrightarrow{\lambda} Cl^0 + e^- \ , \qquad (7)$$

may occur in chloride solutions. The yields for reactions such as (7) are frequently quite high, for example, 5 to 10 product species per 100 eV of energy[10,11] absorbed by the parent species (Cl^- in this case).*

Dissolution of Radiation-Damaged Salt. - Radiation damage produced by gamma rays in NaCl (and in other alkali halides) consists of displaced atoms and of trapped electrons and holes. Chemically, the trapped electrons and holes are reducing and oxidizing agents, respectively, and dissolution of radiation-damaged NaCl results in the injection of oxidizing and reducing agents into the aqueous solution.[13-15] The oxidizing agent entering solution corresponds to Cl_2^- and/or Cl_3^-, while the reducing agent can be treated as a hydrated electron, e_{aq}^-.** The thermal-gradient-induced migration of brine-filled cavities through salt takes place by dissolution of salt at the higher-temperature face of a cavity and precipitation of salt at the lower-temperature face. Accordingly, the migration of brine through radiation-damaged salt will result in the injection of Cl_2^- and/or Cl_3^- and e_{aq}^- into the brine, and the radiochemical result of the dissolution is qualitatively the same as the result of direct absorption of radiation by chloride ions in solution.

10.2.2 Yield of H_2 Upon Absorption of Radiations in Brine

Values for $g'(H_2)$. - Some reported information on $G(H_2)$ in neutral KCl solutions is illustrated in Fig. 10.3.[10] The reported yield increased as the chloride concentration increased, and was about 1.9 at 4 M Cl^-. These G-values refer to the yield of the species as final products of the radiolysis, that is, to the number of the product species which persist after reactions have taken place in the bulk of the solution. The experimental conditions employed in this reported work were such that, for H_2,

---

*For comparison, the yield of OH within spurs is thought to be 5.7 in pure water.[12]

**The reducing agent might be thought of as Na^0. However, the reaction of Na^0 with H_2O would probably produce e_{aq}^- as an intermediate, which could then react to form H_2 and OH^- or undergo other reactions, depending on the solution composition.

$$Na^0 + H_2O \rightarrow Na^+ + e_{aq}^- \qquad (8)$$

$$e_{aq}^- + e_{aq}^- \rightarrow H_2 + 2OH^- \qquad (9)$$

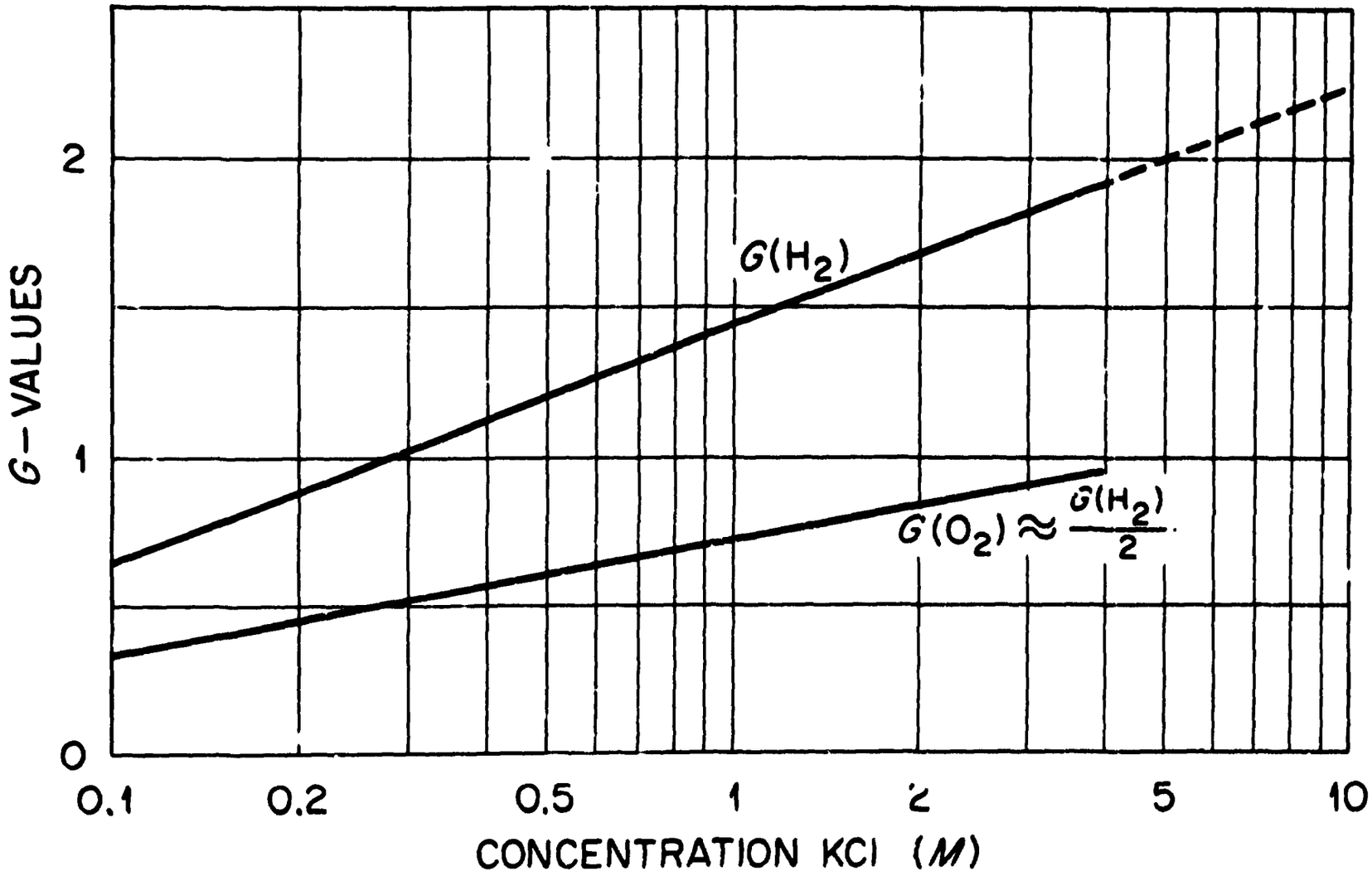

Fig. 10.3. $G(O_2)$ and $G(H_2)$ in KCl Solutions (Brusentseva and Dolin).

the yields for appearance in homogeneous distribution in the initial radiolysis and for appearance as a final product were the same. That is, the G- and g'-values for H_2 were nearly identical.

Now a value of 1.9 for $g'(H_2)$ is surprisingly high as compared with a value of 0.43 in pure water. Furthermore, the high values are not readily explained on the basis of the generally accepted models discussed above. However, they are supported by comparably high values in iodide solutions.[16] Also, they are supported by reported experimental information[17] on $G(Cl_2)$ in chloride solutions at pH 11 (Fig. 10.4) and by a high value for $G(H_2)$ in LiCl solutions exposed to alpha rays. As seen in Fig. 10.4, the reported value of $G(Cl_2)$ at pH 11 exceeded 1.5 at 4 $\underline{M}$ Cl^-. Although $G(H_2)$ was not reported, it must have also exceeded 1.5 in order to satisfy oxidation-reduction balance requirements. Baybarz[18] showed that $G(H_2)$ was equal to 2.36 in the alpha irradiation of concentrated LiCl solutions which also contained HCl at 0.4 to 0 $\underline{M}$. The value of $g'(H_2)$ in pure water undergoing alpha irradiation is 1.5.[19] It can be inferred that the value of $g'(H_2)$ in the LiCl solution was substantially greater than the value in water.

On the basis of the information just discussed, we have assumed that the value of $g'(H_2)$ in the salt-mine brines at normal temperatures may be as high as 2.1, as indicated by extrapolation of the data in Fig. 10.3.

All of the experimental work we have referred to was done at room temperature. Considerations of theoretical and experimental information indicated that values of $g'(H_2)$ will not change appreciably with increasing temperature.[20]

Value for $G(H_2)$.* - The only known reaction by which radiolytic H_2 is removed from water or from chloride solution is:[20]

$$OH + H_2 \rightarrow H + H_2O, \qquad k = 4.5 \times 10^7\ \underline{M}^{-1},\ sec^{-1} \text{ at } 25°C \text{ in water.} \qquad (10)$$

The rate of buildup of dissolved H_2 in the brine, as well as the steady-state concentrations of H_2, will then depend on values of $g'(OH)$ and $g'(H_2)$. They will also depend importantly on the occurrence of scavenger-type reactions in which OH is removed from solution before it can react with

*The number of a species which appears as a final product per 100 eV of absorbed energy is symbolized in this section by $G(H_2)$, $G(O_2)$, etc.

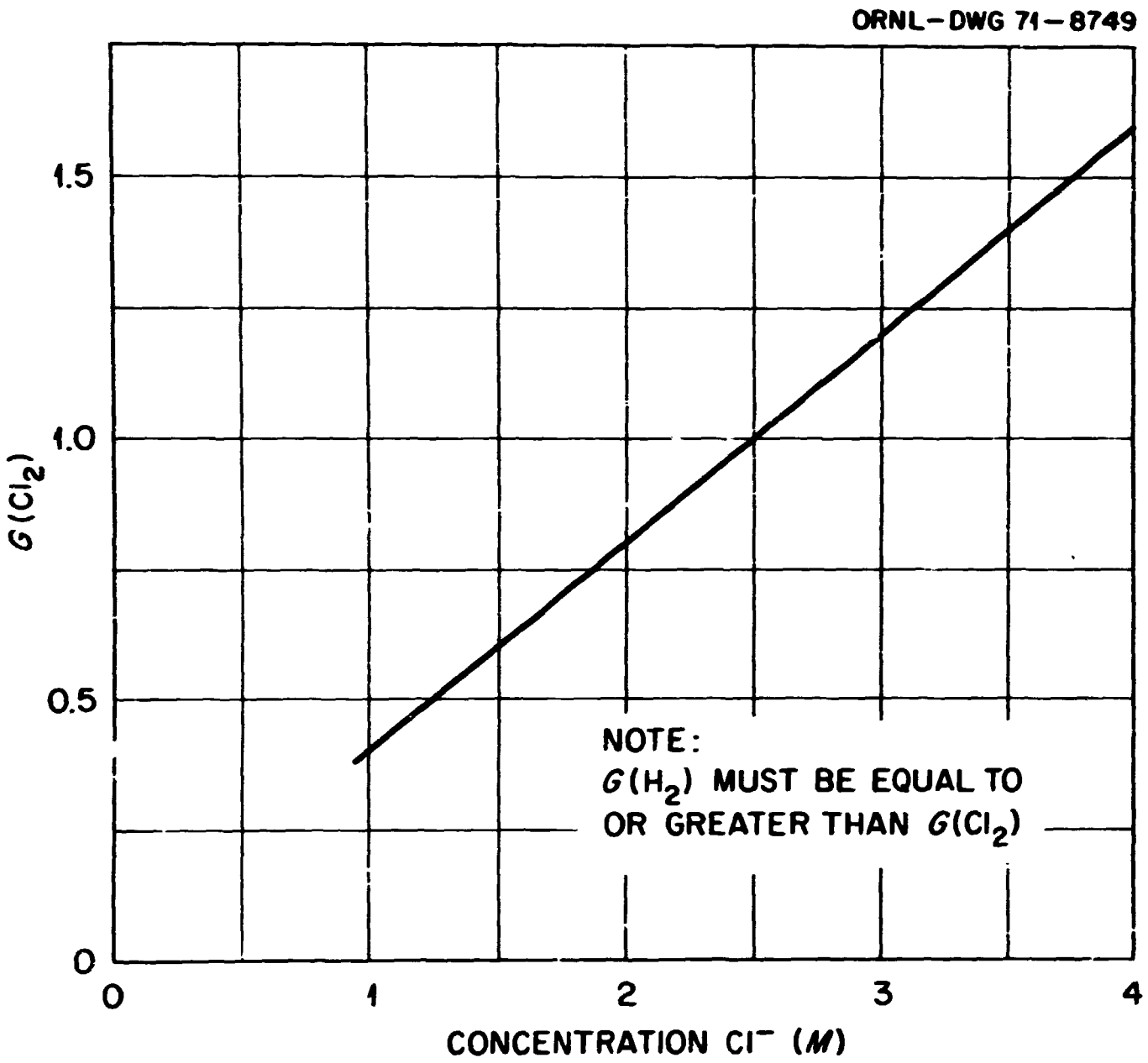

Fig. 10.4. $G(Cl_2)$ in Solutions of KCl, of NaCl, and of $BaCl_2$ at pH 11 (Kabakchi, Gramolin, and Evokhin).

H_2, and on whether H_2 escapes from the irradiated solution and thus escapes the radiation-induced back-reaction within the solution.

It is well known that Br^- is a scavenger for OH radicals. The scavenger reactions are comprised of reaction (11), followed by a reaction between some form of Br^0 and a reducing radical to re-form Br^-:

$$OH + Br^- \rightarrow Br^0 + OH^-, \quad k = 1 \times 10^9 \ \underline{M}^{-1}, \ sec^{-1} \text{ at } 25°C. \qquad (11)$$

Chloride ion is also an effective scavenger in acid solutions. At 10^{-3} $\underline{M}$ H^+ and room temperature, for example, reaction (6) has an equivalent bimolecular rate constant for the reaction between Cl^- and OH of 1.7×10^7 $\underline{M}^{-1}$, sec^{-1}.[21] As mentioned above, the brine solution will be several hundred micromolar in H^+ at elevated temperatures.

Radiolytic gases will escape from the brine into a gas-vapor phase when the pressure of dissolved gases plus water vapor exceeds the overpressure. Most of the brine cavities are completely filled with liquid so that no gas-vapor phase can form unless cavity expansion takes place. In this contained environment, the pressure from dissolved radiolytic gases could be substantial. For example, with 1 $\underline{M}$ H_2, the water vapor--dissolved gas pressures could exceed 19,000, 13,000, and 9,000 psi at 150, 200, and 250°C, respectively.* The bedded salt undergoes plastic deformation (creep) under stress, and the ease of deformation increases with temperature.[23,24] Also, the salt at the edge of the hole will be unsupported until consolidation takes place. After consolidation is complete (including that of the salt in the room above the hole), the pressure on the salt will be about 1000 psi. Considerations of these several factors led to the idea that, in the temperature range 150 to 250°C, cavity expansion will take place before the concentration of dissolved H_2 reaches 1 $\underline{M}$. Recently reported information[24] on cavity expansion in NaCl and KCl lends support to this idea.

Taking the several possible effects into account, we concluded that $G(H_2)$ might equal $g'(H_2)$ at all exposure times and temperatures, both in the unconfined brines and in the encapsulated brine.

---

*We assumed that gas solubility in the brine is the same as that in water.[22] Also, we assumed that the radiolytic H_2 is balanced by radiolytic O_2.

Estimates of the possible effects of dissolution of radiation-damaged salt on the overall yield will be discussed later.

10.2.3 Identities of Oxidized Species

All radiolytic H_2 must be accompanied by a stoichiometrically equivalent number of oxidized species. With respect to the identities of the oxidized species, we can note that Brusentseva and Dolin (Fig. 10.3) measured values of $G(O_2)$ as well as $G(H_2)$ in their neutral solutions. Also they looked for chlorine. As can be seen in Fig. 10.3, the oxygen and hydrogen were formed in approximately stoichiometrically equivalent amounts. Accordingly, since H_2 is the only reduced species in chloride solutions, appreciable amounts of any oxidized species other than oxygen could not have been present. In particular, no appreciable amounts of chlorine would be expected, and none were found. Kubota[25] also reported that no chlorine was formed during gamma-radiolysis of neutral chloride solutions.

It is known that chlorine atoms are formed at high yields as initial products of radiolysis of neutral concentrated chloride solutions. For example, as shown in Fig. 10.5, the reported[21,26] value of $g'(Cl_2^-)$ is 2 at 3 M NaCl.

Oxygen is not a g'-product.

Hydrogen peroxide is a g'-product; however, as shown in Fig. 10.6, the yield is very small in concentrated NaCl.[26]

Our explanation of the occurrence of oxygen in place of chlorine as the oxidized species in neutral chloride solution is that the radiolytic chlorine oxidizes water. The probable reactions are the chain reactions (13) and (14). Chlorine molecules, if formed, would hydrolyze to the hypochlorous acid, HClO, as shown in reaction (12).

$$Cl_2 + H_2O \rightleftarrows Cl^- + H^+ + HClO, \qquad (12)$$

$$Cl_2^- + HClO \rightarrow H^+ + 2Cl^- + ClO^\circ \qquad (13)$$

$$ClO^\circ + HClO \rightarrow H^+ + Cl_2^- + O_2 \qquad (14)$$

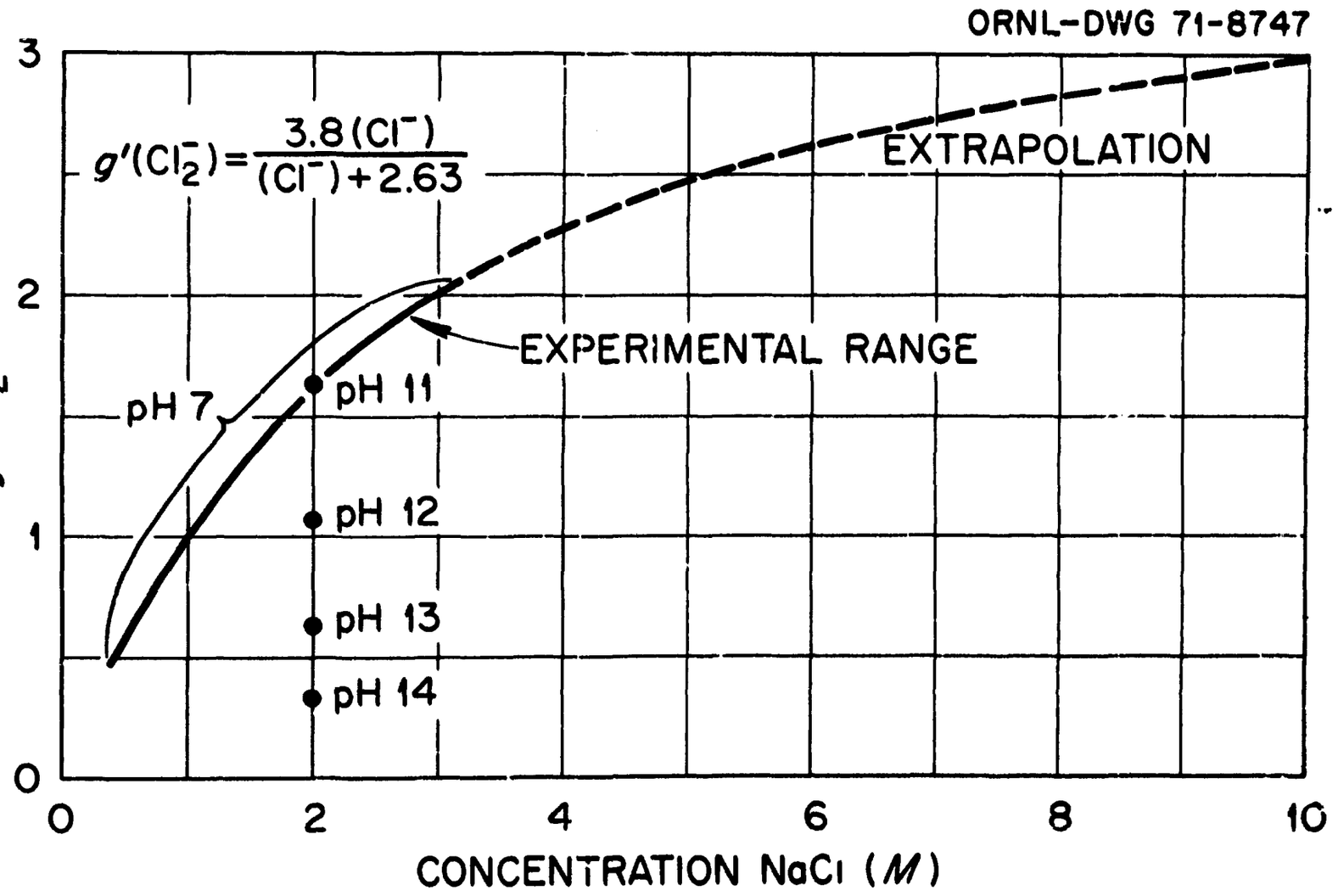

Fig. 10.5. g'-Values for Cl_2^- in NaCl Solutions (Sawai and Hamil, Using Data of Anbar and Thomas).

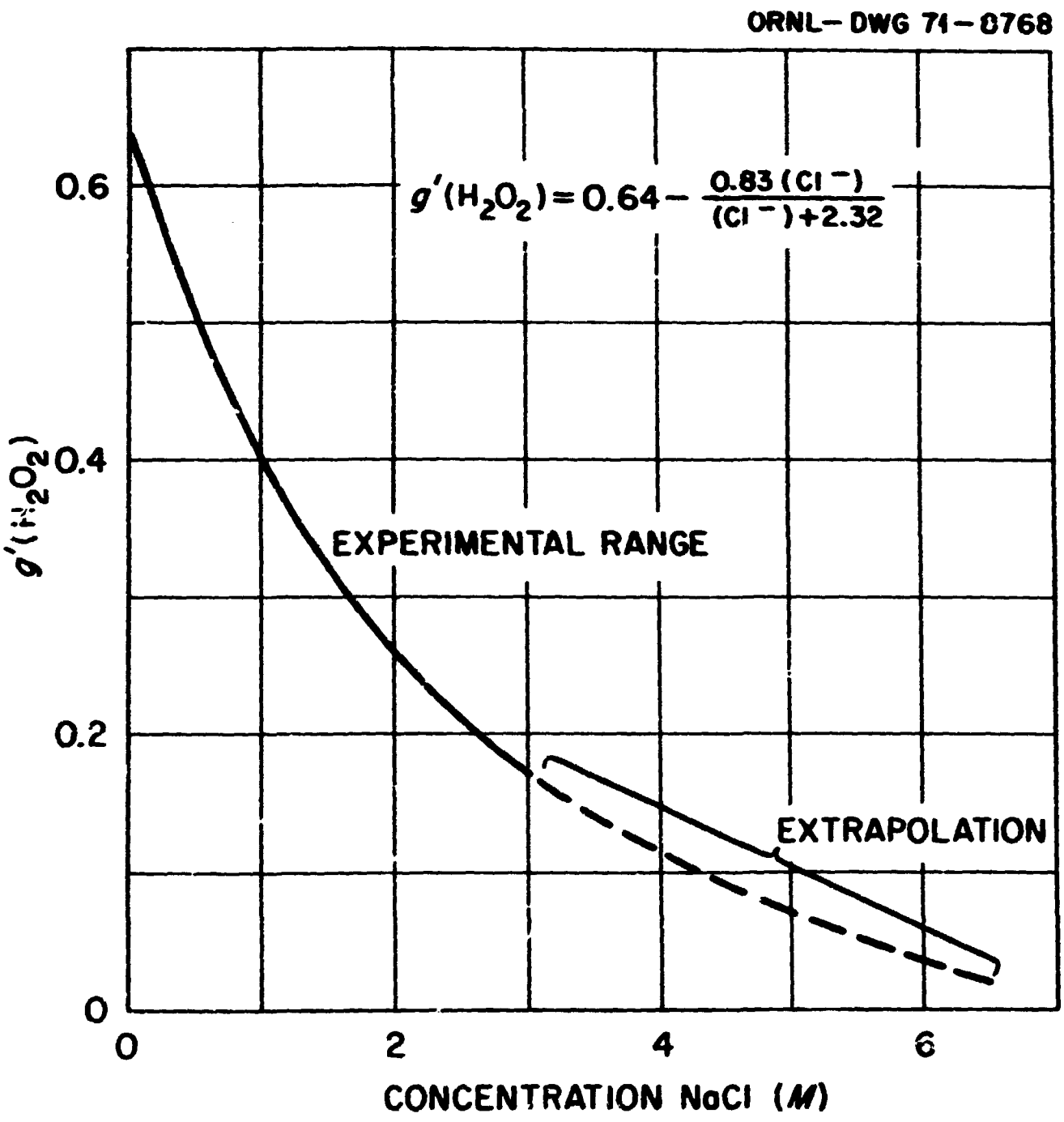

Fig. 10.6. g'-Values for H_2O_2 in NaCl Solutions (Sawai and Hamil).

Reactions analogous to (13) and (14) have been previously postulated by others to explain photolytic oxidation of water by chlorine in aqueous solutions.[27]

We tentatively explain the appreciable values of $G(Cl_2)$ at pH 11 in the reported work discussed above (Sect. 10.2.2) by assuming that ClO^- does not react with Cl_2^-, possibly because the ions have the same charge. The ClO^- ion is the product of ionization of hypochlorous acid, and ionization would have been essentially complete in the reported experiments at pH 11.

On the basis of the experimental and theoretical information discussed above, we believe that oxygen will be the principal oxidized species that is formed during irradiation of confined brines at normal temperatures. However, formation of chlorates in the hydrolysis of chlorine is promoted by increasing temperatures, and we cannot exclude the possibility that chlorate and bromate would be formed in place of some of the oxygen in the high-temperature brine.

The products of radiolysis in unconfined brine around the waste can may differ from those of the encapsulated brine because the unconfined brine may be acid with HNO_3 and HCl and because any gaseous radiolytic products will readily escape from solution. We concluded that the possible radiolytic products under these conditions include Cl_2, Br_2, ClO_3^-, BrO_3^-, ClO_2, ClO_4^-, and ClO_2^-, along with H_2 and O_2. The Cl_2 would react radiolytically to form HCl within the vapor phase.

10.2.4 Hydrolysis of $MgCl_2$ to Form HCl

Magnesium chloride reacts with water (including water of hydration) or steam at high temperatures to form HCl.[28-31] The probable reactions are:

$$MgCl_2 + H_2O \rightleftharpoons MgOHCl + HCl \ , \qquad (15)$$

$$2MgOHCl \rightleftharpoons MgCl_2 + MgO + H_2O \ . \qquad (16)$$

From the available fragmentary data on equilibria in these reactions, we concluded that 50 to 65% of the $MgCl_2$ around the waste can will eventually react to form HCl, providing that the location of the $MgCl_2$ is such that the HCl moves away from the $MgCl_2$. Complete hydrolysis through reaction (16) takes place only at temperatures above 520°C.[31]

10.2.5 Fates of Chlorates and Bromates in Space Around Can[32-35]

Sodium and magnesium chlorates and sodium bromate decompose into perchlorates, halides, and oxygen at elevated temperatures. The perchlorates, in turn, decompose into chlorides and oxygen. The temperatures around a waste can may be below those at which some of the pure compounds would decompose. However, the mixtures of salt that would be present around a waste can probably would decompose at the temperatures prevailing at this location. No chlorine would be expected to be formed from the decomposition.

Magnesium bromate decomposes into magnesium oxide, oxygen, and bromine. Accordingly, some bromine might be formed in the spaces around a can if bromates are, in fact, formed within the migrating brine.

10.2.6 Radiolysis of Vapors Around Can

Ozone is formed in dry or moist air at normal temperatures. However, at low partial pressures of air, its rate of formation would be very low.[36] At high temperatures, any O_3 that might be formed radiolytically would be quickly lost by thermal decomposition and/or by reactions with other species which might be present. Accordingly, we believe that the formation of O_3 will not be a problem in these systems.

Nitric acid is formed by the irradiation of moist air, and its formation might continue in gas mixtures containing low partial pressures of O_2 and N_2 at elevated temperatures.[37-39] The presence of HCl vapor might affect the radiolysis of the moist air; however, there is no information regarding possible effects.

Assumed values of $G(O_3)$ and $G(HNO_3)$, together with calculated values for the corresponding rates of formation of these species, are tabulated in Table 10.3. The G-values refer to energy absorption in the gas-water

Table 10.3 Rates of Formation of HNO_3 and O_3 in Crushed Salt Exposed to 5×10^5 rads/hr

	At Initial Conditions[a]		At Temp. >100°C with $P_{(air)}$ >0.1 atm[b]	
	G-value	Rate of Formation (micromoles/hr)	G-value	Rate of Formation[a] (micromoles/hr)
O_3	7	100	<0.2	<3[c]
HNO_3	1 to 3	15 to 40	1	15

[a]Initial void volume, about 30 liters.

[b]Mixtures of water vapor and air.

[c]Ozone is thermally unstable, as well as reactive, at high temperatures. It is unlikely that O_3 will accumulate.

vapor mixture. Temperatures greater than 100°C will be reached within a few hours after burial in the case of the 5-kW cans. With the 2-kW cans, the minimum temperatures on the cans will exceed 100°C at six months after burial.

10.3 Migration of Brine-Filled Cavities

10.3.1 Theoretical

R. L. Bradshaw[40] was the first to present a theoretical analysis of the process of brine migration in NaCl. He also reported a theoretical relationship between the migration rate of a droplet of pure sodium chloride solution and the temperature gradient and temperature at the droplet. More recently, T. R. Anthony and H. E. Cline have published several papers dealing with their experimental and theoretical work on brine migration in KCl.[41-45] Their theoretical analysis is also applicable to NaCl, and is more complete than that of Bradshaw. Accordingly, we will refer primarily to the work of Anthony and Cline.

The thermomigration of a brine droplet up a temperature gradient results, of course, from an increase in the solubility of the salt with increasing temperature and/or from thermal diffusion effects within the brine (i.e., from the Soret effect). The velocity of droplet migration depends upon several different parameters, including those just mentioned and also droplet size. The migration is also affected by grain boundaries when the droplets are small.

The theoretical expression of Anthony and Cline for the migration velocity of large droplets within the body of a crystal is given by the first term in Eq. (17). The last two terms within the brackets should be ignored for the present.

$$V = \frac{C_\ell}{C_s} \frac{D}{RT} \left[\left(\frac{1}{C_\ell} \frac{\partial C_E}{\partial T} + \sigma \right) G_\ell RT - \frac{4\gamma \bar{V}_s}{XL} - \frac{K}{L} \right] \qquad (17)$$

where

V = migration velocity, cm/sec

C_ℓ = concentration of salt in brine droplet, moles/liter

C_E = equilibrium concentration of salt in brine in contact with salt, moles/liter

C_s = concentration of salt in solid salt, moles/liter

D = diffusivity of salt in brine, cm^2/sec

R = gas constant

T = absolute temperature

RT = $(8.31 \times 10^7)(T)$ ergs/mole

K = kinetic potential, ergs/mole

γ = grain boundary tension, ergs/cm^2

L = dimension of droplet parallel to thermal gradient, cm

X = dimension of droplet perpendicular to thermal gradient, cm

V_s = molar volume of solid salt, cm^3/mole

G_ℓ = temperature gradient in the brine droplet, °C/cm

σ = Soret coefficient of salt in brine, $°C^{-1}$

If the last two terms within brackets in Eq. (17) are ignored, the expression of Anthony and Cline becomes similar to that of Bradshaw. The remaining differences are: (1) the absence of the Soret coefficient

in Bradshaw's expression, and (2) the appearance of molal rather than molar concentrations in the term outside the brackets in Bradshaw's expression.

We will not discuss the theoretical bases for this equation. It can be noted, however, that this expression for large droplets can be derived from Eqs. (18) and (19) if it is assumed that the concentrations of salt in solution at the hot and cold interfaces are equal to the equilibrium concentrations at the respective temperatures.

$$V = -J/C_s \tag{18}$$

$$J = -D\nabla C_\ell - D_\sigma C_\ell \nabla T_\ell \tag{19}$$

Equation (18) results from material balance considerations. J is the flux of salt through the brine in a direction parallel to ∇T_ℓ. Equation (19) states the relationship between the flux and the gradients of concentration ∇C_ℓ and of temperature ∇T_ℓ. D_σ is the thermal diffusion coefficient.

Small droplets and the other terms within the brackets will be discussed next.

According to Anthony and Cline, a frictional force represented by K/L becomes important as the droplet gets smaller. The term K, which is called the kinetic potential, is related to the difference between the chemical potential of salt in the solid and that in the brine solution. The value of K is primarily dependent on the undersaturation required at the dissolving interface in order for dissolution to occur at the rate required to support the rate of migration of the droplet. The value of K increases with the velocity of the droplet, decreasing to zero at zero velocity. It can also be expected that the value of K would depend on other factors that may affect the rate of attainment of equilibrium at the interface. These would include, for example, temperature and structural factors such as dislocations within the path of a migrating droplet.

We do not have any good estimates of the value of K in the naturally occurring rock salt systems in which we are interested. If we assume that the value of K will be about the same as the value in the KCl system at

room temperature, we would guess that the droplet dimension would have to be less than about 1 mm before kinetic factors would influence migration velocities appreciably.

Another force retarding the motion of small droplets occurs at grain boundaries. According to Anthony and Cline, droplets on grain boundaries are in positions of minimum energy; therefore, the thermal-gradient driving force required to propel a droplet across a grain boundary exceeds that for motion through the body of a crystal. Their theoretical expression for the effect of the grain boundary tension force is given by the middle term within the brackets in Eq. (17).

Again we do not have any direct information on the effects of grain boundaries in rock salt. However, using these theoretical relationships, and assuming that the grain boundary energy is approximately the same as the surface energy (and thus equal to several hundred ergs per cm^2), we estimated that temperature gradients of a few degrees Centigrade per centimeter would be required to propel 0.1-mm droplets through the grain boundaries. Larger gradients would, of course, be required with smaller droplets, and vice versa.

10.3.2 Experimental Information

Experimental data on brine migration in rock salt are illustrated in Fig. 10.7. Here, the values for the migration rate up the temperature gradient in inches per year per degree Centigrade per centimeter are plotted on the ordinate, and the exposure temperature is shown on the abscissa. These data were reported by Bradshaw and Sanchez.[40] Their work was done as part of some earlier studies for the salt Repository; the rock salt came from the mine at Hutchinson, Kansas. The naturally occurring brine-filled cavities which they used in their measurements were cubical in shape, and ranged in size from 2 to 10 mm on an edge. That is, they were in the size range above which grain boundary trapping and kinetic retarding effects are unlikely.

In practice, we do not know what fraction of the volume of the brine within the Lyons rock salt is contained within large droplets. Perhaps the most pertinent information on this subject was obtained in the Project

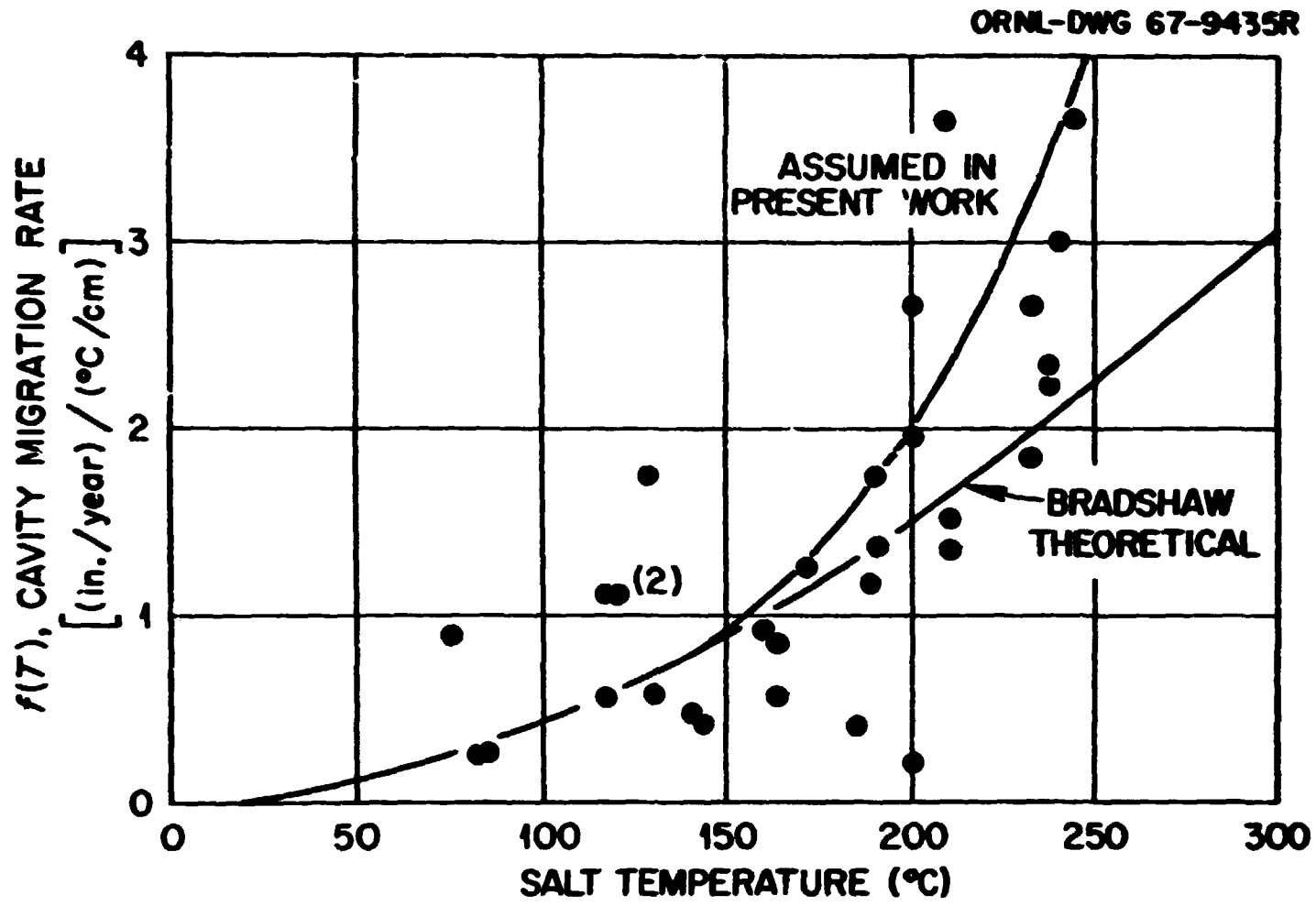

Fig. 10.7. Values of f(T) vs Temperature.

Salt Vault Experiment.[46] From the results of brine-inflow measurements in this experiment, it can be inferred that at least two-thirds, and possibly a much larger fraction, of the inflow took place at times when the electrical power to the heaters had failed and when, as a consequence, the temperature gradient in the salt near the edge of a hole was the reverse of that prevailing during regular operation.

A conceivable explanation of these findings is that a large fraction of the migrating brine droplets was trapped on grain boundaries within the polycrystalline bedded salt, and that these droplets were subsequently released as a result of slight cracking at grain boundaries when the wall temperature was reduced. This cracking would be presumed to result from the reduction of the tangential stress at the wall of the hole which would accompany the cooling of the wall. Also, it is conceivable that the two-phase droplets which were formed upon cooling migrated down the temperature gradient and were thus responsible for some of the Salt Vault results (see Sect. 10.4).

10.3.3 Upper-Limit Estimates of Amounts of Brine Inflow to Burial Holes for 2- and 5-kW Waste Cans (Cases C-1 and C-2)

From the brief review of available theoretical and experimental information on brine migration, it is apparent that we can only make upper-limit estimates of the amounts of brine inflow which will take place in an actual waste disposal hole. We made such estimates for 2- and 5-kW waste cans (10-year-old wastes) using the conservative relationship between migration rate, temperature gradient, and temperature shown by the upper curve in Fig. 10.7. It was assumed that the fractional volume of brine in the salt is 0.5% and that the cavities remain filled with brine until they reach the open spaces around a can. Temperature and temperature gradients (Figs. 10.8 and 10.9) used in these estimates were obtained from the results of the thermal calculations of Cheverton and co-workers.[2]

Figure 10.10 shows the results of the inflow estimates for the 2-kW can. Note that the total inflow is about 30 liters after 50 years. The top curve represents the results obtained when we assumed that the brine

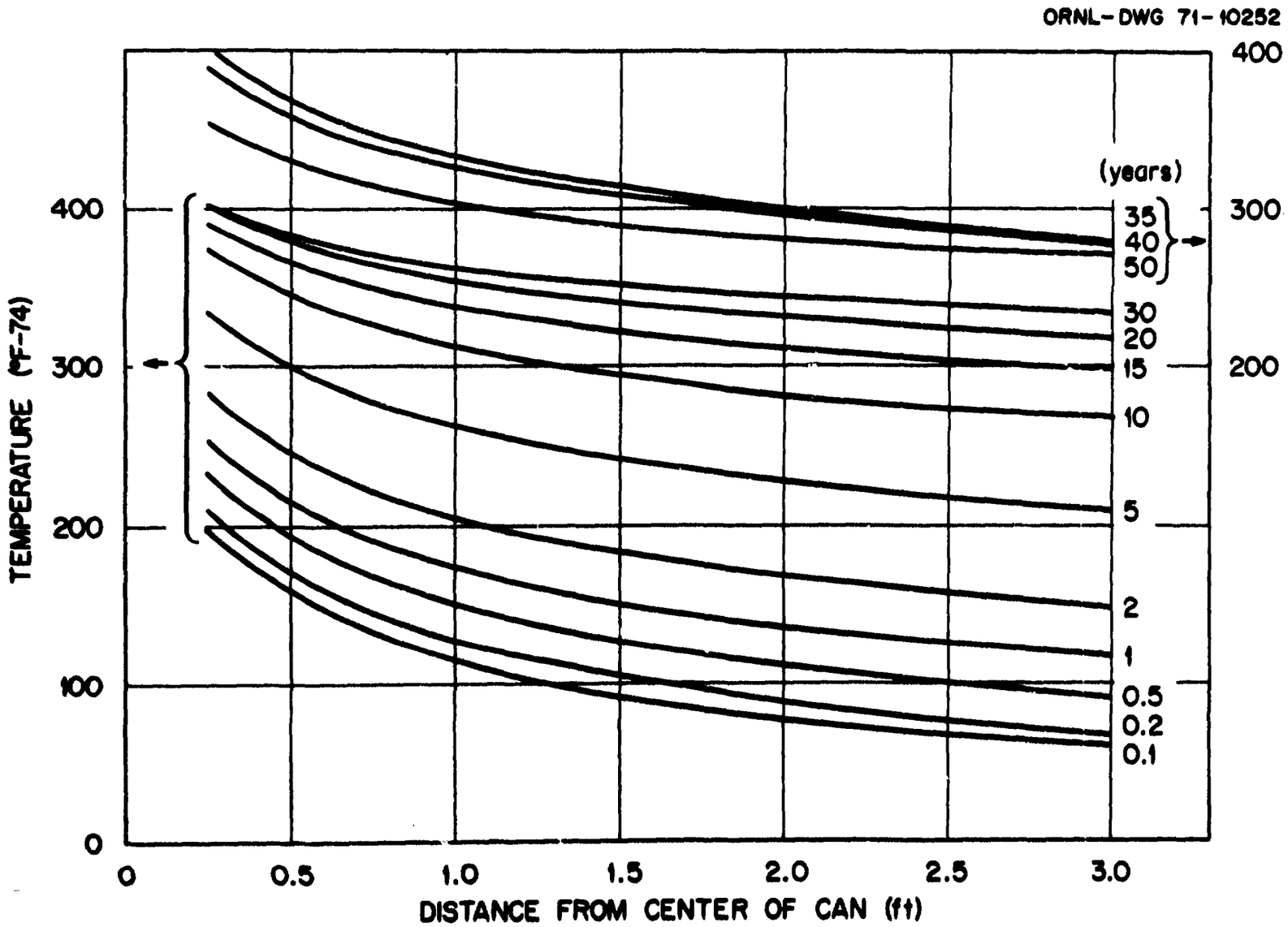

Fig. 10.8. Salt Temperature vs Distance from Center of Can at Several Different Times After Burial, Midplane (Case C-1, 2-kW Can).

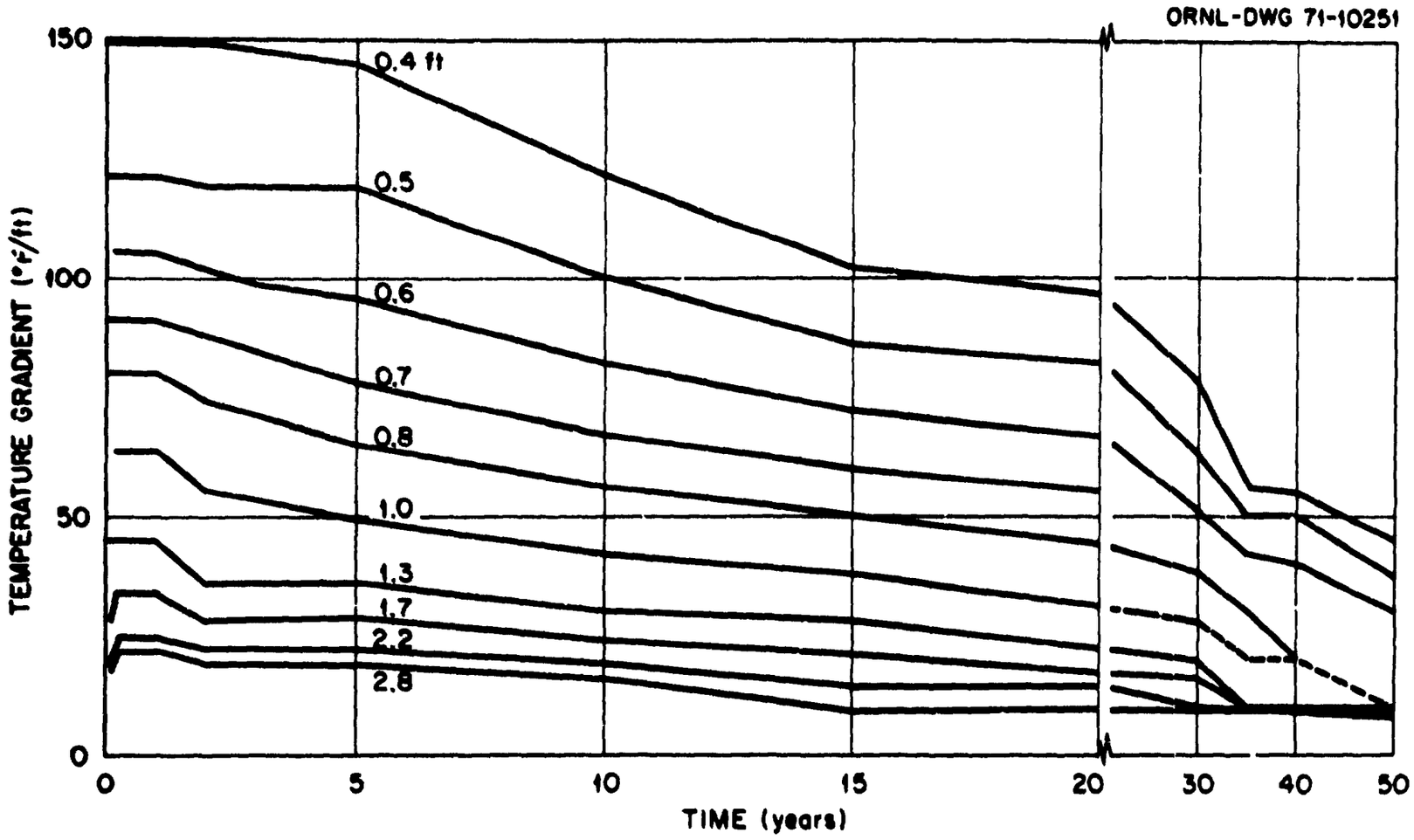

Fig. 10.9. Temperature Gradient vs Time After Burial at Several Different Radii, Midplane (Case C-1, 2-kW Can).

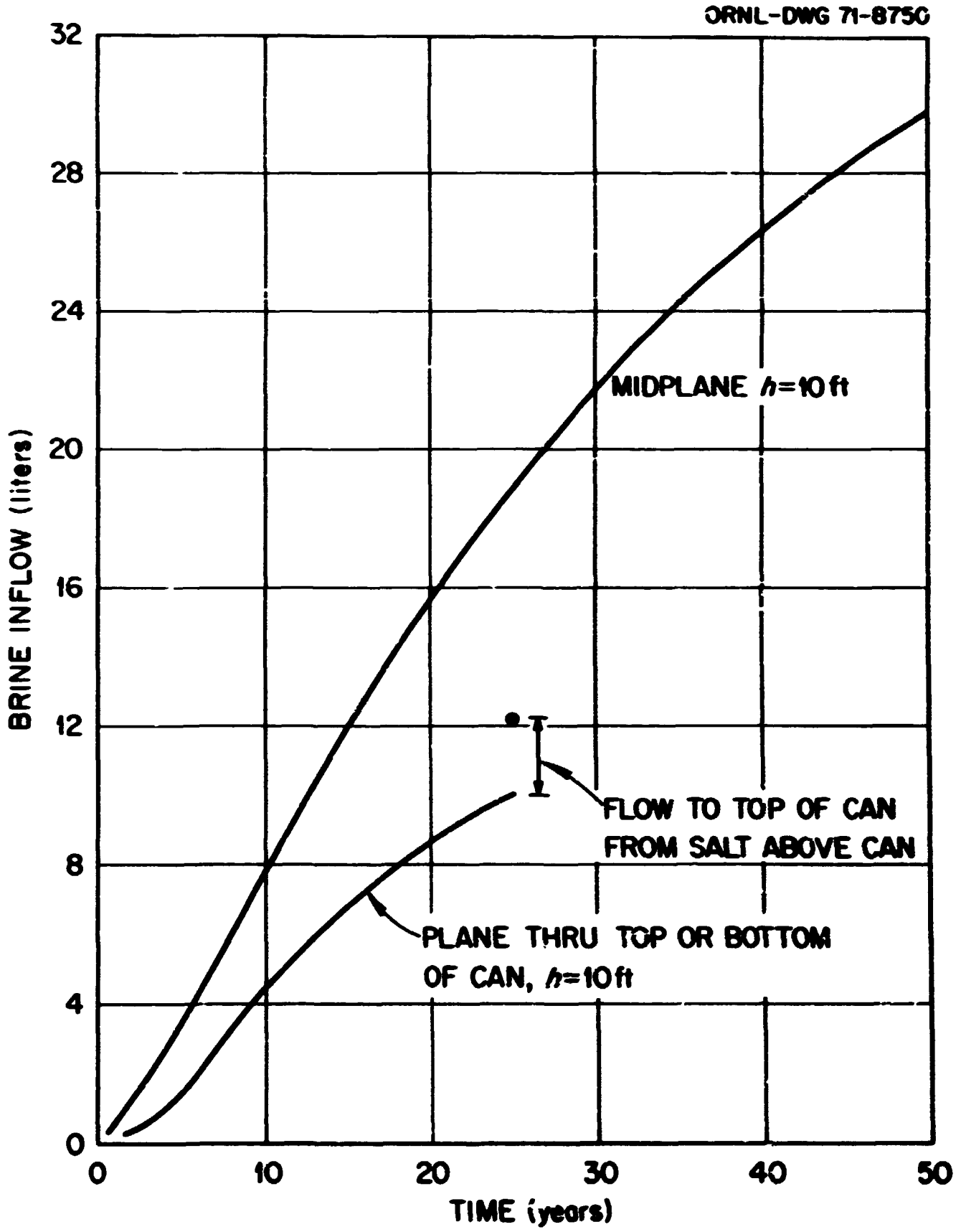

Fig. 10.10. Cumulative Brine Inflow vs Time After Burial (Case C-1, 2-kW Can).

flows into the hole from the cylindrical annulus of salt lying between horizontal planes which pass through the top and bottom of the can. Also, we assumed here that the inflow rate at each elevation was the same as that at the midplane. The bottom curve represents the estimates obtained in the same way, except that the inflow at all elevations was taken to be the same as that at the top or bottom plane.

Estimates of flow to the can from salt lying above and below the can are also shown. In general, we concluded that only a small error was introduced into the estimates by assuming that inflow at the midplane is representative of that at all elevations.

Figure 10.11 shows similarly estimated amounts of inflow for a can containing 5 kW of 10-year-old wastes at burial. Note that the total inflow at 50 years is less than 53 liters. The high initial rates in this case resulted from our assumption that the salt fractures and releases the brine at high temperatures starting at 250°C. The calculated temperatures in this case reached 250°C or above at all radii less than 9 in. (With the 2-kW can, the salt temperature did not exceed 250°C.)

10.4 Migration of Two-Phase Cavities

Anthony and Cline[47] have recently discovered that droplets containing both a gas-vapor phase and a liquid phase will migrate down a temperature gradient. That is, they migrate in a direction opposite to that of brine-filled droplets. The mechanism involves vaporization of liquid at the hot end and condensation of vapor at the cold end.

To date, we have not taken into account possible effects of the down-gradient migration of two-phase droplets. One notable effect which should be recognized is that the concentration of gases within those droplets migrating to the can will be limited to about 1 M or less (see Sect. 10.2.2) due to creation of a gas-vapor phase by cavity expansion at high gas pressure. Upon enlargement, the gas phase and some or all of the liquid would migrate down the temperature gradient.

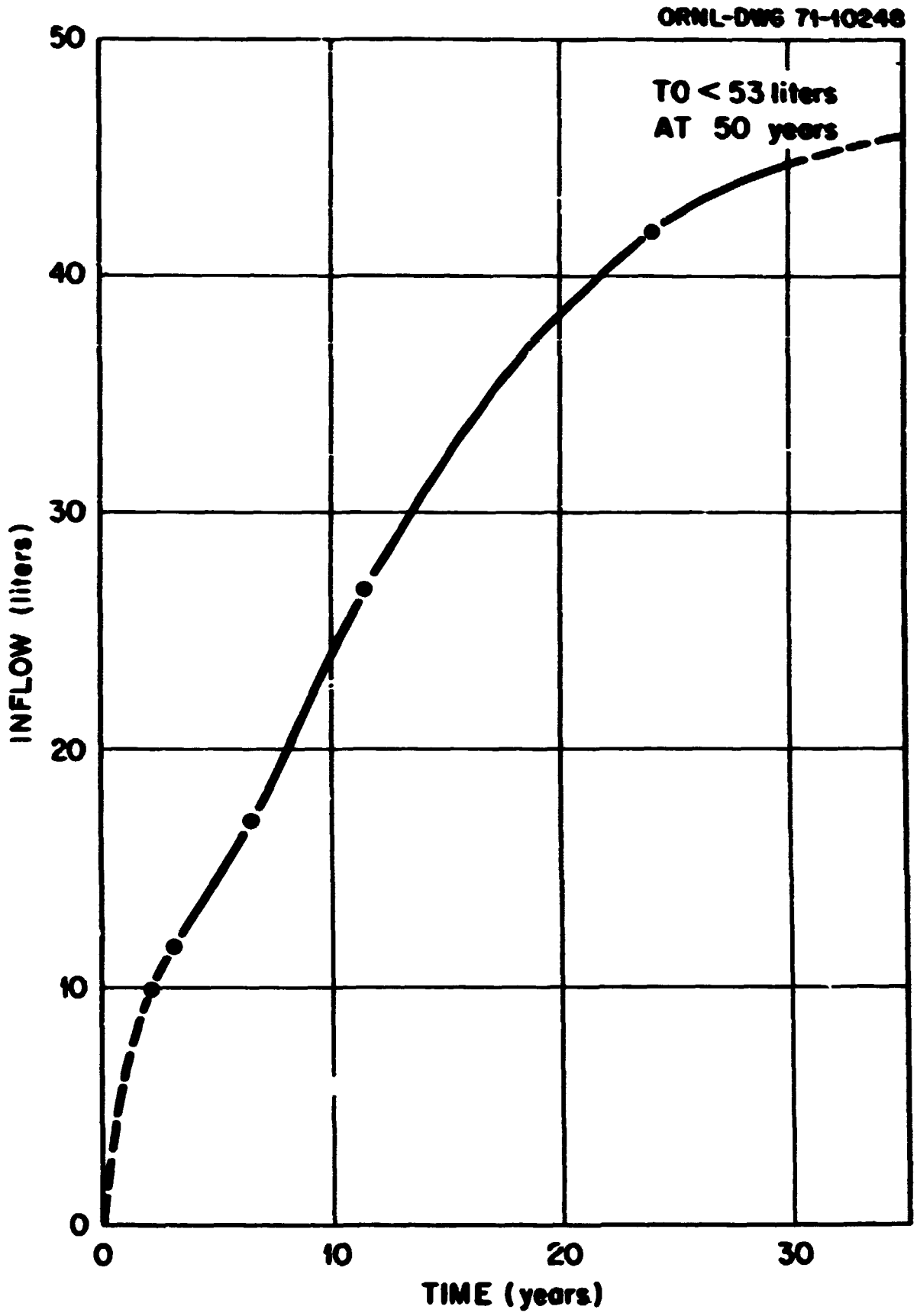

Fig. 10.11. Total Cumulative Brine Inflow vs Time After Burial, Midplane, h = 10 ft (Case C-2, 5-kW Can).

10.5 Effects of Migration of Brine-Filled Cavities on Radiolysis of Brine and on Amounts of Radiation Damage in Salt

The rate, ζ, at which trapped electrons and holes are introduced into a migrating brine droplet will depend upon several parameters as shown approximately by the relationship, Eq. (20):

$$\zeta = 2000 \frac{mC}{X} \text{ (moles liter}^{-1} \text{ year}^{-1}) \ , \qquad (20)$$

where

m = velocity of migration of droplet (cm/year),

X = dimension of droplet perpendicular to thermal gradient (cm),

C = concentration of pairs of trapped electrons and holes in the salt lying in front of the migrating droplet (moles/g).

A radiation annealing constant, k, can be written as in Eq. (21) if it is assumed that the cavities are uniformly dispersed as cubes of dimension, X, and that the amounts and uniformity of this heterogeneous annealing suffice to approximate a homogeneous process,

$$k = \frac{mb}{X} \text{ (year}^{-1}) \ , \qquad (21)$$

where b is the fraction of the salt that is occupied by brine.

Discussions of information relative to these parameters and of estimates of the rates of injection of trapped electrons and holes into migrating brine are presented below.

10.5.1 Concentration of Trapped Electrons and Holes in Salt

The radiation behavior, with respect to accumulation of trapped electrons and holes, of NaCl at the high temperatures and doses that will prevail in the Repository has not been completely established. It has been suggested that the concentrations of defects which can be accumulated at certain high temperatures exceed those which can be accumulated at normal temperatures.[14] Also, it is believed that colloids, rather than F-centers, are the predominant trapped-electron-defects which are present in NaCl after irradiation at certain high temperatures.[14]

Some of the available quantitative data relating stored energy (or concentration of defects) and gamma ray or electron dose at high temperatures[3,13,15,48] are plotted in Fig. 10.12.* Other high-temperature data obtained with samples of salt that were irradiated in the Project Salt Vault Experiment are listed in Table 10.4. Some of the available data from lower-temperature studies (<100°C) are included in Fig. 10.12. Ordinate scales show values both for stored energy and for concentration of pairs of trapped electrons and holes. The values for defect concentrations were obtained from those for stored energy, or vice versa, using a conversion factor of 5.5 eV per defect.** Information on the form of the sample, radiation exposure conditions, and methods of measurements is set forth in the legend in Fig. 10.12 and is also given in Table 10.4.

Consideration of these various data and of other information, including that mentioned above, led to the following conclusions regarding possible maximum concentrations of pairs of trapped electrons and holes in the salt in the Repository.

(1) The amounts of stored energy in the Project Salt Vault samples exceeded, by large factors, those expected for NaCl irradiated at comparable dose rates and doses but at lower temperatures (less than about 60°C). There are unexplained differences between the results of DTA and solution calorimeter measurements. There are also unexplained differences between the

---

*The rock salt sample that gave 14 cal/g (Fig. 10.12) by solution calorimetry gave 21 ± 6 cal/g by scanning differential calorimetry.

**Recent theoretical considerations by Schweinler[49] indicated that the stored energy per defect (displaced atom and vacancy pair) in NaCl is unlikely to exceed 5.5 to 6 eV. Experimental values of 9.2 and 12.4 eV per F-center have been reported, respectively, by Phelps and Pearlstein[50] and by Bunch and Pearlstein.[51] The former workers employed solution calorimetry, and they added 3.6 eV to the measured value of 5.6 eV on the unverified assumption that H_2 and OCl^- were formed upon dissolution of the defects. The latter workers heated the irradiated samples to 400°C and measured the heat released by calorimetry. They employed a plot of stored energy vs $N_F + 2N_M$ in evaluations of their data, and they fitted the data with a straight line. However, they mentioned that the data also could have been fitted with a curve concave upward. In the latter case, their energy per F-center could be substantially less than the reported 12.4 eV.

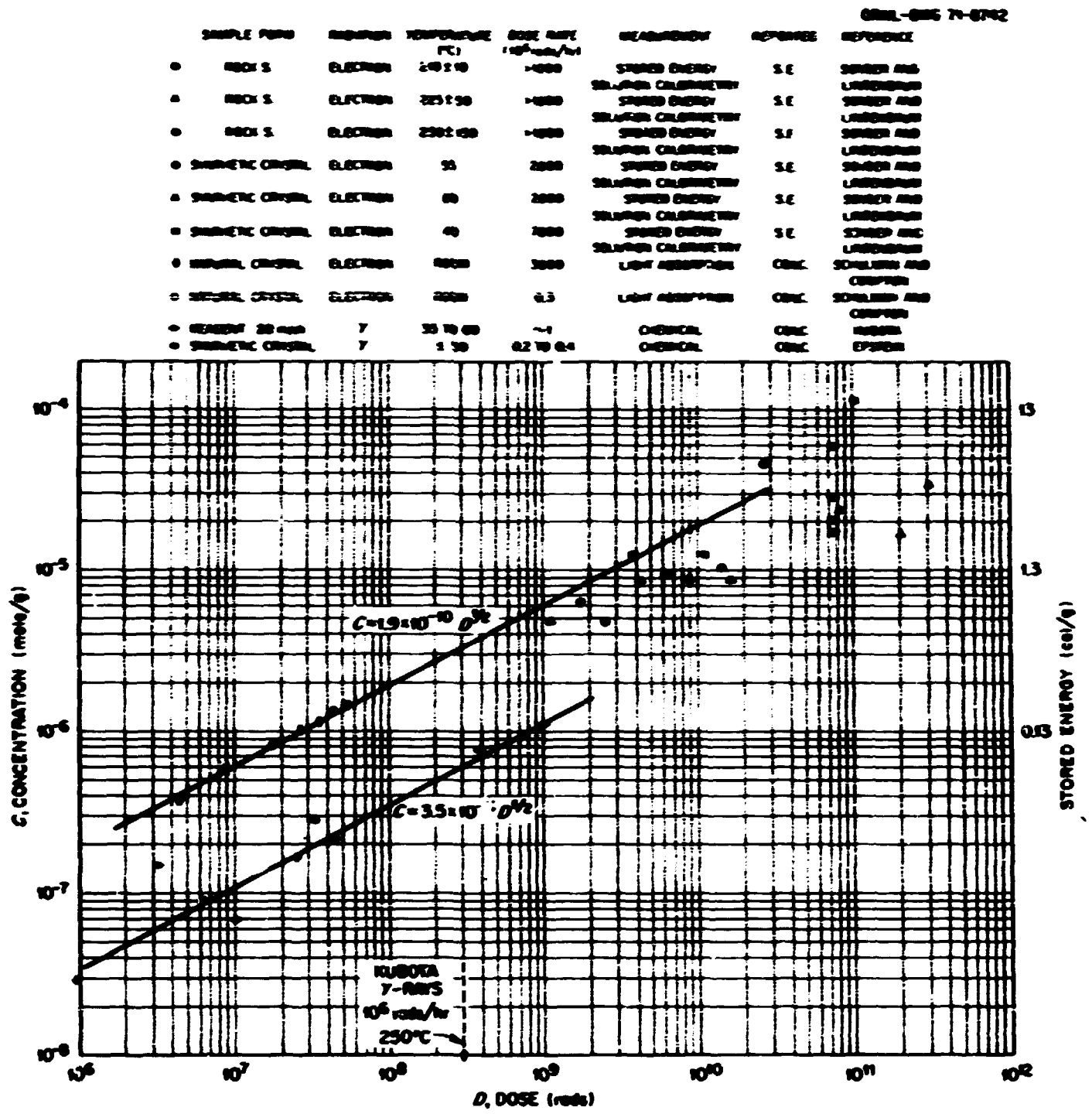

Fig. 10.12. Some Reported Information on Defect Concentration vs Dose in NaCl.

Table 10.4. Stored Energy in Salt Irradiated in Project Salt Vault

Sample Source	Exposure Temp. for Final 80 Days[a] (°C)	Average Dose Rate (Mrads/hr)	Total Dose (Mrads)	Stored Energy (cal/g)	Defect Conc.[b] (micromole/g)	Method	Reference
Hole 2 core	180	0.080	600	0.67 and 0.68[c]	5.0	Soln. Cal.	Mastrolanni et al.[d]
Hole 2 core	165	0.065	490	0.62 and 0.56[c]	4.5	Soln. Cal.	Mastrolanni et al.[d]
Hole 6 core	180	0.080	600	1.2 and 1.6[c]	10.5	Soln. Cal.	Mastrolanni et al.[d]
Hole 6 core	135	0.013	89	1.1	8.5	Soln. Cal.	Mastrolanni et al.[d]
Hole 4 scrapings - 11 ft	160	0.095	700	6	46	DTA	Zeller et al.[e]
Hole 4 scrapings - 9.5 to 11 ft	165-200	0.08	600	0 ± 0.2	-	Soln. Cal.	Sonder et al.[f]
Hole 4 scrapings - 11 ft	160[g]	0.095	700	0 ± 0.2	-	Soln. Cal.	Sonder et al.[f]

[a]The following statements regarding temperatures can be inferred from information in ref. 58: (1) Total time at temperature was about 570 days. (2) Temperatures at the edge of a hole at 100 to 400 days were 40 to 50°C below those at 570 days. Between 400 and 490 days, the temperatures were intermediate between those at 400 and 570 days. Still lower temperatures prevailed prior to 100 days. (3) Salt temperatures away from the edge of the hole also changed during the 570-day exposures, but the changes were probably somewhat less than those at the edge of the hole.

[b]Calculated from stored energy using 5.5 eV per defect.

[c]Duplicate samples.

[d]M. J. Mastrolanni and C. D. Bopp, ORNL, private communication, September 1971. The listed stored energy values were evaluated from the difference between the heats of solution of the irradiated samples and of pure unirradiated NaCl. Average sample.

[e]Eduard Zeller, Gisela Dreschoff, and Harold Yarger, "Energy Storage and Radiation Damage Effects in Rocksalt," Chap. 5, p. 103 in final report, Geology and Hydrology of the Proposed Lyons, Kansas, Waste Repository Site, E. H. Angino and W. W. Hambleton (compilers), prepared for the ORNL and the Union Carbide Corporation by the University of Kansas Center for Research, Inc. (March 1971). Dark crystals were selected for measurement.

[f]For an average sample. See Sect. 9 of this report.

[g]Sonder et al.,[3] listed this exposure temperature as 165-200°C. However, from information in ref. 58, it can be inferred that the maximum temperature at the edge of the hole was 160°C.

results of solution calorimeter measurements on samples exposed to presumably comparable conditions. The maximum experimental values with the Salt Vault samples are adequately represented by Eq. (22):

$$C = 10^{-18} D , \qquad (22)$$

where D is the radiation dose (in rads), and C is as defined above.

(2) There are some theoretical reasons for expecting that, at saturation, the number of defects will not exceed a few percent of the number of atoms in the salt crystal.[3]* The assumptions that saturation occurs at 1% defects (22 cal/g) and that Eq. (22) is valid in the dose range below about 10^9 rads leads to Eq. (23):

$$C = 1.7 \times 10^{-4} \left(1 - e^{-6.0 \times 10^{-10} D}\right) . \qquad (23)$$

(3) The radiation and/or thermal annealing required to bring about the saturation indicated by Eq. (23) would be greater than the migration annealing constant [Eq. (21)] unless the value of X is appreciably less than 1 mm. To be conservative (and for simplicity), we assumed that the droplets are about 1 mm in dimension and that migration annealing will be negligible.

(4) The data in Table 10.4 and Kubota's 250°C datum point in Fig. 10.12 indicate that thermal annealing will limit the amount of energy storage in the salt mine to a few calories per gram or less when the exposure temperature exceeds some value in the range 200 to 250°C.**

(5) Our previous estimates of amounts of migration annealing and of the radiolysis caused by dissolution of trapped electrons and holes were based on the following assumed relationship between defect concentration and dose in the absence of migration

---

*However, additional experimental information is needed to establish the actual defect concentration at saturation at the dose rates and the temperatures that will prevail in the Repository.

**However, additional experimental information is needed to establish this for salt-mine salt that has been irradiated under Repository conditions, including conditions of light and moisture.

annealing,

$$C = 3.2 \times 10^{-10} D^{1/2} . \qquad (24)$$

The recent data and the interpretations discussed above indicate that this was not a conservative assumption for salt exposed within certain temperature ranges (e.g., 130 to 160°C).

10.5.2 Values of m

Brine inflow considerations (see Sect. 10.3) for the 2-kW can (Case C-1) indicated that the brine-migration-velocity remains approximately constant over long periods of exposure; the velocity is about 6 cm/year after a 1.7-year exposure, and 7.5 to 10 cm/year between exposure intervals of 3 and 30 years. Also, the volume of brine at the edge of the burial hole remains approximately constant at the initial value, 0.5 vol %, over long periods of exposure (i.e., 50 years).

The similarly estimated values of m for the 5-kW cans (Case C-2) are 15 cm/year during the first 20 years after burial and 6 cm/year between 20 and 30 years after burial.

10.5.3 Estimates of Rates of Injection of Defects into Migrating Brine

The steady-state value of C from Eq. (23) is 170 micromoles/g. Substituting this value in Eq. (20),

$$\zeta = 2 \times 10^{3} \frac{mC}{X} , \qquad (20)$$

with m and X equal to 6 cm/year and 0.1 cm, respectively, we have

$$\zeta = \frac{(6)(1.7 \times 10^{-4})}{0.1} 2 \times 10^{3} , \qquad (25)$$

or

$$\zeta = 20 \text{ (moles liter}^{-1} \text{ year}^{-1}) .$$

For comparison with the rates at which chlorine is formed by direct absorption of radiation in the brine, we calculate that, with $2g'(H^2) = g'(Cl_2^-) + 2g'(Cl_3^-) = 4.2$, and with dose rate = 8.8×10^8 rads/year (2-kW can), the rate of formation of chlorine is 4.6 moles liter^{-1} year^{-1} (measured as Cl^0). Accordingly, the contribution from the salt could be several times that from direct absorption of radiation if it is assumed that all of the trapped electrons (or Na^0) react to form H_2 upon dissolution.

It is apparent from Eq. (20) how the value of ζ would change with changes in the assumed values of C. a, and X.

10.6 Amounts of $MgCl_2$ and Radiolytic H_2 Entering Open Spaces Around Can with Migrating Brine

Estimated rates at which $MgCl_2$ is introduced into the open spaces around a can with migrating brine in cases C-1 and C-2 are plotted in Figs. 10.13 and 10.14. As indicated in these figures, the concentration of $MgCl_2$ in the brine was assumed to be 3 M.

As discussed above, it is probable that the concentration of radiolytic H_2 within the brine will not exceed 1 M. Assuming that this is the case, the rate of inflow of H_2 would not exceed one-third of that for $MgCl_2$. The plot for H_2 in Fig. 10.13 was made before this probable 1 M limit for H_2 was recognized. The high initial rate of inflow of $MgCl_2$ shown in Fig. 10.14 resulted from the assumption that brine was released by high-temperature fracture of the salt (see Sect. 10.3). The estimated rates of inflow of radiolytic H_2 in this case were less than 200 micromoles/hr during the first five years after burial. After this time, the estimated rates for H_2 would be about one-third of those for the $MgCl_2$.

10.7 Identities and Amounts of Oxidized Species in Brine Around Can at Start of Exposure

The products of radiolysis of unconfined brine around the can may differ from those of the encapsulated brine because the unconfined brine may be acid with HNO_3 and HCl and because any gaseous radiolytic products will readily escape from solution. We concluded that the possible

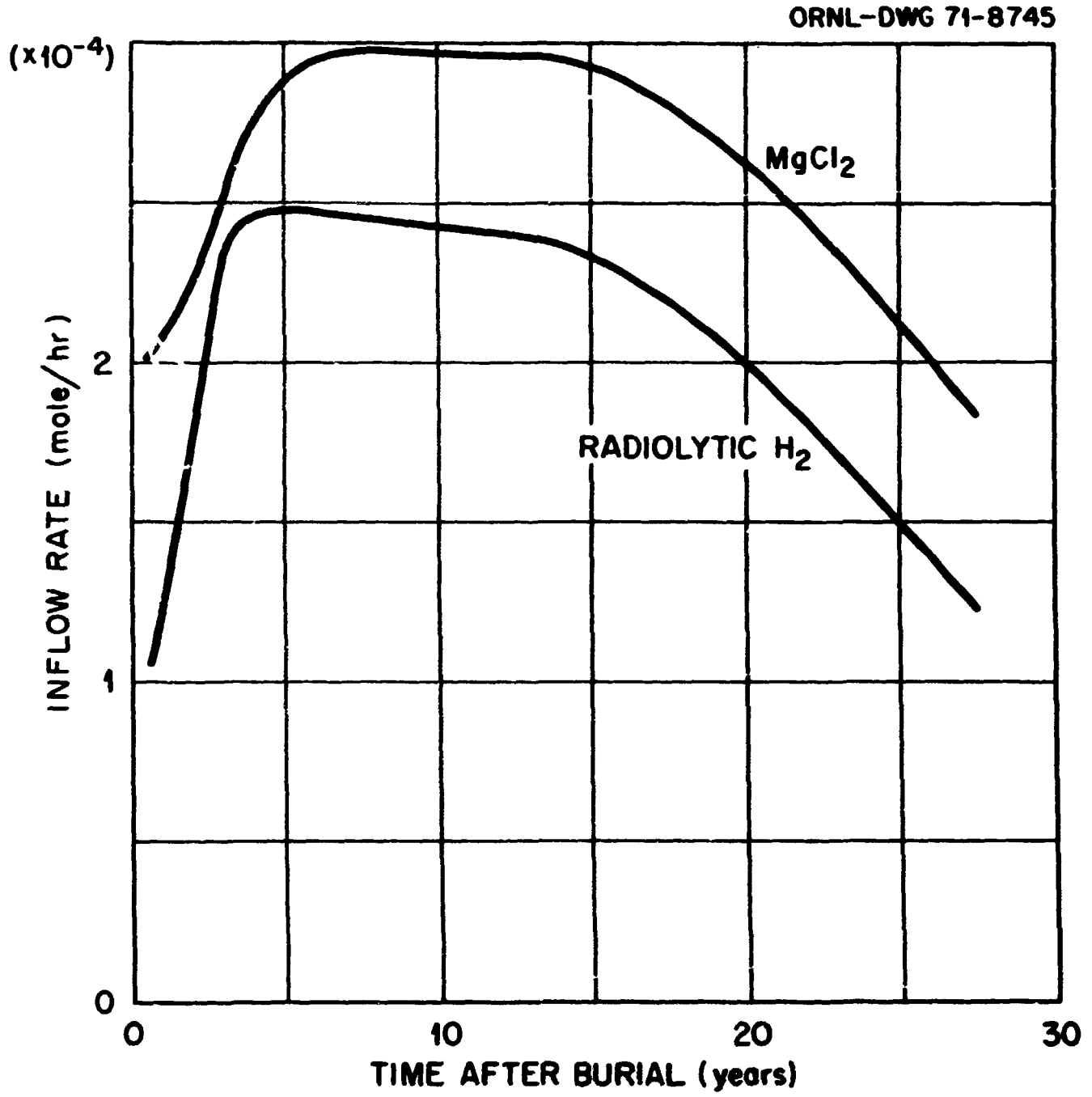

Fig. 10.13. Rates of Flow of Radiolytic H_2 and $MgCl_2$ into Open Spaces Around Can Along with Brine for Case C-1 (2-kW Can). Assumptions: $G(H_2$ = 2.1, $(MgCl_2)$ = 3 M.

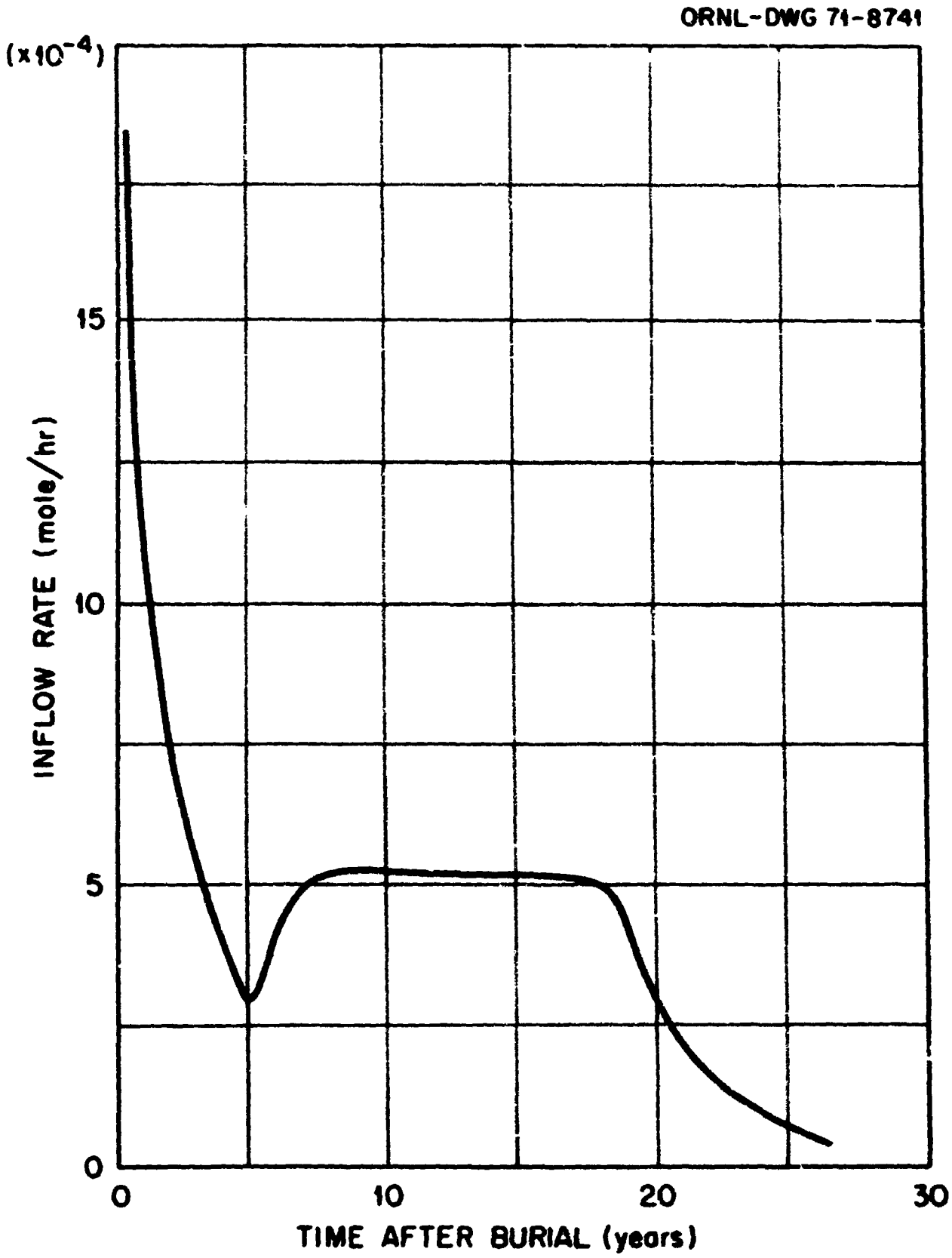

Fig. 10.14. Rate of Inflow of $MgCl_2$ into Open Spaces Around Can with Brine for Case C-2 (5-kW Can). $MgCl_2$ concentration was assumed to be 3 M.

radiolytic products under these conditions include Cl_2, Br_2, ClO_3^-, BrO_3^-, ClO_2, ClO_4^-, and ClO_2^-, along with H_2 and O_2. The Cl_2 would react radiolytically to form HCl within the vapor phase.

It can be shown that the amounts of these products which will be generated before brine-boiling-temperatures are reached will be negligibly small with a 5-kW can. With a 2-kW can, it is possible that rate of H_2 generation would be 0.8 mole/year for a period of about 0.1 year after burial, then decrease to 0.3 mole/year or less for a period of 0.5 year or less. These production rates are much less than the maximum rate at which H_2 may appear around the can as a result of migration of brine to the can (Table 10.5). The maximum amounts of O_2, ClO_3^-, BrO_3^-, and Cl_2 (HCl) would also be well below those associated with the migrating brine. However, the ClO_2, which is a possible product of radiolysis of the unconfined brine, is not a radiolytic product within the migrating brine. Accordingly, its possible production around the can needs to be included in consideration of the possible effects of radiolytic products.

10.8 Significance of the Results of the Work Reported in this Section to the Design and Operation of the High-Level Waste Repository

Table 10.5 presents a summary of our conclusions regarding the identities of the species that will enter the open spaces around a waste can and also regarding the maximum rates of introduction of these species. Active and/or noxious chemicals are included among the species, and their presence may influence the final design and operating procedures for the Repository. Avenues of possible influence which should be considered, or have been considered previously, are discussed below.

It can be noted here that the effects of the species in Table 10.5 on the design and operation of the Repository have not been completely evaluated. However, we have not yet recognized any possibly serious detrimental effect which could not be counteracted by some modification of the design or operation of the Repository. Also, we are presently conducting additional work in a number of different areas, including work in brine migration, radiolysis, and stored energy. The results of this

Table 10.5. Summary of Conclusions Regarding Identities of Species Appearing Around a Waste Can and Maximum Rate of Appearance

Species	Source	Max. Rate of Appearance (moles/year)	Max. Period After Burial (years)	Balancing Oxidized Species	Remarks
H_2	Radiolysis product within encapsulated brine	4	<1	O_2, chlorates, bromates	Comparable rates for 2- and 5-kW cans.
H_2	Radiolysis of solution around can	0.8 followed by a decrease to 0.3	0.1 0.5	O_2, Cl_2, Br_2, ClO_3^-, BrO_3^-	For 2-kW cans. Insignificant radiolysis with 5-kW cans because of rapid heatup.
H_2	Corrosion of can (50 mils/year)	400	<1		Assumed brine inflow rate of 7 liters/year, with all H_2O reacting with can.
HCl	Hydrolysis of $MgCl_2$	20	<1		Assumed brine inflow rate of 7 liters/year, 3 M $MgCl_2$ within brine, and 50% hydrolysis of $MgCl_2$.
HNO_3	Radiolysis of moist mixtures of N_2 and O_2	0.50	<0.1		Likely that all N_2 will have been expelled at <0.1 year after burial.
O_2 and other oxidized species	Radiolysis				To balance radiolytic H_2.

work will help in evaluating the amount and the effects of the radiolysis, hydrolysis, and corrosion products.

It should be emphasized that the rates given in Table 10.5 are maximum values. The analyses in this report were aimed at providing conservative estimates. The actual rates of formation of a species are expected to be equal to, or less than, the value indicated in Table 10.5 and elsewhere in this section.

10.8.1 Reference Information

According to present tentative plans, a burial room will be ventilated with air flowing at 20,000 scfm during operations within the room. These operations will require a period of time no longer than 3 months.[53]

Each room will be backfilled with crushed salt after completion of burial operations. (Backfilling of a section of a room after completion of burial operations in that section could also be done if desired.)[53]

In the case of 5-kW cans, a total of 10 cans will be buried below a single room. The room volume per 5-kW hole will be about 10^4 ft^3.[2]

The fraction of open spaces in the crushed salt backfill, as charged, is expected to range from about 0.27 for mixtures of fine and medium salt to about 0.37 for medium salt.[54] Diffusion through beds of as-charged medium salt is expected to be about three times slower than through free space; diffusion through medium-fine mixture would be about eight times slower than through free space.[54] Consolidation of the crushed salt backfill will take place with accompanying diminution of the fraction of open spaces and possibly of the gas transport capabilities. The times after burial at which the backfill within a hole will have been consolidated have not been established.

The lower ignition limit for mixtures of H_2 in air or oxygen is about 4 vol %.[55] In mixtures of water vapor and H_2 and O_2, the lower limit is about 15 to 20 vol % H_2 plus O_2.[56] The size of the container affects the ignition limit in the latter mixtures under at least some conditions[57,*];

---

*The size of the container also affects the ignition limits in other gas mixtures.[58]

at 200°C, the explosive limit increases from about 15 vol % of $2H_2 + O_2$ to about 50 vol % as the ratio of surface area to gas volume increases from about 1 to 10 in.$^{-1}$.[57] The ratio of surface area to gas volume in the crushed salt will be about 200 or more per in., and it is likely that the lower ignition limits will exceed the 4 vol % mentioned above by substantial factors. However, experimental verification of this hypothesis would be required before use could be made of a given ignition limit in an engineering design. The upper limit of inflammability of an H_2-air mixture is 75% H_2; that for an H_2-O_2 mixture is 94% H_2.[55]

The permissible concentration of HCl in the air within working areas is 5 ppm.

The corrosion of stainless steel at high temperature by vapors containing HCl or Cl_2 may be appreciable (several tens of mils per year),[59] whereas the rate of corrosion by water vapor alone likely would be negligible. The accelerating effects of HCl and Cl_2 on corrosion probably are comparable.[59] There is no information available regarding whether either Cl_2 or HCl catalyzes the reaction between water vapor and stainless steel (i.e., whether the chlorine species would form stable metal halides, and whether corrosion would cease when the chlorine species were thus consumed).

10.8.2 Formation of Explosive Gas Mixtures with Hydrogen Gas

With Gas Transport Properties of Salt Beds Above Can Comparable to Those of Medium Crushed Salt. - (a) Within Waste Disposal Hole. - Our estimates of the transport of H_2 through beds of medium crushed salt indicate that the maximum concentration of H_2 at any elevation above the can would be less than 3 vol % at the maximum rates of generation of H_2 listed in Table 10.5. Thermal and other buoyancy effects would play important parts in transferring the H_2 up through the 8-ft-deep beds and into the room. However, diffusion alone would suffice to hold the H_2 at less than 3 vol % when radiolysis is the only source of H_2.

The situation below the top of the can is less obvious. However, for several reasons, it seems unlikely that an explosive composition would form. In general, gases will tend to be swept out and the remaining gases will tend to be diluted by any steam escaping reaction with the can. Any H_2

that is generated by reaction between the can and water will exercise similar sweeping and dilution effects. In addition, it is likely that O_2 as well as water vapor would react with the can so that, when diluent H_2O is removed from the gas-vapor phase, the O_2 would also be removed.

(b) Room Above Waste Disposal Can. - It can be shown that introduction of H_2 into a burial room at the maximum rates listed in Table 10.5 would present no problem from the standpoint of explosive gas mixtures. Thus, introduction of H_2 at the rate of 4×10^3 moles/year (7.6×10^{-3} mole/min) from ten 5-kW cans buried below a room would result in a maximum H_2 concentration of 3×10^{-5} vol % within the ventilation air. Even with no ventilation, the uniform concentration of H_2 within the volume of air associated with a burial hole would be only 3 vol % at the end of one year. If the room above a waste can is backfilled immediately after the can is buried, the uniform concentration of H_2 within the crushed salt would be 9 vol % after one year, providing that H_2 escapes from the hole at the maximum rate listed in Table 10.5. As mentioned in Sect. 10.8.2, 3 vol % H_2 is at the lower limit for reaction in large containers. The lower ignition limit for gas mixtures within the crushed salt is unknown but is probably in excess of 9 vol % H_2.

With Burial Hole Sealed. - If a gas-tight seal should develop or be imposed within a salt bed above a waste can, it would be possible for an explosive mixture of gases to collect below the plug. Thus for example, assume that a plug forms at an elevation of 2 ft above a can, and assume also that the temperature of the 2-ft length of bed is still below that at which the vapor pressure of water is appreciable. In this case, gases would tend to accumulate in the 2-ft length of bed, and the maximum rate of increase of the partial pressure of radiolytic H_2 would be about 0.03 atm/day. The rate of partial pressure increase is about 4 atm/day when H_2 is generated by corrosion at the maximum rate of 400 moles/year. In order that the gas mixtures be combustible, they must contain O_2. Oxygen is generated along with the radiolytic H_2, and, providing it does not react with the waste can, it would accumulate along with radiolytic H_2 in the gas mixture. Atmospheric oxygen at a partial pressure of about 0.2 atm might be trapped below a plug, and this limited amount might be available for reaction with H_2 produced by corrosion.

Considerations to date have indicated* that an explosion below a plug after the space in the room above the waste can has been backfilled with salt would not lead to ejection of the can from the hole. Also, an explosion at that time would not lead to serious dispersal of radioactivity even though the can is open for some reason at the time of the explosion. This latter conclusion follows from consideration of the maximum amounts of gases which would be available for expulsion from the hole and from the reasonable assumption that the expelled gases will quickly reach an approximate thermal equilibrium with the crushed salt in the room above the can. Thus, for example, assume that 400 moles of H_2 (320 ft^3, STP) accumulate within the space around a can for some unforeseen reason, and also assume that all of the 400 moles are expelled by an explosion. This amount of gas would occupy the gas space associated with a 4-ft length of room containing 5-kW cans. The length of room associated with each can will be at least 40 ft; therefore, it is very unlikely that any expelled gas would reach the room opening.

The considerations made thus far have not led to any definite conclusions as to whether an explosion prior to backfilling would be of any concern.

10.8.3 Introduction of Noxious Gases Other than Radioactive Species into Working Area

It can be shown that introduction of HCl into the room containing ten 5-kW cans at the maximum rate listed in Table 10.5 should cause no concern from the standpoint of exceeding acceptable concentrations. With ventilation at 20,000 scfm and with an HCl injection rate of 20 moles per year per can, the maximum HCl concentration in the ventilation air would be 0.015 ppm. Without ventilation, the tolerance concentration of 5 ppm could be reached after one day. Prolonged loss of ventilation would be precluded by the operational design.[53]

Other species such as Br_2 and HNO_3 would be injected at much lower rates and would reach much lower concentrations in the working areas.

---

*R. D. Cheverton and G. H. Jenks, unpublished analyses, July 1971.

10.8.4 Effects of HCl and Other Active Species on Transport of Fission Product Activities

Project members have not ruled out the possibility that volatile oxychlorides will be formed, and this will be investigated.[60]

10.8.5 Effects of HCl and Other Active Chemical Species on Corrosion of Waste Can

As mentioned in Sect. 10.8.2, it is likely that the corrosion rate for stainless steel in contact with water vapor containing HCl or Cl_2 at high temperatures will be appreciable (i.e., several tens of mils per year). The corrosion of carbon steel is also likely to be substantial. At a maximum, the average rate of corrosion could correspond to that at which the rates of inflow of water and of reaction of water with the can are equal. (Assuming maximum rates and uniform corrosion, the 1/4-in. walls on a 5-kW can would be completely converted to oxide at 15 years after burial.)

10.8.6 Effects of Explosive Reactions of Chlorates and Perchlorates

Chlorates and perchlorates are explosives when they come in contact with oxidizable materials. However, it can be inferred that the explosive energy which could be developed from these materials within a waste hole would be tolerable after the burial room has been backfilled.* The bases for this inference are as follows:

(1) An explosive force equivalent to 1 lb of TNT within a burial hole is considered tolerable.[3]

(2) The maximum rate of formation of chlorate is about 1.3 moles/year (Table 10.5). (The equivalent maximum rate of formation of perchlorate from chlorate is about 1.0 mole/year.) As stated in Sect. 10.2.5, it is believed that these compounds would decompose thermally to form O_2 and halides.

(3) The explosive efficiency of the chlorates and/or perchlorates which might be present within a burial hole is unknown. It is

*No analysis has been made of the situation prior to backfilling.

conservative to assume that the material has an explosive efficiency equivalent to that of TNT, and that the material has an atomic weight of 150.[61]

(4) With the assumption in (3), the maximum explosive force that could be developed from chlorates after one year would be equivalent to about 0.35 lb of TNT. (Much longer times would be required to double the amount of chlorate that could be introduced into a waste hole.)

(5) The situation with respect to dispersal of radioactivity is analogous to that discussed in Sect. 10.8.3.

10.9 References

1. W. C. McClain and R. L. Bradshaw, "Status of Investigations of Salt Formation for Disposal of Highly Radioactive Power-Reactor Wastes," Nucl. Safety 11, 130 (1970).

2. R. D. Cheverton, private communication, July 1971.

3. J. O. Blomeke et al., An Analysis of Energy Storage and Its Effects in the Propoced National Radioactive Waste Repository, ORNL-TM-3403 (June 1971).

4. W. T. Holser, "Chemistry of Brine Inclusions in Permian Salt from Hutchinson, Kansas," pp. 86-95 in Proceedings of the Symposium on Salt, Northern Ohio Geological Society, 1963.

5. W. E. Verplank, Salt in California, Bulletin 175, State of California, Div. of Mines, San Francisco, 1958, p. 33. (Discussion of results of J. Usiglio).

6. International Critical Tables of Numerical Data, Physics, Chemistry and Technology, Vol. IV, prepared by the National Research Council, p. 310, McGraw-Hill, New York, 1928.

7. A. Seidell, Solubilities of Inorganic and Metal Organic Compounds, 3d ed., Vol. 1, p. 966, Van Nostrand, 1953.

8. R. L. Bradshaw and W. C. McClain, Project Salt Vault: A Demonstration of the Disposal of High Activity Waste in Underground Salt Mines, ORNL-4555 (April 1971), p. 45.

9. P. Cohen, "Chemistry of Additives and Contaminants in High Pressure Boilers," J. Eng. Power 92, 89 (1970).

10. S. A. Brusentseva and P. I. Dolin, "The Effect of KBr and KCl Concentrations on the Yield of Molecular Products of Radiolysis in Aqueous Solutions," p. 35 in Radiation Chemistry of Aqueous Solutions (Inorganic and Organic Systems), a portion of the Proceedings of the first All-Union Conference on Radiation Chemistry, Moscow, 1957, Consultants Bureau, Inc., New York, 1959.

11. T. J. Sworski, private communication, January 1971.

12. (a) H. A. Schwarz, "Applications of the Spur Diffusion Model to the Radiation Chemistry of Aqueous Solutions," J. Phys. Chem. 73 1928 (1969).

    (b) A. Appleby and H. A. Schwarz, "Radical and Molecular Yields in Water Irradiated by γ Rays and Heavy Ions," J. Phys. Chem. 73, 1937 (1969).

13. L. M. Epstein, Formation of Chemically Free Halogen by Radiolysis of Solid Potassium Chloride, WERL-0100 (June 1962).

14. W. G. Burns and T. F. Williams, "Chemical Effects Associated with 'Colour Centres' in Alkali Halides," Nature 175, 1043 (1955).

15. R. L. Bradshaw and W. C. McClain, Project Salt Vault: A Demonstration of the Disposal of High Activity Waste in Underground Salt Mines, ORNL-4555 (April 1971), p. 43.

16. A. M. Kabakchi, V. A. Gramolin, and V. M. Erokhin, "Some Data on the Effect of Ionizing Radiation on Concentrated Aqueous Solutions of Inorganic Salts," p. 45 in Radiation Chemistry of Aqueous Sclutions (Inorganic and Organic Systems), a portion of the Proceedings of the first All-Union Conference on Radiation Chemistry, Moscow, 1957, Consultants Bureau, Inc., New York, 1959.

17. A. R. Anderson and D. Knight, cited by W. H. Hamill in "A Model for the Radiolysis of Water," J. Phys. Chem. 73, 1341 (1969).

18. R. D. Baybarz, "Alpha Radiation Effects on Concentrated LiCl Solutions Containing HCl, and the Use of Methanol as an Inhibitor of Acid Radiolysis," J. Inorg. Nucl. Chem. 27, 725 (1965).

19. C. J. Hochanadel, Chap. 42.3 in Vol. 1, "Materials," of The Reactor Handbook, 2d ed., ed. by C. R. Tipton, Jr., pp. 878-81, Interscience, New York, 1960.

20. G. H. Jenks and J. C. Griess, Water Chemistry in Pressurized and Boiling Water Reactors, ORNL-4173 (November 1967).

21. M. Anbar and J. K. Thomas, "Pulse Radiolysis Studies of Aquecus Sodium Chloride Solutions," J. Phys. Chem. 68, 3829 (1964).

22. D. M. Himmelblau, "Solubilities of Inert Gases in Water, °C, to Near the Critical Point of Water," J. Chem. Eng. Data 5, 10 (1960).

23. D. W. Kaufmann, Sodium Chloride, p. 19, Reinhold, New York, 1960.

24. H. E. Cline and T. R. Anthony, "Vaporization of Liquid Inclusions in Solids," Phil. Mag. (1971).

25. Hisashi Kubota, "Chlorine Production by Gamma Radiolysis of Acid Chloride Solutions and Its Effect on Analytical Procedures," Anal. Chem. 40, 271 (1968).

26. Takeshi Sawai and W. H. Hamill, "Evidence for Very Early Effects in the Radiolysis of Water," J. Phys. Chem. 74, 3914 (1970).

27. K. W. Young and A. J. Allmand, "Experiments on the Photolysis of Aqueous Solutions of Chlorine, Hypochlorous Acid, and Sodium Hypochlorite," Can. J. Res. 27B, 318 (1949).

28. W. M. Latimer and J. H. Hildebrand, Reference Book of Inorganic Chemistry, 3d ed., p. 69, Macmillian, New York, 1951.

29. J. W. Mellor, A Comprehensive Treatise on Inorganic and Theoretical Chemistry, Vol. IV, pp. 299-301, Longmans, Green and Co., London, 1922.

30. W. Moldenhaur, "Uber die Einwirkung Von Sauerstoff and Wasserdampf auf Chlormagnesium," Z. Anorg. Chem. 51, 25 (1907).

31. S. V. Kushnir and Y. P. Berkman, "Hydrothermal Decomposition of Kainite," Ukr. Khim. Zh. 26, 531-34 (1960). (Translation 3636, Central Electricity Generating Board, London.)

32. Fritz Ephraim, Inorganic Chemistry, 6th English ed., ed. by P. C. L. Thorne and E. R. Roberts, pp. 396-99, Oliver and Boyd, Ltd. London, 1954.

33. M. M. Markowitz, D. A. Borgta, and H. Stewart, Jr., "Transient Perchlorate Formation During the Pyrolysis of the Alkali Metal Chlorates," J. Phys. Chem. 68, 2282-89 (1954).

34. Mellor's Comprehensive Treatise on Inorganic and Theoretical Chemistry, Suppl. II, Pt. 1, pp. 582-84, Longmans, Green and Co., New York, 1956.

35. Handbook of Chemistry and Physics, 48th ed., Chemical Rubber Publishing Company, Cleveland, Ohio, 1967-68.

36. C. J. Hochanadel, private communication, January 1971.

37. S. C. Lind, Radiation Chemistry of Gases, pp. 232-45, Reinhold, New York, 1961.

38. A. R. Jones, "Radiation Induced Reactions in the N_2-O_2-H_2O System," Radiation Res. 10, 655 (1959).

39. J. Wright, J. K. Linacre, W. R. Marsh, and T. H. Bates, "Effect of Radiation on Heterogeneous Systems of Air or Nitrogen and Water," Proc. Intern. Conf. Peaceful Uses At. Energy, Geneva, 1955 7, 560 (1955).

40. R. L. Bradshaw and F. Sanchez, "Brine Migration Studies," p. 32 in Health Phys. Div. Ann. Progr. Rept. July 31, 1968, ORNL-4316.

41. T. R. Anthony and H. E. Cline, "The Interaction of Liquid Droplets with a Grain Boundary in Large Accelerational Fields," Phil. Mag. 24, 695 (1971).

42. H. E. Cline and T. R. Anthony, "The Thermomigration of Liquid Droplets Through Grain Boundaries in Solids," Acta Met. 19, 491 (1971).

43. T. R. Anthony and H. E. Cline, "The Thermal Migration of Liquid Droplets Through Solids," J. Appl. Phys. 42, 3380 (1971).

44. H. E. Cline and T. R. Anthony, "The Shape Relaxation of Liquid Droplets in Solids," Acta Met. 19, 115 (1971).

45. T. R. Anthony and H. E. Cline, "The Kinetics of Droplet Migration in Solids in an Accelerational Field," Phil. Mag. 22, 893 (1970).

46. R. L. Bradshaw and W. C. McClain, Project Salt Vault: A Demonstration of the Disposal of High Activity Waste in Underground Salt Mines, ORNL-4555 (April 1971), pp. 167-70.

47. T. R. Anthony and H. E. Cline, "The Thermomigration of Biphase Vapor-Liquid Droplets in Solids," unpublished paper (1971).

48. J. H. Schulman and W. D. Compton, Color Centers in Solids, p. 221, Macmillan, New York, 1962.

49. H. C. Schweinler, private communication, June 21, 1971.

0. F. T. Phelps and E. Pearlstein, "Measurement of the Stored Energy in x-Rayed Sodium Chloride," Phys. Rev. 128, 1575 (1962).

51. J. M. Bunch and E. Pearlstein, "Stored Energy in Irradiated Sodium Chloride," Phys. Rev. 181, 1290 (1969).

52. R. L. Bradshaw and W. C. McClain, Project Salt Vault: A Demonstration of the Disposal of High Activity Waste in Underground Salt Mines, ORNL-4555 (April 1971), pp. 161-63 and 172-86.

53. J. O. Blomeke, private communications, January-August 1971.

54. A. P. Malinauskas and G. M. Watson, "Gas Flow Characterization of Various Grades of Carey Kansas Rock Salt," Report No. 3 and 4, by R. B. Evans, III and J. L. Rutherford, May 18, 1971, and June 4, 1971 (private communication).

55. Bernard Lewis and Guenther von Elbe, "Combustion, Flames and Explosions of Gases," 2d ed., pp. 691-703, Academic, New York, 1961.

56. I. M. Macafee, Jr., "Detonation, Explosion and Reaction Limits of Saturated Stoichiometric Hydrogen-Oxygen-Water Mixtures," Syracuse University Research Institute, Chemical Engineering Dept. No. Ch.E. 273-556F4 (July 1956), pp. 57, 66, 67. (Report prepared for Union Carbide Corporation, Oak Ridge, Tenn., under Subcontract No. 548.)

57. Ibid., p. 58.

58. Wilhelm Jost, Explosion and Combustion Processes in Gases, translated by H. O. Craft, p. 27, McGraw-Hill, New York, 1946.

59. M. H. Brown, W. B. DeLong, and J. R. Auld, "Corrosion by Chlorine and by Hydrogen Chloride at High Temperatures," Ind. Eng. Chem. 39, 839 (1947).

60. A. P. Malinauskas, private communication, July 1971.

61. G. F. Kinney, Explosive Shocks in Air, p. 165, Macmillan, New York, 1962.

11. ECOLOGICAL ASSESSMENTS

R. C. Dahlman and Y. Tanaka*

The proposed Repository represents a new approach for isolating large quantities of radioactive wastes from the biotic environment. Long-term integrity of deposited wastes is a primary design objective. As a radioactive waste management procedure, the practice is new and untested; therefore, the Kansas facility has been designated by the AEC as a "demonstration repository." As such, it is important that concurrent ecological investigations accompany early phases of the project to establish base lines and methodologies which can be applied later in subsequent examinations of possible impact on the environment.

Results from ecological studies will provide a framework for assessing alleged or real impacts such as effects accruing from either chronic or accidental releases of radioactivity, particularly ^{90}Sr, ^{137}Cs, and plutonium. Expected distribution and/or fate of these radionuclides in affected ecosystems will be examined for possible reconcentration in food chains, a process which could cause hazardous levels of radioactivity in biota and man. Another potential impact concerns possible thermal effects on surface biota manifested by heat dissipation from high-level waste deposits. Subsidence may comprise another impact, but it is not discussed here because expected land-form fluctuations presumably would affect structures more than biota. Furthermore, plains ecosystems constantly are adapting, via successional processes, to subtle (aeolian erosion) or drastic (highway construction) landscape modification.

Preliminary information on ecological, agricultural, and environmental factors has been assembled for the Environmental Quality Statement and the conceptual design and safety report on the proposed Repository. Initial efforts have focused on: (1) ecological surveys which were carried out by consultants from Kansas State University, (2) identification of environmental pathways of radionuclide movement to man, (3) formulation of predictive models for estimating radioactivity concentrations in ecosystem components, and (4) summarization of meteorological conditions for the central Kansas region. Background information collected during this phase of the assessment has been used to characterize agricultural and ecological

*University of Tennessee. Present address: Forestry Research Center, Weyerhauser Company, Centralia, Washington.

conditions, to establish conceptual designs for evaluating impacts from long-term operations, and to define additional research tasks for collecting missing ecological information. Additional information from on-site research will be used to predict the fate of radioactivity in the environment from either chronic or acute releases. New research also will characterize the on-site thermal and hydrologic regimes in the assessment of potential effects of heat dissipation on the surface environment. The summarizations in this section should be regarded as a progress report on biotic, ecological, and surface environmental features related to the Repository.

11.1 Population Centers

The Repository site is directly northeast of Lyons, Kansas, a population center of 4510. Containing 37% of Rice County's population, Lyons represents the most densely populated area within 25 miles. Hutchinson, located 25 miles to the southeast, is the nearest city to Lyons with a larger population (40,000). The outlying rural population is widely scattered, however, as the density for rural Rice County is approximately 5 individuals per square mile.

The population of Lyons has been somewhat variable over the past five years (Table 11.1), but has been on a downward trend since 1968. Construction and operation of the Repository facility may cause an influx of possibly 500 people, thus increasing the population total over the recent 1968 high of 4922. The anticipated increase is not expected to overburden city resources and utilities.

Table 11.1. Population Data for Lyons, Kansas[a]

Year	Population
1965	4701
1966	4729
1967	4767
1968	4922
1969	4739
1970	4510

[a]Data from Lyons Daily News, April 3, 1970. Population of Lyons was 36.4% and 36.9% of Rice County for 1969 and 1970 respectively.

11.2 Current Status of Agriculture and Ecology

The soils and climate of central Kansas strongly favor grassland vegetation. Dryland farming represents a successful adaptation to this type of environment. Küchler[1] designates the climax vegetation for this area as bluestem-grama prairie, and reversion to a native grassland would quickly follow abandonment of intensive agriculture.

11.2.1 Soils

The Repository site will be located on uplands comprised of loessal-derived soils, which are nearly level or gently sloping. Five different soil series have been mapped, and their textures range from silty clays to clay loams.[2] The soils are well drained and possess a high available water capacity and medium-to-high native fertility. All the soils are well suited for range grasses and dryland agriculture, although crop losses occasionally result from summer drought. Alternatively, water erosion occurs on sloping areas, and wet weather drainage systems may experience flooding during intensive rainstorms.

11.2.2 Agriculture Crops

On-site vegetation currently consists of agricultural crops and pasture. Traces of native endemics, cosmopolitan weeds, shrubs, and trees occur along fence rows, drainages, and roadsides. Small but persistent prairie communities exist along Santa Fe and Missouri-Pacific railroad right-of-ways; and, on occasion, this prairie grass may be cut for winter hay. Practically all the 1000-acre site supports intensive agriculture for which cropping systems may vary from year to year on a given field because planting decisions depend on rotations, markets, allotments, and other commitments. Average on-site acreage plantings followed the pattern for Rice County,[3] with 73% of the land planted in wheat, 18% in sorghum, and pasture-soybeans-hay comprising the balance (Table 11.2). Other grains, such as corn, oats, barley, and rye would account for only a small fraction of total crop production. On-site field observations in midsummer 1970 agreed with these county-wide production data. Future crops in surrounding areas probably would follow the same pattern except for possible future increases in sorghum production.

Table 11.2. Proportional Crop Production in 1968 for 200-square-mile Area Surrounding Lyons

Crop	Area Harvested (Acres)	%	Yield Rate[a,b] (kg/ha)	Total Production (tons[c])
Wheat	49,306	73.2	1,934	34,803
Sorghum	12,077	17.9		
Grain	(11,080)	(16.5)	2,176	8,802
Silage	(637)	(0.9)	24,453	6,325
Corn	679	1.0		
Grain	(277)	(0.4)	5,271	533
Silage	(360)	(0.5)	24,700	3,606
Oats	116	0.2	1,074	46
Barley	75	0.1	2,100	57
Rye	158	0.2	1,128	65
Hay	4,820	7.2	4,940	9,626
Alfalfa	(3,740)	(5.6)	5,434	8,239
Wild	(609)	(0.9)	2,717	666
Seeds (alfalfa, red clover, sweet clover)	507	0.5		21
Soybeans	94	0.1	1,445	27
Pasture land (1964 census)	32,660			

[a]Weight conversion factor: 1 kg/ha = 0.028 bu/acre at 32 lb; = 0.019 bu/acre at 48 lb; = 0.016 bu/acre at 56 lb; and = 0.015 bu/acre at 60 lb.

[b]Grain weight per bushel: wheat, 60 lb; barley, 48 lb; oats, 32 lb; rye, corn, sorghum, and soybeans, 56 lb.

[c]Ton = 2000 lb avoirdupois. Production data summarized from ref. 3.

11.2.3 Livestock

Approximately 14,000 cattle and 3,900 hogs are located in a 200-square-mile area around Lyons. Small numbers of sheep, lambs, and chickens are also raised in this area (Table 11.3). Periodic monitoring of milk samples from 530 milk cows in this vicinity (pro-rata calculation) may be required because the grass-cow-milk-man pathway is an important mode of critical radionuclide ingestion by man. Rural situations where total milk intake is from local sources will require special attention. Otherwise, monitoring of milk from the Wichita milkshed collections probably would be continued according to planned Public Health Department schedules and would satisfy requirements for identifying incipient nuclide accumulation in milk products.

Table 11.3. Livestock on Farms in Rice County and Proportional Number for 200 Square-Mile-Area (Jan. 1968)[a]

	Milk Cows	Other Cattle	All Cattle	Hogs	All Sheep and Lambs	Chickens
Rice County	1,900	49,100	51,000	14,000	3,000	11,000
Proportional	530	13,700	14,230	3,900	830	3,050

[a]Livestock data summarized from ref. 3.

11.2.4 Permanent Vegetation

Ecologists in Kansas strongly recommended that native prairie should be established on the Repository site. Specific advantages of native vegetation include enhanced ecosystem stability, reduced erosion, minimal dispersal of radioactive materials, economical long-term maintenance, control of management influences, and educational-cultural benefits. Revegetation with native flora would change the existing physiognomy, biotic equilibria, and microenvironments. Thus, the projected native grassland ecosystem, at least three to ten years in the future, would exhibit a character greatly different from the present, intensively managed agroecosystems.

Reseeding will result in a 90% native grass community within three to five years. During the next ten years, other native forbs would become established as the vegetation gradually succeeds to that of native prairie.

The inherent stability of such a community would be extremely valuable for assessing real or alleged impacts of the Repository operation on the environment. The terminal species composition of the reseeded grassland will include many individuals which were reported growing along the Santa Fe and Missouri-Pacific railroad right-of-ways. These areas could also serve as a seed source for exotic prairie species that normally would not be present in commercial seed.

11.2.5 Wildlife

More than 1000 taxa were identified in the 1970 ecological surveys as being associated with either local agroecosystems, aquatic environments, or projected grassland ecosystems. Understandably, the inventory is incomplete (Table 11.4), but it suggests the most representative flora and fauna which would be expected in a native terrestrial ecosystem. The more conspicuous animals would be herbivorous birds (bobwhite, pheasant, dove, meadowlark), carnivorous birds (hawk, owl, kingbird, sparrow), herbivorous mammals (rabbit, mouse, vole, ground squirrel, prairie-dog [introduced]), and insects (beetles and wasps). Later introduction of a large animal grazer (i.e., buffalo) would be a stabilizing factor in the surface grassland ecosystem.

11.2.6 Site Management

Reversion to a native grassland community will simplify future management because of the natural interactions among soil-grass-consumer-decomposer components. A managed herd of large grazers would remove excess vegetation, thereby striking a balance between grass growth and harvest. Occasional hay cutting, harvest, or burning management may be necessary during developmental phases of the operation.

11.3 Ecological Impact

Isolation of radioactive wastes in a salt formation assuredly removes hazardous materials from the environment. The secure integrity and projected infinitesimally small risks notwithstanding, effects on ecology or human health and safety could accrue either from an accumulation of low-intensity chronic actions or from direct acute impacts resulting from an accident.

Table 11.4. Expected Minimum Numbers of Plants and Animals at Repository Site

Organism	Taxonomic Level	Number of Taxa
Higher plants (woody, grass, forbs)	Species	90+
Lower plants (bacteria, actinomycetes, fungi)	Genus	14+
Mammals (wild, domestic)	Species	52
Birds (summer, winter, transient)	Species	229
Reptiles and Amphibians (aquatic and terrestrial)	Species	36+
Fish	Species	20
Insects (aquatic and terrestrial)	Order, family and species	600+
Total		1,041+

Rational judgment concerning real or alleged ecological impacts is possible, provided a well-designed data acquisition program parallels facility development and operation. The 1970 ecology surveys only indeterminately allude to possible effects, and additional research on ecological processes is essential to improve our understanding of radionuclide movement in the Lyons vicinity. In spite of voids in the data base, information from the surveys and literature sources has allowed us to describe, at least partially, the behavior of ^{90}Sr, which could conceivably have long-term effects on man and his ecosystem. Similarly, the energy balance for grassland and heat flux for soil were evaluated from calculations based on average data from records maintained by the Agriculture Experiment Station.

11.3.1 Ecosystem Character

Reversion from a cultivated state to a native condition would greatly increase the number and diversity of species. Over 1000 taxa of a prospective grassland community (Table 11.4) would fill nearly all niches, and the resulting distribution of many species among producer-consumer-decomposer trophic levels would contribute to a balanced and stable ecosystem. Such a taxonomic and trophic mixture also would ensure ecological diversity of the ecosystem. A native community would enhance long-term aesthetic and recreational benefits, and, more importantly, would provide a frame of reference for examining long-term environmental effects of Repository operations in perpetuity.

11.3.2 Radioecological Processes

An infinite number of pathways would exist for radionuclide movement in an ecosystem containing more than 1000 interacting species. Such a situation is obviously too complex to evaluate in detail; alternatively, however, the potential hazard to humans and other organisms can be identified from most probable pathways of radionuclide movement through ecosystems and ultimately to man (Figure 11.1). Trophic level concentration factors[4] will also be useful guidelines for initial identification of potential radioecological problems. Following initial deposition, most radionuclides are dispersed in terrestrial environments, but some are

ORNL - DWG 71-686

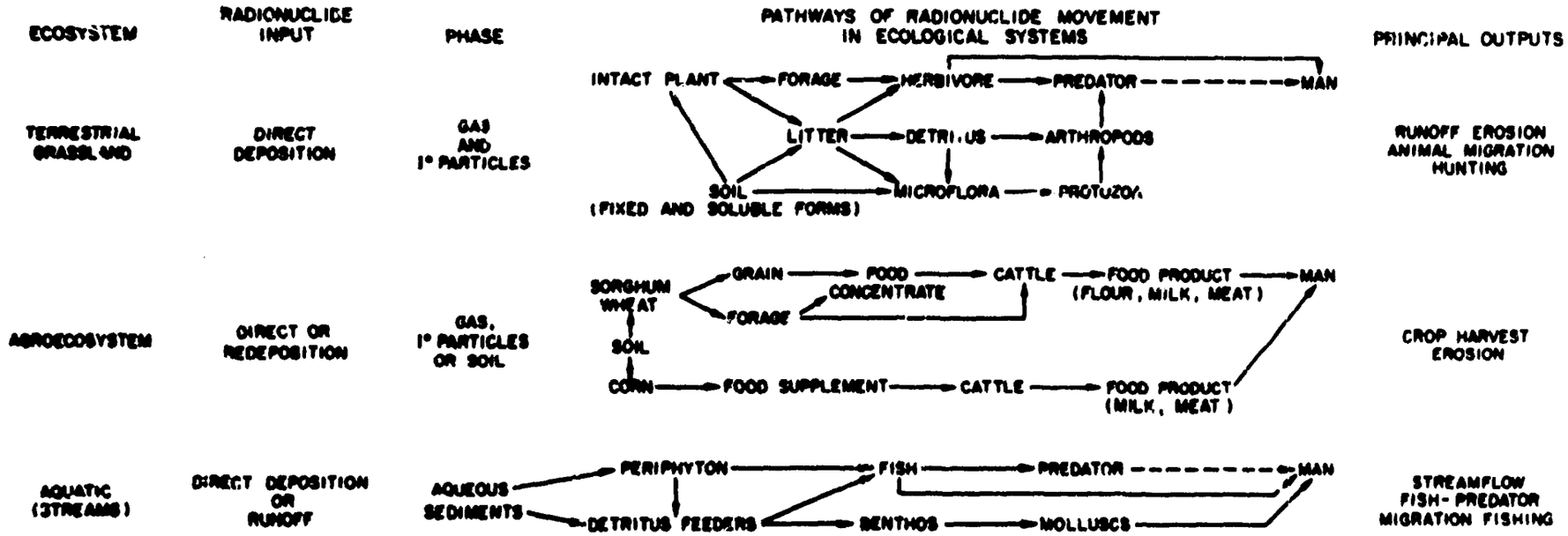

Fig. 11.1. Major Ecosystems and Pathways Responsible for Radionuclide Movement to Man.

concentrated in aquatic systems. Magnitudes of movement can be predicted from compartmental[5] or specific activity models,[4,6] provided that basic data on metabolic, population, environmental, and transport function parameters exist and assuming that information on radionuclide and mineral element behavior in these components is available.

11.3.3 Models of Radionuclide Movement

Proximity to the source of radioactivity will determine initial concentrations in different environments. Chronic, low-level releases will be dispersed over the environs, with the air concentration diminishing as a function of distance from the center of operations. Nearby ecosystems would receive the highest levels of radioactivity, and distant ecosystems considerably less. Radioecological analyses, therefore, will focus on the proposed on-site grassland and adjacent agroecosystems, with distant landscape and aquatic systems commanding a lower priority.

The behavior of principal fission products can be approximated from models of commodity flow in an ecosystem.[5] For example, a framework for describing the important components and transfers among the soil-plant segments is depicted in a simplified systems diagram (Fig. 11.2). If the input, transfer rates, and initial conditions are given, the distribution of a nuclide among different plant and soil components can be predicted as a function of time after initial deposition. This procedure will apply to both chronic and acute inputs, provided transfer parameters are based on "pulse" experimental data. The model can estimate various secondary source terms (foliage, root, litter), which, in turn, serve as potential inputs to ecological and agricultural food chains. While this example describes radiostrontium dynamics in the grass-litter-soil component, similar modeling techniques can be used to illustrate radionuclide movement or concentration for other organisms and pathways of the ecosystem. Specific activity models[4] are most applicable for predicting radionuclide concentrations in aquatic systems, provided sufficient information exists on the stable chemistry of the environments and organisms.

ORNL-DWG 70-15248

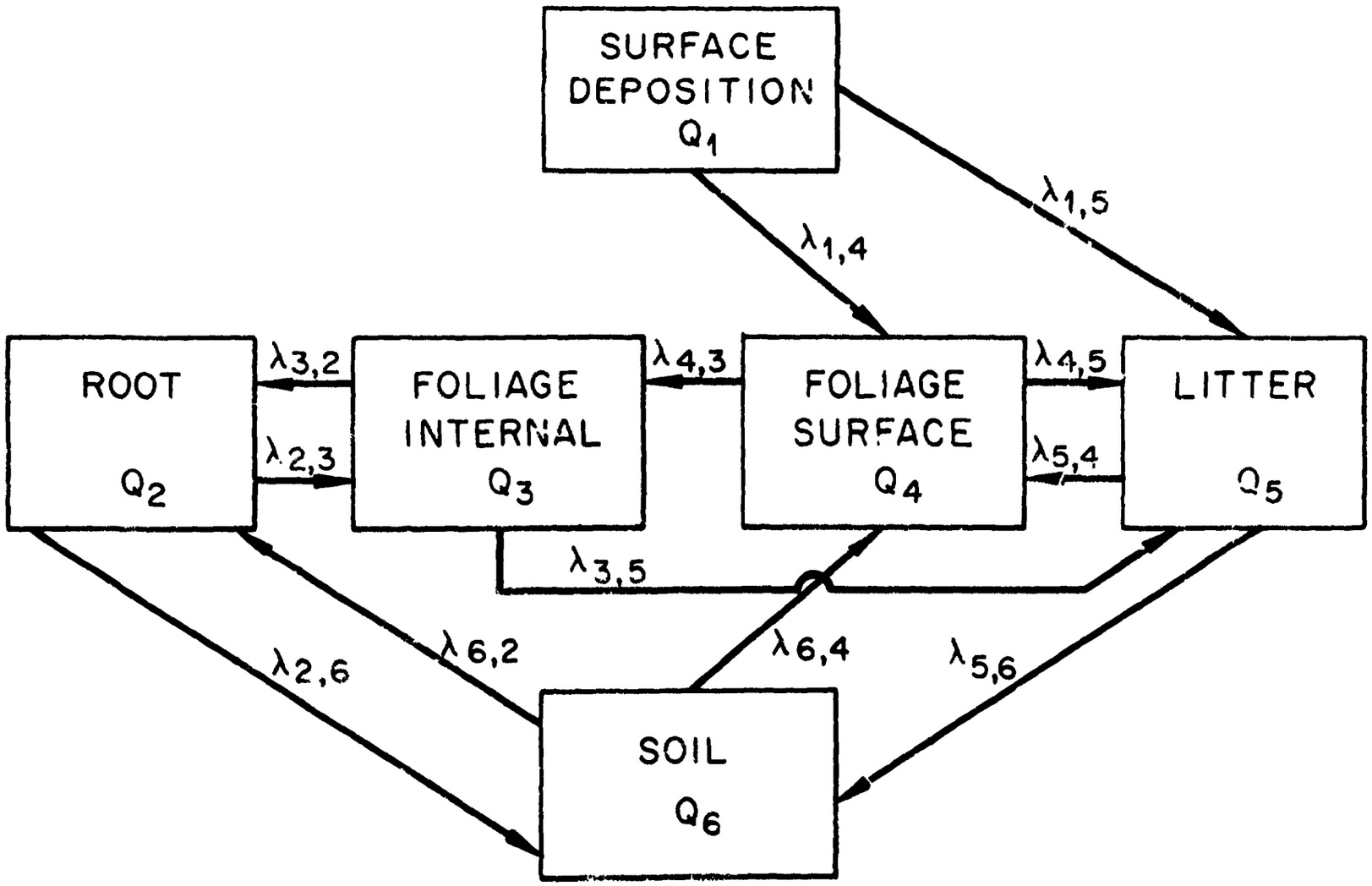

Fig. 11.2. Pathways of ^{90}Sr Movement Among Plant-Soil Segments of a Grassland Ecosystem.

An important advantage of the compartmental modeling approach is that the basic design of the flow model can apply to evaluations of different contaminants; thus base-line ecological data can be used for several specific nuclide assessments. For purposes of preliminary hazard assessment, and as an illustration of how the technique can predict distribution of a contaminant throughout the system, the dynamics of ^{90}Sr is evaluated for a generalized grassland ecosystem. Since this nuclide will constitute about one-third of the routine fission-product release, and it possesses a relatively high health-hazard potential, it is of major interest in this case. Compartmental variables and transfer parameters are defined and enumerated in Tables 11.5 and 11.6, respectively, for grass-litter-soil segments of an "average" grassland. Attendant assumptions and calculations of transfer functions are given in Table 11.7. Examination of these derivations will show that oversimplification was often necessary because the essential data for assessing radiostrontium movement in the environment were not available.

Table 11.5. Initial Conditions of Compartments

Compartment	Definition	Initial Condition (pCi/m^2)
Q_1	Surface deposition	0.86
Q_2	Root	6
Q_3	Internal portion of foliage	30
Q_4	Foliage surface	120
Q_5	Litter	150
Q_6	Soil	270,000

For the grass-soil segments of the ecosystem, based on various flow rates, the model partitions the nuclide among different foodbase components. In turn, these components can serve as source terms for herbivorous and detritus-feeding organisms. Determination of ^{90}Sr and other nuclide movement, dispersion, or concentration through principal trophic levels and food chains are assessment tasks that remain to be accomplished. When

Table 11.6. Fractional Transfer for Flows Among Compartments

Flow	Definition	Fractional Transfer (day^{-1})
$\lambda_{1,4}$	Deposition on foliage	0.15
$\lambda_{1,5}$	Deposition on litter	0.85
$\lambda_{4,3}$	Direct uptake by foliage	0.005
$\lambda_{4,5}$	Fraction lost from foliage surface to litter	0.017
$\lambda_{3,5}$	Loss due to defoliation	0.0055
$\lambda_{3,2}$	Translocation from leaf to root	0.00006
$\lambda_{5,4}$	Fraction moved back to foliage as dust from litter	0.000027
$\lambda_{5,6}$	Fraction lost from litter to soil (mineralization)	0.005
$\lambda_{6,4}$	Fraction redeposited on foliage as dust from soil	0.000001
$\lambda_{6,2}$	Fraction taken up by roots	0.0000045
$\lambda_{2,3}$	Translocation from root to leaf	0.35
$\lambda_{2,6}$	Fraction transferred back to soil	0.00069

Table 11.7. Calculations for Transfer Functions for ^{90}Sr Movement in a Generalized Grassland Ecosystem

Flow	Calculation
$\lambda_{1,4}$	Deposition on foliage (0.15), inferred from Krieger et al.[7] results on permanent grass pasture.
$\lambda_{1,5}$	Deposition on litter, 1.0 - 0.15 = 0.85.
$\lambda_{4,3}$	Internal uptake from surface deposition (0.005), inferred from the maximum rate of translocation found for foliar-applied ^{85}Sr in corn.[8]
$\lambda_{4,5}$	Thirty days were required for radioactivity of leaves to decrease by a factor of 2 when ^{85}Sr was deposited on foliage permanent grass pasture.[9] Daily loss would be 0.017 (0.5 x 1/30), assuming a linear weathering process.
$\lambda_{3,5}$	Radionuclides in leaves are lost as litter at the time of defoliation. Hence maximum daily transfer function would be 1/180 = 0.0055 (180 days/year). Daily foliar attrition is assumed rather than end of season pulse.
$\lambda_{3,2}$	Translocation of ^{85}Sr from leaf to root has been reported to be no more than 0.006% of total applied on corn leaves.[8] Hence daily transfer function would be 0.00006.
$\lambda_{5,4}$	Assuming 1%/year moves from litter to foliage as dust, daily transfer would be 0.01 x 1/360 = 0.000027.
$\lambda_{5,6}$	The loss rate from litter to soil was 0.01/day for subhumid conditions.[10] Slower decomposition and mineral turnover would be expected in drier Kansas grassland; hence a lower loss rate function was assumed (0.01 x 1/2 = 0.005).
$\lambda_{6,4}$	Radionuclides on the ground surface are expected to be redeposited as dust. No experimental data are available on the rate of this movement; however, it would be less than that from soil to litter, possibly 1/25 of redeposition from litter to foliage ($\lambda_{5,4}$). Daily transfer would be 0.000027 x 1/25 = 0.000001.
$\lambda_{6,2}$	Radioactivity surveillance data from Kansas showed that grass foliage had 0.00031% (0.0000031) of radioactivity in soil (Table 11.5). Calculated daily uptake by grass from soil was 0.0000058 (ref. 7). Hence, daily uptake rate from soil was based on average of these values or 0.0000045.
$\lambda_{2,3}$	For tomato plants grown in a 1 ppm strontium nutrient solution, 39% of root strontium moved to leaves in 4 days.[11] Root and solution concentrations were roughly equivalent; thus total root uptake was estimated as 1.0 + 0.39 = 1.39 units, and daily root to shoot transfer would be 1.39 x 0.25 = 0.35.
$\lambda_{2,6}$	Annual turnover of grass roots to soil has been reported to be 25% of total dry weight.[12] Hence daily turnover of roots and minerals would be $0.25 \times \frac{1}{360} = 6.9 \times 10^{-4} \times day^{-1}$.

sufficient quantitative data become available from the site or ecosystems adjacent to the Repository, it will be possible to estimate concentration levels and their attendant hazards more precisely.

Provisional estimates of dynamic distribution of a chronic ^{90}Sr input throughout the grassland system were determined using the transfer and compartmental parameters of Tables 11.6 and 11.7. Change in state of a compartment is a function of inflows and outflows, each of which specifies a term in a difference equation. By using linear transfer functions, which are actually oversimplifications of nuclide movement between principal components, the behavior of ^{90}Sr is given for five compartments from the solution of five differential equations. Program CSS[13] was used to facilitate the large number of calculations for various time intervals.

Chronic input was calculated from estimated releases and deposition velocities (Table 11.8) which gave a daily deposition to the grassland ecosystem of 0.86 pCi/m^2. The redistribution of ^{90}Sr throughout the grass-soil components as a function of time is graphed in Fig. 11.3. The greatest increase in radioactivity occurs in the litter compartment (i.e., the activity nearly triples in two to three years). Relative to background levels, the concentration decreases slightly for roots and increases by 50% for foliage as new equilibria become established. A decrease in soil radioactivity is predicted from this simulation (Table 11.9) because the total input (860 and 8600 pCi/m^2 for 1000 and 10,000 days) initially was an insignificant fraction of the background level after 2.5 and 25 years, respectively, and the decrease in radiostrontium from physical decay exceeds new deposition. Reequilibrium in the biological components occurs within 1 to 2 years. The state conditions of these components may vary somewhat, depending on the verity of the transfer coefficients, but probably by less than a factor of 3 to 5. The dynamic character of the ecosystem precludes significant ^{90}Sr accumulation or concentration in the plant-soil components, and additional analyses will be done to determine if a similar condition would exist for faunal components.

Major pathways of radionuclide redistribution to other organisms are indicated for the grassland ecosystem (Fig. 11.1). Some of these involve transfers through herbivore, omnivore, and carnivore trophic levels.

Table 11.8. Calculations for Initial Conditions of ^{90}Sr in Compartments in Fig. 11.2

Compartment	Initial Condition (pCi/m^2)	Calculation
Q_1 (surface deposition)	0.86	Radiostrontium deposition to the on-site terrestrial landscape was calculated from data in ref. 14, Table 10-1, where concentration in the atmosphere is given as $\sim 1 \times 10^{-14}$ Ci/m^3. This was assumed to be a steady-state value where ground deposition is balanced by input from mine exhaust. A deposition velocity[15] of 10^{-3} m/sec was used to estimate rate of movement from atmosphere to surface features. Thus, $(1 \times 10^{-14}$ $Ci/m^3) \times (10^{-3}$ m/sec) = 1×10^{-17} Ci m^{-2} sec^{-1} or 8.64×10^{-13} Ci m^{-2} day^{-1}.
Q_2 (root)	6.0	Guliakin and Yudintseva's[16] water-culture data show that about 1/25 of total ^{89}Sr absorbed by wheat remained in roots. Since 150 pCi/m^2 was found for foliage in Butler County,[17] radioactivity in roots would be 6 pCi/m^2.
Q_3 (internal foliage)	30.0	Radiostrontium content of foliage samples from Butler County[17] was 485 pCi/kg. Estimating 300 g m^{-2} $year^{-1}$ dry matter production for grassland, the content in grass would be $485 \times 0.3 \approx 150$ pCi/m^2. From field fallout studies, it was estimated that 20% of grass radiostrontium was from root uptake, and 80% was from deposition;[7] then $Q_3 = 150 \times 0.20 = 30$ pCi/m^2 and $Q_4 = 150 \times 0.80 = 120$ pCi/m^2.
Q_4 (external foliage)	120.0	
Q_5 (litter)	150.0	Equal amounts of radioactivity are assumed to be present in litter as in foliage in grassland. Litter accumulation seldom exceeds annual production because of rapid decomposition.
Q_6 (soil)	270,000	Average of two soil samples from Butler County.

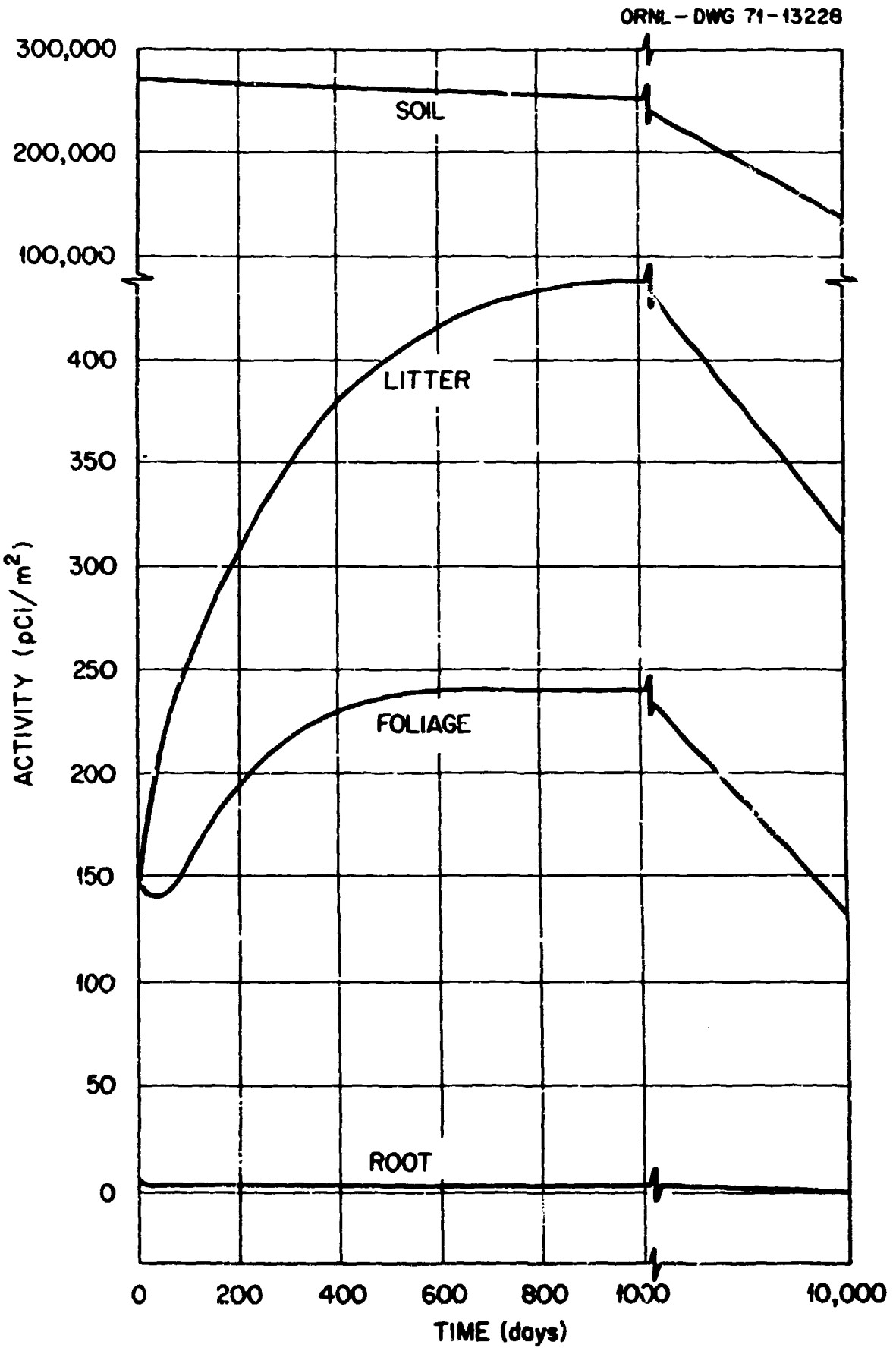

Fig. 11.3. Change in ^{90}Sr Concentration for Plant-Soil Segment of a Grassland Ecosys. m Following Chronic Deposition of 0.86 pCi m^{-2} day^{-1}. Values corrected for decay. Note different scale for soil compartment and for 10^3 to 10^4 time interval. Decrease was nearly linear from 10^3 to 10^4 days.

Table 11.9. Calculated Concentrations of ^{90}Sr in Each Compartment Following Deposition of 0.86 pCi m^{-2} day^{-1} for Selected Time Intervals

(Values from Fig. 11.3)

	(pCi/m^2)				
	Initial	10 days	100 days	1000 days	10,000 days
Foliage	150	141	156	238	133
Root	6	10	12	11	6
Litter	150	170	259	438	316
Soil	270,000	270,000	268,000	252,000	135,000
Total deposition[a]	9	9	86	860	8,600

[a]Values not corrected for decay.

Several pathways may lead to man (grass-deer, rabbit-man, pheasant-man), although food consumption habits would provide limited hazard to humans from ingestion. Except for the milk pathway, most radionuclides would be dispersed rather than concentrated as they move through the terrestrial ecosystem because fission-product concentration factors are usually less than 1 for many terrestrial food chains according to Reichle et al.[4] Certain tissues (thyroid, bone, milk) may concentrate specific fission products (I, Sr) to higher levels than whole-body averages, but, in most cases, accumulation will not exceed that of the food base by more than a factor of 3 to 5. Provisionally then, one would not expect ^{90}Sr levels of native animal populations to be more than three to five times the level indicated for plant parts (Table 11.9). For such conclusions, however, one must recognize that faunal population densities, food habits, and feeding ranges also influence concentration magnitudes, and it is inappropriate to estimate the nuclide dynamics of these components in the absence of population, biomass, and food-web data for the herbivore-omnivore-carnivore components of the ecosystem.

Other pathways of radionuclide movement are identified for major ecosystems in the vicinity of the proposed site (Fig. 11.1). Analysis of the dynamics of ^{90}Sr in the plant-soil components of the grassland ecosystem showed only small increases in biotic components relative to existing residual fallout. Additionally, the extent of potential hazards should be evaluated for adjacent agroecosystems, particularly for the aquatic ecosystems. While the initial concentration of radioactivity deposited in aquatic environments would be substantially less than that closer to the Repository site, potential hazards should be examined because aquatic organisms characteristically concentrate radionuclides by several orders of magnitude. Additional stream chemical (including stable and radioactive elements) data, coupled with probabilistic models of population dynamics, will be required to determine the extent of radiological hazard associated with aquatic systems. Although subject to considerably smaller radioactivity inputs, pathways of movement in the agroecosystem should be examined in greater detail because this system provides the most direct route for entry of nuclides via human ingestion. Data on domestic animal

management and local food consumption will be required in order to determine if a peculiar hazard may exist in the vicinity of the Repository.

11.3.4 Acute Situations

Ecosystem models of radionuclide dynamics will serve dual roles: (1) assessment of long-term effects from chronic releases (discussed above), and (2) evaluation of the fate of contaminants in the event of an accidental release. The same modeling efforts can predict the extent of contamination equally well for both chronic and acute events, provided model parameters are derived from acute input data. The same ecosystem structural and process information would apply in both situations. Data on ecosystem processes and nuclide behavior should be readily available for rational assessment of possible consequences in an emergency situation. Judgments for contingency actions, then, could be based on the best available information on environmental factors coupled with predictive models and computer simulations, rather than on assumption and speculation.

11.3.5 Thermal Effects

The dissipation of waste heat from high-level wastes may increase the temperature of the soil surface. However, a heat flux of 10 times the geothermal rate is not expected to change the surface temperature more than a fraction of a degree Fahrenheit – a negligible amount when compared with observed seasonal variations (Fig. 11.4). Daily bidirectional radiation flux in the soil surface ranges from 0 to 0.1 cal/cm^2, which is at least 1000 times greater than the predicted heat flux from waste deposits. As compared with calculations in radiant energy balance and resultant soil heat flux, the increases in the surface temperature from waste heat will be small or negligible.

Specific low-intensity effects on energy balance components include the following:

(1) Net radiation (Rn) would decrease slightly, possibly 0.01 langley/min, because outgoing long-wave radiation is proportional to the fourth power of the surface temperature. (2) Evapotranspiration (E) could be affected by a 10% increase in the

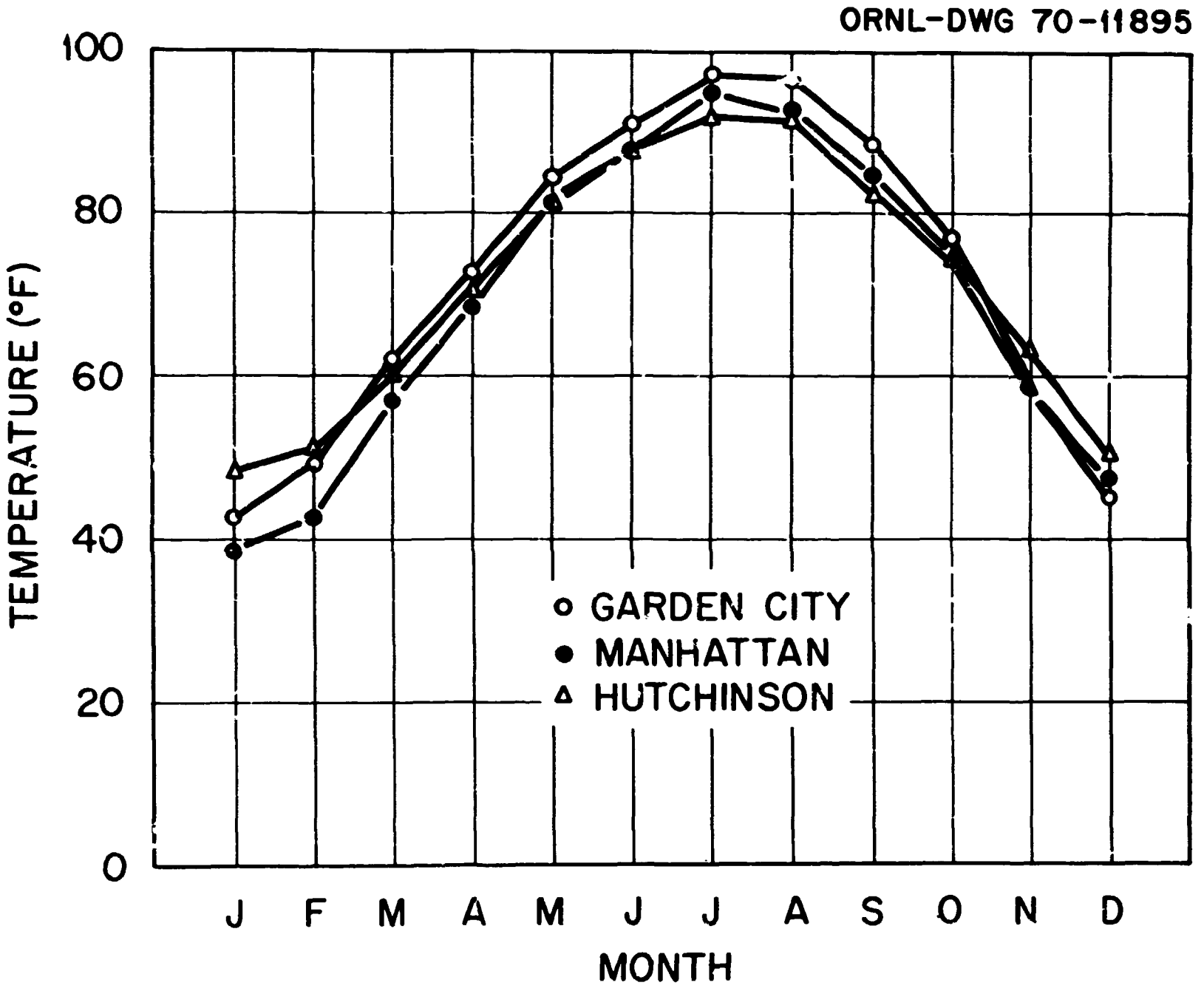

Fig. 11.4. Maximum Soil Temperature (Average for Nine Years of Data).

vapor pressure gradient, one factor of the evaporation equation. Other complex processes affect E, but not all of them are directly influenced by temperature.

(3) Sensible heat fluxes of air and soil also are dependent on several factors (e.g., water, eddy diffusivity, conductance, soil texture, and organic content), and specific effects of additional heat are not easily identified.

Some biological processes that may be affected by subtle changes in soil temperature include the following:

(1) Seed germination and seedling development could be advanced by only slightly higher temperatures, but death of the emerging plant could also result if the event were not synchronized with other facets of the environment.

(2) Insect life cycles and phenology conceivably could be affected because their reproductive responses are triggered by temperature-controlled metabolic development.

(3) Increased metabolism from slightly higher temperatures of plant storage organs could lead to carbohydrate deficits and decreased vigor.

(4) With increased geothermal fluxes as the driving force, a slight redistribution of soil moisture could occur, vertically as well as horizontally. This phenomenon could influence water reserves in the subsoil on which deep-rooted plants depend during periods of drought stress.

The fact that physical and biotic effects could occur from an increased geothermal flux does not necessarily mean that devastating consequences will result. The identification of reasonable impacts should be followed by more detailed analysis of those manifestations which substantively could be detrimental over centuries of biotic exposure to such a heat source. Experience concerning low-level effects from chronic heat sources is very limited, however.

11.4 Meteorology

Weather history was evaluated in order to identify normal, as well as extreme, climatic conditions that must be considered in the design and operation of a Repository. Wind summaries will be used as provisional input to hazard assessment models which predict atmospheric dispersion from either normal or accidental releases. Approximate magnitudes of principal meteorological parameters were identified from regional data summarizations. Estimates of regional meteorological patterns will aid the design of preoperational, on-site meteorological measurements. Average and extreme climatological data provided estimates of microclimatic conditions, which, in turn, provided guidelines for other field and laboratory studies of ecological processes. Records of 14 weather bureau stations in central Kansas[18-28] (Table 11.10, Fig. 11.5[29]) were examined to determine average, variance, and extremes because only precipitation data have been collected at Lyons.

11.4.1 Precipitation[18-21,26,30,31]

Thirty years of data on monthly mean precipitation at Lyons (see dotted line in Fig. 11.6) were compared with the average and variance of the 11 nearby stations. Summer maxima and winter minima characterize the seasonal rainfall distribution in central Kansas. The trend at Lyons follows closely the seasonal pattern of the 11-station average, exceeding the 95% confidence interval only during July, August, September, and December (Fig. 11.6). Analysis of variance, which considers year-to-year variation of all stations for 30 years, showed a significant difference between Lyons and the 11-station average only in September, however.

Annual precipitation at Lyons was 25.9 in., approximately midpoint between the high (31.0 - Wichita) and the low (Dodge City - 21.0). Grouping the stations according to Duncan's multiple range test ($P = 0.05$) showed three distinct aggregations reflecting similarities in total rainfall. The most inclusive grouping (Table 11.11) contained 10 stations, excluding Wichita and Dodge City. This implies that, relative to rainfall, the weather phenomena at 10 of 12 stations do not deviate significantly from

Table 11.10. Locations and General Characteristics of Weather Stations Used for Climatological Summaries

Station[a]	County	Latitude (N)	Longitude (W)	Elevation (ft)	Reference
Concordia WB City	Cloud	39° 34'	97° 40'	1375	18-22
Dodge City WB AP	Ford	37° 46'	99° 58'	2594	18-20, 22, 23
Garden City Exp. Station	Fenney	37° 59'	100° 49'	2840	20
Geneseo	Rice	38° 31'	98° 09'	1755	18-20
Great Bend	Great Bend	38° 22'	98° 46'	1940	18-20, 24
Hutchinson Exp. Field[b]	Reno	37° 56'	98° 02'	1570	18-20, 25
Kanopolis Dam	Ellsworth	38° 36'	97° 57'	1492	18-20
Lyons	Rice	38° 19'	98° 12'	1696	18-20, 26
Manhattan Agronomy Farm	Riley	39° 12'	96° 36'	1106	20
McPherson	McPherson	38° 20'	97° 40'	1495	18-20
Russell FAA AP	Russell	38° 52'	98° 49'	1864	18-20
Salina FAA AP	Salina	38° 49'	97° 34'	1271	18-20, 27
Sterling	Rice	38° 13'	98° 12'	1636	18-20
Wichita WB AP	Sedgwick	37° 39'	97° 25'	1321	18-20, 28

[a]AP-Airport; FAA-Federal Aviation Administration; WB-Weather Bureau.

[b]Air temperature data from Hutchinson KWBW were used when those from experimental field were not available.

ORNL-DWG 70-8225R

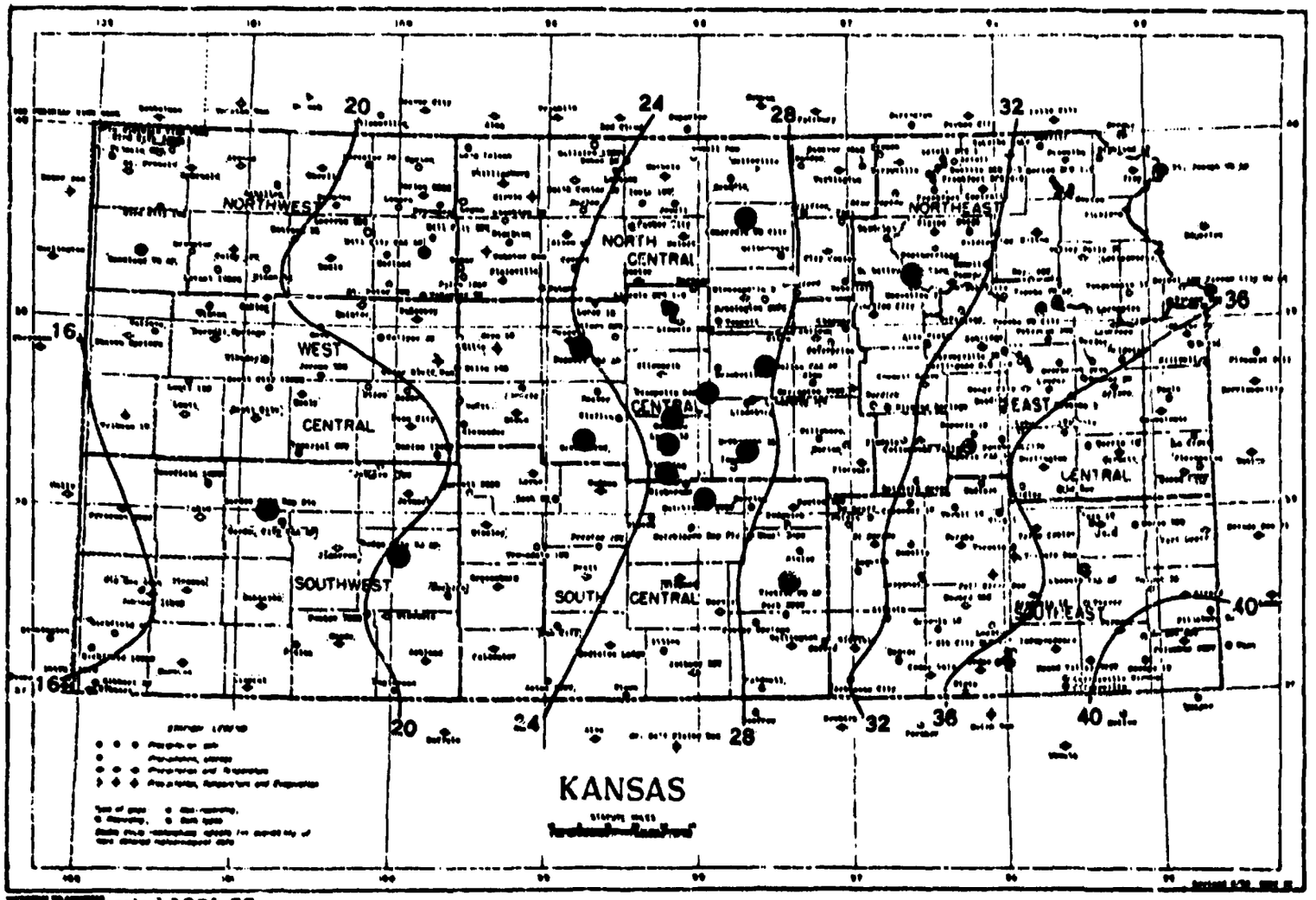

Based on period 1931-55

Isolines are drawn through points of approximately equal value. Caution should be used in interpolating on these maps.

Fig. 11.5. Mean Annual Precipitation (in Inches) Gradient Across State of Kansas. Locations of stations used in meteorological summaries indicated with black dots. Map from ref. 29.

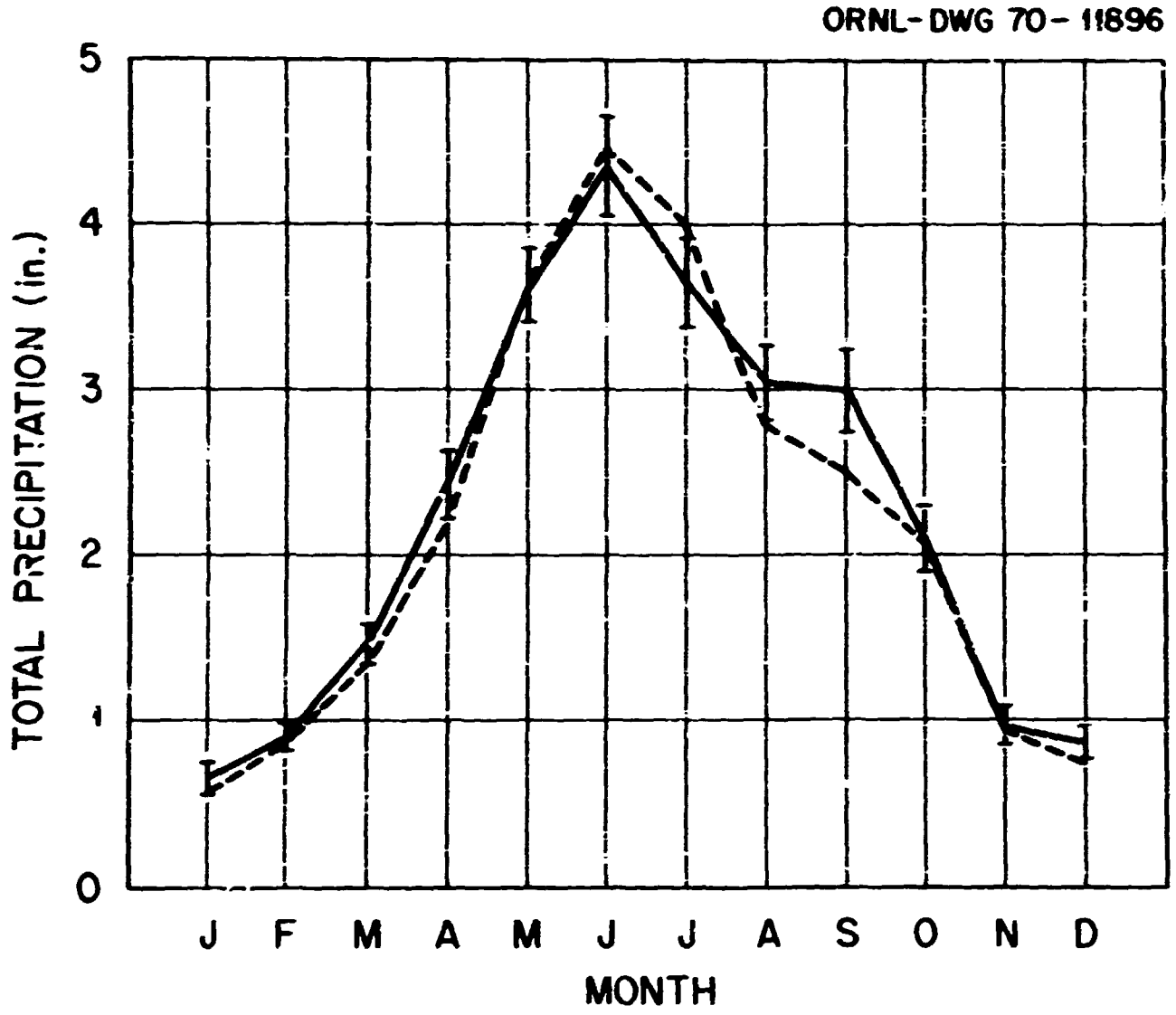

Fig. 11.6. Monthly Mean Precipitation for 11 Stations, Including 95% Confidence Intervals, and Monthly Mean Precipitation for Lyons (Average of 30 Years of Data).

Table 11.11. Duncan's Grouping (0.05) of Stations According to Annual Total Precipitation[a]

Station	Annual Total Precipitation (in.)	Grouping[b]
Wichita	30.95	
McPherson	29.31	
Hutchinson	29.00	
Salina	28.34	
Concordia	27.24	
Geneseo	27.14	
Russell	26.77	
Lyons	25.94	
Kanopolis Dam	25.61	
Sterling	25.46	
Great Bend	25.43	
Dodge City	21.02	

[a]Average for 30 years of data.

[b]Any two means not included within the same bracket are significantly different at 0.05 level.

regional average conditions; thus climatological data from these 10 can provisionally be used to infer a general rainfall (and possibly a climatic) regime for Lyons.

Precipitation extremes are evaluated because of their relationship to storms, surface runoff, and lowland flooding. Maximum monthly precipitation at Lyons was 14.1 in. (June 1965); however, hourly or daily rates for this extreme at Lyons are unknown. Daily maxima in central Kansas have been as high as 8 in. (Wichita, 1911, see Table 11.12), but such events are highly localized because a given extreme seldom has been registered at more than one station. The frequency of recurrence of different rainfall intensities for Rice County is given in Table 11.13. One could expect a rainfall event of the magnitude of 3 in./hr or 5.5 in./24 hr intensity once during the next 25 years. Catastrophic flooding within the confines of the Repository areas would not be expected from these rainfall intensities, although local experience should be consulted on this subject. We should have no difficulty in circumventing hazards from extensive rainfall in the Repository design.

11.4.2 Temperature[18-21,30,31]

Ambient-temperature data were not available for the Lyons site; therefore, 30-year data from the 11 nearby stations were averaged to estimate this parameter for the Repository. Monthly and annual averages, accompanied by 95% confidence limits, are given in Table 11.14. Monthly means ranged from a low of 29°F (January) to a high of 80°F (July), and the annual average was 55°F for all stations. Air temperatures were more uniform (annual means range from 56.6°F at Wichita to 53.7°F at Concordia) and exhibited less variance than precipitation. Analysis of variance of monthly means showed statistically significant differences among stations for five months (November-February, and April), and five different groupings of annual means were determined from Duncan's multiple range test (Table 11.15). Both Sterling and Geneseo, which are Rice County stations, appear in one of the groupings; therefore, averaging their data would provide the best temperature estimate for Lyons. The annual average of 55.2°F for these stations agreed remarkably well with the grand average (55.3°F) for 11 stations (see Table 11.14).

Table 11.12. Extremes of Temperature and Precipitation, Including Snowfall, at Four Stations

Station	Highest[a] Temperature (°F)	Lowest[b] Temperature (°F)	Maximum Monthly Precipitation		Maximum Rainfall		Maximum Snowfall	
			Amount (in.)	Date	Rate (in./hr)	Date	Rate (in./24 hr)	Date
Concordia[c]	116	-25			6.46	May 1950	17.2	March 1924
Dodge City[d]	109	-26	12.82	May 1881	6.03	June 1899	17.5	March 1922
Wichita[e]	114	-22	14.43	June 1923	7.99	Sept. 1911		
McPherson[f]	117	-27			4.52	July 1897	20.0	Feb. 1912

[a]Maximum temperature for each station occurred in August 1936.

[b]Minimum temperature for each station occurred in February 1899.

[c]Data taken from ref. 21.

[d]Data taken from ref. 31.

[e]Data taken from ref. 30.

[f]Data taken from ref. 32.

Table 11.13. Frequency of Specified Amounts of Rainfall During Stated Time Intervals in Rice County[a]

Length of Return Period (years)	Total Rainfall (in.) for Various Time Intervals						
	30 min	1 hr	2 hr	3 hr	6 hr	12 hr	24 hr
1	1.1	1.3	1.5	1.6	1.9	2.0	2.3
2	1.6	1.6	1.9	2.0	2.4	2.6	3.0
5	1.7	2.1	2.5	2.7	3.2	3.5	4.0
10	2.0	2.4	2.9	3.1	3.7	4.2	4.6
25	2.3	2.9	3.4	3.6	4.4	4.9	5.5
50	2.7	3.3	3.9	4.2	5.0	5.7	6.2
100	3.0	3.7	4.4	4.7	5.7	6.4	7.0

[a]Frequency table taken from ref. 26.

Note: This table shows the expected frequency of rainfall events of a specified duration for return periods ranging from 1 to 100 years. For example, in a 24-hr period, 2.3 in. or more of rainfall may be expected once a year; 4.6 in. or more, once in 10 years; and 7.0 in. or more, once in 100 years.

Table 11.14. Monthly Mean Air Temperature of 11 Stations, Including 95% Confidence Limits

Month	Mean Ambient Temperature (°F)[a]	95% Confidence Limits
January	29.4	±0.6
February	34.4	±0.6
March	41.7	±0.7
April	54.7	±0.5
May	64.8	±0.4
June	74.8	±0.4
July	80.2	±0.4
August	78.8	±0.4
September	69.6	±0.4
October	48.8	±0.4
November	43.3	±0.4
December	33.0	±0.5
Annual	55.3	±0.2

[a]Based on 235 to 239 observations per monthly value. Data taken from refs. 18, 19, 33.

Table 11.15. Duncan's Grouping (0.05) of Stations According to Annual Mean Temperature

Station	Annual Mean Temperature (°F)	Grouping
Wichita	56.6	
Hutchinson	56.2	
McPherson	56.1	
Great Bend	56.0	
Sterling	55.6	
Salina	55.1	
Dodge City	55.0	
Geneseo	54.8	
Kanopolis Dam	54.3	
Russell	54.0	
Concordia	53.7	

[a]Any two means not included within the same bracket are significantly different at 0.05 level.

Material transfer and storage operations will be designed to withstand temperature extremes of both summer and winter seasons. Ambient temperatures greater than 100°F occur an average of 15 days per year in central Kansas. Extremes ranged from a high of 117°F to a low of -27°F, both of which occurred at McPherson but not in the same year. The fact that three other stations exhibited all-time highs and lows on the same occasion (Table 11.12) is further evidence of a general uniformity of climate in this area of the Great Plains.

11.4.3 Wind[22-25,27,28]

Knowledge of the atmospheric dispersion of radioactive materials requires an in-depth understanding of wind conditions. Wind data presently are not available for Lyons or the Repository site, and only short-term records can be expected from preoperational measurements; therefore, meteorological data from six stations were summarized to characterize the wind regime for central Kansas and Rice County. Estimates of radioactivity dispersion were calculated[14] using a diffusion model and atmospheric data from the Wichita station.

Estimates of wind velocity and direction for Lyons can confidently be made from average data from surrounding stations because of the consistency and uniformity of prevailing wind over broad expanses of the Great Plains region. Annual average wind velocity and variance as a function of direction is illustrated in Fig. 11.7. The maximum velocity is from a southerly direction, the wind path which would disperse radionuclides away from the Lyons population center. Confidence intervals of approximately 1 mph indicate high directional uniformity among six different areas in central Kansas. Summarized as a wind rose (Fig. 11.8), directional frequency is greatest from a southerly direction. Thus, the maximum-velocity winds most frequently come from the south, and fair-weather winds were also from this direction for 11 months of the year. The exception was February, when wind frequency is slightly greater from the north. Slightly more than 60% of the wind velocities occurred in the 13- to 24-mph class (Table 11.16), and the maximum wind velocity exceeded the 32- to 46-mph class for only 0.5% of vernal winds at Dodge City.

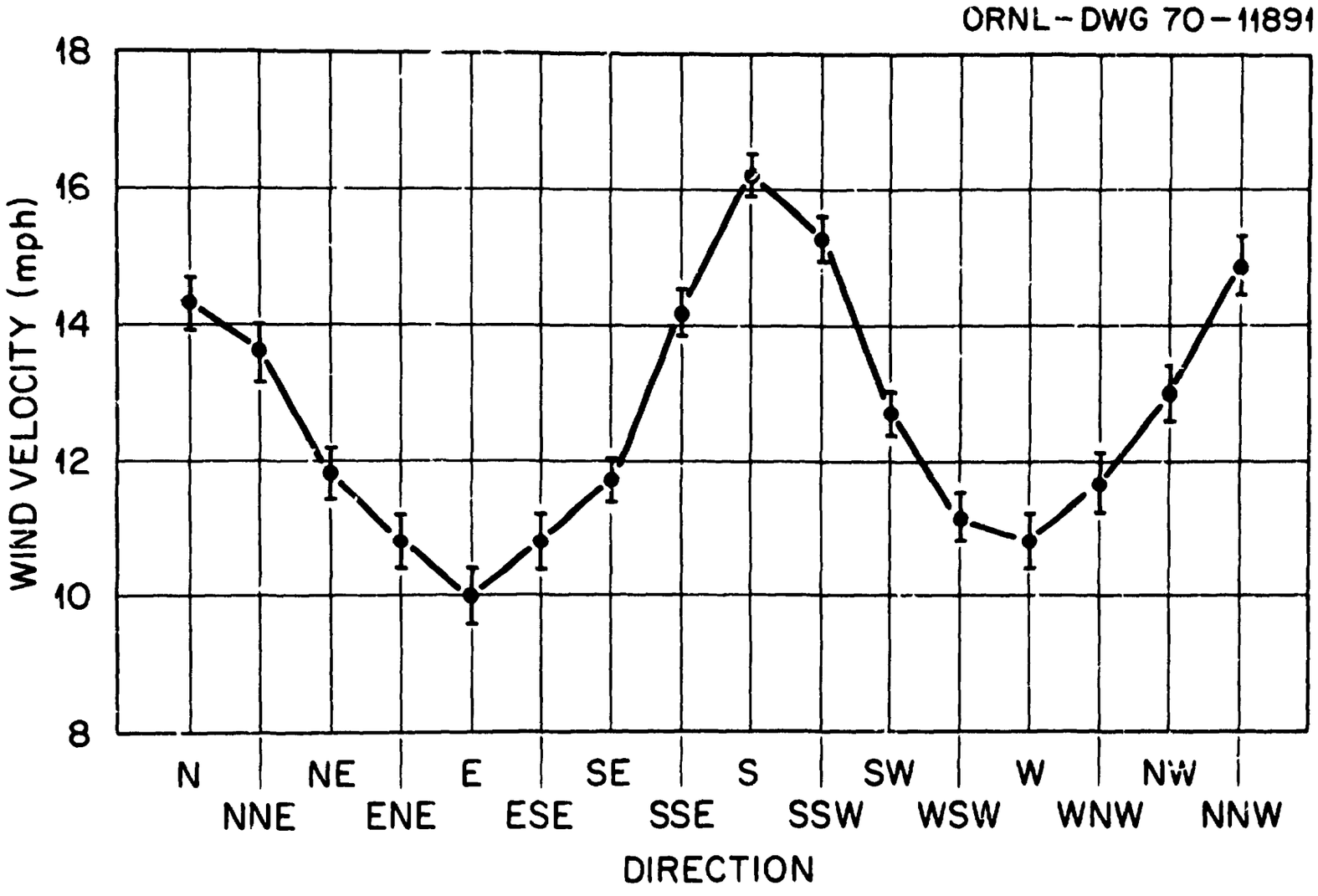

Fig. 11.7. Average Mean Wind Velocity of Six Stations at Each Direction Including 95% Confidence Intervals.

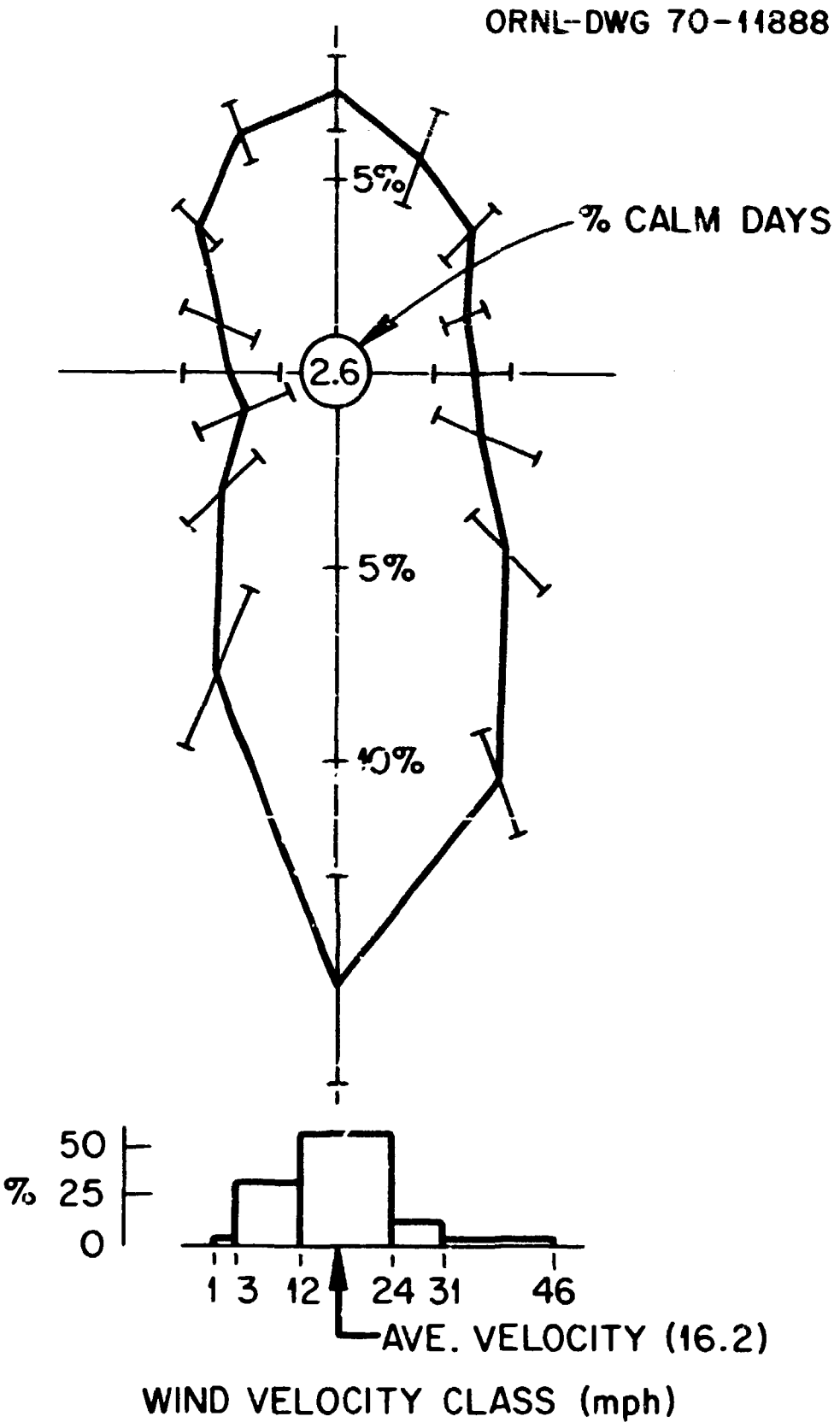

Fig. 11.8. Percentage Frequency of (1) Wind Direction Including 95% Confidence Intervals and (2) Wind Velocity from Prevailing Direction.

Table 11.16. Percentage Frequency of Wind Velocity from South (Prevailing Direction)

Wind Velocity Class (mph)	Frequency (%)
1-3[a]	1.0
4-12	27.8
13-24	61.6
25-31	8.6
32-46	1.2
46 or over[b]	
Average wind velocity from prevailing wind direction	16.2

[a]Average of three stations: Great Bend, Wichita, and Dodge City.

[b]Observed 0.2% of February and March winds at Dodge City station only.

Despite the apparent uniformity of the wind regime of central Kansas, significant differences were observed among stations. Using a model that considers the cyclical character of the wind parameters (Figs. 11.7 and 11.9), analysis of variance and multiple-range tests indicated that annual velocities were similar for Dodge City and Great Bend and for Hutchinson and Wichita. Concordia and Salina were in categories by themselves (Table 11.17). Although annual mean differences were small, it appears that local factors, possibly topography or fetch, also influence air movement patterns. Adequate assessment of the on-site wind patterns will require a meteorology station or network to measure velocity, direction, and seasonal variations.

Inversion conditions tend to localize atmospheric contents of radioactivity, but inversions will occur only during periods of relatively calm air. The percentage of calm days ranged from 0.1 (Dodge City) to 3.1 (Salina), averaging 2.6 for six stations. Low inversion frequencey would be expected on the basis of the infrequent occurrence of calm days. Again, on-site observations of this phenomenon would be necessary because the analysis of variance and similarity groupings (Table 11.18) indicate that only Concordia and Wichita are similar in this regard.

11.5 Extreme Weather

11.5.1 Tornado Events

Tornadoes result from violent storms of the Great Plains region and occur most frequently in summer. Over a 34-year-period, the average annual frequency of tornadoes in Kansas was 2.1 per 1000 square miles.[34] According to Thom,[35] the probability of a tornado striking a given square mile is calculated from the following relationship:

$$P = \frac{Z \cdot \bar{t}}{A} ,$$

where

P = mean probability of a tornado striking any given square-mile area,

Z = mean path of a tornado (for Kansas, length and width = 10 and 0.25 miles, respectively; thus, Z = 2.5 square miles)

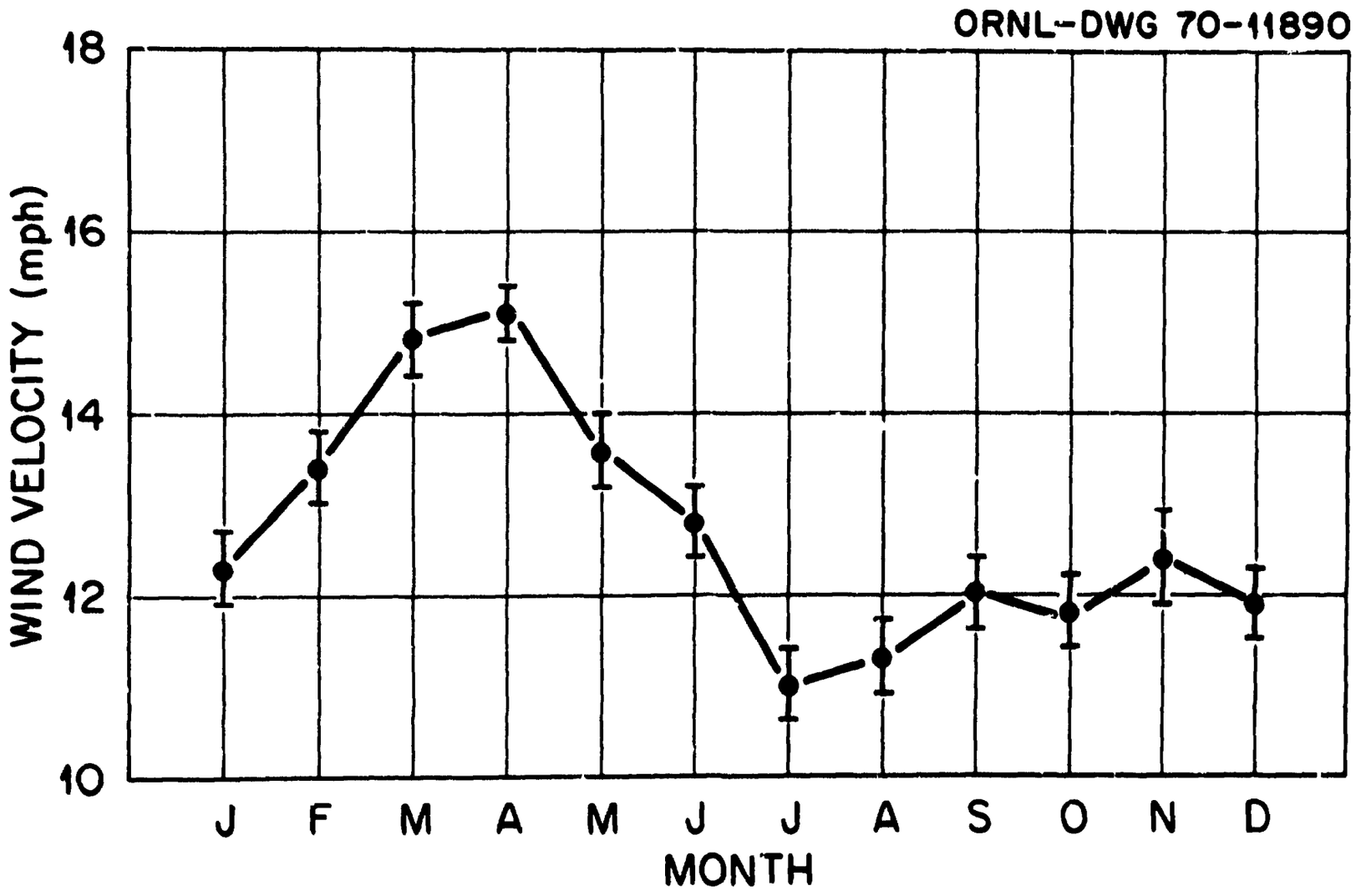

Fig. 11.9. Average Mean Wind Velocity of Six Stations in Each Month Including 95% Confidence Intervals.

Table 11.17. Duncan's Grouping (0.05) of Stations According to Wind Velocity

Station	Annual Mean Wind Velocity (mph)	Grouping[a]
Dodge City	13.9	}
Great Bend	13.7	}
Hutchinson	12.8	}
Wichita	12.6	}
Concordia	12.0	
Salina	11.2	

[a]Any two means not included within the same bracket are significantly different at 0.05 level.

Table 11.18. Duncan's Grouping (0.05) of Stations According to Percentage Frequency of Calm Days

Station	Mean Percentage of Calm Days	Grouping[a]
Salina	8.1	
Hutchinson	4.0	
Concordia	1.5	}
Wichita	1.2	}
Great Bend	0.4	
Dodge City	0.1	

[a]Any two means not included within the same bracket are significantly different at 0.05 level.

$\bar{t}$ = mean number of tornadoes per year = 2.1,

A = 10,000 square miles.

The calculated annual probability is 5.25×10^{-4}. Adjusted for increased frequencies in central Kansas (1.1 times the Kansas average according to Flora[34]), the adjusted probability (P') for the Lyons vicinity becomes 5.8×10^{-4}. Summation of annual probabilities for 25 years (i.e., the expected life of the facility) gives a probability of 0.014 for a tornado interacting with a given square-mile area in central Kansas. The probability (P") for a 1000-acre area would be 0.023. By using the relationship

$$R = 1/P'$$

or

$$R = 1/P'' \quad ,$$

the mean recurrence intervals (R) are 1730 and 1107 years for 11-square-mile and 1000-acre areas, respectively. If the Repository site should experience a tornado (P" = 0.023), then this event is unlikely to occur again during the restricted 25-year period of operations. Tornado phenomenology cannot, of course, be expected to follow strictly the laws of probability, and actual events may occur at lesser or greater frequencies.

By recognizing that the Lyons site lies in a region of relatively high tornado activity and that exposed containers of radioactive materials on the ground surface could be dispersed widely by tornado forces, then appropriate design considerations regarding structural integrity and handling procedures can be incorporated into the advance stages of planning the proposed facility. Precautionary measures to secure materials during periods of tornado watches and warnings would minimize the potential hazards from accidental release and dissemination of radioactivity over the landscape.

11.5.2 Hailstorms[36]

Crop damage from hailstorms in Kansas averages $10 million per year (ten times the damage from tornadoes). Although hail damage per se to a Repository facility is not anticipated, the commonality and the severity of hailstorms are indicators of storm violence which can be expected in the Kansas plains region. More than 75% of the hailstorms occur during May, June, and July, with nearly all the damage being to the wheat crop.

11.6 Program Plan for Future Ecological Research and Assessment

From the preceding assessment, it is apparent that additional information will be required to evaluate ecological characteristics, ecosystem processes, and related radionuclide behavior in major ecosystems of the Lyons vicinity. Additional data and parameters are needed in order to assess accurately the environmental fate of either chronic or acute releases of radioactivity from Repository operations. By using dose estimation models and data based on radioactivity pathways and concentrations in the environment, the radiation dose to man will be calculated for different sources of release and modes of exposure. The evaluation of thermal effects on surface biota also requires further investigation of potential impact on energy and water balance from the long-term, chronic heat flux that emanates from high-level wastes deposited in the salt formation. Research will focus on three different ecosystems: Cow Creek - a stream with a variable flow rate; a grassland pasture - the projected community for the Repository site; and a wheat agroecosystem - the predominant crop of the area.

An ecology program has been designed to provide technical information for assessing conceivable chronic or accidental impacts on biotic populations, ecosystems, and man during Repository operations and periods of postoperation surveillance. A primary objective of on-site ecological investigations will be to determine the structure and function of ecosystems and to examine those ecological processes which influence radionuclide fluxes in the vicinity of the waste Repository. An additional outcome of on-site research will be the formulation of base-line references for evaluating thermal or radioecological effects (either real or alleged)

related to routine operations or emergency situations. Since the Repository has been designated as a demonstration project, it is extremely important that future comparative evaluations be scientifically sound and that they be referenced against well-documented base-line conditions. Types of ecological research tasks which will be required to achieve these objectives include: (1) verification of principal food chains identified in preliminary studies (Fig. 11.1), (2) determination of the composition and abundance of important species for the major food chains, (3) evaluation of population behavior and seasonal fluctuation of principal species, and (4) analyses of environmental and biotic phenomena which may influence the behavior of radioactive or stable forms of plutonium, strontium, and cesium, and (5) determination of radioactive and stable chemical forms of contaminants for application to specific activity models. Many of these tasks, by necessity, will be carried out at the Repository site or in adjacent agroecosystems, and the work probably will be performed by ecologists from Kansas.

Field data on aquatic and terrestrial ecosystem processes will be combined with general concepts of radionuclide metabolism in organisms and with existing information on the behavior of radioactivity in the environment. Therefore, an important related objective is to couple ecological field data with ecosystem models to predict the fate of chronically or accidentally released radioactivity in the environment. For example, the capability of grassland and aquatic models to predict more accurately the behavior of ^{90}Sr in these ecosystems will be further refined from on-site ecological and environmental data collected at the Repository site. Much of this work will be performed by ORNL because several groups already possess expertise and experience in modeling and systems analysis. Sui generis model refinement will proceed concurrently with on-site ecological research, and reciprocal feedback of information between modeling-synthesis efforts and data collection will strengthen the predictability of ecosystem models as well as improve the guidelines for field and laboratory research. ORNL also will perform preliminary maximum credible assessments, a procedure that will identify potential problems in the systems context.

Schedules for completion call for assessment and model development commencing in mid-1972, with initial efforts being directed toward critical problem identification and establishment of guidelines for evaluating long-term impacts. During 1973 and 1974, when native populations have become stabilized on the Repository site, field work will concentrate on grassland and aquatic ecosystems. The research and assessment programs will be completed in 1975, at which time the results will be summarized in a final environmental and safety analysis report.

11.7 References

1. A. W. Küchler, Potential Natural Vegetation of the Conterminous United States, Am. Geog. Soc. Special Publication No. 36, American Geography Society, 1964.
2. Marcellus Horsh, "Soil Survey of Rice County," Soil Conservation Service (first draft).
3. Kansas State Board of Agriculture, Farm Facts 1968-1969.
4. D. E. Reichle, P. B. Dunaway, and D. J. Nelson, "Turnover and Concentration of Radionuclides in Food Chains," Nucl. Safety 11, 43-56 (1970).
5. F. E. Smith, "Analysis of Ecosystems," pp. 7-18 in Analysis of Temperate Forest Ecosystems, ed. by D. E. Reichle, Springer-Verlag, New York, 1970.
6. D. J. Nelson, and S. V. Kaye, "The Specific Activity Concept Applied to Aquatic Ecosystems, pp. 735-46 in Nuclear Techniques in Environmental Pollution, IAEA-SM-142a/48, 1971.
7. H. L. Krieger, B. Kahn, and S. Cummings, "Deposition and Uptake of ^{90}Sr and ^{137}Cs in an Established Pasture," pp. 59-72 in Radioecological Concentration Processes, ed. by B. Åberg and F. P. Hungate, Pergamon, Oxford, 1966.
8. J. E. Ambler, "Translocation of Strontium from Leaves of Bean and Corn Plants," Radiation Botany 4, 259-65 (1964).
9. R. Kirchmann, E. Fagniart, and S. Van Puyrnbrseck, "Studies on Foliar Contamination by Radiocesium and Radiostrontium." pp. 475-83 in Radioecological Concentration Processes, ed. by B. Åberg and F. P. Hungate Pergamon, Oxford, 1966.

10. M. R. Koelling and C. L. Kucera, "Dry Matter Losses and Mineral Leaching in Blue Stem Standing Crop and Litter," Ecology 46 529-32 (1965).
11. J. H. Rediske and A. A. Selders, "The Absorption and Translocation of Strontium by Plants," Plant Physiol. 28, 594-603 (1953).
12. R. C. Dahlman and C. L. Kucera, "Root Productivity and Turnover in Native Prairie," Ecology 46, 84-89 (1965).
13. P. Sollins, CSS: A Computer Program for Modeling Ecological Systems, ORNL-IBP-71-5 (1971).
14. Kaiser Engineers, Inc., Oak Ridge National Laboratory, and the U.S. Atomic Energy Commission, Conceptual Design and Safety Report, Federal Repository, (In press).
15. Environmental Statement for Federal Waste Repository, ORNL-CF-70-7-45 (1970).
16. I. V. Guliakin and E. V. Yudintseva, 1957. "Plant Uptake of Fission Products from Soil," in On the Behavior of Radioactive Fission Products in Soil, Their Absorption by Plants and Their Accumulation in Crops, ed. by Klechovsky, USAEC-tr-2869.
17. G. W. Campbell, personal communication, 1970. ("A Report on the Environmental Surveillance Performed in the State of Kansas, Jan. 1969 to June 1969").
18. U. S. Department of Commerce, Weather Bureau Climatic Summary of the United States 11-12. Suppl. for 1931-1952.
19. U. S. Department of Commerce, Weather Bureau Climatic Summary of the United States 86-12. Suppl. for 1951-1960.
20. U. S. Department of Commerce, Weather Bureau Climatological Data, No. 13. Annual Summary 1961 to 1969.
21. U. S. Department of Commerce, ESSA, Local Climatological Data, Annual Summary with Comparative Data. Concordia, Kansas.
22. U. S. Department of Commerce, Weather Bureau, Surface Wind Rose, Concordia, Kansas, Job No. 5780, 1964.
23. U. S. Department of Commerce, Weather Bureau National Weather Records Center, Surface Wind Rose, Dodge City, Kansas, Job No. 9068, 1959.
24. Air Weather Service, Surface Winds, Percentage Frequency of Occurrence of Directions by Velocity Groups - Great Bend Data Control Unit 13940.

25. Chief of Naval Operations, Naval Weather Service Division, Summary of Monthly Aerological Records. Hutchinson, Kansas.

26. U. S. Department of Commerce, Weather Bureau, Rainfall Frequency Atlas of the United States for Duration from 30 Minutes to 24 Hours and Return Period from 1 to 100 Years, Tech. Paper 50, 1961.

27. Air Weather Service, Directorate of Climatology Data Control Division. Percentage Frequency of Occurrence Directions by Speed Groups. Salina.

28. U. S. Department of Commerce, Decennial Census of United States Climate Climatography of the U. S. No. 82-14. Wichita, Kansas, 1963.

29. U. S. Department of Commerce, Weather Bureau Climates of the States, Kansas. Climatography of the United States No. 60-14.

30. U. S. Department of Commerce, ESSA, Local Climatological Data, Annual Summary with Comparative Data. Wichita, Kansas, 1969.

31. U. S. Department of Commerce, ESSA, Local Climatological Data, Annual Summary with Comparative Data. Dodge City, Kansas.

32. U. S. Department of Commerce, Weather Bureau, Climatography of the United States, No. 20-14, McPherson, Kansas.

33. U. S. Department of Commerce, Annual Summary of Climatological Data, No. 13. Kansas. Vols. 75 to 83, 1961-1969.

34. S. D. Flora, Tornadoes of the United States, University of Oklahoma Press, Norman, Okla., 1953.

35. H. C. S. Thom, "Tornado Probabilities," Monthly Weather Review 91, 730-36 (1963).

36. S. D. Flora, "Hailstorms of the United States," University of Oklahoma Press, Norman, Okla., 1956.

12. SAFETY ANALYSIS

J. P. Nichols

Safety and protection of the environment are of primary concern in the development and design of the proposed Repository; consequently, these subjects constitute the principal theme of this section. Included in this section are the following: a discussion of the formal procedures that have been established for analysis and review of the safety of the project, an outline of radiological safety criteria that are being used for design, estimates of the consequences of normal operations and accidents, and, finally, some thoughts with respect to long-term safety after the Repository has been decommissioned.

12.1 Safety Analysis and Reviews

An "Environmental Impact Statement" for the Repository project has been published. A draft of the Conceptual Design and Safety Analysis Report has been prepared and is currently being reviewed within the Laboratory and the AEC. Progressively more detailed and complete versions of these documents will be prepared during the design, construction, and preoperational phases of the project.

An impressive number of committees and agencies have been charged with reviewing the safety of the Repository and making known their views. Among these are:

(1) a committee of senior ORNL staff members who are not directly associated with the project,

(2) a panel of consultants to the Laboratory in the fields of geology and geophysics,

(3) various divisions of the AEC, including those who have promotional as well as those who have regulatory responsibilities,

(4) the Advisory Committee on Reactor Safeguards,

(5) the Presidential Advisory Council, a special Council of nine persons, at least three of whom will represent the state of Kansas,

(6) the Joint Congressional Committee on Atomic Energy,

(7) various agencies of the Kansas State Government, including the Kansas Geological Survey, the Kansas Department of Health, and the Kansas Advisory Council on Ecology,

(8) various other federal agencies, including, in particular, the Department of the Interior, the Environmental Protection Agency, and the Council on Environmental Quality.

Decisions with respect to approval or disapproval of the project will, no doubt, be made at the very highest levels in our Government.

12.2 Safety Criteria

There are a number of federal regulations which form a basis for the safety criteria that will be used for the design and operation of the Repository. Radiation control and monitoring systems for the Repository will be in conformance with the AEC Manual, Chapter 0524. These standards have basically the same provisions and limits as those required of AEC licensees by 10 CFR 20. The regulations governing mine safety will be the Bureau of Mines "Health and Safety Standards for Underground Mines," as published in Title 30, Part 57 of the Code of Federal Regulations. The standards for industrial safety will be in conformance with the AEC Manual, Chapter 0550, and with 41 CFR 50-204, which contains Department of Labor Regulations pursuant to the Walsh-Healy Act. The criteria for transportation safety are those of the AEC and the Department of Transportation. These regulations, in turn, require compliance with a variety of other regulations that specifically apply to such items as construction, explosives, motor vehicles, fire protection, industrial hygiene, and environmental protection.

In addition to the guidelines provided by the AEC Manual, certain other specific radiation criteria that have been found to constitute good practice among the AEC prime contractors are to be implemented at the Repository. For example, the following criteria applicable to the protection of Repository personnel will be included:

1. Radiation shields and contamination limits, together with the degree of occupancy of the affected zones, will be selected such that the

weekly averaged dose or dose commitment to operating personnel will be no more than 40% of the radiation protection standards prorated for one week of exposure. For continuously occupied zones, these limits correspond to a penetrating radiation dose rate no greater than 1.0 mrem/hr and to levels of transferable surface contamination no greater than 300 dis min^{-1} dm^{-2} from alpha radiation and 10,000 dis min^{-1} dm^{-2} from beta-gamma radiation.

2. Posted, controlled access "Radiation Zones" and "Contamination Zones" will be established in those areas which have significant potential for higher levels of radiation or contamination. Contamination control will be accomplished through the use of physical confinement barriers and the maintenance of a flow of air in the direction of increasing contamination potential.

3. "Regulated" zones with physical confinement barriers will be provided as a buffer between contamination zones and the environment.

4. Area radiation monitors will be provided in all areas in which there is potential hazard from penetrating radiation or airborne contamination.

The following criteria applicable to radiation protection of the public will also be included:

1. Releases of airborne radioactive materials from the Repository will be maintained at the lowest practical levels and well below applicable standards by:

(a) accepting no radioactive nuclides in gaseous form (other than the very small quantities that result from nuclear transmutation of solid species),

(b) providing decontamination operations to maintain surfaces in contact with ventilation streams as free of transferable contamination as practical, and

(c) passing all air from zones of potential contamination through high-efficiency particulate air (HEPA) filters, which are suitably equipped to permit periodic in-situ testing and replacement without compromising the integrity of the confinement system.

2. It is planned that there will be no discharges of radioactive materials to surface streams or to the sanitary sewer system. Solid wastes generated within the Repository will be packaged and buried in the mine. Aqueous wastes will be recycled, with any excess water being evaporated and vented to the atmosphere.

3. Confinement barriers (including critical structures and ventilation systems) and personnel protection and instrument systems will be designed, tested, routinely inspected, and maintained to ensure that the necessary confinement potential and radiation safety are sustained following exposure to any credible internal and external forces.

4. Filter systems will be physically isolated from operating areas; preceded by a series of roughing filters; protected from external forces with check valves; and tested routinely to provide protection against pressure surges, plugging, and deterioration.

5. Personnel and vehicle access to zones of any significant radiation or contamination hazard within the Repository site will be limited by an exclusion fence that surrounds surface facilities.

12.3 Radiological and Physiological Safety

The current state of technology in confinement systems is such that concentrations of physiologically hazardous materials in working areas and off-site can be maintained at an extremely low level with respect to concentrations that are considered acceptable for occupational exposure and exposure of the public.

Table 12.1 presents currently acceptable air concentrations for exposure of the public and estimates of background levels for the radioactive nuclides that will probably be of primary importance in effluents from the Repository. From the point of view of radiation exposure, the controlling nuclides in airborne waste particles will be ^{90}Sr, ^{137}Cs, and Pu; these same nuclides are also the most hazardous of the long-lived nuclides in the fallout from nuclear weapons tests. The most important gaseous materials that will be produced from spontaneous fission and decay of the wastes are believed to be ^{85}Kr, ^{3}H, ^{222}Rn, and ^{220}Rn. Although tritium is produced naturally in

Table 12.1. Concentration Guides and Estimated Concentrations of Radionuclides in the Air and Soil Near Lyons

Nuclide	Concentration Guide for Public Exposure (Ci/m^3)	Concentration in the Troposphere (Ci/m^3)	Concentration in the Soil (Ci/m^2)
^{90}Sr	1×10^{-11}	1×10^{-14}	7×10^{-8}
^{137}Cs	2×10^{-10}	1×10^{-14}	1×10^{-7}
Pu	2×10^{-14}	2×10^{-16}	1×10^{-9}
^{85}Kr	1×10^{-7}	2×10^{-11}	-
^{3}H	7×10^{-8}	2×10^{-11}	-
^{222}Rn	1×10^{-9}	1×10^{-10}	-
^{220}Rn	3×10^{-9}	5×10^{-12}	-

the atmosphere, most of the tritium presently in the biosphere was placed there by nuclear weapons tests. The radon isotopes of mass 222 and 220 are generated naturally, in relatively high concentrations, by the decay of uranium and thorium in oceans and in the earth's crust.

The guides for exposure of the public are one-third of the values listed in Table 2 of 10 CFR 20 and correspond nominally to an exposure rate of 170 mrem/year.

The surface concentrations of strontium, cesium, and plutonium that have resulted from fallout are based on measurements made in Colorado.[1,2] The corresponding atmospheric concentrations of these nuclides are based on typical experimental values of resuspension factors. From these values, we estimate that the current near-surface air concentration of ^{90}Sr corresponds to about 0.1% of the guides and that the air concentration of plutonium may be as high as 1% of the guides.

The concentrations of ^{85}Kr and ^{3}H in the atmosphere are in the range of 0.02 to 0.03% of the guides, and each contributes about 0.05 mrem of exposure per year.[3] Radon-222 occurs naturally at a concentration that is about 10 to 15% of the guides, corresponding to 20-30 mrem of exposure per year.

It should be pointed out, however, that recent measurements in the salt mine at Lyons, Kansas, have shown that the concentration of radon in the mine is about a factor of 10 higher than the average concentration of the atmosphere (or roughly 10^{-9} Ci/m^3).[4] However, this concentration is only about 3% of the level that is currently considered acceptable for occupational exposure in mines.

Table 12.2 shows estimates of the maximum concentrations of physiologically hazardous materials that are expected within work areas of the Repository under projected full-scale operations. Air that is exhausted from these work areas will, of course, be routed through HEPA filters; therefore, the concentrations passing to the atmosphere will be lower by factors of 1000 to 10,000.

Table 12.2. Typical Maximum Concentrations of Hazardous Materials in Air Expected Within Work Areas of the Repository (Before Filtration)

	Concentration in Air (% of Guides for Occupational Exposure)	
	In Surface Buildings	In Mine Exhaust Tunnels
Waste Particles	< 20	< 20
^{85}Kr		0.0002
^{3}H		0.00003
^{220}Rn and ^{222}Rn		3
H_2		1
HCl		40
Exhaust Fumes		<30

In spite of the acceptance criteria which will require shipping containers and waste packages to be relatively free of surface contamination, it is reasonable to expect that work areas of surface buildings will eventually develop contamination and that some of the material will become airborne by resuspension. On the basis of experience, periodic decontamination operations in the work areas (vacuuming, washing, and painting of work rooms, etc.) will be sufficient to maintain airborne concentrations of solid particles below 20% of the acceptable levels for occupational exposure.

Ventilation air from sections of the mine that have been exposed to waste will contain small concentrations of radioactive particles and gases, chemically noxious gases, and salt particles. Maximum concentrations of these materials will occur in the normally unoccupied mine exhaust tunnels.

The mine operating policy (i.e., the covering of waste containers with crushed salt, progressive backfilling of the utilized rooms and corridors, and eventually, backfilling of the entire mine and sealing of the shafts) will provide that once buried, virtually no radioactive particles can be transported from the wastes to the mine ventilation air and, thus, to the surface.

The maximum concentration of radioactive particles in the mine ventilation air is estimated to be 20% of the permissible concentration for occupational exposure. This would result from resuspension of minor levels of contamination that may eventually develop on surfaces exposed to the ventilation streams. We believe that these areas can be decontaminated by scraping the salt walls.

The rate at which gases are released from the mine is determined by the rate of production of the gases, the rate of temperature rise, and the rate of convergence of the mine. The waste containers will be designed to remain leakproof for at least the time that is required for backfilling of the room with crushed salt. Following perforation of the containers, gases (Xe, Kr, Rn, He, and H_2) produced by spontaneous fission and decay, as well as small volumes of H_2 and HCl from radiolysis and decomposition of the brine, will migrate slowly from the room into active air corridors.

The time required for gases to migrate through the backfilled room to the ventilation stream is such that ^{85}Kr and ^{3}H (half-lives, 10.76 and 12.26 years, respectively) will be the only radioisotopes that are released in measurable concentrations.

It is estimated that the air in the ventilation tunnels will contain radon isotopes, essentially entirely from natural sources, at concentrations of about 1×10^{-9} Ci per cubic meter.

Fumes from diesel equipment in the mine and an aerosol of salt will also be discharged into the ventilation system air. The total rate of purge air has been selected to provide for adequate dilution of diesel exhaust gases in conformance with regulations of the U.S. Bureau of Mines. Practically all of the soot from the diesel exhaust and salt that have become airborne in the mining operations will be removed by the mine exhaust filters.

Atmospheric transport will be the primary mechanism for the dispersion of material that is released from Repository stacks. We have estimated the maximum concentrations of physiologically hazardous materials that would be present in air off-site as the result of unit continuous and "puff" releases of radioactive materials from the stacks. These estimates were made using ORNL atmospheric dispersion codes and meteorological data from the Wichita weather station. The derived maximum average annual concentration at the southern site boundary for a continuous source of 1 Ci/sec is 8.6×10^{-6} Ci/m^3, which occurs at the southern boundary of the site. The maximum off-site exposure from a "puff" release of 1 Ci has been estimated as 5.5×10^{-3} Ci-sec/m^3, if the wind is blowing toward the west at the time of the release. Concentrations and exposures will decrease rapidly with distance from the Repository – approximately in inverse proportion to the 3/2 power of the distance from the stack.

Table 12.3 presents estimates of the maximum annual rate at which physiologically hazardous materials will be released from the Repository and the resultant off-site concentrations, expressed as a percentage of the guides for public exposure and the estimated concentrations that are currently present in the atmosphere.[5]

Table 12.3. Average Annual Release Rates and Off-Site Concentrations of Airborne Materials

Material	Release Rate	Concentration (%) Based On: Guides	Present Values
Waste Particles	0.007 Ci/year	0.02[a]	5.0
^{85}Kr	0.014 Ci/year	0.000004[a]	0.02
^{3}H	0.0009 Ci/year	0.0000004[a]	0.002
Natural Radon	0.9 Ci/year	0.02[a]	0.2
H_2	4 scfm	0.0002[b]	4
HCl	0.1 scfm	0.005[b]	100
Exhaust Fumes	50 scfm	<0.01[b]	<10

[a]Based on 10 CFR 20, Table II, Column 1.

[b]Based on ACGIH threshold limit values.

The primary source of waste particles is from the high-level waste receiving cell (a zone that is essentially always unoccupied), assuming that the typical air concentration in the cell would be about 100 times the level from occupational exposure.

The estimated average annual off-site concentrations of airborne radioactive materials that originate in the wastes are seen to be no greater than 0.02% of the guides and no greater than 5% of the concentrations that currently persist in the area. Off-site concentrations of radon released from the Repository are estimated to be very small, both with respect to the guides and the current concentrations. The estimated concentrations of the important nonradioactive materials are well below the limits imposed by guides, but the HCl concentrations may be equal to the present, relatively low concentration of HCl in the troposphere.

The maximum level of off-site surface contamination contributed by sources in the Repository over its 25-year life is estimated as approximately 10^{-9} Ci/m^2. This estimate is based on washout and fallout with a pessimistically high effective deposition velocity of 0.01 m/sec. This level of surface contamination is less than 1% of the level that presently exists from man-made sources and is well below the guidelines of the Federal Radiation Council. Experience has shown that the materials cannot be reconcentrated to hazardous levels in food chains at these levels of surface contamination.

12.4 Consequences of Upper Limit Accidents

Certain highly improbably dispersive events, which could result from operation of the Repository, have been considered to provide some relative appreciation for the maximum consequences that could result from unplanned or unforeseen circumstances.

Combustion of alpha waste, accompanied by rupture of the involved container(s), has the potential of generating more radioactive aerosol than any other type of accident that has been postulated for the alpha waste. The release to the atmosphere following such a fire would be

maximized if this accident were to take place in the alpha waste receiving building, since a large fraction of the contaminated smoke would reach the filters. By comparison, smoke from a fire involving an exposed container in the mine would travel with low superficial velocity through many tortuous passages and be deposited largely on exposed surfaces upstream of the filters. Because of the filtration capability and decreased diffusivity of gases in thick layers of crushed salt, no detectable release of aerosols would be expected to occur from smoldering combustion within containers after they are backfilled.

Consequences of a fire in the alpha waste receiving building have been estimated by assuming there is a fire of 30-min duration that involves the contents of many packages of alpha waste. The rationale for this accident is that the contents of a single package containing undetected solid oxidants, such as nitrate-soaked rags, are ignited by spontaneous combustion. The resulting fire is assumed to rupture the package and spread to other packages within the burial unit, as well as to any adjacent burial units. The 30-min period is believed to be a very conservative overestimate of the time that would be required for complete combustion of the contents of the package containing solid oxidants and subsequent extinguishment (by the sprinkler system) of the combustion in other containers.

For this accident, it is assumed that the waste within the container contains plutonium at the maximum acceptable concentration of 5 g/ft^3 and that the waste (cloth, tissue paper, and plastic) has a bulk density of 5 lb/ft^3. Assuming that 2% ash and soot result from combustion, the plutonium concentration per gram of airborne particulate matter would be 0.11 g.

The release of plutonium to the atmosphere through the HEPA filters is estimated by assuming that the concentration of particles in the filter effluent is 0.02 mg/m^3 and that the flow rate of air and smoke is 2600 cfm in each case. This concentration is in the upper range of measurements for filter systems that have been exposed to high loadings of unaged, submicron-size solid particles. This concentration may also be derived

as a theoretical upper limit based on self-preserving aerosol size distributions and filter efficiencies as a function of particle size.

Based on the above assumptions, the estimated release of plutonium from the stack of the Alpha-Operations Facility would be approximately 5 mg. The maximum quantity of plutonium inhaled by a hypothetical person standing at the site boundary during the entire period of release would be approximately 0.01 μg. This hypothetical intake, corresponding to 20% of the maximum permissible body burden or a bone dose commitment of 30 rem, is considered acceptable in view of its very low probability of occurrence.

The upper-limit accident in the High-Level Facility is assumed to result from complete dispersal of the contents of a can of high-level waste in the air of the high-level transfer cell. Such an accident occurring in the mine would result in a much lower release to the atmosphere. In particular, virtually no off-site exposure would result from dropping a can in the waste shaft since it is planned that there will be no sustained flow of air from the shaft into either the mine or surface facilities.

A maximum release of 9 mCi of high-level waste to the atmosphere is estimated, based on a filter effluent concentration of 0.02 mg/m^3 for one complete volume change of the air in the high-level transfer cell. The estimated maximum quantity of high-level waste that could be inhaled by a hypothetical person standing at the site boundary is 0.02 μCi. This intake by inhalation corresponds to 1% of the maximum acceptable body burden for occupational exposure and a bone dose commitment of 0.3 rem.

12.5 Long-Term Safety

The primary objective of radioactive waste disposal is that of minimizing the risk of radiation exposure of the population within the foreseeable limits of technology. In view of technical alternatives, this objective negates the intentional discharge of wastes to the atmosphere or to surface waters. On the other hand, perpetual storage of wastes

in surface vaults is subject to uncertainties with respect to the longevity of governments and forces involving sabotage and war.

The most reasonable alternative is the disposal of the waste in an isolated, natural, solid environment (deep underground). Long-term safety is promoted by (1) a high degree of confinement; (2) the option of retrievability in the event that it becomes necessary; and (3) storage of the waste in a relatively dilute form such that the average concentration is not tremendously higher than the concentration of similar radioactive materials that occur naturally.

In our opinion, the salt-mine repository provides the best method of satisfying these objectives.

Table 12.4 relates projections of the average radiation density of waste materials in the salt bed after decommissioning to the radiation density that occurs naturally in the earth's crust. Rather than comparing activity densities, per se, however, we compare the densities weighted by the appropriate concentration guide for ingestion such that we have a more precise measure of the relative potential of these materials for contamination of surface waters.

These figures show that, at the time of decommissioning, the ingestion hazard of the salt bed in the high-level portion of the Repository is about 190,000 times the hazard of an average of the earth's crust containing about 6 ppm of uranium and 12 ppm of thorium. The relative hazard decreases to unity after about 1 million years. Initially, the hazard is caused predominantly by ^{90}Sr. After progressively longer periods of decay, the most important nuclides are ^{241}Am, ^{243}Am, ^{226}Ra, and ^{129}I.

On the same basis, the relative hazard of the salt bed of the alpha facility is initially 230 – caused predominantly by ^{241}Pu and ^{241}Am – and becomes unity after about 200,000 years when most of the ^{239}Pu has decayed.

This analysis provides perhaps the most pessimistic view of the containment time that is required for the waste. Another measure of the containment time may be made by estimating the time which is required such that, if the salt and radioactive constituents were dissolved by water, the ingestion hazard of the resulting salt water would be determined

Table 12.4. Radiation Ingestion Hazard of the Salt Bed Relative to That from U-Th in the Earth's Crust

Time Since Decommissioning (years)	High-Level Waste (900 acres by 300 ft)	Alpha Waste (180 acres by 300 ft)
0	190,000 (^{90}Sr)	230 (^{241}Pu)
100	16,000 (^{90}Sr)	220 (^{241}Am)
1,000	15 (^{241}Am)	70 (^{241}Am)
10,000	4 (^{243}Am)	19 (^{239}Pu)
100,000	2 (^{226}Ra)	4 (^{239}Pu)
1,000,000	0.9 (^{129}I)	0.5 (^{237}Np)
10,000,000	0.5 (^{129}I)	0.01 (^{223}Ra)

more by its salinity than its radionuclide content. Assuming that the acceptable upper limit of salt content is 500 ppm, an acceptably low radiation density would be attained after about 1000 years in the high-level facility and 10,000 years in the alpha facility.

While these types of considerations certainly do not provide a final answer (we need to know more about solubility and mobility), they do indicate that the hazard associated with this facility will be diminished appreciably after periods of 1000 to 10,000 years (which are relatively short periods from the geologic point of view).

12.6 Alpha Waste Hazard

This section reviews very briefly the rationale that has been used to decide on the concentration of alpha waste that will require disposal in the salt mine as opposed to conventional burial in carefully selected surface burial grounds.[6]

Table 12.5 shows relative ingestion hazards of ores and various assumed types of wastes. An average of the earth's crust, formed several billion years ago, has a combined ^{238}U and ^{232}Th activity of about 0.0034 μCi/kg. If 1 kg of this average material were dissolved, it would contaminate a volume of about 0.14 m^3 to the concentration corresponding to the radiation concentration guide for exposure of the public, the hazard being dictated by the ^{226}Ra daughter. On the same basis, a typical uranium ore would contaminate about 26 m^3 of water per kilogram. An upper limit value of 10 μCi per kilogram of alpha waste has been selected on the basis that material of this contamination level would pose no greater hazard to surface water around carefully selected burial grounds than the relatively abundant deposits of uranium having concentrations intermediate between the average concentration in the earth's crust and that of uranium ore.

The ingestion hazards for wastes at these concentrations and the post-separation time at which the waste attains this maximum hazard are shown in Table 12.5. It is interesting to note that, on this basis, plutonium is the least hazardous of the common fuel materials. However, the

Table 12.5. Relative Ingestion Hazards of Ores and Wastes Containing 10 μCi of Alpha Radioactivity per Kilogram

	Parent Alpha Activity (μCi/kg)	Time Since Isolation (years)	Volume (m^3) of Water at RCG per kg Dissolved
Earth's crust (U-Th)	0.0034	4.5×10^9	0.14 (^{226}Ra)
Uranium ore	0.59	4.5×10^9	26 (^{226}Ra)
Natural U	10	1,000,000	433 (^{226}Ra)
Natural Th	10	25	346 (^{228}Ra)
93% ^{235}U	10	1,000,000	36 (^{223}Ra)
^{233}U	10	30,000	19 (^{225}Ra)
LWR Pu	10	30	5.2 (^{241}Am)

differences are not great, and it is a fair approximation to assume that all types of alpha waste have equal potential hazard on a curie basis.

12.7 References

1. P. W. Krey and E. P. Hardy, Plutonium in Soil Around the Rocky Flats Plant, HASL-235 (August 1970).

2. Federal Radiation Council Protective Action Guides, Hearings before the Joint Committee on Atomic Energy, June 29 and 30, 1965.

3. Environmental Effects of Producing Electric Power, Hearings before the Joint Committee on Atomic Energy, Oct. 28, 29, 30, and 31, Nov. 4, 5, 6, and 7, 1969, pp. 254-55.

4. F. M. Empson and J. W. Poston, Oak Ridge National Laboratory, unpublished data (September 1971).

5. C. E. Junge, Air Chemistry and Radioactivity, Academic, New York, 1963.

6. M. J. Bell and R. S. Dillon, The Long-Term Hazard of Radioactive Wastes Produced by the Enriched Uranium, Pu-^{238}U, and ^{233}U-Th Fuel Cycles, ORNL-TM-3548 (November 1971).